

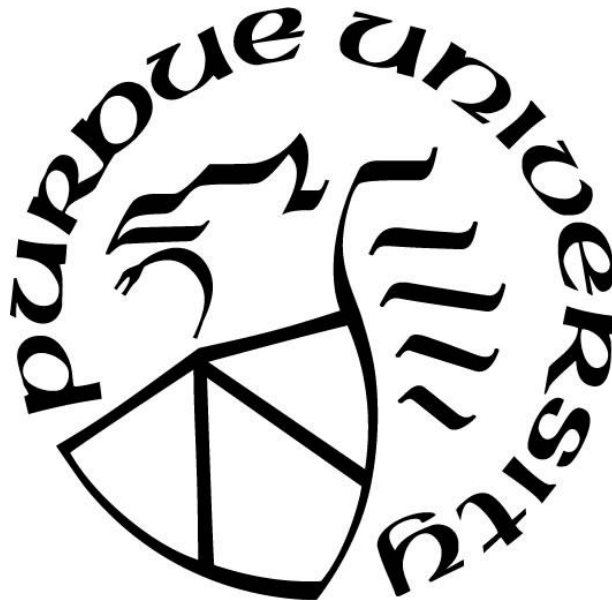
***IN VITRO AND IN VIVO INVESTIGATIONS OF CARBOHYDRATES  
WITH DIFFERENT DIGESTIBILITIES FOR IMPROVED SATIETY AND  
METABOLIC HEALTH***

by  
**Anna M.R. Hayes**

**A Dissertation**

*Submitted to the Faculty of Purdue University  
In Partial Fulfillment of the Requirements for the degree of*

**Doctor of Philosophy**



Department of Food Science  
West Lafayette, Indiana  
May 2021

**THE PURDUE UNIVERSITY GRADUATE SCHOOL  
STATEMENT OF COMMITTEE APPROVAL**

**Dr. Bruce R. Hamaker, Chair**

Department of Food Science

**Dr. Kee-Hong Kim**

Department of Food Science

**Dr. Richard D. Mattes**

Department of Nutrition Science

**Dr. Mario G. Ferruzzi**

Department of Food, Bioprocessing, and Nutrition Sciences  
North Carolina State University

**Dr. Buford L. Nichols, Jr., M.D.**

Baylor College of Medicine

**Approved by:**

Dr. Arun Bhunia

*To those who persevere*

## ACKNOWLEDGMENTS

Many thanks to the Graduate School at Purdue University for the support in form of the Frederick N. Andrews Fellowship, which supported coverage of my stipend/salary and tuition during part of my time at Purdue University.

The research described in Chapters 3 and 4 of this dissertation was supported by the Whistler Center for Carbohydrate Research. Additionally, this research was made possible in part by the support of the American People provided to the Feed the Future Innovation Lab for Collaborative Research on Sorghum and Millet through the United States Agency for International Development (USAID). The contents are the sole responsibility of the authors and do not necessarily reflect the views of USAID or the United States Government. Program activities are funded by USAID under Cooperative Agreement No. AID-OAA-A-13-00047.

The research experiments described in Chapter 5 were supported in part by research funds from USDA ARS 6250- 51000-052 including the MS and the Mouse Metabolic Research Units. The Comprehensive Lab Animal Monitor system was supported by NIH grant number S10RR024629. The investigation was part of the Texas Medical Center Digestive Diseases Center (NIH DK58338) and Whistler Center for Carbohydrate Research (internal funding).

The research project detailed in Appendix Chapter B was supported by Mondelēz International and the Whistler Center for Carbohydrate Research.

Aside from the sponsors who made this research possible, I must acknowledge the numerous individuals who have supported me as I have pursued my Ph.D.

First, I am grateful and so fortunate to have had Dr. Bruce Hamaker as my advisor and mentor. He has enabled me to participate in many collaborations and engage in various pursuits during my time in his lab – both for research and beyond. Along with this, he has helped me to enhance my understanding of dietary carbohydrates and advance the field of dietary carbohydrates as a whole. I am also especially thankful for his patience and support when I had to take time off from graduate school to improve my own health and well-being. Having the reassurance that “there would still be a place for me in the lab when I was better” was incredible.

I am also appreciative of the support of my committee – Drs. Mario Ferruzzi, Kee-Hong Kim, Richard Mattes, and Buford Nichols. I am so honored to be guided by such a distinguished group. You have all helped me improve my critical thinking skills, both related to my research and

beyond, and provided a firm foundation these past years that I am excited to build upon in the future.

As for research collaborators, I am thankful for the teamwork and friendship of Aminata Diatta and Fanny Gozzi, both of whom helped with preparing the self-made millet foods and conducting the human study described in this dissertation. To the team at the University of California, Davis – Dr. Gail Bornhorst, Clay Swackhamer, Dr. Yamile Mennah-Govela, Erik Sewalt, and Danny Tagle – thank you for all your guidance and help with the Human Gastric Simulator experiments while I was a visiting scholar there. To Dr. Mario Martinez, currently at Aarhus University – I am most grateful for your guidance, training, friendship, and overall support throughout my research. To Dr. Susann Bellmann and Tom Gorissen as well as the rest of the group at TNO/The TIM Company in the Netherlands – thank you for your generous support, assistance, and kindness when we conducted the TIMagc experiments during my time in the Netherlands. To Dr. Buford Nichols and his collaborative team – Dr. Nancy Butte, Dr. Erwin Sterchi, Dr. Ursi Lugenbuhl, Firoz Vohra, Stephen Avery, and Dr. Roberto Quezada-Calvillo – your contributions to the mouse indirect calorimetry experiments are much appreciated.

Past and present Hamaker Lab members have also given me countless support and guidance. To past members – Dr. Mohammad Chegeni, Dr. Tingting Chen, Dr. Sarah Corwin, Dr. Fang Fang, Rachel Jackson, Dr. Moustapha Moussa, Dr. Elizabeth Pletsch, Dr. Leigh Schmidt, and Dr. Xiaowei Zhang – thank you for your friendship and encouragement. To current members – Emmanuel Ayua, Nuseybe Bulut, Dr. Thaisa Cantu-Jungles, Aminata Diatta, Dr. Marwa El Hindawy, Enosh Kazem, Dr. Jongbin Lim, Dr. Oguz Ozturk, Monica Richmond, Dr. Yony Roman Ochoa, Oluwatoyin “Ola” Sangokunle, Pablo Torres-Aguilar, and Tianming Yao – you have been a wonderful group to finish my Ph.D. with and I am grateful for all the memories we have together (especially the ups and downs of dealing with a pandemic!).

I am also most appreciative of the support and assistance of the Purdue Food Science Department. I will miss all the staff, faculty, and students. I am especially grateful to Mitzi Barnett for her constant guidance as I have navigated my Ph.D.

A special note of thanks to Dr. Edward Fox in the Department of Psychological Sciences at Purdue for his collaboration, support, and inspiration as I approached him about learning more in the area of neuroscience related to the control of food intake and ingestive behavior. Dr. Fox – you have helped me discover a fascinating area of research that I will be pursuing in the near future.

Without your encouragement and belief in me as a student and researcher, none of this would have unfolded.

Finally, I have innumerable family and friends to thank. First, I am eternally grateful for the support and love from my family – Tom, Patti, David, Micaela, Fr. John, Daniel, and now little Sophia. Thank you for always being there and cheering me on. Second, I am so thankful for the friendship of Dr. Simran Kaur; little did I know when I agreed to room with you when I was first starting at Purdue that I would find a lifelong friend! Thank you for everything these past years. There are many others to thank for so many reasons. To Dr. Dennis Cladis, Dr. Da Chen, Dr. Cecilia Espinoza, Enrico Federici, Ryan Kawakita, Anbuhkani “Connie” Muniandy, Dr. Amudhan Ponrajan, Dr. Veronica Rodriguez, Hector Rodriguez, Dr. Laura Roman, Dr. Shreya Sahasrabudhe-Kulkarni, Troy Tonner, and Dr. Adrienne Voelker – thank you for your support and I have many fond memories with you all! I also must thank Deb and Steve Belter for their support these past years. Finally, I am especially grateful to my partner-in-crime, Clay Swackhamer. You have helped me in ways I cannot adequately express. Notably, though, I am so fortunate to have you as a constant source of support and companionship. I am excited for what the future holds!

Through God, all things are possible.

# TABLE OF CONTENTS

LIST OF TABLES .....	12
LIST OF FIGURES .....	15
LIST OF ABBREVIATIONS.....	20
ABSTRACT.....	22
CHAPTER 1. INTRODUCTION .....	25
1.1 Introduction.....	25
1.2 Specific objectives and research hypotheses .....	26
1.3 Significance of work.....	27
1.4 Thesis organization .....	28
1.5 References.....	29
CHAPTER 2. LITERATURE REVIEW .....	33
2.1 Abstract.....	33
2.2 Introduction.....	33
2.3 Carbohydrate structure and digestion .....	34
2.4 Gastric emptying, the ileal brake, and the gut-brain axis .....	39
2.5 Carbohydrate metabolism – oxidation and metabolic flexibility.....	43
2.6 <i>In vitro</i> , <i>in vivo</i> , and mathematical modeling approaches related to starch digestion, gastric emptying, and metabolism.....	46
2.7 Conclusions.....	50
2.8 References.....	50
CHAPTER 3. PEARL MILLET ( <i>PENNISETUM GLAUCUM</i> ) COUSCOUS BREAKS DOWN FASTER THAN WHEAT COUSCOUS IN THE HUMAN GASTRIC SIMULATOR, THOUGH HAS SLOWER STARCH HYDROLYSIS .....	70
3.1 Abstract.....	70
3.2 Introduction.....	71
3.3 Materials and Methods.....	72
3.3.1 Raw material preparation.....	72
Couscous materials.....	72
Couscous pre-processing.....	72

Couscous preparation .....	73
3.3.2 Couscous characterization .....	73
Rapid Visco Analyzer analysis .....	73
Starch fine structure .....	73
Light microscopy.....	74
3.3.3 Simulated oral and gastric digestion.....	74
Simulated saliva formulation .....	74
Simulated gastric juice formulation .....	74
Simulated oral and gastric digestion procedure .....	74
3.3.4 Moisture content .....	75
3.3.5 pH measurement .....	75
3.3.6 Particle size analysis .....	75
3.3.7 Starch hydrolysis analysis.....	76
3.3.8 Relative gastric emptying of solids from the HGS .....	77
3.3.9 Statistical analysis.....	77
3.4 Results.....	78
3.4.1 Couscous properties.....	78
Rapid Visco Analyzer analysis .....	78
Starch fine structure .....	78
Light microscopy.....	78
3.4.2 Particle size analysis .....	79
3.4.3 Starch hydrolysis in the HGS .....	80
3.4.4 Moisture content .....	80
3.4.5 pH .....	80
3.4.6 Relative gastric emptying of solids from the HGS .....	81
3.5 Discussion .....	81
3.6 Conclusions.....	86
3.7 References.....	86
CHAPTER 4. SOME PEARL MILLET-BASED FOODS PROMOTE SATIETY OR REDUCE GLYCEMIC RESPONSE IN A CROSSOVER TRIAL .....	104
4.1 Abstract.....	104

4.2	Introduction.....	105
4.3	Methods.....	106
4.3.1	Participants and study design.....	106
4.3.2	Pre-preparation of test meals foods .....	107
4.3.3	Test day preparation of test meal foods.....	108
4.3.4	Test day procedures .....	109
4.3.5	Glycemic response.....	110
4.3.6	Appetitive sensations .....	110
4.3.7	Gastric emptying.....	110
4.3.8	Analysis of relationship between gastric emptying and glycemic response.....	111
4.3.9	Breath hydrogen.....	111
4.3.10	<i>In vitro</i> gastric compartment pressure profiles.....	112
4.3.11	Statistical analysis .....	112
4.4	Results.....	113
4.4.1	Participant characteristics .....	113
4.4.2	Glycemic response.....	113
4.4.3	Appetitive sensations .....	114
4.4.4	Gastric emptying.....	114
4.4.5	Analysis of relationship between gastric emptying and glycemic response.....	115
4.4.6	Breath hydrogen.....	115
4.4.7	<i>In vitro</i> gastric compartment pressure profiles .....	116
4.5	Discussion.....	116
4.6	References.....	119
CHAPTER 5. MODERATING CARBOHYDRATE DIGESTION PROMOTES FAT OXIDATION AND MAY ENHANCE METABOLIC FLEXIBILITY .....		143
5.1	Abstract.....	143
5.2	Introduction.....	144
5.3	Materials and Methods.....	147
5.3.1	Animals.....	148
5.3.2	Experimental diets .....	148
5.3.3	Amyloglucosidase (AMG) supplementation .....	149

5.3.4	Indirect calorimetry – Respiratory Exchange Ratio (RER).....	149
5.3.5	Modeling of RER using sine equation.....	150
5.3.6	Calculation of Percent Relative Cumulative Frequency (PRCF) of RER .....	151
5.3.7	Modeling of PRCF.....	151
5.3.8	Mean RER per 24 h .....	152
5.3.9	Body weight.....	153
5.3.10	<i>Ex vivo</i> assay of jejunal enzyme activities .....	153
5.3.11	Statistical analysis .....	153
5.4	Results and Discussion .....	154
5.4.1	Starch digestibility, percent amylose, and food quotient of experimental diets .....	154
5.4.2	Effect of diet, genotype, and AMG supplementation on RER .....	156
5.4.3	Effect of diet, genotype, and AMG supplementation on PRCF of RER .....	158
	Data analyzed per individual mice .....	158
	Data analyzed as pooled from all mice .....	163
	Weibull Cumulative Distribution.....	163
	Mixed Weibull Cumulative Distribution .....	165
	Notable differences among PRCF approaches .....	171
5.4.4	Mean RER per 24 h .....	173
5.4.5	Body weight.....	173
5.4.6	<i>Ex vivo</i> assay of jejunal enzyme activities.....	173
5.4.7	Strengths and potential limitations .....	174
5.5	Conclusion .....	175
5.6	Acknowledgements.....	177
5.7	References.....	178
CHAPTER 6.	CONCLUSION.....	229
6.1	Summary and overall conclusions .....	229
6.2	Future directions .....	231
6.3	References.....	233
APPENDIX A.	SUPPLEMENTARY MATERIALS.....	235

APPENDIX B. INVESTIGATING THE POTENTIAL OF SLOW-RETROGRADING STARCHES TO REDUCE STALING IN SOFT SAVORY BREAD AND SWEET CAKE MODEL SYSTEMS .....	246
VITA.....	302

## LIST OF TABLES

Table 2.1 Approximate oxidation characteristics for carbohydrate, fat, and protein and corresponding respiratory exchange ratio (RER) values. Based off Ferrannini (1988). .....	63
Table 3.1 Types of couscous. Source of each couscous is given in addition to its initial (before digestion, dry) particle size as determined by sieving. ....	92
Table 3.2 Starch structural characterization of initial (undigested) couscous as well as for flour starting materials used for self-made couscous types. Values in each column that do not share a letter (abc) represent significant differences ( $p<0.05$ ) between different types of couscous or flour. DP = degree of polymerization. If no letter is shown, there were no statistically significant differences. ....	93
Table 3.3 Median particle size, quantified by Rosin-Rammler $x_{50}$ (Equation 1), and particle size distribution spread parameter, quantified by Rosin-Rammler $b$ (Equation 1), for particles in digesta withdrawn from the HGS at different time points and for different types of couscous. All values are means of multiple runs in the HGS ( $n=3$ runs, except for millet small which was $n=4$ ) $\pm$ standard deviation. Values in each column that do not share a letter (abc) represent significant differences ( $p<0.05$ ) within a certain type of couscous across different digestion times. Values in each row that do not share a letter (zyx) represent significant differences ( $p<0.05$ ) within a certain time point across different types of couscous. If no letter is shown, there were no statistically significant differences. ....	94
Table 3.4 Percent starch hydrolysis (%) of digesta withdrawn from the HGS at different time points and for different types of couscous (not expressed per unit area). All values are means of multiple runs in the HGS ( $n=3$ runs, except for millet small which was $n=4$ ) $\pm$ standard deviation. Values in each column that do not share a letter (abc) represent significant differences ( $p<0.05$ ) within a certain type of couscous across different digestion times. Values in each row that do not share a letter (zyx) represent significant differences ( $p<0.05$ ) within a certain timepoint across different types of couscous. If no letter is shown, there were no statistically significant differences. ....	95
Table 3.5 Moisture content (dry basis, g water/g dry mass) and pH of digesta withdrawn from the HGS at different time points and for different types of couscous. All values are means of multiple runs in the HGS ( $n=3$ runs, except for millet small which was $n=4$ ) $\pm$ standard deviation. Values in each column that do not share a letter (abc) represent significant differences ( $p<0.05$ ) within a certain type of couscous across different digestion times. Values in each row that do not share a letter (zyx) represent significant differences ( $p<0.05$ ) within a certain time point across different types of couscous. If no letter is shown, there were no statistically significant differences. ....	96
Table 3.6 Parameters of the modified power-exponential model (Equations 2 and 3) for gastric emptying. Values in each column that do not share a letter (abc) represent significant differences ( $p<0.05$ ) between different types of couscous. ....	97
Table 4.1 Test meal foods. ....	124
Table 4.2 Values used for correction of endogenous $^{13}\text{C}$ for percent dose recovery per timepoint for gastric emptying assessment of millet-based meals. Values are means from testing with a	

subgroup of 4 participants (n=4). Values shown were used for the millet thick porridge, millet couscous (self-made), and millet couscous (commercial) test meals. Endogenous <sup>13</sup> C for white rice and wheat couscous were nearly negligible.....	125
Table 4.3 Parameters from modelling percent dose recovery (PDR) and cumulative percent dose recovery (CPDR) of <sup>13</sup> C (corrected for endogenous <sup>13</sup> C) for each participant. These parameters were used for calculating gastric half-emptying time, lag phase, and gastric emptying coefficient. ....	126
Table 4.4 Mean lag phase and gastric emptying coefficient values (n=14) <sup>a</sup> . ....	128
Table 4.5 Participant baseline characteristics (n=15) <sup>a</sup> . ....	129
Table 4.6 Glycemic response characteristics <sup>a</sup> . ....	130
Table 5.1 Experimental diet compositions.....	184
Table 5.2 Starch contents in different diets <sup>a</sup> . ....	186
Table 5.3 Contents of rapidly digestible, slowly digestible, and resistant starches in different diets (% , dry starch basis). <sup>a</sup> Mean values shown with ± standard deviation as applicable. ....	187
Table 5.4 Sine equation parameters for curve fitting of respiratory exchange ratio (RER) for individual mice, per diet type, per cycle (with vs. without AMG). Value are means ± standard error the mean. Groups not sharing the same letters or symbols are significantly different (p<0.05). ....	188
Table 5.5 Statistical analysis for sine equation parameters for curve fitting of respiratory exchange ratio (RER) for individual mice, per diet type, genotype (null vs. wild-type), per cycle (with vs. without AMG).....	190
Table 5.6 Mixed Weibull Cumulative Distribution parameter estimates ( $\alpha$ , $x_{50\_1}$ , $b_1$ , $x_{50\_2}$ , $b_2$ ) for respiratory exchange ratio (RER) from individual percent relative cumulative frequency (PRCF) analyses. $R^2$ is also shown as an indicator of goodness of fit. Values are means ± standard error of the mean. Groups not sharing the same letters or symbols are significantly different (p<0.05).....	191
Table 5.7 Parameter estimates, confidence intervals, statistical groupings, and visualization of genotype and amyloglucosidase (AMG) effects for median respiratory exchange ratio ( $x_{50}$ RER) from pooled percent relative cumulative frequency (PRCF) using the Weibull Cumulative Distribution function. ....	193
Table 5.8 Parameter estimates, confidence intervals, statistical groupings, and visualization of genotype and amyloglucosidase (AMG) effects for the distribution breadth constant ( $b$ ) of respiratory exchange ratio (RER) from pooled percent relative cumulative frequency (PRCF) using the Weibull Cumulative Distribution function. ....	195
Table 5.9 Parameter estimates, confidence intervals, statistical groupings, and visualization of genotype and amyloglucosidase (AMG) effects for the $\alpha$ parameter from modeling of respiratory exchange ratio (RER) from pooled percent relative cumulative frequency (PRCF) using the Mixed Weibull Cumulative Distribution function. ....	197

Table 5.10 Parameter estimates, confidence intervals, statistical groupings, and visualization of genotype and amyloglucosidase (AMG) effects for the median RER ( $x_{50\_1}$ ) parameter from modeling of respiratory exchange ratio (RER) from pooled percent relative cumulative frequency (PRCF) using the Mixed Weibull Cumulative Distribution function. .... 199

Table 5.11 Parameter estimates, confidence intervals, statistical groupings, and visualization of genotype and amyloglucosidase (AMG) effects for the median RER  $b_1$  parameter from modeling of respiratory exchange ratio (RER) from pooled percent relative cumulative frequency (PRCF) using the Mixed Weibull Cumulative Distribution function. .... 201

Table 5.12 Parameter estimates, confidence intervals, statistical groupings, and visualization of genotype and amyloglucosidase (AMG) effects for the median RER ( $x_{50\_2}$ ) parameter from modeling of respiratory exchange ratio (RER) from pooled percent relative cumulative frequency (PRCF) using the Mixed Weibull Cumulative Distribution function. .... 203

Table 5.13 Parameter estimates, confidence intervals, statistical groupings, and visualization of genotype and amyloglucosidase (AMG) effects for the median RER  $b_2$  parameter from modeling of respiratory exchange ratio (RER) from pooled percent relative cumulative frequency (PRCF) using the Mixed Weibull Cumulative Distribution function. .... 205

Table 5.14 Mean RER per 24 h for each group (diet  $\times$  genotype  $\times$  cycle [without/with AMG]). Mean values shown with  $\pm$  standard error of the mean. Values not sharing the same letter are significantly different ( $p < 0.05$ ; diet  $\times$  genotype  $\times$  cycle was significant [ $p = 0.0001$ ], so *post hoc* comparisons were made among the 24 groups). Arrows in columns for genotype and AMG breakdown the effects of these two factors *within* each diet. .... 207

Table 5.15 Effect of dietary condition and genotype on *ex vivo* jejunal enzyme activities (U/gm protein) for maltodextrin and sucrose substrates sampled by military time (MT),  $n = 4$  per group. Mean values are shown  $\pm$  standard error of the mean.  $p$ -values indicate statistical comparisons between genotype per diet for the two substrates. .... 208

## LIST OF FIGURES

Figure 2.1 Representation of the protein organization of the MGAM and SI complexes. Both MGAM and SI have a small cytosolic domain (~26 residues), and transmembrane domain (~20 residues), an O-glycosylated linker (~55 residues), and two homologous catalytic subunits (NtMGAM, CtMGAM, NtSI, CtSI; each ~900 residues). Percentages shown indicate the proportion of sequence identities between the catalytic subunits. Originally published in Sim et al. (2008), used with permission. CtMGAM, C-terminal maltase glucoamylase; CtSI, C-terminal sucrase isomaltase; MGAM, maltase glucoamylase; NtMGAM, N-terminal maltase glucoamylase; NtSI, N-terminal sucrase isomaltase; O-link, O-glycosylated linker; SI, sucrase isomaltase; TMD, transmembrane domain. .... 64

Figure 2.2 Enteroendocrine cell types divided into pan-GI-tract (throughout the gastrointestinal tract), gastric-selective, and intestinal-selective cells. For each of the cell types, the main secretory product and the original Wiesbaden nomenclature (W-type) are indicated. The lighter maroon color indicates that some of the peptides are less expressed in these segments. \*Some enteroendocrine cells have been shown to co-express GIP and GLP-1 (Grigoryan et al., 2012). Adapted from Engelstoft et al. (2013), used with permission. CCK, cholecystokinin; EE, enteroendocrine; GIP, glucose-dependent insulinotropic peptide; GLP-1, glucagon-like peptide 1; GLP-2, glucagon-like peptide 2; PYY, peptide YY; W-type, Wiesbaden nomenclature..... 65

Figure 2.3 Photo of the TIM system with an advanced gastric compartment (TIMagc). Developed by TNO in the Netherlands and now commercialized with The TIM Company..... 66

Figure 2.4 Photos of the Human Gastric Simulator (HGS). Initially developed by Kong and Singh (2010) at the University of California, Davis, and later refined to the current version in the laboratory of Dr. Gail Bornhorst at the University of California, Davis. Entire system when not in use (A) and close-up of the gastric compartment while in use (B)..... 67

Figure 2.5 Representation of the Weibull Cumulative Distribution function fit to data. PRCF, percent relative cumulative frequency; RER, respiratory exchange ratio. .... 68

Figure 2.6 Representation of the Weibull Cumulative Distribution function fit to data. PRCF, percent relative cumulative frequency; RER, respiratory exchange ratio. .... 69

Figure 3.1 Diagram of the Human Gastric Simulator (HGS). .... 98

Figure 3.2 RVA profiles of wheat couscous (●), wheat flour (▲), millet couscous (◆), and millet flour (★). Error bars represent the standard deviation of two runs and in some cases may be too small to be seen. Viscosity was recorded every 4 seconds, but for clarity a symbol has been placed on every fifth data point (every 20 s)..... 99

Figure 3.3 Light micrographs (A-H) of the initial flour and couscous samples: millet flour (A), small millet couscous (B), large millet couscous (C), commercial millet couscous (D), wheat flour (E), small wheat couscous (F), large wheat couscous (G), commercial wheat couscous (H). ... 100

Figure 3.4 Particles per gram dry matter of for digesta of small wheat couscous (■), commercial wheat couscous (■), small millet couscous (■), large millet couscous (■), and commercial millet

couscous (■) during vitro gastric digestion (initial = no digestion; oral = 30 s simulated oral digestion; 30-180 min = corresponding simulated gastric digestion time). Error bars represent standard deviation of either three or four digestions in the HGS. .... 101

Figure 3.5 Percent starch hydrolysis per unit area of particles in the HGS for small wheat couscous (●), commercial wheat couscous (▲), small millet couscous (\*), large millet couscous (■), and commercial millet couscous (★). Error bars represent the standard error of three runs except for millet small (four runs). .... 102

Figure 3.6 Relative solids remaining in the HGS (%), representative of relative gastric emptying, for small wheat couscous (●), commercial wheat couscous (▲), small millet couscous (\*), large millet couscous (■), and commercial millet couscous (★). Error bars represent the standard deviation of three digestions except for small millet couscous (four digestions). Lines represent the model fit (Equation 2). .... 103

Figure 4.1 Participant recruitment and participation flow diagram. .... 131

Figure 4.2 Example percent dose recovery (PDR) and cumulative percent dose recovery (CPDR) graphs and modelling for determining gastric half-emptying times of the different test meal foods for one participant. A: White rice. B: Millet thick porridge. C: Millet couscous (self-made). D: Millet couscous (commercial). E: Wheat couscous. All figures labelled 1 show PDR, while all figures labelled 2 depict CPDR. .... 132

Figure 4.3 Mean glucose expressed as mean  $\Delta$ Glucose (glucose difference from baseline) for carbohydrate-based test meals. Error bars represent standard error of the mean (SEM). Means not sharing the same letter are significantly different ( $p < 0.05$ ) in main effects: All millet foods and wheat couscous had significantly lower glycemic response than white rice [ $p < 0.0001$  for millet couscous (commercial), millet thick porridge, wheat couscous vs. white rice;  $p = 0.05$  for millet couscous (self-made) vs. white rice]. Millet thick porridge had significantly lower glycemic response than both types of millet couscous (commercial and self-made;  $p = 0.01$  and  $p < 0.0001$ , respectively) and wheat couscous ( $p < 0.0001$ ). Millet couscous (self-made) also had significantly higher glycemic response than millet couscous (commercial) and wheat couscous ( $p < 0.0001$ ). A significant effect for time was also evident ( $p < 0.0001$ ). .... 133

Figure 4.4 Mean hunger ratings (Visual Analog Scale) immediately prior to and 4 h following consumption of carbohydrate-based test meal foods. Error bars represent standard error of the mean (SEM). Means not sharing the same letter are significantly different ( $p < 0.05$ ) in main effects: Millet couscous (self-made) was significantly lower than white rice ( $p < 0.0001$ ), wheat couscous ( $p = 0.02$ ), millet thick porridge ( $p = 0.008$ ), and millet couscous (commercial) ( $p = 0.002$ ). A significant effect for time was also evident ( $p < 0.0001$ ). .... 134

Figure 4.5 Mean fullness ratings (Visual Analog Scale) immediately prior to and 4 h following consumption of carbohydrate-based test meal foods. Error bars represent standard error of the mean (SEM). Means not sharing the same letter are significantly different ( $p < 0.05$ ) in main effects: Millet couscous (self-made) was significantly higher than white rice ( $p < 0.0001$ ), millet couscous (commercial) ( $p < 0.0001$ ), and millet thick porridge ( $p = 0.0004$ ). A significant effect for time was also evident ( $p < 0.0001$ ). .... 135

Figure 4.6 Mean gastric half-emptying times for each carbohydrate-based test food displayed as a box-plot, with either all values (A) or outliers removed (B) ( $n = 14$ ). No statistically significant

differences were found ( $p=0.15$ ). Circles represent values from individual participants per test meal. Central red marks indicate the median. Bottom and top edges of the blue box represent the 25<sup>th</sup> and 75<sup>th</sup> percentiles, respectively. Note that instances for which the percent dose recovery of the tracer did not decrease by more than 1% of its peak value during the monitoring period were deemed outliers (4 values greater than 10 h). ..... 136

Figure 4.7 Gastric half-emptying times by participant averaged across all test meal foods ( $n=15$ , includes participant 61 who withdrew during the study). Exploratory data visualization, so no statistical analysis was conducted. Circles represent values for individual test meal foods per participant. Central red mark indicates the median. Bottom and top edges of the blue box represent the 25<sup>th</sup> and 75<sup>th</sup> percentiles, respectively. Note that instances for which the percent dose recovery of the tracer did not decrease by more than 1% of its peak value during the monitoring period were deemed outliers (4 values greater than 10 h). ..... 137

Figure 4.8 Example of included (A) and excluded (B) percent dose recovery (PDR) modelling curves for gastric half-emptying time. Excluded modelling curves (and therefore gastric half-emptying times) did not decrease by more than 1% of their peak value during the monitoring period, such as the curve seen in (B), were deemed outliers. .... 138

Figure 4.9 Mean gastric half-emptying time for each carbohydrate-based test food (excluding 4 outlier values) as determined using the <sup>13</sup>C octanoic breath test. Error bars represent  $\pm$  standard error of the mean (SEM). No statistically significant differences were found ( $p=0.18$ ). ..... 139

Figure 4.10 Relationship between gastric half-emptying time (h) and glucose incremental area under the curve from 0-120 min (iAUC<sub>0-120min</sub>; mg $\times$ min/dL; A, D),  $\Delta$ Peak glucose value (mg/dL; B, E), and peak glucose time (min; C, F) ( $n=14$ ). Analyses in two instances of inclusion of gastric half-emptying time values are shown. A-C: no values removed. D-F: outliers removed. Note that instances in which the percent dose recovery of the tracer did not decrease by more than 1% of its peak value during the monitoring period were deemed outliers. .... 140

Figure 4.11 Mean breath hydrogen during the 4 h postprandial period for each test meal ( $n=14$ , excluding one participant due to outlier values and one additional outlier value) as a general indicator of potential fermentation of the test meals. As breath hydrogen values never rose above baseline for any of the treatments, it was concluded that fermentability was not a confounding factor in the study. .... 141

Figure 4.12 Mean pressure values within the gastric compartment during *in vitro* gastrointestinal experiments for white rice, millet thick porridge, millet couscous (self-made), and wheat couscous. Means represent values from duplicate runs from experiments lasting 6 h. .... 142

Figure 5.1 Diagram of indirect calorimetry experiments protocol per diet. Figure made using BioRender. AMG, amyloglucosidase. .... 209

Figure 5.2 Modeled respiratory exchange ratio (RER) for Conventional starch diet. AMG, amyloglucosidase. .... 210

Figure 5.3 Modeled respiratory exchange ratio (RER) for 53% Resistant starch diet. AMG, amyloglucosidase. .... 211

Figure 5.4 Modeled respiratory exchange ratio (RER) for 35% Resistant starch diet. AMG, amyloglucosidase. .... 212

Figure 5.5 Modeled respiratory exchange ratio (RER) for 18% Resistant starch diet. AMG, amyloglucosidase.....	213
Figure 5.6 Modeled respiratory exchange ratio (RER) for Sucrose diet. AMG, amyloglucosidase. ....	214
Figure 5.7 Modeled respiratory exchange ratio (RER) for High-fat diet. AMG, amyloglucosidase. ....	215
Figure 5.8 Sine curves for average sine parameters from RER data fit for all null mice per diet (diet × mouse genotype [null] × cycle). AMG, amyloglucosidase.....	216
Figure 5.9 Sine curves for average sine parameters from RER data fit for all wild-type mice per diet (diet × mouse genotype [wild-type] × cycle). AMG, amyloglucosidase.....	217
Figure 5.10 Sine curves for average sine parameters from RER data fit for all mice per diet (diet × mouse genotype × cycle), illustrated without AMG only [cycle 2]. AMG, amyloglucosidase. ....	218
Figure 5.11 Sine curves for average sine parameters from RER data fit for all mice per diet (diet × mouse genotype × cycle), illustrated with AMG only [cycle 3]. AMG, amyloglucosidase.....	219
Figure 5.12 Sine curves for average sine parameters from RER data fit for all mice per diet (diet × mouse genotype × cycle). Split per genotype and cycle: null cycle 2 [without AMG] (A), null cycle 3 [without AMG] (B), wild-type cycle 2 [without AMG] (C), wild-type cycle 3 [with AMG] (D). AMG, amyloglucosidase.....	220
Figure 5.13 Relationships between carbohydrate components and <i>c</i> parameter values from sine equation curve fitting for null mice fed the Conventional starch diet, 53% Resistant starch diet, 35% Resistant starch diet, and 18% Resistant starch diet, all without the amyloglucosidase (AMG) supplement. Correlation between amylose percentage and <i>c</i> (A). Correlation between resistant starch amount and <i>c</i> (B). Correlation coefficients and <i>p</i> -values from linear regression are shown for both analyses. ....	221
Figure 5.14 Median RER values from the bimodal PRCF distributions of RER modeled for individual mice using the Mixed Weibull Cumulative Distribution function. <i>x</i> 50_1 represents the median RER for the first mode, while <i>x</i> 50_2 represents the median RER for the second mode. Error bars indicate ± standard error of the mean. Groups not sharing the same letters within each parameter are significantly different in main effect for diet ( <i>p</i> <0.05). Statistically significant main effects for cycle (with vs. without AMG) and genotype (null vs. wild-type) were observed for the <i>x</i> 50_1 parameter ( <i>p</i> <0.05), and a statistically significant main effect for cycle (with vs. without AMG) was observed for the and <i>x</i> 50_2 parameter ( <i>p</i> <0.05). AMG, amyloglucosidase.....	222
Figure 5.15 Distribution breadth constants (slopes) from the bimodal PRCF distributions of RER modeled for individual mice using the Mixed Weibull Cumulative Distribution function. <i>b</i> _1 represents the median RER for the first mode, while <i>b</i> _2 represents the median RER for the second mode. Error bars indicate ± standard error of the mean. Groups not sharing the same letters within each parameter are significantly different in main effect for diet ( <i>p</i> <0.05). Statistically significant main effects for cycle (with vs. without AMG) and genotype (null vs. wild-type) were observed for the <i>b</i> _2 parameter ( <i>p</i> <0.05). AMG, amyloglucosidase. ....	223

Figure 5.16 Percent relative cumulative frequency (PRCF) curves for pooled RER data from all mice per diet (diet × mouse genotype × cycle). Split per diet: Conventional starch (A), 53% Resistant starch (B), 35% Resistant starch (C), 18% Resistant starch (D). ..... 224

Figure 5.17 Percent relative cumulative frequency (PRCF) curves for pooled RER data from all mice per diet (diet × mouse genotype × cycle). Split by genotype: null (A), wild-type (B). AMG, amyloglucosidase. .... 226

Figure 5.18 Percent relative cumulative frequency (PRCF) curves for pooled RER data from all mice per diet (diet × mouse genotype × cycle). Split by cycle: without AMG (A), with AMG (B). AMG, amyloglucosidase. .... 227

Figure 5.19 Median  $a$  values from the bimodal PRCF distributions of RER modeled for pooled data from all mice using the Mixed Weibull Cumulative Distribution function. Error bars indicate  $\pm$  standard error of the mean. Groups not sharing the same letters within each parameter are significantly different ( $p < 0.05$ ). AMG, amyloglucosidase. .... 228

## LIST OF ABBREVIATIONS

<b>AgRP</b>	Agouti-related peptide
<b>AMG</b>	Amyloglucosidase
<b>CART</b>	Cocaine-and amphetamine-regulated transcript
<b>CGM</b>	Continuous glucose monitor
<b>CPDR</b>	Cumulative percent dose <sup>13</sup> C recovery
<b>CRH</b>	Corticotropin-releasing hormone
<b>DASH</b>	Dietary Approaches to Stop Hypertension
<b>DNS</b>	Dinitrosalicylic acid
<b>DOB</b>	Delta over baseline
<b>DP</b>	Degree of polymerization
<b>DPP-4</b>	Dipeptidyl peptidase-4
<b>EE</b>	Energy expenditure
<b>GIP</b>	Glucose-dependent insulinotropic peptide
<b>GLP-1</b>	Glucagon-like peptide 1
<b>GLUT2</b>	Glucose transporter 2
<b>GSM</b>	Gastric Simulation Model
<b>HGS</b>	Human Gastric Simulator
<b>HPSEC</b>	High performance size-exclusion chromatography
<b>iAUC</b>	Incremental area under the curve
<b>MCH</b>	Melanin-concentrating hormone
<b>MGAM</b>	Human maltase glucoamylase
<b>Mgam</b>	Mouse maltase-glucoamylase
<b>NPY</b>	Neuropeptide Y
<b>PDR</b>	Percent dose <sup>13</sup> C recovery
<b>POMC</b>	Proopiomelanocortin
<b>PRCF</b>	Percent relative cumulative frequency
<b>PYY</b>	Peptide YY
<b>RDS</b>	Rapidly digestible starch

<b>RER</b>	Respiratory exchange ratio
<b>RQ</b>	Respiratory quotient
<b>RS</b>	Resistant starch
<b>RVA</b>	Rapid Visco Analyzer
<b>SD</b>	Standard deviation
<b>SDS</b>	Slowly digestible starch
<b>SEM</b>	Standard error of the mean
<b>SGLT1</b>	Sodium-glucose cotransporter 1
<b>Si</b>	Mouse sucrase isomaltase
<b>SI</b>	Human sucrase-isomaltase
<b>TIM</b>	Gastrointestinal digestion system
<b>TIMagc</b>	TIM system with an advanced gastric compartment
<b>VAS</b>	Visual analog scale
<b>V<sub>O2</sub></b>	Carbon dioxide production
<b>V<sub>CO2</sub></b>	Oxygen consumption

## ABSTRACT

Obesity and nutrition-related non-communicable diseases continue to be major challenges that are increasing in severity worldwide. Science-centered carbohydrate dietary strategies may be a viable approach to help address such challenges. Recent reports from our laboratory indicate that certain carbohydrates with slow digestion profiles have the ability to trigger the gut-brain axis and reduce food intake and to slow gastric emptying and potentially affect appetite. Slow carbohydrate digestion may have other impacts on energy metabolism that have not been explored. In the current investigations, we sought to better understand the delayed gastric emptying profile of pearl millet-based foods as well as to understand how altering carbohydrate digestion rate impacts substrate utilization for energy.

In the first study, the physical breakdown of pearl millet couscous particles in a simulated gastric environment (Human Gastric Simulator) was studied compared to wheat couscous matched in particle size, and select physicochemical properties of each type of couscous were characterized. Because we previously showed that pearl millet couscous had a marked delay in gastric emptying compared to white rice, boiled potatoes, and pasta in a human study in Mali, the objective of the first investigation was to test the hypothesis that pearl millet couscous was more resistant to breakdown in the stomach than wheat couscous and would take longer to empty. Our findings indicated that pearl millet couscous instead broke down into smaller, more numerous particles than wheat couscous. However, pearl millet had a slower starch hydrolysis property compared to wheat couscous per unit surface area. Pearl millet also had a smaller amylose chain length (839-963 DP) compared to wheat (1225-1563 DP), which may enable a denser packing of millet starch molecules that hinders hydrolysis. We also visually observed that the pearl millet particles formed a paste while breaking down that could reasonably generate viscosity in the stomach to potentially delay gastric emptying.

Based off the findings from simulated gastric digestion, we next conducted a human study ( $n=14$ ) in the U.S. to test the hypothesis that pearl millet-based foods (couscous – commercial and self-made, thick porridge) would reduce glycemic response, increase satiety, and delay gastric emptying compared to wheat couscous and white rice. We complemented this human study with additional *in vitro* work using an advanced gastrointestinal digestion system (TIMage) to determine if the viscosity of pearl millet couscous particles as they were breaking down in the

stomach was contributing to a decrease in gastric emptying. Our findings indicated that all the pearl millet-based foods and wheat couscous had lower overall glycemc response than white rice, but only the self-made millet couscous showed higher satiety through subjective appetitive response ratings. Surprisingly, there were no differences in gastric emptying among the foods. Additionally, the half-emptying times for these foods were all ~3 h, which is similar to the comparably low half-emptying times observed for white rice, boiled potatoes, and pasta in the previous Mali study. We now hypothesize that there may be diet-induced changes in gut-brain axis signaling when slowly digestible carbohydrates are consumed repeatedly over time, perhaps through modulating the number or sensitivity of small intestinal L-cells. We also found that millet couscous did not exhibit high viscosity in the TIMagc, suggesting that viscosity was not impacting its rate of gastric emptying. We conclude that at least some pearl millet-based foods possess a slow digestion property that may act to trigger the gut-brain axis or ileal brake to increase feelings of satiety or slow gastric emptying, but the discrepancy between U.S. and Malian populations requires further study.

In the final investigation, we examined how altering carbohydrate digestion affected partitioning of carbohydrate versus fat for oxidation as well as the efficiency of switching oxidation between these two substrates (termed “metabolic flexibility”) in mice. Metabolic flexibility has been associated with good health related to decreased adipose tissue in the body and improved insulin sensitivity and may have implications on weight management. Carbohydrate digestion was adjusted by: (1) testing mice that lacked a complete set of enzymes by knocking out maltase-glucoamylase (Mgam; null) for moderating starch digestion versus testing wild-type mice; (2) using diets in these two groups of mice to moderate starch digestion that had different levels of resistant starch (53%, 35%, and 18%), had only raw corn starch or sucrose, or were high in fat; and (3) providing a supplement of fungal amyloglucosidase (AMG) to the mice treatment groups to increase starch digestion. Respiratory exchange ratio (RER) was measured through indirect calorimetry and mathematical modeling was used to characterize the diurnal shifts in RER (sine equation) as well as carbohydrate versus fat oxidation and metabolic flexibility (percent relative cumulative frequency [PRCF] with Weibull and Mixed Weibull Cumulative Distribution functions). Our results suggest that null mice lacking Mgam had somewhat increased metabolic flexibility than wild-type mice despite exhibiting minimal to no effects on carbohydrate oxidation. Intriguingly, the raw corn starch diet increased fat oxidation and generally promoted metabolic

flexibility, although it did not increase carbohydrate oxidation relative to the other carbohydrate-predominant diets. Increasing carbohydrate digestion through AMG supplementation increased carbohydrate oxidation, and generally prompted earlier shifts to carbohydrate oxidation than without AMG supplementation. These findings provide a basis for better understanding the metabolic consequences of altering carbohydrate digestion and establish novel tools that can be utilized in future investigations. Overall, we propose that moderating carbohydrate digestion provides the ideal combination of balancing carbohydrate and fat oxidation while promoting metabolic flexibility.

In conclusion, a slow digestion property may enable some types of pearl millet to trigger the ileal brake and gut-brain axis feedback systems to decrease glycemic response and increase satiety. Moreover, consuming carbohydrates with slow digestion may optimize substrate utilization for energy by the body. In addition to triggering the ileal brake and gut-brain axis, modulating carbohydrate digestion to more effectively switch between carbohydrate and fat for oxidation may be beneficial for weight management and metabolic disease prevention.

# CHAPTER 1. INTRODUCTION

## 1.1 Introduction

Dietary carbohydrates constitute the main source of energy from the average human diet (Shan et al., 2019) and are broadly categorized as digestible (e.g. starch, sugar) and indigestible (e.g. fiber). The increasing prevalence of obesity worldwide indicates a widespread impairment in the regulation of food intake and energy balance (Abarca-Gómez et al., 2017; Hales et al., 2020). Strategies to prevent or help treat obesity and associated nutrition-related non-communicable diseases are becoming increasingly imperative.

Consumption of digestible carbohydrates is often viewed unfavorably due to purported negative effects of such carbohydrates on health (Kroemer et al., 2018). For example, epidemiological evidence from 18 countries across five continents indicated a high intake of carbohydrates (>70% of total daily energy) was associated with increased risk of total mortality (Dehghan et al., 2017), and diets with a high ratio of carbohydrate-to-cereal fiber and starch-to-cereal fiber were associated with increased risk for incident coronary heart disease in U.S. men and women (AlEissa et al., 2018). However, results from a different epidemiological study showed that moderate intake of carbohydrates (50-55% of total daily energy) was associated with decreased risk of mortality in U.S. men and women (Seidemann et al., 2018), indicating the importance of consuming an intermediate level of carbohydrates.

Although carbohydrates have been associated with negative health effects (AlEissa et al., 2018; Dehghan et al., 2017), certain types of carbohydrates can have beneficial impacts on health. Not all carbohydrates are the same, even within digestible carbohydrates. Classification systems, such as the glycemic index (Jenkins et al., 1981) and Englyst assay system (i.e. designations of rapidly digestible starch, slowly digestible starch, and resistant starch) (Englyst et al., 1992), have been developed to differentiate carbohydrates based on their digestibility. Carbohydrates that are more slowly digestible may have positive effects on the body (Zhang et al., 2015; Zhang & Hamaker, 2009). In fact, emerging evidence from our lab group has indicated that starch entrapped microspheres, a form of slowly digestible carbohydrate, trigger the gut-brain axis to decrease food intake (Hasek et al., 2018) and incrementally slow gastric emptying rate (Hasek et al., 2020) in

rats. These findings indicate use of certain slowly digestible carbohydrates may be a potential strategy to help address the pandemic proportions of obesity worldwide.

## 1.2 Specific objectives and research hypotheses

In order to make strides in determining how carbohydrates could potentially be used to help combat obesity, we first focused on studying the digestive properties of pearl millet, a purported slowly digestible carbohydrate, that relate to satiety and the control of food intake through *in vitro* experiments and an *in vivo* human study. We then explored the metabolic consequences of altering the digestibility of carbohydrates in mice and how they relate to metabolic flexibility, which is a marker of good health (Goodpaster & Sparks, 2017; Muoio, 2014).

Pearl millet (*Pennisetum glaucum*) is an ideal crop for regions such as the dry, semi-arid West African Sahel, because it is sturdy and drought-resistant (Chand et al., 2017; Lemgharbi et al., 2016; Yadav et al., 2016). However, pearl millet has benefits beyond efficient growth and production, for many consumers of pearl millet in this region anecdotally report that eating pearl millet makes them feel “full” for extended periods of time. These individuals prefer to consume pearl millet in order to go for long periods of time without feeling the need to eat. From an ingestive behavior standpoint, these anecdotal reports indicate that pearl millet foods promote satiety. Indeed, previous researchers have found that pearl millet has a nutritionally beneficial *in vitro* slow digestion property (Annor et al., 2015, 2017). However, the relationship between the anecdotal satiety property and apparent slow digestion property of pearl millet had not been explored until recently, when previous work from our group indicated that pearl millet foods in the form of couscous and thick porridge substantially delayed gastric emptying rate compared to white rice, boiled potatoes, and well-cooked pasta in a Malian population (Cisse et al., 2018). This study established a potential physiological basis for the satiety property of pearl millet, as slower gastric emptying is related to satiety (Halawi et al., 2017; Hellström & Näslund, 2001). Yet, the mechanism was unknown. Through a series of *in vitro* and *in vivo* experiments, we have explored potential mechanisms for the satiety property of pearl millet and provided further evidence for its slow digestion. We hypothesized that a slow carbohydrate digestion property of pearl millet (and not the food physical properties of particle breakdown or viscosity) was the basis of its slow gastric emptying and high satiety, as well as that we would observe consistent gastric emptying and satiety

responses in a U.S. population compared to the Malian population in the previous study (Cisse et al., 2018).

In our third experimental study for this thesis, we examined the partitioning between carbohydrate and fat as substrates for energy metabolism (i.e. oxidation) in response to different dietary conditions in mice that were lacking the maltase-glucoamylase (Mgam) enzyme and wild-type mice. This allowed us to gain insight into metabolic flexibility, or the efficiency of the body to freely switch between using carbohydrate and fat for energy (Muoio, 2014). Metabolic flexibility has generally been studied in relation to type 2 diabetes (Meex et al., 2010; van de Weijer et al., 2013), adipose tissue in the body (Sparks et al., 2009), exercise and insulin sensitivity (Malin et al., 2013), energy use governed by neurons in the brain (Bernier et al., 2020; Reichenbach et al., 2018), and even cancer (Kreuzaler et al., 2020; Woolbright et al., 2019). To our knowledge, it has not been well-studied related to different diets with the exception of two studies, which found that saturated fat-based diets reduced metabolic flexibility compared to polyunsaturated fat-based diets (Duivenvoorde et al., 2015), as well as that female mice (but not male) had improved metabolic flexibility for a resistant starch-based diet (i.e. high-amylose) fed for 3 weeks immediately after weaning compared to a rapidly digestible carbohydrate diet (i.e. 100% amylopectin) (Fernández-Calleja et al., 2018); however, for both of these studies metabolic flexibility was assessed for a challenge meal during fasting and re-feeding, while in our approach we fed mice *ad libitum*. In our study, we altered carbohydrate digestion by using mice that lacked the Mgam enzyme (vs. wild-type mice with a full set of enzymes), feeding diets with different carbohydrate digestibilities, and providing an amyloglucosidase supplement. Additionally, we devised and employed innovative mathematical modeling approaches to better assess metabolic flexibility from respiratory exchange ratio (RER) data. We hypothesized that the Mgam knockout (null) mice would have reduced RER and higher metabolic flexibility compared to wild-type mice, that reduced carbohydrate digestion would reduce RER and lead to greater metabolic flexibility, and that supplementation with AMG to increase carbohydrate digestion would result in higher RER and decreased metabolic flexibility.

### **1.3 Significance of work**

This research helps reveal steps toward a better understanding of how carbohydrates with different digestibilities may act to affect gastric emptying rate and satiety, which have implications

on the ileal brake and gut-brain axis signaling systems to influence food intake, as well as alter substrate oxidation for energy and metabolic flexibility. Specifically, understanding the underlying basis for the slow gastric emptying of pearl millet-based foods may lead to greater insight into their anecdotal satiety property. As pearl millet is an existing food, better knowledge of the reason(s) for its beneficial properties may help identify strategies that can be implemented to design new carbohydrate-based foods with similar benefits. Additionally, insights gained about substrate oxidation and metabolic flexibility will reveal ways in which carbohydrates affect metabolism that relate to energy expenditure, which is beneficial from a ‘whole body’ level of weight management. The findings from this work may also have implications on reducing the risk of developing or perhaps even helping treat obesity and type 2 diabetes.

#### **1.4 Thesis organization**

This thesis is organized into six chapters as follows:

Chapter 1 is an introduction of the project background, hypotheses, and significance.

Chapter 2 is a literature review of the structure and digestion of digestible (starch-based) carbohydrates; the post-ingestive processes in the body as they relate to such carbohydrates, including gastric emptying, the ileal brake, and gut-brain axis; key concepts of substrate oxidation and glycemic response in metabolism; and select approaches using *in vitro*, *in vivo*, and mathematical modeling for studying carbohydrates in these collective areas.

Chapter 3 is an experimental chapter exploring the breakdown profile of pearl millet couscous in a simulated gastric environment and its physicochemical properties compared to wheat couscous (matched in particle size). The goal of this chapter was to determine if either particle breakdown or a slow starch digestion property was contributing to the delayed gastric emptying rate observed for pearl millet couscous in humans in Mali in Cisse et al. (2018).

Chapter 4 is an experimental chapter investigating the subjective satiety, glycemic response, and gastric emptying for pearl millet in the forms of couscous and thick porridge compared to wheat couscous and white rice in a U.S. population as well as examining the viscosity of these foods in the stomach using an *in vitro* advanced gastrointestinal digestion system. The objective of this chapter was to determine how the pearl millet foods would perform relative to wheat couscous (matched in particle size to one type of the millet couscous), because this had not been

tested previously, as well as to reveal if viscosity or a slow carbohydrate digestion property were contributing to delayed gastric emptying.

Chapter 5 is a final experimental chapter focused on improving our understanding of how alterations in carbohydrate digestion affect utilization of carbohydrate for energy (i.e. substrate oxidation) as well as the body's ability to switch between using carbohydrate and fat for energy. This chapter involves new mathematical modeling tools to advance our understanding of metabolic flexibility, which has not been well-studied related to carbohydrate digestion.

Chapter 6 is an overall summary of the key findings from this thesis work as well as recommendations for future research.

Additionally, Appendix Chapter B describes an experimental investigation of how altering the structure of starch (i.e. fragmenting amylopectin chains through extrusion) impacts staling of breads and cakes, and is a published study that was conducted during this thesis period.

## 1.5 References

- Abarca-Gómez, L., Abdeen, Z. A., Hamid, Z. A., Abu-Rmeileh, N. M., Acosta-Cazares, B., Acuin, C., Adams, R. J., Aekplakorn, W., Afsana, K., Aguilar-Salinas, C. A., Agyemang, C., Ahmadvand, A., Ahrens, W., Ajlouni, K., Akhtaeva, N., Al-Hazzaa, H. M., Al-Othman, A. R., Al-Raddadi, R., Al Buhairan, F., ... Ezzati, M. (2017). Worldwide trends in body-mass index, underweight, overweight, and obesity from 1975 to 2016: a pooled analysis of 2416 population-based measurement studies in 128·9 million children, adolescents, and adults. *The Lancet*, *390*(10113), 2627–2642. [https://doi.org/10.1016/S0140-6736\(17\)32129-3](https://doi.org/10.1016/S0140-6736(17)32129-3)
- AlEsa, H. B., Cohen, R., Malik, V. S., Adebamowo, S. N., Rimm, E. B., Manson, J. A. E., Willett, W. C., & Hu, F. B. (2018). Carbohydrate quality and quantity and risk of coronary heart disease among US women and men. *American Journal of Clinical Nutrition*, *107*(2), 257–267. <https://doi.org/10.1093/ajcn/nqx060>
- Annor, G. A., Marcone, M., Corredig, M., Bertoft, E., & Seetharaman, K. (2015). Effects of the amount and type of fatty acids present in millets on their in vitro starch digestibility and expected glycemic index (eGI). *Journal of Cereal Science*, *64*, 76–81. <https://doi.org/10.1016/j.jcs.2015.05.004>
- Annor, G. A., Tyl, C., Marcone, M., Ragaee, S., & Marti, A. (2017). Why do millets have slower starch and protein digestibility than other cereals? *Trends in Food Science & Technology*, *66*, 73–83. <https://doi.org/10.1016/j.tifs.2017.05.012>
- Bernier, L. P., York, E. M., Kamyabi, A., Choi, H. B., Weiling, N. L., & MacVicar, B. A. (2020). Microglial metabolic flexibility supports immune surveillance of the brain parenchyma. *Nature Communications*, *11*(1). <https://doi.org/10.1038/s41467-020-15267-z>
- Chand, G., Morya, K., Mishra, H. S., Shakya, S., Bahadur, R., & Yadav, K. N. (2017). *Millets : The Indigenous Food Grains*. *6*(1), 447–452.

- Cisse, F., Erickson, D. P., Hayes, A. M. R., Opekun, A. R., Nichols, B. L., & Hamaker, B. R. (2018). Traditional Malian solid foods made from sorghum and millet have markedly slower gastric emptying than rice, potato, or pasta. *Nutrients*, *10*(2), 124. <https://doi.org/10.3390/nu10020124>
- Dehghan, M., Mente, A., Zhang, X., Swaminathan, S., Li, W., Mohan, V., Iqbal, R., Kumar, R., Wentzel-Viljoen, E., Rosengren, A., Amma, L. I., Avezum, A., Chifamba, J., Diaz, R., Khatib, R., Lear, S., Lopez-Jaramillo, P., Liu, X., Gupta, R., ... Mapanga, R. (2017). Associations of fats and carbohydrate intake with cardiovascular disease and mortality in 18 countries from five continents (PURE): a prospective cohort study. *The Lancet*, *390*(10107), 2050–2062. [https://doi.org/10.1016/S0140-6736\(17\)32252-3](https://doi.org/10.1016/S0140-6736(17)32252-3)
- Duivenvoorde, L. P. M., van Schothorst, E. M., Swarts, H. M., Kuda, O., Steenbergh, E., Termeulen, S., Kopecky, J., & Keijer, J. (2015). A Difference in Fatty Acid Composition of Isocaloric High-Fat Diets Alters Metabolic Flexibility in Male C57BL/6JOLA<sup>Hsd</sup> Mice. *PLOS ONE*, *10*(6), e0128515. <https://doi.org/10.1371/journal.pone.0128515>
- Englyst, H. N., Kingman, S. M., & Cummings, J. H. (1992). Classification and measurement of nutritionally important starch fractions. *European Journal of Clinical Nutrition*, *46 Suppl 2*, S33-50. <http://www.ncbi.nlm.nih.gov/pubmed/1330528>
- Fernández-Calleja, J., Bouwman, L., Swarts, H., Oosting, A., Keijer, J., & van Schothorst, E. (2018). Direct and Long-Term Metabolic Consequences of Lowly vs. Highly-Digestible Starch in the Early Post-Weaning Diet of Mice. *Nutrients*, *10*(11), 1788. <https://doi.org/10.3390/nu10111788>
- Goodpaster, B. H., & Sparks, L. M. (2017). Metabolic Flexibility in Health and Disease. *Cell Metabolism*, *25*(5), 1027–1036. <https://doi.org/10.1016/j.cmet.2017.04.015>
- Halawi, H., Camilleri, M., Acosta, A., Vazquez-Roque, M., Oduyebo, I., Burton, D., Busciglio, I., & Zinsmeister, A. R. (2017). Relationship of gastric emptying or accommodation with satiation, satiety, and postprandial symptoms in health. *American Journal of Gastrointestinal and Liver Physiology*, *313*, G442–G447. <https://doi.org/10.1152/ajpgi.00190.2017>
- Hales, C. M., Carroll, M. D., Fryar, C. D., & Ogden, C. L. (2020). Prevalence of obesity and severe obesity among adults: United States, 2017-2018. *NCHS Data Brief*, *360*, 1–7. <https://www.cdc.gov/nchs/products/index.htm>
- Hasek, L. Y., Phillips, R. J., Hayes, A. M. R., Kinzig, K., Zhang, G., Powley, T. L., & Hamaker, B. R. (2020). Carbohydrates designed with different digestion rates modulate gastric emptying response in rats. *International Journal of Food Sciences and Nutrition*. <https://doi.org/10.1080/09637486.2020.1738355>
- Hasek, L. Y., Phillips, R. J., Zhang, G., Kinzig, K. P., Kim, C. Y., Powley, T. L., & Hamaker, B. R. (2018). Dietary slowly digestible starch triggers the gut-brain axis in obese rats with accompanied reduced food intake. *Molecular Nutrition & Food Research*, *62*(5), 1700117. <https://doi.org/10.1002/mnfr.201700117>
- Hellström, P. M., & Näslund, E. (2001). Interactions between gastric emptying and satiety, with special reference to glucagon-like peptide-1. *Physiology & Behavior*, *74*(4–5), 735–741.
- Jenkins, D. J., Wolever, T. M., Taylor, R. H., Barker, H., Fielden, H., Baldwin, J. M., Bowling, A. C., Newman, H. C., Jenkins, A. L., & Goff, D. V. (1981). Glycemic index of foods: a physiological basis for carbohydrate exchange. *The American Journal of Clinical Nutrition*, *34*(3), 362–366. <https://doi.org/10.1093/ajcn/34.3.362>

- Kreuzaler, P., Panina, Y., Segal, J., & Yuneva, M. (2020). Adapt and conquer: Metabolic flexibility in cancer growth, invasion and evasion. *Molecular Metabolism*, *33*, 83–101. <https://doi.org/10.1016/j.molmet.2019.08.021>
- Kroemer, G., López-Otín, C., Madeo, F., & de Cabo, R. (2018). Carbotoxicity—Noxious Effects of Carbohydrates. *Cell*, *175*(3), 605–614. <https://doi.org/10.1016/j.cell.2018.07.044>
- Lemgharbi, M., Belhadi, B., Souilah, R., Terbag, L., Djabali, D., & Nadjemi, B. (2016). Biodiversity of Pearl Millet [*Pennisetum glaucum*] in Southern Algeria (Hoggar Region). *American Journal of Plant Sciences*, *07*(12), 1673–1684. <https://doi.org/10.4236/ajps.2016.712158>
- Malin, S. K., Haus, J. M., Solomon, T. P. J., Blaszcak, A., Kashyap, S. R., & Kirwan, J. P. (2013). Insulin sensitivity and metabolic flexibility following exercise training among different obese insulin-resistant phenotypes. *American Journal of Physiology-Endocrinology and Metabolism*, *305*(10), E1292–E1298. <https://doi.org/10.1152/ajpendo.00441.2013>
- Meex, R. C. R., Schrauwen-Hinderling, V. B., Moonen-Kornips, E., Schaart, G., Mensink, M., Phielix, E., van de Weijer, T., Sels, J.-P., Schrauwen, P., & Hesselink, M. K. C. (2010). Restoration of Muscle Mitochondrial Function and Metabolic Flexibility in Type 2 Diabetes by Exercise Training Is Paralleled by Increased Myocellular Fat Storage and Improved Insulin Sensitivity. *Diabetes*, *59*(3), 572–579. <https://doi.org/10.2337/db09-1322>
- Muoio, D. M. (2014). Metabolic inflexibility: When mitochondrial indecision leads to metabolic gridlock. *Cell*, *159*(6), 1253–1262. <https://doi.org/10.1016/j.cell.2014.11.034>
- Reichenbach, A., Stark, R., Mequinion, M., Denis, R. R. G., Goularte, J. F., Clarke, R. E., Lockie, S. H., Lemus, M. B., Kowalski, G. M., Bruce, C. R., Huang, C., Schittenhelm, R. B., Mynatt, R. L., Oldfield, B. J., Watt, M. J., Luquet, S., & Andrews, Z. B. (2018). AgRP Neurons Require Carnitine Acetyltransferase to Regulate Metabolic Flexibility and Peripheral Nutrient Partitioning. *Cell Reports*, *22*(7), 1745–1759. <https://doi.org/10.1016/j.celrep.2018.01.067>
- Seidemann, S. B., Claggett, B., Cheng, S., Henglin, M., Shah, A., Steffen, L. M., Folsom, A. R., Rimm, E. B., Willett, W. C., & Solomon, S. D. (2018). Dietary carbohydrate intake and mortality: a prospective cohort study and meta-analysis. *The Lancet Public Health*, *3*(9), e419–e428. [https://doi.org/10.1016/S2468-2667\(18\)30135-X](https://doi.org/10.1016/S2468-2667(18)30135-X)
- Shan, Z., Rehm, C. D., Rogers, G., Ruan, M., Wang, D. D., Hu, F. B., Mozaffarian, D., Zhang, F., & Bhupathiraju, S. N. (2019). Trends in Dietary Carbohydrate, Protein, and Fat Intake and Diet Quality Among US Adults, 1999–2016. *JAMA*, *322*(12), 1178. <https://doi.org/10.1001/jama.2019.13771>
- Sparks, L. M., Ukropcova, B., Smith, J., Pasarica, M., Hymel, D., Xie, H., Bray, G. A., Miles, J. M., & Smith, S. R. (2009). Relation of adipose tissue to metabolic flexibility. *Diabetes Research and Clinical Practice*, *83*(1), 32–43. <https://doi.org/10.1016/j.diabres.2008.09.052>
- van de Weijer, T., Sparks, L. M., Phielix, E., Meex, R. C., van Herpen, N. A., Hesselink, M. K. C., Schrauwen, P., & Schrauwen-Hinderling, V. B. (2013). Relationships between Mitochondrial Function and Metabolic Flexibility in Type 2 Diabetes Mellitus. *PLoS ONE*, *8*(2), e51648. <https://doi.org/10.1371/journal.pone.0051648>
- Woolbright, B. L., Rajendran, G., Harris, R. A., & Taylor, J. A. (2019). Metabolic Flexibility in Cancer: Targeting the Pyruvate Dehydrogenase Kinase:Pyruvate Dehydrogenase Axis. *Molecular Cancer Therapeutics*, *18*(10), 1673–1681. <https://doi.org/10.1158/1535-7163.MCT-19-0079>

- Yadav, H. P., Gupta, S. K., Rajpurohit, B. S., & Pareek, N. (2016). Pearl Millet. In M. Singh & S. Kumar (Eds.), *Broadening the Genetic Base of Grain Cereals* (pp. 205–224). Springer India. [https://doi.org/10.1007/978-81-322-3613-9\\_8](https://doi.org/10.1007/978-81-322-3613-9_8)
- Zhang, G., & Hamaker, B. R. (2009). Slowly Digestible Starch: Concept, Mechanism, and Proposed Extended Glycemic Index. *Critical Reviews in Food Science and Nutrition*, 49(10), 852–867. <https://doi.org/10.1080/10408390903372466>
- Zhang, G., Hasek, L. Y., Lee, B.-H., & Hamaker, B. R. (2015). Gut feedback mechanisms and food intake: a physiological approach to slow carbohydrate bioavailability. *Food Funct.*, 6(4), 1072–1089. <https://doi.org/10.1039/C4FO00803K>

## CHAPTER 2. LITERATURE REVIEW

### 2.1 Abstract

The rising prevalence of obesity and nutrition-related non-communicable diseases worldwide is indicative of a widespread disruption in the balance of food intake and body weight, which broadly involves energy consumed and expended. As starch-based carbohydrates are the primary source of energy for most diets, they are uniquely positioned to serve as a strategy to help address or prevent such rising levels of overweight and obesity and disease. The purpose of this review is to provide a general context for improving understanding of starch-based carbohydrates and their roles in health. This will be achieved by examining: (1) the structure and digestion of starch-based carbohydrates; (2) the post-ingestive processes in the body as they relate to starch-based carbohydrates; (3) key aspects of carbohydrate oxidation and glycemic response in metabolism; and (4) select *in vitro*, *in vivo*, and mathematical modeling approaches for studying carbohydrates related to these areas. Although carbohydrates are often associated only with glycemic response, they may influence physiological and neurobiological responses with impacts on health outcomes related to food intake and body weight.

### 2.2 Introduction

Carbohydrates are the primary source of energy for an average human diet (Shan et al., 2019). Carbohydrates provide an estimated 4 kcal per gram, and a key energy-delivering component of diets is starch. Before starch can be used for energy, it must be digested into glucose and absorbed. Subsequent blood glucose levels are generally highly regulated to maintain glucose homeostasis. Among the general public, starch-based carbohydrates are often negatively perceived because of their potential, with over-consumption, to promote weight gain and type 2 diabetes (Kroemer et al., 2018). These are generally fast digesting carbohydrates that lead to high glycemic response. Less widely recognized among the general population, is the fact that there are starches that have the capability to slow down or evade the body's digestion and absorption processes. Recent research indicates that certain starch-based carbohydrates with a slow digestion property can elicit specific beneficial physiological and neurobiological responses (Cisse et al., 2017, 2018; Hasek et al., 2018, 2020; Komuro et al., 2019; E.-S. Lee et al., 2018; Martinussen et al., 2019).

This includes the potential to control of food intake (Hasek et al., 2018; E.-S. Lee et al., 2018). Thus, carbohydrates with a slow digestion property may help address or even prevent one of the pandemics afflicting the world: obesity. Obesity is associated with a host of nutrition-related non-communicable diseases, such as metabolic disease, type 2 diabetes, hypertension, coronary artery disease, and stroke (Kopelman, 2007). Our ultimate research goals are to better understand (1) how dietary carbohydrates affect physiological systems related to the gut-brain axis and ileal brake, and (2) how carbohydrates can be designed or utilized to prevent or help reduce the damaging effects of obesity and related non-communicable diseases. This review examines the structure and digestion of starch-based carbohydrates; their post-ingestive processes in the body; key aspects of carbohydrate oxidation and glycemic response in metabolism; and select *in vitro*, *in vivo*, and mathematical modeling approaches for studying carbohydrates related to these areas. Together, these subjects establish a framework for enhancing the understanding of starch-based carbohydrates and their implications on health.

### **2.3 Carbohydrate structure and digestion**

Structurally, starches are units of glucose bonded covalently by either  $\alpha$ -1,4 or  $\alpha$ -1,6 glycosidic linkages to form polymers. The  $\alpha$ -1,4 linkages form linear chains that constitute the long chain lengths of the smaller amylose and shorter chain lengths of very large amylopectin, and the  $\alpha$ -1,6 form branch points that are few in amylose and frequent in amylopectin. The patterns of these two types of linkages in a starch molecule give rise to fine structural features that can have important impacts on the functionality and digestibility of starch (Benmoussa et al., 2007; Bertoft et al., 2016; Matalanis et al., 2009; Roman et al., 2020; Vamadevan & Bertoft, 2015; Zhang et al., 2008). Notably, amylopectin with a much lower or higher amount of the short-chain fraction to long-chain fraction weight ratio ( $<13$  DP or  $\geq 17$  DP) contributes to a greater proportion of starch with a slow digestion property (Zhang et al., 2008). Starch that is physically entrapped (Venkatachalam et al., 2009) or has a propensity to form intermolecular associations after gelatinization (Martinez et al., 2018) are other key characteristics leading to slowly digestible starch. A thorough discussion of all the structural features and specific physicochemical properties contributing to different starch functionalities and digestion profiles are beyond the scope of this review, but they are important to recognize. Additionally, it is central to understand the processes

occurring in the body once foods are consumed in order to discern how some starches are more slowly digested than others.

Before being used for energy by the body, starch must undergo digestion to glucose (glucogenesis) and absorption in the small intestine. The  $\alpha$ -linked glucose units comprising starch differentiate digestible starch from  $\beta$ -linked indigestible fiber because the starch digesting enzymes in the body can act on  $\alpha$ -linkages but not  $\beta$ -linkages (BeMiller, 2007; B.-H. Lee et al., 2013). However, some types of starch are resistant to digestion by passing through the upper gastrointestinal tract and traveling into the large intestine to be fermented by certain gut bacteria. Additionally, some starches are more susceptible to rapid enzymatic digestion, while others are more slowly digested. Rapidly digestible starches result in large fluctuations in glycemic response within the body concurrent with substantial demands on insulin function, which can be detrimental to health, while slowly digestible starches result in a slow and prolonged release of glucose, which is thought to be better for health by moderating glycemic and insulin responses, among other factors (Miao et al., 2015; Zhang & Hamaker, 2009).

To account for these different impacts on glycemic response, the glycemic index was proposed as a means to classify carbohydrate-containing foods according to their effects on postprandial glycemia (Jenkins et al., 1981). The glycemic index is defined as the incremental area under the blood glucose curve during the first 2-hours after consumption of a standard amount of carbohydrate from a test food compared to either white bread or glucose (Jenkins et al., 1981; Ludwig, 2002). Another widely recognized classification is that of glycemic load, which is the weighted average glycemic index of a specific food multiplied by its percentage of dietary energy consumed as carbohydrate (Ludwig, 2002); that is, glycemic load integrates glycemic response and the amount of carbohydrate consumed.

Although these forms of classification have been widely adopted, they are limited in their ability to describe starches with different digestion profiles, and they do not account for differences in starch properties and preparation (e.g. structure; botanical sources; particle size; matrix effects; retrogradation, or the reassociation of amylose and amylopectin helices after gelatinization [heating in excess water]; food form). There are conflicting reports in the literature regarding whether consumption of low glycemic carbohydrate foods improves biomarkers for glucose homeostasis. Several studies in humans have found that consumption of slowly digestible carbohydrates (e.g. “biscuits” produced using a rotary-molding technology) had favorable impacts

on glycemic response compared to rapidly digestible carbohydrates (e.g. extruded flakes), such as reduced postprandial glycemia, decreased plasma exogenous glucose appearance, and improved glycemic control at a subsequent meal (Nazare et al., 2010; Péronnet et al., 2015; Vinoy et al., 2013). Alternatively, results from a 5-week randomized crossover-controlled feeding trial published in 2014 showed that low glycemic index diets did not improve insulin sensitivity, lipid levels, or systolic blood pressure compared to high glycemic index diets (Sacks et al., 2014); however, the diets used in this trial were based on the dietary approaches to stop hypertension (DASH) diet and not an average U.S. diet. Another crossover study found that slowly and rapidly digestible starch-based foods had similar glycemic responses (Eelderink et al., 2012), but their results also indicated the slowly digestible starch-based foods had slower intestinal glucose uptake concomitant with lower postprandial insulin and glucose-dependent insulinotropic polypeptide (GIP) levels than the rapidly digestible starch-based foods. Therefore, the lack of difference in glycemic responses was attributed to a slower glucose clearance rate for the slowly digestible starch-based foods than the rapidly digestible versions. The authors of this study concluded that the glycemic index may not adequately identify starch-based foods with slow digestion properties (Eelderink et al., 2012).

To identify and characterize starches or starch fractions according to their digestion rate using an *in vitro* approach, Englyst et al. (1992) developed a classification system based on an assay involving the *in vitro* hydrolysis of starch using the enzymes pancreatin and amyloglucosidase. Rapidly digestible starch (RDS) is hydrolyzed to glucose within 20 min, slowly digestible starch (SDS) is hydrolyzed to glucose from 20-120 min, and resistant starch (RS) is the starch remaining unhydrolyzed after 120 min. The Englyst assay has been studied extensively and validated with *in vivo* glycemic response (H. N. Englyst et al., 1992; K. N. Englyst et al., 1999, 2003, 2018), and it is now widely adopted by food researchers as a means to characterize nutritionally relevant starch fractions. Starch ingredients usually contain all three of these classes (RDS, SDS, RS) which cannot be easily isolated from one another because this classification system is based on a time-dependent experimental outcome, not a distinct chemical or structural feature (Zhang & Hamaker, 2009). The Englyst assay involves the use of a fungal amyloglucosidase, which differs in its enzymatic property related to  $\alpha$ -linkage hydrolysis compared to the mammalian  $\alpha$ -glucosidases (B.-H. Lee et al., 2016; Lin et al., 2016; Shin et al., 2019). These limitations speak to the need for better approaches to examine and classify starches

according to their digestibility, and some promising advancements in this area have been recently described (Martinez, 2021). Altogether, emphasis should be placed on understanding the limitations and constraints of a particular method or approach instead of forgoing its use. For the purpose of this review, we will use the term slowly digestible carbohydrate to refer to carbohydrates with a slow digestion property as a differentiation from the SDS classification term.

In order to better understand the limitations of existing approaches in classifying and characterizing starch-based carbohydrates according to their digestibility, we must take a deeper look at the process of digestion itself within the body. Starch digestion begins in the mouth by the action of salivary  $\alpha$ -amylase and continues in the small intestine by the action of pancreatic  $\alpha$ -amylase and the small intestinal  $\alpha$ -glucosidases. Both salivary and pancreatic  $\alpha$ -amylases act on internal linear segments of  $\alpha$ -1,4 linked glucose units and are thus termed endoglycosidases (Fujii & Kawamura, 1985; Robyt & French, 1967). Products of the action of these enzymes are maltose, maltotriose, maltotetraose, and the branched  $\alpha$ -limit dextrins (mostly in the oligosaccharide size range). Importantly, little free glucose is generated and therefore additional enzymatic digestion by the  $\alpha$ -glucosidases is required. The two small intestinal  $\alpha$ -glucosidases, sucrase isomaltase (SI) and maltase glucoamylase (MGAM), both have N-terminal and C-terminal domains (Dahlqvist & Telenius, 1969; Nichols et al., 2003; Sauer et al., 2000; Sim et al., 2008). SI is only expressed in the intestine, while MGAM is also expressed in other tissues such as the kidney, bone marrow, spleen, and stomach (Fagerberg et al., 2014). Both enzymes are anchored to the luminal surface of small intestinal enterocytes and are found concentrated in lipid rafts, with the N-terminal subunits located near the membrane and the C-terminal subunits as the second enzymes extending into the intestinal lumen (Figure 1) (Dahlqvist & Telenius, 1969; Sim et al., 2008). The body has a coordinated, complex response to digest starch, such that the activities of the  $\alpha$ -glucosidases are amplified by the products of  $\alpha$ -amylase digestion (Chegeni et al., 2018; Sim et al., 2008). Intriguingly, in the human infant,  $\alpha$ -amylase secretion is developmentally delayed until weaning (McClellan & Weaver, 1993), but the mucosal  $\alpha$ -glucosidases are present in their mature form at birth (Auricchio et al., 1965). The four maltase activities of the  $\alpha$ -glucosidases (2 maltase activities from SI and 2 maltase activities from MGAM) have been well-studied *in vitro* and independently characterized (Dahlqvist & Telenius, 1969; Frandsen et al., 2002; Frandsen & Svensson, 1998; Nichols et al., 2003; Stoffer et al., 1993). All have the ability to hydrolyze maltose and maltosides from the non-reducing end as  $\alpha$ -exoglucosidases, yet each domain has unique substrate

specificities. Specifically, the N-terminal of the SI, isomaltase, has a strong affinity for  $\alpha$ -1,6 linkages, which comprise the branched structure of amylopectin, and the C-terminal of SI, sucrase, has a strong affinity for  $\alpha$ -1,2 linkages, as can be found in sucrose (non-starch carbohydrate). As for MGAM, its N-terminal has hydrolytic activity for  $\alpha$ -1,4 linkages in short glucose oligomer chains and also is most adept at hydrolyzing  $\alpha$ -1,2 and  $\alpha$ -1,3 linkages (B.-H. Lee et al., 2016), while its C-terminal has a strong affinity for all  $\alpha$ -1,4 linkages in glucose oligomers and longer linear  $\alpha$ -glucans including intact starch polymers (hence its name “glucoamylase”). The catalytic sites of each of these maltase enzymes have been characterized by crystallography to confirm their congruency with the substrate specificities (Dahlqvist, 1962; Dahlqvist & Borgstrom, 1961; Dahlqvist & Telenius, 1969; Frandsen et al., 2002).

Results from *in vitro* experimentation have informed the hypothesized concept that the four specific mucosal maltase activities complement each other and interact with the activity of secreted  $\alpha$ -amylase. For one, activity of secreted  $\alpha$ -amylase has been found to amplify the activity of MGAM 2-fold and SI 10-fold, and, in return, increased concentrations of maltase can suppress  $\alpha$ -amylase activity (Quezada-Calvillo, Robayo-Torres, Opekun, et al., 2007). Suppression of MGAM glucoamylase activity occurs with increased concentrations of maltotriose, maltotetraose, and maltosides; however, there is no evidence to support that SI activities are regulated by substrate availability (Quezada-Calvillo, Robayo-Torres, Ao, et al., 2007). Therefore, it appears that MGAM is sensitive to substrate availability, while SI is not. It is also notable that the activities of all the  $\alpha$ -glucosidases vary according circadian rhythms (e.g. increase in mice during their nocturnal feeding cycle) (Saito, 1972; Santos et al., 1992; Stevenson et al., 1975). Although these advancements from *in vitro* experiments have improved our understanding of the enzymatic system of starch  $\alpha$ -glucogenesis, more work *in vivo* is needed. Notably, as mentioned above, recent findings indicate differences in enzymatic properties of enzymes from fungal and mammalian sources (B.-H. Lee et al., 2016; Shin et al., 2019).

Following digestion of starch through the coordinated action of  $\alpha$ -amylase and  $\alpha$ -glucosidases, the final digestion product of glucose is finally ready to be absorbed through enterocytes lining the small intestine. Such absorption involves the action of the sodium-glucose cotransporter 1 (Na<sup>+</sup>-D-glucose cotransporter 1; SGLT1) and glucose transporter 2 (GLUT2) (Uldry & Thorens, 2004; Wright et al., 2011). SGLT1 actively transports the uptake of low concentrations of glucose across the brush-border membrane, whereas GLUT2 typically mediates

facilitated glucose transport across the basolateral membrane. (Note that there are other types of glucose transporters located in various areas of the body (Uldry & Thorens, 2004), but a discussion of them is beyond the scope of this review.) Following high loads of glucose (e.g. a meal high in starch), some GLUT2 migrates to the brush-border membrane, but this was found to have only a minor impact on glucose absorption in the small intestine in a mouse study (Gorboulev et al., 2012). However, in the same mouse study, some evidence suggested that, in the contexts of continuous feeding of sugar-rich diets or having diabetes, the influence of GLUT2 in glucose absorption may become substantial (Gorboulev et al., 2012). Regardless, following transport across the brush-border and basolateral membranes, glucose passes into the bloodstream to affect blood glucose levels (glycemia) and be taken up into the liver and muscle tissues to be used for energy or stored.

#### **2.4 Gastric emptying, the ileal brake, and the gut-brain axis**

In addition to the chemical breakdown of starch through starch-digesting enzymes and absorption of glucose through the brush-border and basolateral membranes of the small intestine, glucose and other starch digestion products are sensed by enteroendocrine cells to affect various processes in the body, including processes that are physiological, hormonal, or neurological in nature. The key aspects of focus are largely related to gastric emptying, the ileal brake, and the gut-brain axis.

Gastric emptying describes how quickly or slowly stomach contents pass into the small intestine. Numerous methods exist for measuring gastric emptying *in vivo*, including scintigraphy (the gold standard method) (Ma et al., 2015; Spiegel et al., 1994), <sup>13</sup>C breath tests (Ghoos et al., 1993; Sanaka & Nakada, 2010), magnetic resonance imaging (Marciani, 2011), and the paracetamol absorption test (Medhus et al., 2001; Willems et al., 2001). Before reaching the stomach, mastication and saliva in the mouth facilitate initial physical and chemical breakdown of food. Upon being swallowed and traveling through the esophagus to the stomach, a bolus of food then undergoes continued physical breakdown through the action of the stomach. The acidic environment coupled with active pepsin and lipase secreted from the lining of the stomach facilitate protein hydrolysis and softening of food texture. From an engineering perspective, the stomach has been described as a tank, mixer, grinder, and sieve (Bornhorst & Paul Singh, 2014; Meyer, 1980). Essentially, the stomach prepares food for later digestion in the rest of the gastrointestinal tract. The physical properties of foods can affect how much “processing” they need

to undergo in the stomach as well as at what rate they are emptied into the small intestine. More specifically, factors such as food physical form (Collins et al., 1996; Hellmig et al., 2006; Santangelo et al., 1998), composition (Giezenaar, Lange, et al., 2018; Moore et al., 1981), viscosity (Marciani et al., 2001; Sirois et al., 1990; Zhu et al., 2013), particle size (Meyer, 1980; Sirois et al., 1990), and caloric content (Calbet & MacLean, 1997; Camps et al., 2016; McHugh & Moran, 1979; Moore et al., 1981) affect gastric emptying rate. On the macronutrient level, the ileal brake system has long been known to slow or brake gastric emptying rate (Spiller et al., 1984). Protein and fat have been most studied to delay gastric emptying, though a number of studies also show that carbohydrate also triggers the ileal brake (Burn-Murdoch et al., 1978; Giezenaar et al., 2017; Giezenaar, Lange, et al., 2018; Giezenaar, Van Der Burgh, et al., 2018). In the majority of these studies, glucose was used as the carbohydrate, indicating that no digestion was required for the carbohydrate component being examined. Yet, in a different trial that did compare glucose to protein (gelatin) in beverages, glucose tended to delay gastric half-emptying to a greater extent than protein ( $P = 0.06$ ) (Karamanlis et al., 2007). Furthermore, previous research from our group has shown that starch-based carbohydrates with decreasing digestibilities, that locationally digested starch into the ileum, incrementally decreased gastric emptying rate according to the level of slowly digestible carbohydrate (Hasek et al., 2020). The mechanism behind this delayed gastric emptying is hypothesized to be related to post-ingestive feedback signals from digestion and absorption – specifically the ileal brake and perhaps the gut-brain axis.

As nutrients pass from the stomach and into the small intestine for digestion and absorption, they are sensed by specialized enterocytes lining the intestinal epithelium called enteroendocrine cells. Although these cells constitute only 1% of the cell population in the intestinal epithelium, they secrete a variety of hormones and neurotransmitters that regulate glucose homeostasis, gut motility, epithelial proliferation, and appetite (Reimann et al., 2012; Spreckley, 2015). There are at least 11 different types of enteroendocrine cells, each found in different abundances within the gastrointestinal tract and proposed to secrete specific peptide hormones (Figure 2) (Engelstoft et al., 2013; Rindi et al., 2004). Although the distinctions among enteroendocrine cells is blurred by evidence suggesting co-expression of hormones beyond those originally proposed for one type of cell (Grigoryan et al., 2012), in general, L-cells found in the small intestine secrete the peptide hormone glucagon-like peptide-1 (GLP-1), and L-cells in the distal small intestine and large intestine secrete a combination of GLP-1 and peptide YY (PYY) (Engelstoft et al., 2013; Habib et

al., 2012). Both of these hormones are implicated in the control of food intake. Among other outcomes, GLP-1 stimulates insulin secretion, inhibits glucagon secretion, slows gastric emptying, and reduces hepatic glucose metabolism (Diakogiannaki et al., 2012; Holst, 2007; Sandoval & D'Alessio, 2015). GLP-1 is secreted in a locational gradient, and it is thought that defects in GLP-1 secretion and/or signaling may contribute to overeating in obesity (Robert E. Steinert et al., 2017). GLP-1 has been targeted for numerous pharmaceutical applications largely due to its incretin effect and connection to type 2 diabetes (Daoudi et al., 2011; Yu et al., 2010). Meanwhile, studies have shown that PYY may aid in glycemic control by: 1) improving insulin sensitivity, at least under some conditions (Van Den Hoek et al., 2004), 2) tonically stimulating islet-cell proliferation and inhibiting  $\beta$ -cell apoptosis in mice (Persaud & Bewick, 2014; Sam et al., 2012), or 3) decreasing gastric emptying via the ileal brake mechanism and thus reducing glycemia. Considering these positive health effects, modulated rise in L-cell number and distribution could result in increased release of GLP-1 and PYY, along with improved glucose tolerance and control of food intake. In accordance with this concept, some researchers have hypothesized that endogenous GLP-1 production can be increased or controlled through adaptation of L-cells or their gene transcription (Daoudi et al., 2011). However, little is known about the mechanism controlling L-cell number and distribution. A compelling hypothesis holds that dietary exposure can impact not only L-cells, but also other enteroendocrine cells.

The interest in L-cells is closely tied to their ability to secrete GLP-1 and a cascade of events in the body that have potential implications on food intake, namely two phenomena known as the ileal brake and gut-brain axis. The ileal brake has been described as a “nutrient-triggered, neurohormonally-mediated, primary inhibitory feedback mechanism” (Barreto et al., 2017) that occurs due to the presence of nutrients in the distal small intestine (the ileum). It results in inhibition of upper gastrointestinal tract motility (i.e. delayed gastric emptying rate) and is implicated in satiation (i.e. short-term signals and processes that lead to cessation of food intake within a meal) and satiety (i.e. longer-term signals and processes occurring between meals that prevent the initiation of eating). The main mechanism underlying this braking effect is thought to be GLP-1, as it acts locally as well as on the vagus nerve to transmit signals to the brain to slow gastric emptying (Abbott et al., 2005; Hayes et al., 2011; Kanoski et al., 2011; Labouesse et al., 2012) and can travel through the blood to cross the blood-brain barrier and directly act on the brain (Kanoski et al., 2011; Labouesse et al., 2012) (however, this latter part may occur to a lesser extent

because GLP-1 is quickly cleaved by dipeptidyl peptidase-4 [DPP-4] and converted into an inactive form). These actions either directly or indirectly act on the stomach to delay gastric emptying in a dose-dependent manner (Nauck et al., 1997; Schirra et al., 1996; Schirra & Göke, 2005). The potential of GLP-1 to help treat obesity and control food intake has been recently reviewed (Grill, 2020; Krieger, 2020; R. E. Steinert et al., 2016), and its relationship to the ileal brake has also been described (Barreto et al., 2017; Schirra & Göke, 2005). Recent findings show that slowly digestible carbohydrates (i.e. isomaltodextrin, isomaltulose) selectively increased GLP-1 secretion in both rats (Komuro et al., 2019) and humans (Martinussen et al., 2019), suggesting that carbohydrates with a slow digestion property offer potential to trigger the ileal brake and associated beneficial effects on food intake.

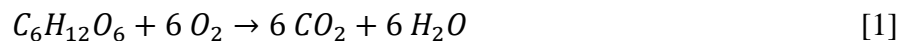
Likely even more influential than the ileal brake, the gut-brain axis is another mechanism by which slowly digestible carbohydrates are proposed to affect appetite, food intake, and body weight. The gut-brain axis is the bidirectional communication between the gastrointestinal tract and the brain through neurological, metabolic, and humoral signals (Hussain & Bloom, 2013; Soty et al., 2017; Weltens et al., 2018). Although it is often associated with the microbiome, by which it is purported to have an additional role in mental health and mental disorders (de Vadder & Mithieux, 2018; Mason, 2017; Treisman, 2017), it also encompasses nutrient sensing in the upper gastrointestinal tract (Beutler et al., 2017; Soty et al., 2017). Despite advancements made in recent years, the exact mechanism(s) and associated pathways composing this bidirectional communication system are incompletely understood. The vagus nerve and enteroendocrine cells, such as L-cells, are important in this system, yet evidence for changes in vagal afferent signaling (Al Helaili et al., 2020; de Lartigue & Xu, 2018) or L-cell population (Cani et al., 2007; Kaji et al., 2011; Richards et al., 2016) due to dietary exposure blur the lines of exactly how gut-brain dynamics ultimately affect the control of food intake and body weight. This is further obscured by the numerous other factors that can affect food intake, such as social norms related to eating and food reward (at least in humans). However, some of these factors can at least be partially distinguished by studying the brain, as different regions of the brain have been identified to play roles in specific functions in the body or in behavioral actions. Namely, the hypothalamus has long been known as the “feeding center” of the brain (Anand & Brobeck, 1951), and the area postrema and nucleus of the solitary tract have for many years been recognized for their roles in receiving and transmitting food intake-related signals (Hyde & Miselis, 1983). Within the hypothalamus,

agouti-related peptide (AgRP), neuropeptide Y (NPY), and melanin-concentrating hormone (MCH) have been identified as orexigenic (appetite-stimulating) neuropeptides; and proopiomelanocortin (POMC), cocaine-and amphetamine-regulated transcript (CART), and corticotropin-releasing hormone (CRH) have been identified as anorexigenic (appetite-reducing) neuropeptides (Hussain & Bloom, 2013). Alterations in expression of these neuropeptides are thought to serve as an indication of gut-brain axis signaling. In a previous study in diet-induced obese Sprague Dawley rats, our group found that feeding a high-fat diet containing slowly digestible carbohydrate in the form of fabricated starch-entrapped microspheres for 12 weeks significantly decreased the expression of the orexigenic neuropeptides NPY and AgRP as well as decreased food intake relative to feeding a high-fat diet containing rapidly digestible carbohydrate in the form of pregelatinized high-amylopectin corn starch (Hasek et al., 2018). This study serves as a “proof-of-concept” to support the capability of slowly digestible carbohydrates to have marked effects on the control of food intake with implications for obesity.

Intriguingly, more recent evidence supports that the hippocampus is also involved in what has been widely recognized as homeostatic control of food intake – in addition to its identified roles in food seeking, memory, and reward – among other aspects that can influence food intake (Davidson et al., 2007; Hsu et al., 2015; Suarez et al., 2020). How consumption of carbohydrates with different digestibilities impacts gut-brain axis signaling related to these different brain regions may be a promising area for future research.

## **2.5 Carbohydrate metabolism – oxidation and metabolic flexibility**

After glucose is sensed in the small intestine and absorbed into the bloodstream, it is eventually drawn into cells through the action of insulin. Within cells, it can finally be used for energy through the action of mitochondria. The overall chemical breakdown of glucose can be summarized in the following chemical equation [Equation 1]:



For each molecule of glucose metabolized, a net total of 36 ATP molecules are produced. Glycolysis, the citric acid cycle, and oxidative phosphorylation (the electron transport chain) are all summarized in this chemical equation (Lodish et al., 2000). Other carbohydrate metabolic processes include gluconeogenesis (converting non-carbohydrate molecules into glucose), glycogenolysis (breaking down glycogen [stored carbohydrate in bodily tissues]), glycogenesis

(synthesizing glycogen, or storing carbohydrate as glycogen in the body), fructose metabolism (metabolizing fructose instead of glucose, which involves different steps), and galactose metabolism (metabolizing galactose instead of glucose or fructose). The metabolism of carbohydrates (e.g. glucose) can be measured relative to the metabolism of fats via indirect calorimetry. This technique allows for the measurement of the type and rate of substrate utilization for metabolism based on the gas exchange measurements of oxygen (O<sub>2</sub>) consumption and carbon dioxide (CO<sub>2</sub>) production (Ferrannini, 1988). This is possible because each type of “fuel” (carbohydrate, fat, protein) generally requires a certain amount of O<sub>2</sub> in order to produce a specific amount of CO<sub>2</sub> (Table 1). To more clearly describe these differences, the respiratory exchange ratio (RER) can be calculated as follows [Equation 2]:

$$RER = \frac{VCO_2}{VO_2} \quad [2]$$

Where  $VCO_2$  is the volume of carbon dioxide gas produced in the indirect calorimetry chamber system, and  $VO_2$  is the volume of oxygen gas consumed in the indirect calorimetry chamber system. When applied to the different macronutrients, carbohydrate is characterized by an RER of approximately 1.00, fat by 0.70-0.71, and protein by 0.80. There is a continuum of ranges in RER values observed *in vivo* because foods with different mixtures of macronutrient compositions are consumed. Thus, RER is generally used to only differentiate carbohydrate oxidation from fat oxidation (and not protein oxidation). RER is sometimes used synonymously with respiratory quotient (RQ), yet there is a subtle but important difference between these two parameters: RER is a measurement of  $VCO_2$  and  $VO_2$  gas volumes in respired air and does not involve invasive measures, while RQ is a measurement of  $VCO_2$  and  $VO_2$  at the tissue level (and thus more invasive procedures, such as arterial and venous catheters, are required) (Deuster & Heled, 2008; Patel et al., 2020). Because carbohydrates produce more CO<sub>2</sub> per mole O<sub>2</sub> consumed than fat, the RER (and RQ) representing carbohydrate oxidation is higher than the RER (and RQ) representing fat oxidation. (This can also be inferred by the RER values of 1.00 for carbohydrate and 0.70-0.71 for fat.) In this sense, RER (and RQ) can be used as an indication of substrate partitioning for energy. However, it is worthy to note that different fatty acids have been shown to result in different RER metabolic responses in humans (Polley et al., 2018), indicating that RER may vary within different types of fats. One study in mice found increased carbohydrate oxidation in females, but not males, when a diet with low starch digestibility (high in amylose) was compared to a highly digestible-starch diet (high in amylopectin) (Fernández-Calleja et al., 2019), suggesting there may also be

variations in RER for starches with different digestibilities. However, to our knowledge, this area is largely unexplored and may be a promising area for future research.

In addition to measuring substrate oxidation for metabolism, indirect calorimetry can also serve as a means to measure metabolic flexibility. Broadly defined, metabolic flexibility is “the ability of an organism to respond or adapt according to changes in metabolic or energy demand as well as the prevailing conditions or activity” (Goodpaster & Sparks, 2017). More specifically related to oxidation, metabolic flexibility can be considered the ability to “toggle” or switch between carbohydrate and fat as substrates for oxidation. First used to describe the ability of helminths (parasitic worms) to respond and adapt to changes in their environment (Kohler, 1985), lack of metabolic flexibility was later found to be associated with obesity, insulin resistance, and type 2 diabetes (Kelley & Mandarino, 2000; Meex et al., 2010; Sparks et al., 2009; Stull et al., 2010). In essence, metabolic flexibility is the response by the body to address a nutritional or environmental challenge (e.g. high-carbohydrate meal, fasting, intense activity, oxygen restriction); to optimally address the challenge at hand, the body must switch metabolic substrates efficiently (Duivenvoorde et al., 2015). Possessing metabolic flexibility is a marker of good health, while having metabolic *inflexibility* is a marker of poor health. For example, individuals with obesity may have impaired metabolic flexibility (Kelley et al., 1999). Although RER can be an indicator of metabolic flexibility by describing time-specific RER values, it does not readily characterize the toggling between carbohydrate oxidation and fat oxidation. To address this, some researchers have used an approach called Percent Relative Cumulative Frequency (PRCF) (Riachi et al., 2004). This approach can be used for analyzing RER as well as energy expenditure values collected over time and is reportedly capable of detecting subtle differences in energy metabolism. In the same study reporting sex-related differences in RER for lowly versus highly digestible-starch diets described above, there were also sex-based differences in metabolic flexibility (Fernández-Calleja et al., 2019). A diet high in saturated fatty acids was found to result in poorer metabolic flexibility in mice compared to a diet high in polyunsaturated fatty acids (Duivenvoorde et al., 2015). Metabolic flexibility has been widely studied in relation to aspects of body composition, notably skeletal muscle and adipose tissue, but, aside from the aforementioned studies by Fernández-Calleja et al. (2019) and Duivenvoorde et al. (2015), to our knowledge it has not been studied related to different dietary carbohydrate or fat compositions (or digestibilities).

## 2.6 *In vitro*, *in vivo*, and mathematical modeling approaches related to starch digestion, gastric emptying, and metabolism

There are many methods, tools, and approaches to study and characterize food digestion and metabolism. As already described, the glycemic index, glycemic load, and Englyst assay classification systems specifically characterize carbohydrates. RER and RQ more broadly describe carbohydrate, fat, and protein macronutrients. In order to better understand different approaches and techniques applied in the investigations for this thesis, we will visit some key relevant details here.

Beyond the Englyst assay classification system to characterize starch as RDS, SDS, and RS, there are increasing numbers of *in vitro* digestion systems being developed. Namely, currently existing systems include the TIM gastrointestinal digestion system (and its various iterations) (Bellmann, Gorissen, et al., 2016; Bellmann, Lelieveld, et al., 2016; Minekus et al., 1995), which is a sophisticated, multi-compartmental digestion system that mimics the stomach and small intestine (and one iteration involves the large intestine) (Figure 3, TIM with an advanced gastric compartment [TIMagc]); the Human Gastric Simulator (HGS; and its later iterations) (Figure 4), which is an advanced system that specifically mimics the peristaltic motion of the stomach as it breaks down food (Kong & Singh, 2010); a Human Gastric Digestion Simulator, which is another advanced system focusing on digestive processes in the stomach (Kozu et al., 2016); SoGut, a stomach-based system that takes a unique approach to mimic the peristaltic muscle movements of the stomach (Dang et al., 2020); and the Gastric Simulation Model (GSM), which was created to reproduce the geometry and motility of the human stomach in a sophisticated way (Li et al., 2019); among others. Some of these systems have been reviewed relatively recently (Dupont et al., 2019; Kozu, 2015). The experiments in Chapter 3 of this dissertation involved the use of the HGS, and the experiments in Chapter 4 involved the use of the TIMagc. In addition to these models, there are numerous less complex *in vitro* digestion methods that more simply involve a shaking water bath or are static. The plethora of model systems has led to inconsistencies in methodology and endpoint measurements, and thus a coordinated effort among researchers has resulted in the development of the INFOGEST protocol (and a refined iteration) (Brodkorb et al., 2019; Minekus et al., 2014). Although it is specific to static *in vitro* digestion methods, this protocol promotes harmonization within the field of general *in vitro* digestion. In terms of all the different dynamic

models, researchers should strive to select the appropriate approach according to their project objectives and hypotheses.

To study gastric emptying *in vivo*, methods of scintigraphy (the gold standard method) (Ma et al., 2015; Spiegel et al., 1994),  $^{13}\text{C}$  breath tests (Ghoos et al., 1993; Sanaka & Nakada, 2010), magnetic resonance imaging (Marciani, 2011), and the paracetamol absorption test (Medhus et al., 2001; Willems et al., 2001) are used. Each method has its own set of constraints and limitations, and these should inform which is the most suitable to use for a specific project.

Our lab has used the  $^{13}\text{C}$  octanoic acid breath test to examine potential differences in gastric emptying for different solid carbohydrate-based foods in humans (Cisse et al., 2017, 2018; Pletsch & Hamaker, 2018). The basis of this method lies in the fact that the rate-limiting step for an orally consumed tracer to appear in the breath is how quickly it empties from the stomach. In this method, a standard amount of  $^{13}\text{C}$  octanoic acid is added to each carbohydrate-based test meal, which participants then consume.  $^{13}\text{C}$  sodium acetate has also been used. Breath samples are collected at 15-min intervals for the first 2 h postprandially, and then at 30-min intervals from 2 to 4 h postprandially. These breath samples are then analyzed using a specialized spectrophotometer (e.g. POcone breath analyzer, Otsuka Electronics Co., Ltd., Osaka, Japan) compared to a baseline breath sample collected before the participant consumed the test meal. The  $^{13}\text{CO}_2/^{12}\text{CO}_2$  ratio of a breath sample compared to the ratio for baseline breath is recorded as  $^{13}\text{CO}_2$  delta over baseline (DOB, ‰). Given these values, the percent dose  $^{13}\text{C}$  recovery (PDR) per hour and cumulative percent dose  $^{13}\text{C}$  recovery (CPDR) can be calculated (Sanaka & Nakada, 2010) and are then normalized for each participant's body surface area (Haycock et al., 1978) to model gastric half-emptying time and lag phase for the test meal using the following two equations [Equations 3 and 4]:

$$y = at^b c^{-ct} \quad [3]$$

Where  $y$  = PDR per hour (%),  $t$  = time (h), and  $a$ ,  $b$ , and  $c$  = constants.

$$y = m(1 - e^{-kt})^\beta \quad [4]$$

Where  $y$  = CPDR over time (%),  $t$  = time (h), and  $m$ ,  $k$ , and  $\beta$  = constants (where  $m$  = total cumulative dose recovery when time is infinite).

From these equations, lag phase ( $T_{lag}$ ) and gastric half-emptying time ( $T_{1/2}$ ) are calculated using Equations 5 and 6 as follows:

$$T_{lag} = (\ln\beta)/k \quad [5]$$

$$(T_{1/2}) = \left(-\frac{1}{k}\right) \times \ln \left(1 - 2^{-\frac{1}{\beta}}\right) \quad [6]$$

Where  $\beta$  and  $k$  are constants calculated from Equation 5. In this approach, lag phase ( $T_{lag}$ ) specifically represents the time required for the  $^{13}\text{CO}_2$  excretion rate to attain its maximal level, which is used as an indicator of the time it takes for a food to break down within the stomach, and gastric half-emptying time ( $T_{1/2}$ ) is the time necessary for half of the  $^{13}\text{C}$  dose to be metabolized, which is used to represent the time for half of the test meal food to empty from the stomach (Perri et al., 2005; Sanaka & Nakada, 2010). Although an assumption made with this approach is that the tracer is evenly distributed within the test meal food and thus empties from the stomach at the same rate as the food, it is not as invasive as many of the other approaches to assess gastric emptying and has been widely used.

From a whole-body perspective, there are a number of comprehensive approaches to model dynamics in *in vivo* energy metabolism as they relate to body weight, body composition, and activity (Alpert, 1979; Antonetti, 1973; Guo & Hall, 2009; Hall, 2012a, 2012b). A discussion of such approaches is beyond the scope of this review, but they do bring into question how adaptations in metabolism may contribute to whole-body energy regulation.

In Chapter 5 of this thesis, we attempt to model a specific aspect of metabolism related to substrate utilization for oxidation, which involves the concepts of RER and metabolic flexibility discussed above. In our investigation, we devise and apply new modeling approaches to our percent relative cumulative frequency (PRCF) analysis of RER to gain insight into metabolic flexibility. To do this, we employ the Weibull Cumulative Distribution function (Figure 5) as well as the Mixed Weibull Cumulative Distribution function (Figure 6) (Rinne, 2008). The Weibull Distribution is extensively used in many different fields—from biology to engineering to economics—and is rooted in statistics. When fit to empirical data, it benefits from defined parameters that can be interpreted according to the conditions of the experiment. The main distinction between these two Weibull-based functions is that the (normal) Weibull Cumulative Distribution function represents a unimodal distribution, while the Mixed Weibull Cumulative Distribution represents a bimodal distribution. When considering our application of these distributions to RER and PRCF, the Weibull Cumulative Distribution function is given as Equation 7 and the Mixed Weibull Cumulative Distribution function is given as Equation 8, both below:

$$y = 1 - \exp\left(-\left[\frac{x}{x_{50}}\right]^b \ln(2)\right) \quad [7]$$

$$y = \alpha \left( 1 - \exp \left( - \left[ \frac{x}{x_{50.1}} \right]^{b.1} \right) \right) + (1 - \alpha) \left( 1 - \exp \left( - \left[ \frac{x}{x_{50.2}} \right]^{b.2} \right) \right) \quad [8]$$

Where for Eq. 7:

$y$  = percent relative cumulative frequency (PRCF; 0 to 100%);

$x_{50}$  = median respiratory exchange ratio (median RER);

$b$  = distribution breadth constant (dimensionless), indicative of slope;

And for Eq. 8:

$y$  = percent relative cumulative frequency (PRCF; 0 to 100%);

$\alpha$  = mixing weight parameter that represents the proportion of the first mode;

$x_{50.1}$  = median respiratory exchange ratio (median RER) for the first mode;

$b_{.1}$  = distribution breadth constant for first mode (dimensionless), indicative of slope for the first mode;

$x_{50.2}$  = median respiratory exchange ratio (median RER) for the second mode;

$b_{.2}$  = distribution breadth constant for the second mode (dimensionless), indicative of slope for the second mode.

In addition to these proposed modeling approaches to examine the toggling between carbohydrate oxidation and fat oxidation, for the investigation in Chapter 5 we also employ modeling of RER over time using the sine equation [Equation 9].

$$y = a \sin(bx + c) + d \quad [9]$$

Where  $a$  indicates the amplitude,  $b$  indicates the period (breadth or width),  $c$  indicates the horizontal shift on the  $x$ -axis, and  $d$  indicates the vertical shift on the  $y$ -axis for the sinusoidal curve. We have taken this approach in order to better characterize the diurnal patterns in RER, with the idea that we can gain insight into metabolic flexibility by this alternative means.

Although the *in vitro*, *in vivo*, and mathematical modeling approaches related to starch digestion, gastric emptying, and metabolism discussed here are by no means comprehensive, a general familiarity with them may be beneficial for developing improved techniques and tools to improve our understanding of carbohydrate consumption and health.

## 2.7 Conclusions

In this review, we have explored a number of key aspects that are important for the connection between carbohydrates and health. Carbohydrates with different digestibilities are often thought of specifically in relation to glycemic response, but they can impact or be associated with many other physiological responses, neurobiological responses, and health-related outcomes. Considering the high and growing levels of obesity and nutrition-related non-communicable diseases worldwide, pursuits to prevent and help treat these diseases will remain relevant and impactful. Slowly digestible carbohydrates may play a role in such endeavors.

## 2.8 References

- Abbott, C. R., Monteiro, M., Small, C. J., Sajedi, A., Smith, K. L., Parkinson, J. R. C., Ghatei, M. A., & Bloom, S. R. (2005). The inhibitory effects of peripheral administration of peptide YY3–36 and glucagon-like peptide-1 on food intake are attenuated by ablation of the vagal–brainstem–hypothalamic pathway. *Brain Research*, *1044*(1), 127–131. <https://doi.org/10.1016/j.brainres.2005.03.011>
- Al Helaili, A., Park, S. J., & Beyak, M. J. (2020). Chronic high fat diet impairs glucagon like peptide-1 sensitivity in vagal afferents. *Biochemical and Biophysical Research Communications*, *533*(1), 110–117. <https://doi.org/10.1016/j.bbrc.2020.08.045>
- Alpert, S. S. (1979). A two-reservoir energy model of the human body. *The American Journal of Clinical Nutrition*, *32*(8), 1710–1718. <https://doi.org/10.1093/ajcn/32.8.1710>
- Anand, B. K., & Brobeck, J. R. (1951). Localization of a “Feeding Center” in the Hypothalamus of the Rat. *Experimental Biology and Medicine*, *77*(2), 323–325. <https://doi.org/10.3181/00379727-77-18766>
- Antonetti, V. W. (1973). The equations governing weight change in human beings. *The American Journal of Clinical Nutrition*, *26*(1), 64–71. <https://doi.org/10.1093/ajcn/26.1.64>
- Auricchio, S., Rubino, A., & Muerset, G. (1965). Intestinal glycosidase activities in the human embryo, fetus, and newborn. *Pediatrics*, *35*, 944–954.
- Barreto, S. G., Soenen, S., Chisholm, J., Chapman, I., & Kow, L. (2017). Does the ileal brake mechanism contribute to sustained weight loss after bariatric surgery? *ANZ Journal of Surgery*. <https://doi.org/10.1111/ans.14062>
- Bellmann, S., Gorissen, T., & Minekus, M. (2016). *An in vitro gastrointestinal model for studying the gastric behavior of formulas for infants suffering from gastroesophageal reflux*.
- Bellmann, S., Lelieveld, J., Gorissen, T., Minekus, M., & Havenaar, R. (2016). Development of an advanced in vitro model of the stomach and its evaluation versus human gastric physiology. *Food Research International*, *88*, 191–198. <https://doi.org/10.1016/j.foodres.2016.01.030>
- BeMiller, J. N. (2007). *Carbohydrate Chemistry for Food Scientists* (Second Edi). AACC International, Inc.
- Benmoussa, M., Moldenhauer, K. A. K., & Hamaker, B. R. (2007). Rice amylopectin fine structure variability affects starch digestion properties. *Journal of Agricultural and Food Chemistry*, *55*(4), 1475–1479. <https://doi.org/10.1021/jf062349x>

- Bertoft, E., Annor, G. A., Shen, X., Rumpagaporn, P., Seetharaman, K., & Hamaker, B. R. (2016). Small differences in amylopectin fine structure may explain large functional differences of starch. *Carbohydrate Polymers*, *140*, 113–121. <https://doi.org/10.1016/j.carbpol.2015.12.025>
- Beutler, L. R., Chen, Y., Ahn, J. S., Lin, Y.-C., Essner, R. A., & Knight, Z. A. (2017). Dynamics of Gut-Brain Communication Underlying Hunger. *Neuron*, *96*(2), 461–475.e5. <https://doi.org/10.1016/j.neuron.2017.09.043>
- Bornhorst, G. M., & Paul Singh, R. (2014). Gastric Digestion In Vivo and In Vitro: How the Structural Aspects of Food Influence the Digestion Process. *Annual Review of Food Science and Technology*, *5*(1), 111–132. <https://doi.org/10.1146/annurev-food-030713-092346>
- Brodkorb, A., Egger, L., Alminger, M., Alvito, P., Assunção, R., Ballance, S., Bohn, T., Bourlieu-Lacanal, C., Boutrou, R., Carrière, F., Clemente, A., Corredig, M., Dupont, D., Dufour, C., Edwards, C., Golding, M., Karakaya, S., Kirkhus, B., Le Feunteun, S., ... Recio, I. (2019). INFOGEST static in vitro simulation of gastrointestinal food digestion. *Nature Protocols*, *14*(4), 991–1014. <https://doi.org/10.1038/s41596-018-0119-1>
- Burn-Murdoch, R. A., Fisher, M. A., & Hunt, J. N. (1978). The slowing of gastric emptying by proteins in test meals. *The Journal of Physiology*, *274*(1), 477–485. <https://doi.org/10.1113/jphysiol.1978.sp012161>
- Calbet, J. A., & MacLean, D. A. (1997). Role of caloric content on gastric emptying in humans. *The Journal of Physiology*, *498* ( Pt 2(1997)), 553–559.
- Camps, G., Mars, M., De Graaf, C., & Smeets, P. A. M. (2016). Empty calories and phantom fullness: A randomized trial studying the relative effects of energy density and viscosity on gastric emptying determined by MRI and satiety. *American Journal of Clinical Nutrition*, *104*(1), 73–80. <https://doi.org/10.3945/ajcn.115.129064>
- Cani, P. D., Hoste, S., Guiot, Y., & Delzenne, N. M. (2007). Dietary non-digestible carbohydrates promote L-cell differentiation in the proximal colon of rats. *British Journal of Nutrition*, *98*(1), 32–37. <https://doi.org/10.1017/S0007114507691648>
- Chegeni, M., Amiri, M., Nichols, B. L., Naim, H. Y., & Hamaker, B. R. (2018). Dietary starch breakdown product sensing mobilizes and apically activates  $\alpha$ -glucosidases in small intestinal enterocytes. *FASEB Journal*, *32*(7), 3903–3911. <https://doi.org/10.1096/fj.201701029R>
- Cisse, F., Erickson, D. P., Hayes, A. M. R., Opekun, A. R., Nichols, B. L., & Hamaker, B. R. (2018). Traditional Malian solid foods made from sorghum and millet have markedly slower gastric emptying than rice, potato, or pasta. *Nutrients*, *10*(2), 124. <https://doi.org/10.3390/nu10020124>
- Cisse, F., Pletsch, E. A., Erickson, D. P., Chegeni, M., Hayes, A. M. R., & Hamaker, B. R. (2017). Preload of slowly digestible carbohydrate microspheres decreases gastric emptying rate of subsequent meal in humans. *Nutrition Research*, *45*, 46–51. <https://doi.org/10.1016/j.nutres.2017.06.009>
- Collins, P. J., Horowitz, M., Maddox, A., Myers, J. C., & Chatterton, B. E. (1996). Effects of increasing solid component size of a mixed solid/liquid meal on solid and liquid gastric emptying. *The American Journal of Physiology*, *271*(4 Pt 1), G549-54. <http://www.ncbi.nlm.nih.gov/pubmed/8897871>
- Dahlqvist, A. (1962). Specificity of the human intestinal disaccharidases and implications for hereditary disaccharide intolerance. *Journal of Clinical Investigation*, *41*(3), 463–470.
- Dahlqvist, A., & Borgstrom, B. (1961). Digestion and absorption of disaccharides in man. *Biochemical Journal*, *81*(2), 411–418. <https://doi.org/10.1042/bj0810411>

- Dahlqvist, A., & Telenius, U. (1969). Column chromatography of human small-intestinal maltase, isomaltase and invertase activities. *Biochemical Journal*, *111*(2), 139–146. <https://doi.org/10.1042/bj1110139>
- Dang, Y., Liu, Y., Hashem, R., Bhattacharya, D., Allen, J., Stommel, M., Cheng, L. K., & Xu, W. (2020). SoGut: A Soft Robotic Gastric Simulator. *Soft Robotics*, soro.2019.0136. <https://doi.org/10.1089/soro.2019.0136>
- Daoudi, M., Hennuyer, N., Borland, M. G., Touche, V., Duhem, C., Gross, B., Caiazzo, R., Kerr–Conte, J., Pattou, F., Peters, J. M., Staels, B., & Lestavel, S. (2011). PPAR $\beta/\delta$  Activation Induces Enteroendocrine L Cell GLP-1 Production. *Gastroenterology*, *140*(5), 1564–1574. <https://doi.org/10.1053/j.gastro.2011.01.045>
- Davidson, T. L., Kanoski, S. E., Schier, L. A., Clegg, D. J., & Benoit, S. C. (2007). A potential role for the hippocampus in energy intake and body weight regulation. *Current Opinion in Pharmacology*, *7*(6), 613–616. <https://doi.org/10.1016/j.coph.2007.10.008>
- de Lartigue, G., & Xu, C. (2018). Mechanisms of vagal plasticity influencing feeding behavior. *Brain Research*, *1693*, 146–150. <https://doi.org/10.1016/j.brainres.2018.03.030>
- de Vadder, F., & Mithieux, G. (2018). Gut-brain signaling in energy homeostasis: The unexpected role of microbiota-derived succinate. *Journal of Endocrinology*, *236*(2), R105–R108. <https://doi.org/10.1530/JOE-17-0542>
- Deuster, P. A., & Heled, Y. (2008). Testing for Maximal Aerobic Power. In *The Sports Medicine Resource Manual* (pp. 520–528). Elsevier. <https://doi.org/10.1016/B978-141603197-0.10069-2>
- Diakogiannaki, E., Gribble, F. M., & Reimann, F. (2012). Nutrient detection by incretin hormone secreting cells. *Physiology & Behavior*, *106*(3), 387–393. <https://doi.org/10.1016/j.physbeh.2011.12.001>
- Duivenvoorde, L. P. M., van Schothorst, E. M., Swarts, H. M., Kuda, O., Steenbergh, E., Termeulen, S., Kopecky, J., & Keijer, J. (2015). A Difference in Fatty Acid Composition of Isocaloric High-Fat Diets Alters Metabolic Flexibility in Male C57BL/6JOLA $Hsd$  Mice. *PLOS ONE*, *10*(6), e0128515. <https://doi.org/10.1371/journal.pone.0128515>
- Dupont, D., Alric, M., Blanquet-Diot, S., Bornhorst, G., Cueva, C., Deglaire, A., Denis, S., Ferrua, M., Havenaar, R., Lelieveld, J., Mackie, A. R., Marzorati, M., Menard, O., Minekus, M., Miralles, B., Recio, I., & Van den Abbeele, P. (2019). Can dynamic in vitro digestion systems mimic the physiological reality? *Critical Reviews in Food Science and Nutrition*, *59*, 1546–1562. <https://doi.org/10.1080/10408398.2017.1421900>
- Eelderink, C., Schepers, M., Preston, T., Vonk, R. J., Oudhuis, L., & Priebe, M. G. (2012). Slowly and rapidly digestible starchy foods can elicit a similar glycemic response because of differential tissue glucose uptake in healthy men. *American Journal of Clinical Nutrition*, *96*(5), 1017–1024. <https://doi.org/10.3945/ajcn.112.041947>
- Engelstoft, M. S., Egerod, K. L., Lund, M. L., & Schwartz, T. W. (2013). Enteroendocrine cell types revisited. *Current Opinion in Pharmacology*, *13*(6), 912–921. <https://doi.org/10.1016/j.coph.2013.09.018>
- Englyst, H. N., Kingman, S. M., & Cummings, J. H. (1992). Classification and measurement of nutritionally important starch fractions. *European Journal of Clinical Nutrition*, *46 Suppl 2*, S33–50. <http://www.ncbi.nlm.nih.gov/pubmed/1330528>
- Englyst, K. N., Englyst, H. N., Hudson, G. J., Cole, T. J., & Cummings, J. H. (1999). Rapidly available glucose in foods: An in vitro measurement that reflects the glycemic response. *American Journal of Clinical Nutrition*, *69*(3), 448–454.

- Englyst, K. N., Goux, A., Meynier, A., Quigley, M., Englyst, H., Brack, O., & Vinoy, S. (2018). Inter-laboratory validation of the starch digestibility method for determination of rapidly digestible and slowly digestible starch. *Food Chemistry*, 245(August 2017), 1183–1189. <https://doi.org/10.1016/j.foodchem.2017.11.037>
- Englyst, K. N., Vinoy, S., Englyst, H. N., & Lang, V. (2003). Glycaemic index of cereal products explained by their content of rapidly and slowly available glucose. *British Journal of Nutrition*, 89(3), 329–339. <https://doi.org/10.1079/BJN2002786>
- Fagerberg, L., Hallström, B. M., Oksvold, P., Kampf, C., Djureinovic, D., Odeberg, J., Habuka, M., Tahmasebpour, S., Danielsson, A., Edlund, K., Asplund, A., Sjöstedt, E., Lundberg, E., Szigyarto, C. A.-K., Skogs, M., Takanen, J. O., Berling, H., Tegel, H., Mulder, J., ... Uhlén, M. (2014). Analysis of the Human Tissue-specific Expression by Genome-wide Integration of Transcriptomics and Antibody-based Proteomics. *Molecular & Cellular Proteomics*, 13(2), 397–406. <https://doi.org/10.1074/mcp.M113.035600>
- Fernández-Calleja, J. M. S., Bouwman, L. M. S., Swarts, H. J. M., Billecke, N., Oosting, A., Keijer, J., & van Schothorst, E. M. (2019). A Lowly Digestible-Starch Diet after Weaning Enhances Exogenous Glucose Oxidation Rate in Female, but Not in Male, Mice. *Nutrients*, 11(9), 2242. <https://doi.org/10.3390/nu11092242>
- Ferrannini, E. (1988). The theoretical bases of indirect calorimetry: A review. *Metabolism*, 37(3), 287–301. [https://doi.org/10.1016/0026-0495\(88\)90110-2](https://doi.org/10.1016/0026-0495(88)90110-2)
- Frandsen, T. P., Palcic, M. M., & Svensson, B. (2002). Substrate recognition by three family 13 yeast  $\alpha$ -glucosidases. *European Journal of Biochemistry*, 269(2), 728–734. <https://doi.org/10.1046/j.0014-2956.2001.02714.x>
- Frandsen, T. P., & Svensson, B. (1998). Plant  $\alpha$ -glucosidases of the glycoside hydrolase family 31. Molecular properties, substrate specificity, reaction mechanism, and comparison with family members of different origin. *Plant Molecular Biology*, 37(1), 1–13.
- Fujii, M., & Kawamura, Y. (1985). Synergistic action of  $\alpha$ -amylase and glucoamylase on hydrolysis of starch. *Biotechnology and Bioengineering*, 27(3), 260–265. <https://doi.org/10.1002/bit.260270308>
- Ghoos, Y. F., Maes, B. D., Geypens, B. J., Mys, G., Hiele, M. I., Rutgeerts, P. J., & Vantrappen, G. (1993). Measurement of gastric emptying rate of solids by means of a carbon-labeled octanoic acid breath test. *Gastroenterology*, 104(6), 1640–1647. [https://doi.org/http://dx.doi.org/10.1016/0016-5085\(93\)90640-X](https://doi.org/http://dx.doi.org/10.1016/0016-5085(93)90640-X)
- Giezenaar, C., Lange, K., Hausken, T., Jones, K., Horowitz, M., Chapman, I., & Soenen, S. (2018). Acute Effects of Substitution, and Addition, of Carbohydrates and Fat to Protein on Gastric Emptying, Blood Glucose, Gut Hormones, Appetite, and Energy Intake. *Nutrients*, 10(10), 1451. <https://doi.org/10.3390/nu10101451>
- Giezenaar, C., Trahair, L. G., Luscombe-Marsh, N. D., Hausken, T., Standfield, S., Jones, K. L., Lange, K., Horowitz, M., Chapman, I., & Soenen, S. (2017). Effects of randomized whey-protein loads on energy intake, appetite, gastric emptying, and plasma gut-hormone concentrations in older men and women. *American Journal of Clinical Nutrition*, 106(3), 865–877. <https://doi.org/10.3945/ajcn.117.154377>
- Giezenaar, C., Van Der Burgh, Y., Lange, K., Hatzinikolas, S., Hausken, T., Jones, K. L., Horowitz, M., Chapman, I., & Soenen, S. (2018). Effects of substitution, and adding of carbohydrate and fat to whey-protein on energy intake, appetite, gastric emptying, glucose, insulin, ghrelin, cck and glp-1 in healthy older men—a randomized controlled trial. *Nutrients*, 10(2), 1–14. <https://doi.org/10.3390/nu10020113>

- Goodpaster, B. H., & Sparks, L. M. (2017). Metabolic Flexibility in Health and Disease. *Cell Metabolism*, 25(5), 1027–1036. <https://doi.org/10.1016/j.cmet.2017.04.015>
- Gorboulev, V., Schurmann, A., Vallon, V., Kipp, H., Jaschke, A., Klessen, D., Friedrich, A., Scherneck, S., Rieg, T., Cunard, R., Veyhl-Wichmann, M., Srinivasan, A., Balen, D., Breljak, D., Rexhepaj, R., Parker, H. E., Gribble, F. M., Reimann, F., Lang, F., ... Koepsell, H. (2012). Na<sup>+</sup>-D-glucose Cotransporter SGLT1 is Pivotal for Intestinal Glucose Absorption and Glucose-Dependent Incretin Secretion. *Diabetes*, 61(1), 187–196. <https://doi.org/10.2337/db11-1029>
- Grigoryan, M., Kedeas, M. H., Charron, M. J., Guz, Y., & Teitelman, G. (2012). Regulation of Mouse Intestinal L Cell Progenitors Proliferation by the Glucagon Family of Peptides. *Endocrinology*, 153(7), 3076–3088. <https://doi.org/10.1210/en.2012-1120>
- Grill, H. J. (2020). A Role for GLP-1 in Treating Hyperphagia and Obesity. *Endocrinology*, 161(8), 1–40. <https://doi.org/10.1210/endocr/bqaa093>
- Guo, J., & Hall, K. D. (2009). Estimating the Continuous-Time Dynamics of Energy and Fat Metabolism in Mice. *PLoS Computational Biology*, 5(9), e1000511. <https://doi.org/10.1371/journal.pcbi.1000511>
- Habib, A. M., Richards, P., Cairns, L. S., Rogers, G. J., Bannon, C. A. M., Parker, H. E., Morley, T. C. E., Yeo, G. S. H., Reimann, F., & Gribble, F. M. (2012). Overlap of endocrine hormone expression in the mouse intestine revealed by transcriptional profiling and flow cytometry. *Endocrinology*, 153(7), 3054–3065. <https://doi.org/10.1210/en.2011-2170>
- Hall, K. D. (2012a). Modeling Metabolic Adaptations and Energy Regulation in Humans. *Annual Review of Nutrition*, 32(1), 35–54. <https://doi.org/10.1146/annurev-nutr-071811-150705>
- Hall, K. D. (2012b). Metabolism of mice and men. *Current Opinion in Clinical Nutrition and Metabolic Care*, 15(5), 418–423. <https://doi.org/10.1097/MCO.0b013e3283561150>
- Hasek, L. Y., Phillips, R. J., Hayes, A. M. R., Kinzig, K., Zhang, G., Powley, T. L., & Hamaker, B. R. (2020). Carbohydrates designed with different digestion rates modulate gastric emptying response in rats. *International Journal of Food Sciences and Nutrition*. <https://doi.org/10.1080/09637486.2020.1738355>
- Hasek, L. Y., Phillips, R. J., Zhang, G., Kinzig, K. P., Kim, C. Y., Powley, T. L., & Hamaker, B. R. (2018). Dietary slowly digestible starch triggers the gut-brain axis in obese rats with accompanied reduced food intake. *Molecular Nutrition & Food Research*, 62(5), 1700117. <https://doi.org/10.1002/mnfr.201700117>
- Haycock, G. B., Schwartz, G. J., & Wisotsky, D. H. (1978). Geometric method for measuring body surface area: A height-weight formula validated in infants, children, and adults. *The Journal of Pediatrics*, 93(1), 62–66. [https://doi.org/10.1016/S0022-3476\(78\)80601-5](https://doi.org/10.1016/S0022-3476(78)80601-5)
- Hayes, M. R., Kanoski, S. E., De Jonghe, B. C., Lechner, T. M., Alhadeff, A. L., Fortin, S. M., Arnold, M., Langhans, W., & Grill, H. J. (2011). The common hepatic branch of the vagus is not required to mediate the glycemic and food intake suppressive effects of glucagon-like-peptide-1. *American Journal of Physiology-Regulatory, Integrative and Comparative Physiology*, 301(5), R1479–R1485. <https://doi.org/10.1152/ajpregu.00356.2011>
- Hellmig, S., Von Schöning, F., Gadow, C., Katsoulis, S., Hedderich, J., Fölsch, U. R., & Stüber, E. (2006). Gastric emptying time of fluids and solids in healthy subjects determined by <sup>13</sup>C breath tests: influence of age, sex and body mass index. *Journal of Gastroenterology and Hepatology*, 21(12), 1832–1838. <https://doi.org/10.1111/j.1440-1746.2006.04449.x>
- Holst, J. J. (2007). The Physiology of Glucagon-like Peptide 1. *Physiological Reviews*, 87(4), 1409–1439. <https://doi.org/10.1152/physrev.00034.2006>

- Hsu, T. M., Hahn, J. D., Konanur, V. R., Lam, A., & Kanoski, S. E. (2015). Hippocampal GLP-1 Receptors Influence Food Intake, Meal Size, and Effort-Based Responding for Food through Volume Transmission. *Neuropsychopharmacology*, 40(2), 327–337. <https://doi.org/10.1038/npp.2014.175>
- Hussain, S. S., & Bloom, S. R. (2013). The regulation of food intake by the gut-brain axis: Implications for obesity. *International Journal of Obesity*, 37(5), 625–633. <https://doi.org/10.1038/ijo.2012.93>
- Hyde, T. M., & Miselis, R. R. (1983). Effects of area postrema/caudal medial nucleus of solitary tract lesions on food intake and body weight. *American Journal of Physiology - Regulatory Integrative and Comparative Physiology*, 13(4). <https://doi.org/10.1152/ajpregu.1983.244.4.r577>
- Jenkins, D. J., Wolever, T. M., Taylor, R. H., Barker, H., Fielden, H., Baldwin, J. M., Bowling, A. C., Newman, H. C., Jenkins, A. L., & Goff, D. V. (1981). Glycemic index of foods: a physiological basis for carbohydrate exchange. *The American Journal of Clinical Nutrition*, 34(3), 362–366. <https://doi.org/10.1093/ajcn/34.3.362>
- Kaji, I., Karaki, S. I., Tanaka, R., & Kuwahara, A. (2011). Density distribution of free fatty acid receptor 2 (FFA2)-expressing and GLP-1-producing enteroendocrine L cells in human and rat lower intestine, and increased cell numbers after ingestion of fructo-oligosaccharide. *Journal of Molecular Histology*, 42(1), 27–38. <https://doi.org/10.1007/s10735-010-9304-4>
- Kanoski, S. E., Fortin, S. M., Arnold, M., Grill, H. J., & Hayes, M. R. (2011). Peripheral and Central GLP-1 Receptor Populations Mediate the Anorectic Effects of Peripherally Administered GLP-1 Receptor Agonists, Liraglutide and Exendin-4. *Endocrinology*, 152(8), 3103–3112. <https://doi.org/10.1210/en.2011-0174>
- Karamanlis, A., Chaikomin, R., Doran, S., Bellon, M., Bartholomeusz, F. D., Wishart, J. M., Jones, K. L., Horowitz, M., & Rayner, C. K. (2007). Effects of protein on glycemic and incretin responses and gastric emptying after oral glucose in healthy subjects. *The American Journal of Clinical Nutrition*, 86(5), 1364–1368. <https://doi.org/10.1093/ajcn/86.5.1364>
- Kelley, D. E., Goodpaster, B., Wing, R. R., & Simoneau, J. A. (1999). Skeletal muscle fatty acid metabolism in association with insulin resistance, obesity, and weight loss. *American Journal of Physiology - Endocrinology and Metabolism*, 277(6), 40-6. <https://doi.org/10.1152/ajpendo.1999.277.6.e1130>
- Kelley, D. E., & Mandarino, L. J. (2000). Fuel selection in human skeletal muscle in insulin resistance: a reexamination. *Diabetes*, 49(5), 677–683. <https://doi.org/10.2337/diabetes.49.5.677>
- Kohler, P. (1985). The strategies of energy conservation in helminths. *Molecular and Biochemical Parasitology*, 17(1), 1–18. [https://doi.org/10.1016/0166-6851\(85\)90124-0](https://doi.org/10.1016/0166-6851(85)90124-0)
- Komuro, Y., Kondo, T., Hino, S., Morita, T., & Nishimura, N. (2019). Oral intake of slowly digestible  $\alpha$ -glucan, isomaltodextrin, stimulates GLP-1 secretion in the small intestine of rats. *British Journal of Nutrition*, 1–26. <https://doi.org/10.1017/S0007114519003210>
- Kong, F., & Singh, R. P. (2010). A Human Gastric Simulator (HGS) to study food digestion in human stomach. *Journal of Food Science*, 75(9), E627–E635. <https://doi.org/10.1111/j.1750-3841.2010.01856.x>
- Kopelman, P. (2007). Health risks associated with overweight and obesity. *Obesity Reviews*, 8(s1), 13–17. <https://doi.org/10.1111/j.1467-789X.2007.00311.x>
- Kozu, H. (2015). *Development of human gastric models for characterization of food digestion phenomena*. University of Tsukuba.

- Kozu, H., Kobayashi, I., Nakajima, M., Neves, M. A., Uemura, K., & Ichikawa, S. (2016). Mixing Characterization of Liquid Contents in Human Gastric Digestion Simulator Equipped with Gastric Secretion and Emptying. *Biochemical Engineering Journal*. <https://doi.org/10.1016/j.bej.2016.10.013>
- Krieger, J.-P. (2020). Intestinal glucagon-like peptide-1 effects on food intake: Physiological relevance and emerging mechanisms. *Peptides*, *131*, 170342. <https://doi.org/10.1016/j.peptides.2020.170342>
- Kroemer, G., López-Otín, C., Madeo, F., & de Cabo, R. (2018). Carbotoxicity—Noxious Effects of Carbohydrates. *Cell*, *175*(3), 605–614. <https://doi.org/10.1016/j.cell.2018.07.044>
- Labouesse, M. A., Stadlbauer, U., Weber, E., Arnold, M., Langhans, W., & Pacheco-López, G. (2012). Vagal Afferents Mediate Early Satiety and Prevent Flavour Avoidance Learning in Response to Intraperitoneally Infused Exendin-4. *Journal of Neuroendocrinology*, *24*(12), 1505–1516. <https://doi.org/10.1111/j.1365-2826.2012.02364.x>
- Lee, B.-H., Bello-Pérez, L. A., Lin, A. H.-M., Kim, C. Y., & Hamaker, B. R. (2013). Importance of Location of Digestion and Colonic Fermentation of Starch Related to Its Quality. *Cereal Chemistry*, *90*(4), 335–343. <https://doi.org/10.1094/CCHEM-05-13-0095-FI>
- Lee, B.-H., Rose, D. R., Lin, A. H.-M., Quezada-Calvillo, R., Nichols, B. L., & Hamaker, B. R. (2016). Contribution of the Individual Small Intestinal  $\alpha$ -Glucosidases to Digestion of Unusual  $\alpha$ -Linked Glycemic Disaccharides. *Journal of Agricultural and Food Chemistry*, *64*(33), 6487–6494. <https://doi.org/10.1021/acs.jafc.6b01816>
- Lee, E.-S., Shin, H., Seo, J.-M., Nam, Y.-D., Lee, B.-H., & Seo, D.-H. (2018). Effects of raw potato starch on body weight with controlled glucose delivery. *Food Chemistry*, *256*, 367–372. <https://doi.org/10.1016/j.foodchem.2018.02.150>
- Li, Y., Fortner, L., & Kong, F. (2019). Development of a Gastric Simulation Model (GSM) incorporating gastric geometry and peristalsis for food digestion study. *Food Research International*, *125*(March), 108598. <https://doi.org/10.1016/j.foodres.2019.108598>
- Lin, A. H.-M., Lee, B.-H., & Chang, W.-J. (2016). Small intestine mucosal  $\alpha$ -glucosidase: A missing feature of in vitro starch digestibility. *Food Hydrocolloids*, *53*, 163–171. <https://doi.org/10.1016/j.foodhyd.2015.03.002>
- Lodish, H., Berk, A., Zipursky, S., Matsudaira, P., Baltimore, D., & Darnell, J. (2000). *Molecular Biology* (4th editio). W. H. Freeman.
- Ludwig, D. S. (2002). The Glycemic Index. *JAMA*, *287*(18), 2414. <https://doi.org/10.1001/jama.287.18.2414>
- Ma, J., Jesudason, D. R., Stevens, J. E., Keogh, J. B., Jones, K. L., Clifton, P. M., Horowitz, M., & Rayner, C. K. (2015). Sustained effects of a protein “preload” on glycaemia and gastric emptying over 4 weeks in patients with type 2 diabetes: A randomized clinical trial. *Diabetes Research and Clinical Practice*, *108*(2), e31–e34. <https://doi.org/10.1016/j.diabres.2015.02.019>
- Marciani, L. (2011). Assessment of gastrointestinal motor functions by MRI: a comprehensive review. *Neurogastroenterology & Motility*, *23*(5), 399–407. <https://doi.org/10.1111/j.1365-2982.2011.01670.x>
- Marciani, L., Gowland, P. A., Spiller, R. C., Manoj, P., Moore, R. J., Young, P., & Fillery-Travis, A. J. (2001). Effect of meal viscosity and nutrients on satiety, intragastric dilution, and emptying assessed by MRI. *American Journal of Physiology. Gastrointestinal and Liver Physiology*, *280*(6), G1227–G1233.

- Martinez, M. M. (2021). Starch nutritional quality: beyond intraluminal digestion in response to current trends. *Current Opinion in Food Science*, 38, 112–121. <https://doi.org/10.1016/j.cofs.2020.10.024>
- Martinez, M. M., Li, C., Okoniewska, M., Mukherjee, I., Vellucci, D., & Hamaker, B. (2018). Slowly digestible starch in fully gelatinized material is structurally driven by molecular size and A and B1 chain lengths. *Carbohydrate Polymers*, 197, 531–539. <https://doi.org/10.1016/j.carbpol.2018.06.021>
- Martinussen, C., Bojsen-Møller, K. N., Dirksen, C., Svane, M. S., Kristiansen, V. B., Hartmann, B., Holst, J. J., & Madsbad, S. (2019). Augmented GLP-1 Secretion as Seen After Gastric Bypass May Be Obtained by Delaying Carbohydrate Digestion. *The Journal of Clinical Endocrinology & Metabolism*, 104(8), 3233–3244. <https://doi.org/10.1210/jc.2018-02661>
- Mason, B. L. (2017). Feeding Systems and the Gut Microbiome: Gut-Brain Interactions with Relevance to Psychiatric Conditions. *Psychosomatics*. <https://doi.org/10.1016/j.psym.2017.06.002>
- Matalanis, A. M., Campanella, O. H., & Hamaker, B. R. (2009). Storage retrogradation behavior of sorghum, maize and rice starch pastes related to amylopectin fine structure. *Journal of Cereal Science*, 50(1), 74–81. <https://doi.org/10.1016/j.jcs.2009.02.007>
- McClellan, P., & Weaver, L. T. (1993). Ontogeny of human pancreatic exocrine function. *Archives of Disease in Childhood*, 68(1 Spec No), 62–65. [https://doi.org/10.1136/adc.68.1\\_Spec\\_No.62](https://doi.org/10.1136/adc.68.1_Spec_No.62)
- McHugh, P. R., & Moran, T. H. (1979). Calories and gastric emptying: a regulatory capacity with implications for feeding. *American Journal of Physiology*, 236(5), R254-60.
- Medhus, A. W., Lofthus, C. M., Bredesen, J., & Husebye, E. (2001). Gastric emptying: the validity of the paracetamol absorption test adjusted for individual pharmacokinetics. *Neurogastroenterology and Motility*, 13(3), 179–185. <https://doi.org/10.1046/j.1365-2982.2001.00249.x>
- Meex, R. C. R., Schrauwen-Hinderling, V. B., Moonen-Kornips, E., Schaart, G., Mensink, M., Phielix, E., van de Weijer, T., Sels, J.-P., Schrauwen, P., & Hesselink, M. K. C. (2010). Restoration of Muscle Mitochondrial Function and Metabolic Flexibility in Type 2 Diabetes by Exercise Training Is Paralleled by Increased Myocellular Fat Storage and Improved Insulin Sensitivity. *Diabetes*, 59(3), 572–579. <https://doi.org/10.2337/db09-1322>
- Meyer, J. H. (1980). Gastric emptying of ordinary food: effect of antrum on particle size. *American Journal of Physiology-Gastrointestinal and Liver Physiology*, 239(3), G133–G135. <https://doi.org/10.1152/ajpgi.1980.239.3.G133>
- Miao, M., Jiang, B., Cui, S. W., Zhang, T., & Jin, Z. (2015). Slowly Digestible Starch—A Review. *Critical Reviews in Food Science and Nutrition*, 55(12), 1642–1657. <https://doi.org/10.1080/10408398.2012.704434>
- Minekus, M., Alminger, M., Alvito, P., Ballance, S., Bohn, T., Bourlieu, C., Carrière, F., Boutrou, R., Corredig, M., Dupont, D., Dufour, C., Egger, L., Golding, M., Karakaya, S., Kirkhus, B., Le Feunteun, S., Lesmes, U., Macierzanka, A., Mackie, A., ... Brodtkorb, A. (2014). A standardised static in vitro digestion method suitable for food - an international consensus. *Food & Function*, 5(6), 1113–1124. <https://doi.org/10.1039/c3fo60702j>
- Minekus, M., Marteau, P., Havenaar, R., & Huis in 't Veld, J. (1995). A multi compartmental dynamic computer-controlled model simulating the stomach and small intestine. *Alternatives to Laboratory Animals (ATLA)*, 23, 197–209.

- Moore, J. G., Christian, P. E., & Coleman, R. E. (1981). Gastric emptying of varying meal weight and composition in man. *Digestive Diseases and Sciences*, 26(1), 16–22. <https://doi.org/10.1007/BF01307971>
- Nauck, M. A., Niedereichholz, U., Ettl, R., Holst, J. J., Ørskov, C., Ritzel, R., & Schmiegel, W. H. (1997). Glucagon-like peptide 1 inhibition of gastric emptying outweighs its insulinotropic effects in healthy humans. *American Journal of Physiology - Endocrinology and Metabolism*, 273(5 36-5), 981–988. <https://doi.org/10.1152/ajpendo.1997.273.5.e981>
- Nazare, J.-A., de Rougemont, A., Normand, S., Sauvinet, V., Sothier, M., Vinoy, S., Désage, M., & Laville, M. (2010). Effect of postprandial modulation of glucose availability: short- and long-term analysis. *British Journal of Nutrition*, 103(10), 1461–1470. <https://doi.org/10.1017/S0007114509993357>
- Nichols, B. L., Avery, S., Sen, P., Swallow, D. M., Hahn, D., & Sterchi, E. (2003). The maltase-glucoamylase gene: Common ancestry to sucrase-isomaltase with complementary starch digestion activities. *Proceedings of the National Academy of Sciences*, 100(3), 1432–1437. <https://doi.org/10.1073/pnas.0237170100>
- Patel, H., Kerndt, C. C., & Bhardwaj, A. (2020). *Physiology, Respiratory Quotient*. StatPearls Publishing.
- Péronnet, F., Meynier, A., Sauvinet, V., Normand, S., Bourdon, E., Mignault, D., St-Pierre, D. H., Laville, M., Rabasa-Lhoret, R., & Vinoy, S. (2015). Plasma glucose kinetics and response of insulin and GIP following a cereal breakfast in female subjects: Effect of starch digestibility. *European Journal of Clinical Nutrition*, 69(6), 740–745. <https://doi.org/10.1038/ejcn.2015.50>
- Perri, F., Pastore, M. R., & Annese, V. (2005). 13C-octanoic acid breath test for measuring gastric emptying of solids. *European Review for Medical and Pharmacological Sciences*, 9(5 Suppl 1), 3–8.
- Persaud, S. J., & Bewick, G. A. (2014). Peptide YY: more than just an appetite regulator. *Diabetologia*, 57(9), 1762–1769. <https://doi.org/10.1007/s00125-014-3292-y>
- Pletsch, E. A., & Hamaker, B. R. (2018). Brown rice compared to white rice slows gastric emptying in humans. *European Journal of Clinical Nutrition*, 72(3), 367–373. <https://doi.org/10.1038/s41430-017-0003-z>
- Polley, K. R., Miller, M. K., Johnson, M., Vaughan, R., Paton, C. M., & Cooper, J. A. (2018). Metabolic responses to high-fat diets rich in MUFA v. PUFA. *British Journal of Nutrition*, 120(1), 13–22. <https://doi.org/10.1017/S0007114518001332>
- Quezada-Calvillo, R., Robayo-Torres, C. C., Ao, Z., Hamaker, B. R., Quaroni, A., Brayer, G. D., Sterchi, E. E., Baker, S. S., & Nichols, B. L. (2007). Luminal Substrate “Brake” on Mucosal Maltase-glucoamylase Activity Regulates Total Rate of Starch Digestion to Glucose. *Journal of Pediatric Gastroenterology and Nutrition*, 45(1), 32–43. <https://doi.org/10.1097/MPG.0b013e31804216fc>
- Quezada-Calvillo, R., Robayo-Torres, C. C., Opekun, A. R., Sen, P., Ao, Z., Hamaker, B. R., Quaroni, A., Brayer, G. D., Wattler, S., Nehls, M. C., Sterchi, E. E., & Nichols, B. L. (2007). Contribution of Mucosal Maltase-Glucoamylase Activities to Mouse Small Intestinal Starch  $\alpha$ -Glucogenesis. *The Journal of Nutrition*, 137(7), 1725–1733. <https://doi.org/10.1093/jn/137.7.1725>
- Reimann, F., Tolhurst, G., & Gribble, F. M. (2012). G-protein-coupled receptors in intestinal chemosensation. *Cell Metabolism*, 15(4), 421–431. <https://doi.org/10.1016/j.cmet.2011.12.019>

- Riachi, M., Himms-Hagen, J., & Harper, M. E. (2004). Percent relative cumulative frequency analysis in indirect calorimetry: Application to studies of transgenic mice. *Canadian Journal of Physiology and Pharmacology*, 82(12), 1075–1083. <https://doi.org/10.1139/y04-117>
- Richards, P., Pais, R., Habib, A. M., Brighton, C. A., Yeo, G. S. H., Reimann, F., & Gribble, F. M. (2016). High fat diet impairs the function of glucagon-like peptide-1 producing L-cells. *Peptides*, 77, 21–27. <https://doi.org/10.1016/j.peptides.2015.06.006>
- Rindi, G., Leiter, A. B., Kopin, A. S., Bordi, C., & Solcia, E. (2004). The “normal” endocrine cell of the gut: Changing concepts and new evidences. *Annals of the New York Academy of Sciences*, 1014, 1–12. <https://doi.org/10.1196/annals.1294.001>
- Rinne, H. (2008). *The Weibull Distribution - A Handbook*. CRC Press.
- Robyt, J. F., & French, D. (1967). Multiple attack hypothesis of  $\alpha$ -amylase action: Action of porcine pancreatic, human salivary, and *Aspergillus oryzae*  $\alpha$ -amylases. *Archives of Biochemistry and Biophysics*, 122(1), 8–16. [https://doi.org/10.1016/0003-9861\(67\)90118-X](https://doi.org/10.1016/0003-9861(67)90118-X)
- Roman, L., Yee, J., Hayes, A. M. R., Hamaker, B. R., Bertoft, E., & Martinez, M. M. (2020). On the role of the internal chain length distribution of amylopectins during retrogradation: Double helix lateral aggregation and slow digestibility. *Carbohydrate Polymers*, 246, 116633. <https://doi.org/10.1016/j.carbpol.2020.116633>
- Sacks, F. M., Carey, V. J., Anderson, C. A. M., Miller, E. R., Copeland, T., Charleston, J., Harshfield, B. J., Laranjo, N., McCarron, P., Swain, J., White, K., Yee, K., & Appel, L. J. (2014). Effects of High vs Low Glycemic Index of Dietary Carbohydrate on Cardiovascular Disease Risk Factors and Insulin Sensitivity. *JAMA*, 312(23), 2531. <https://doi.org/10.1001/jama.2014.16658>
- Saito, M. (1972). Daily rhythmic changes in brush border enzymes of the small intestine and kidney in rat. *Biochimica et Biophysica Acta (BBA) - General Subjects*, 286(1), 212–215. [https://doi.org/10.1016/0304-4165\(72\)90108-0](https://doi.org/10.1016/0304-4165(72)90108-0)
- Sam, A. H., Gunner, D. J., King, A., Persaud, S. J., Brooks, L., Hostomska, K., Ford, H. E., Liu, B., Ghatei, M. A., Bloom, S. R., & Bewick, G. A. (2012). Selective Ablation of Peptide YY Cells in Adult Mice Reveals Their Role in Beta Cell Survival. *Gastroenterology*, 143(2), 459–468. <https://doi.org/10.1053/j.gastro.2012.04.047>
- Sanaka, M., & Nakada, K. (2010). Stable isotope breath tests for assessing gastric emptying: A comprehensive review. *Journal of Smooth Muscle Research*, 46(6), 267–280.
- Sandoval, D. A., & D'Alessio, D. A. (2015). Physiology of proglucagon peptides: Role of glucagon and GLP-1 in health and disease. *Physiological Reviews*, 95(2), 513–548. <https://doi.org/10.1152/physrev.00013.2014>
- Santangelo, A., Peracchi, M., Conte, D., Fraquelli, M., & Porrini, M. (1998). Physical state of meal affects gastric emptying, cholecystokinin release and satiety. *British Journal of Nutrition*, 80, 521–527.
- Santos, B. K. S.-D., Goda, T., & Koldovsky, O. (1992). Dietary-induced increases of disaccharidase activities in rat jejunum. *British Journal of Nutrition*, 67(2), 267–278. <https://doi.org/10.1079/BJN19920030>
- Sauer, J., Sigurskjold, B. W., Christensen, U., Frandsen, T. P., Mirgorodskaya, E., Harrison, M., Roepstorff, P., & Svensson, B. (2000). Glucoamylase: structure/function relationships, and protein engineering. *Biochimica et Biophysica Acta (BBA) - Protein Structure and Molecular Enzymology*, 1543(2), 275–293. [https://doi.org/10.1016/S0167-4838\(00\)00232-6](https://doi.org/10.1016/S0167-4838(00)00232-6)
- Schirra, J., & Göke, B. (2005). The physiological role of GLP-1 in human: Incretin, ileal brake or more? *Regulatory Peptides*, 128(2), 109–115. <https://doi.org/10.1016/j.regpep.2004.06.018>

- Schirra, J., Katschinski, M., Weidmann, C., Schäfer, T., Wank, U., Arnold, R., & Göke, B. (1996). Gastric emptying and release of incretin hormones after glucose ingestion in humans. *Journal of Clinical Investigation*, 97(1), 92–103. <https://doi.org/10.1172/JCI118411>
- Shan, Z., Rehm, C. D., Rogers, G., Ruan, M., Wang, D. D., Hu, F. B., Mozaffarian, D., Zhang, F. F., & Bhupathiraju, S. N. (2019). Trends in Dietary Carbohydrate, Protein, and Fat Intake and Diet Quality Among US Adults, 1999-2016. *JAMA*, 322(12), 1178. <https://doi.org/10.1001/jama.2019.13771>
- Shin, H., Seo, D.-H., Seo, J., Lamothe, L. M., Yoo, S.-H., & Lee, B.-H. (2019). Optimization of in vitro carbohydrate digestion by mammalian mucosal  $\alpha$ -glucosidases and its applications to hydrolyze the various sources of starches. *Food Hydrocolloids*, 87(August 2018), 470–476. <https://doi.org/10.1016/j.foodhyd.2018.08.033>
- Sim, L., Quezada-Calvillo, R., Sterchi, E. E., Nichols, B. L., & Rose, D. R. (2008). Human Intestinal Maltase–Glucoamylase: Crystal Structure of the N-Terminal Catalytic Subunit and Basis of Inhibition and Substrate Specificity. *Journal of Molecular Biology*, 375(3), 782–792. <https://doi.org/10.1016/j.jmb.2007.10.069>
- Sirois, P. J., Amidon, G. L., Meyer, J. H., Doty, J., & Dressman, J. B. (1990). Gastric emptying of nondigestible solids in dogs: a hydrodynamic correlation. *The American Journal of Physiology*, 258(1 Pt 1), G65-72. <http://www.ncbi.nlm.nih.gov/pubmed/2301585>
- Soty, M., Gautier-stein, A., Rajas, F., & Mithieux, G. (2017). Perspective Gut-Brain Glucose Signaling in Energy Homeostasis. *Cell Metabolism*, 25(6), 1231–1242. <https://doi.org/10.1016/j.cmet.2017.04.032>
- Sparks, L. M., Ukropcova, B., Smith, J., Pasarica, M., Hymel, D., Xie, H., Bray, G. A., Miles, J. M., & Smith, S. R. (2009). Relation of adipose tissue to metabolic flexibility. *Diabetes Research and Clinical Practice*, 83(1), 32–43. <https://doi.org/10.1016/j.diabres.2008.09.052>
- Spiegel, T. A., Kaplan, J. M., Alavi, A., Kim, P. S. Y., & Tse, K. K. M. (1994). Effects of soup preloads on gastric emptying and fullness ratings following an egg sandwich meal. *Physiology and Behavior*, 56(3), 571–575. [https://doi.org/10.1016/0031-9384\(94\)90303-4](https://doi.org/10.1016/0031-9384(94)90303-4)
- Spiller, R. C., Trotman, I. F., Higgins, B. E., Ghatei, M. A., Grimble, G. K., Lee, Y. C., Bloom, S. R., Misiewicz, J. J., & Silk, D. B. (1984). The ileal brake--inhibition of jejunal motility after ileal fat perfusion in man. *Gut*, 25(4), 365–374. <https://doi.org/10.1136/gut.25.4.365>
- Spreckley, E. (2015). The L-cell in nutritional sensing and the regulation of appetite. *Frontiers in Nutrition*, 2(23). <https://doi.org/10.3389/fnut.2015.00023>
- Steinert, R. E., Beglinger, C., & Langhans, W. (2016). Intestinal GLP-1 and satiation: from man to rodents and back. *International Journal of Obesity*, 40(2), 198–205. <https://doi.org/10.1038/ijo.2015.172>
- Steinert, Robert E., Feinle-Bisset, C., Asarian, L., Horowitz, M., Beglinger, C., & Geary, N. (2017). Ghrelin, CCK, GLP-1, and PYY(3–36): Secretory Controls and Physiological Roles in Eating and Glycemia in Health, Obesity, and After RYGB. *Physiological Reviews*, 97(1), 411–463. <https://doi.org/10.1152/physrev.00031.2014>
- Stevenson, N. R., Ferrigni, F., Parnicky, K., Day, S., & Fierstein, J. S. (1975). Effect of changes in feeding schedule on the diurnal rhythms and daily activity levels of intestinal brush border enzymes and transport systems. *Biochimica et Biophysica Acta (BBA) - Biomembranes*, 406(1), 131–145. [https://doi.org/10.1016/0005-2736\(75\)90048-6](https://doi.org/10.1016/0005-2736(75)90048-6)
- Stoffer, B., Frandsen, T. P., Busk, P. K., Schneider, P., Svendsen, I., & Svensson, B. (1993). Production, purification and characterization of the catalytic domain of glucoamylase from *Aspergillus niger*. *Biochemical Journal*, 292(1), 197–202. <https://doi.org/10.1042/bj2920197>

- Stull, A. J., Galgani, J. E., Johnson, W. D., & Cefalu, W. T. (2010). The contribution of race and diabetes status to metabolic flexibility in humans. *Metabolism*, *59*(9), 1358–1364. <https://doi.org/10.1016/j.metabol.2009.12.020>
- Suarez, A. N., Liu, C. M., Cortella, A. M., Noble, E. E., & Kanoski, S. E. (2020). Ghrelin and Orexin Interact to Increase Meal Size Through a Descending Hippocampus to Hindbrain Signaling Pathway. *Biological Psychiatry*, *87*(11), 1001–1011. <https://doi.org/10.1016/j.biopsych.2019.10.012>
- Treisman, G. J. (2017). The Role of the Brain – Gut – Microbiome in Mental Health and Mental Disorders. In *The Microbiota in Gastrointestinal Pathophysiology*. Elsevier Inc. <https://doi.org/10.1016/B978-0-12-804024-9/00042-2>
- Uldry, M., & Thorens, B. (2004). The SLC2 family of facilitated hexose and polyol transporters. *Pflugers Archiv European Journal of Physiology*, *447*(5), 480–489. <https://doi.org/10.1007/s00424-003-1085-0>
- Vamadevan, V., & Bertoft, E. (2015). Structure-function relationships of starch components. *Starch/Staerke*, *67*(1–2), 55–68. <https://doi.org/10.1002/star.201400188>
- Van Den Hoek, A. M., Heijboer, A. C., Corssmit, E. P. M., Voshol, P. J., Romijn, J. A., Havekes, L. M., & Pijl, H. (2004). PYY3-36 reinforces insulin action on glucose disposal in mice fed a high-fat diet. *Diabetes*, *53*(8), 1949–1952. <https://doi.org/10.2337/diabetes.53.8.1949>
- Venkatachalam, M., Kushnick, M. R., Zhang, G., & Hamaker, B. R. (2009). Starch-Entrapped Biopolymer Microspheres as a Novel Approach to Vary Blood Glucose Profiles. *Journal of the American College of Nutrition*, *28*(5), 583–590. <https://doi.org/10.1080/07315724.2009.10719790>
- Vinoy, S., Normand, S., Meynier, A., Sothier, M., Louche-Pelissier, C., Peyrat, J., Maitrepierre, C., Nazare, J. A., Brand-Miller, J., & Laville, M. (2013). Cereal Processing Influences Postprandial Glucose Metabolism as Well as the GI Effect. *Journal of the American College of Nutrition*, *32*(2), 79–91. <https://doi.org/10.1080/07315724.2013.789336>
- Weltens, N., Iven, J., Van Oudenhove, L., & Kano, M. (2018). The gut-brain axis in health neuroscience: implications for functional gastrointestinal disorders and appetite regulation. *Annals of the New York Academy of Sciences*, *1428*(1), 129–150. <https://doi.org/10.1111/nyas.13969>
- Willems, M., Otto Quatero, A., & Numans, M. E. (2001). How Useful Is Paracetamol Absorption as a Marker of Gastric Emptying? *Digestive Diseases and Sciences*, *46*(10), 2256–2262.
- Wright, E. M., Loo, D. D. F., & Hirayama, B. A. (2011). Biology of Human Sodium Glucose Transporters. *Physiological Reviews*, *91*(2), 733–794. <https://doi.org/10.1152/physrev.00055.2009>
- Yu, Y., Liu, L., Wang, X., Liu, X., Liu, X., Xie, L., & Wang, G. (2010). Modulation of glucagon-like peptide-1 release by berberine: In vivo and in vitro studies. *Biochemical Pharmacology*, *79*(7), 1000–1006. <https://doi.org/10.1016/j.bcp.2009.11.017>
- Zhang, G., Ao, Z., & Hamaker, B. R. (2008). Nutritional property of endosperm starches from maize mutants: A parabolic relationship between slowly digestible starch and amylopectin fine structure. *Journal of Agricultural and Food Chemistry*, *56*(12), 4686–4694. <https://doi.org/10.1021/jf072822m>
- Zhang, G., & Hamaker, B. R. (2009). Slowly Digestible Starch: Concept, Mechanism, and Proposed Extended Glycemic Index. *Critical Reviews in Food Science and Nutrition*, *49*(10), 852–867. <https://doi.org/10.1080/10408390903372466>

Zhu, Y., Hsu, W. H., & Hollis, J. H. (2013). The Impact of Food Viscosity on Eating Rate, Subjective Appetite, Glycemic Response and Gastric Emptying Rate. *PLoS ONE*, 8(6), e67482. <https://doi.org/10.1371/journal.pone.0067482>

Table 2.1 Approximate oxidation characteristics for carbohydrate, fat, and protein and corresponding respiratory exchange ratio (RER) values. Based off Ferrannini (1988).

<b>Macronutrient (g)</b>	<b>Oxygen consumed (L/g)</b>	<b>Carbon dioxide produced (L/g)</b>	<b>Respiratory exchange ratio (RER, unitless)</b>
Carbohydrate	0.83	0.83	1.00
Fat	2.02	1.42	0.70 <sup>a</sup>
Protein	0.97	0.77	0.80

<sup>a</sup>Can also be designated as 0.71.

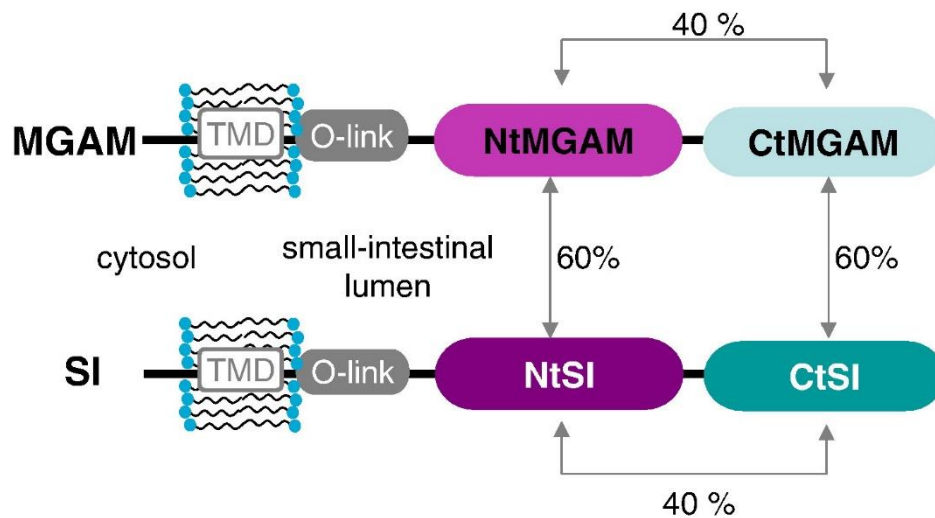


Figure 2.1 Representation of the protein organization of the MGAM and SI complexes. Both MGAM and SI have a small cytosolic domain (~26 residues), and transmembrane domain (~20 residues), an O-glycosylated linker (~55 residues), and two homologous catalytic subunits (NtMGAM, CtMGAM, NtSI, CtSI; each ~900 residues). Percentages shown indicate the proportion of sequence identities between the catalytic subunits. Originally published in Sim et al. (2008), used with permission. CtMGAM, C-terminal maltase glucoamylase; CtSI, C-terminal sucrose isomaltase; MGAM, maltase glucoamylase; NtMGAM, N-terminal maltase glucoamylase; NtSI, N-terminal sucrose isomaltase; O-link, O-glycosylated linker; SI, sucrose isomaltase; TMD, transmembrane domain.

	W-type	Peptide hormone / monoamine	Stomach	Small Intestine		Large Intestine	
				Proximal	Distal	Proximal	Distal
Pan GI-tract EE cell types	D-cell	Somatostatin					
	ECcell	Substance-P/5-HT					
Gastric EE cell types	ECLcell	? peptide/histamine					
	G-cell	Gastrin					
	X/A-like	Ghrelin		(+Motilin)			
Intestinal EE cell types	S-cell	Secretin				mRNA	mRNA
	K-cell*	GIP					
	I-cell	CCK					
	L-cell*	GLP-1/GLP-2					
	N-cell	Neurotensin					
	(L-cell)	PYY					

Figure 2.2 Enteroendocrine cell types divided into pan-GI-tract (throughout the gastrointestinal tract), gastric-selective, and intestinal-selective cells. For each of the cell types, the main secretory product and the original Wiesbaden nomenclature (W-type) are indicated. The lighter maroon color indicates that some of the peptides are less expressed in these segments. \*Some enteroendocrine cells have been shown to co-express GIP and GLP-1 (Grigoryan et al., 2012). Adapted from Engelstoft et al. (2013), used with permission. CCK, cholecystokinin; EE, enteroendocrine; GIP, glucose-dependent insulinotropic peptide; GLP-1, glucagon-like peptide 1; GLP-2, glucagon-like peptide 2; PYY, peptide YY; W-type, Wiesbaden nomenclature.

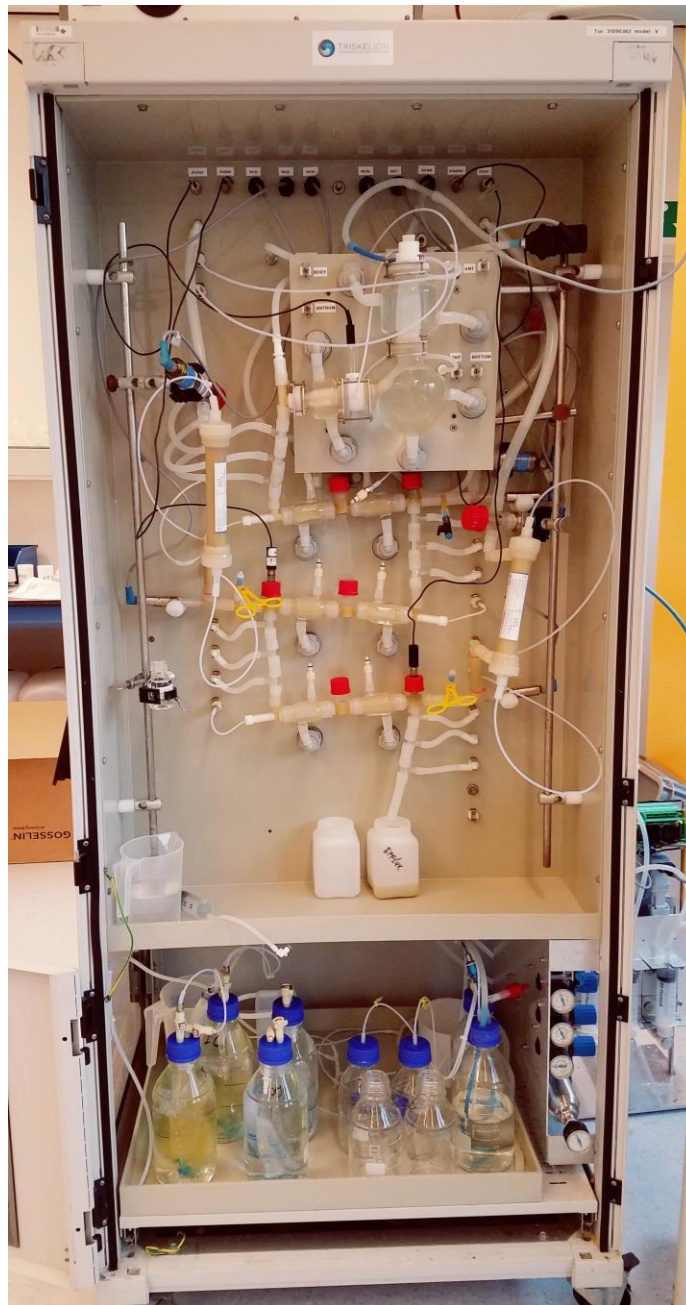


Figure 2.3 Photo of the TIM system with an advanced gastric compartment (TIMAgc). Developed by TNO in the Netherlands and now commercialized with The TIM Company.

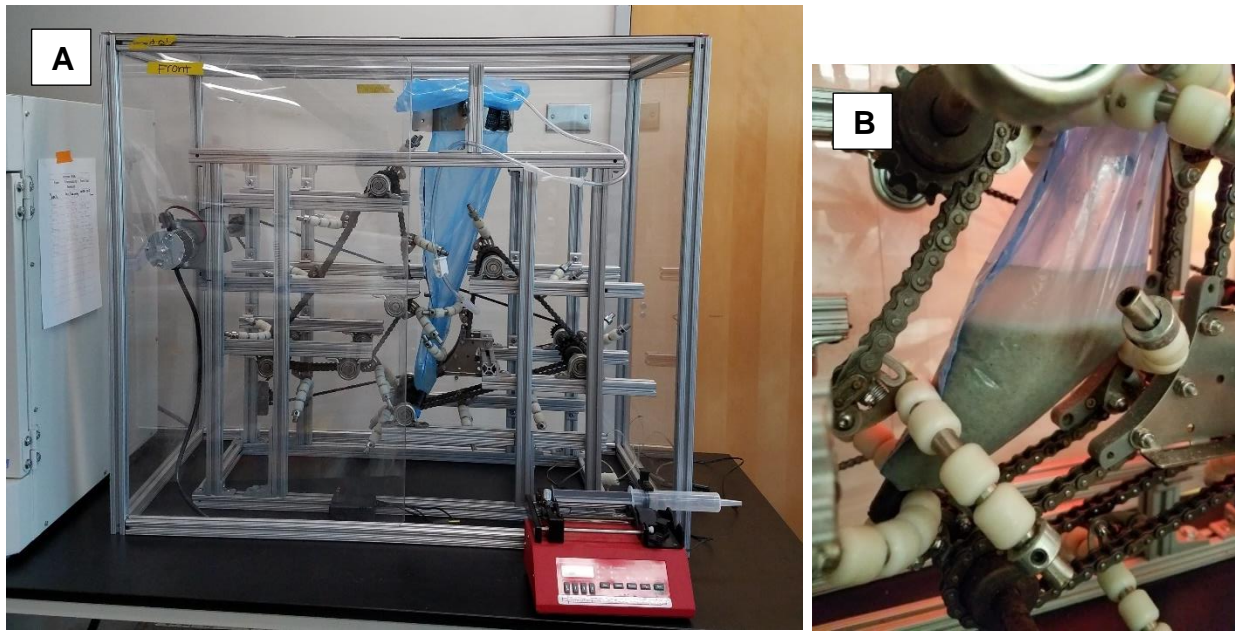


Figure 2.4 Photos of the Human Gastric Simulator (HGS). Initially developed by Kong and Singh (2010) at the University of California, Davis, and later refined to the current version in the laboratory of Dr. Gail Bornhorst at the University of California, Davis. Entire system when not in use (A) and close-up of the gastric compartment while in use (B).

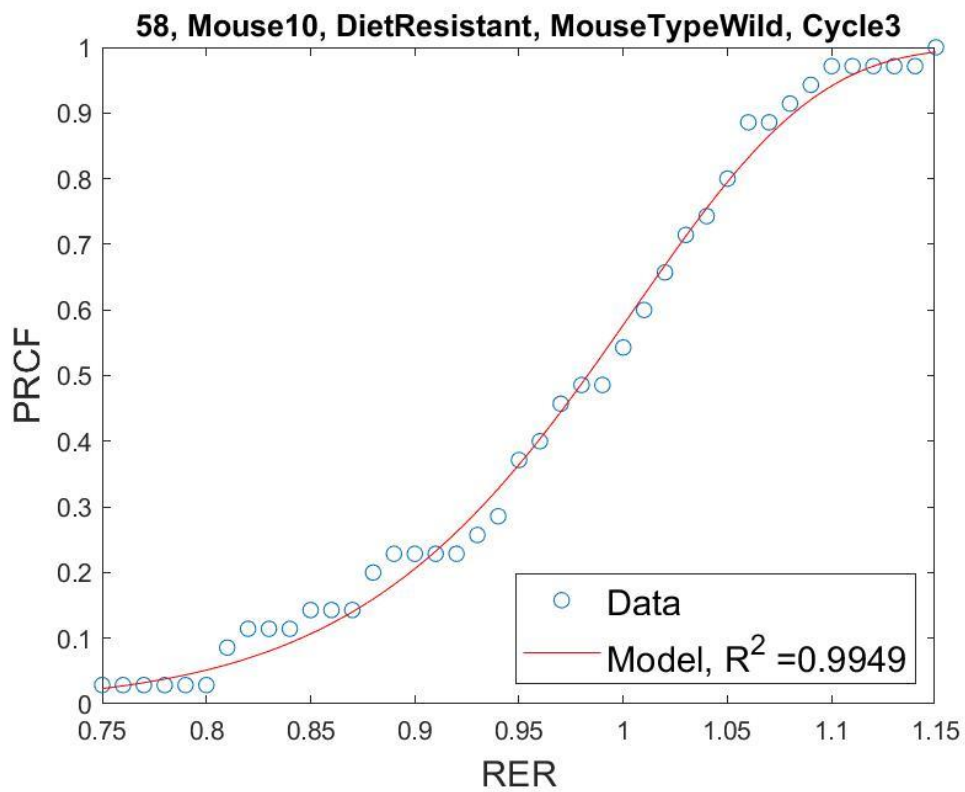


Figure 2.5 Representation of the Weibull Cumulative Distribution function fit to data. PRCF, percent relative cumulative frequency; RER, respiratory exchange ratio.

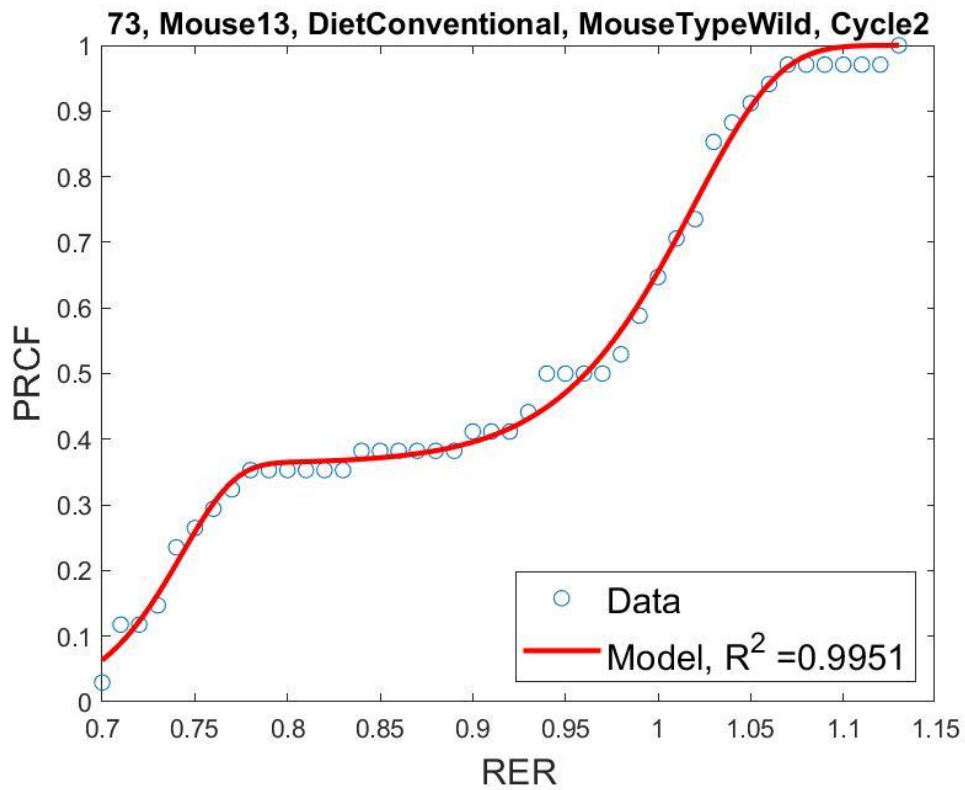


Figure 2.6 Representation of the Weibull Cumulative Distribution function fit to data. PRCF, percent relative cumulative frequency; RER, respiratory exchange ratio.

## CHAPTER 3. PEARL MILLET (*Pennisetum glaucum*) COUSCOUS BREAKS DOWN FASTER THAN WHEAT COUSCOUS IN THE HUMAN GASTRIC SIMULATOR, THOUGH HAS SLOWER STARCH HYDROLYSIS

Reprinted with permission. Full citation:

Hayes, A. M. R., Swackhamer, C., Mennah-Govela, Y. A., Martinez, M. M., Diatta, A., Bornhorst, G. M., & Hamaker, B. R. (2020). Pearl millet (*Pennisetum glaucum*) couscous breaks down faster than wheat couscous in the Human Gastric Simulator, though has slower starch hydrolysis. *Food & Function*, 11(1), 111-122. doi: 10.1039/c9fo01461f.

### 3.1 Abstract

Consumption of traditional West African pearl millet (*Pennisetum glaucum*) couscous delayed gastric emptying in our recent human study compared to other starch-based foods (white rice, boiled potatoes, pasta). The objective of this study was to determine whether physical properties of pearl millet couscous affect particle breakdown and starch hydrolysis during simulated gastric digestion to understand the basis of the slow gastric emptying. Starch fine structure and viscosity were analyzed for initial millet and wheat couscous samples by high performance size-exclusion chromatography and the Rapid Visco Analyzer, respectively. Couscous samples were subjected to simulated gastric digestion using the Human Gastric Simulator (HGS), a dynamic model of human gastric digestion. Digesta was collected from the HGS at 30 min intervals over 180 min. Particle size and percent starch hydrolysis of couscous in the digesta were evaluated at each time point. The number of particles per gram of dry mass substantially increased over digestion time for millet couscous ( $p < 0.05$ ), while changed little for the wheat couscous samples. Millet couscous showed lower starch hydrolysis per unit surface area of particles than wheat couscous ( $p < 0.05$ ). Slower starch hydrolysis was associated with smaller ( $p < 0.05$ ) amylose chain length for millet (839-963 DP) than for wheat (1225-1563 DP), which may enable a denser packing of millet starch molecules that impedes hydrolysis. We hypothesize that the slow gastric emptying rate of millet couscous observed in humans may be explained by its slow starch hydrolysis property that could activate the ileal brake system, independent of high particle breakdown rate in the stomach.

## 3.2 Introduction

Increasing prevalence of obesity is indicative of dysregulation in the control of appetite and energy homeostasis. Thus, there is a need for foods with satiating properties that can better promote health. Slow gastric emptying is associated with increased satiety (Halawi et al., 2017; Hellström & Näslund, 2001). Our recent human study showed that couscous made from pearl millet (*Pennisetum glaucum*), a traditional West African food, substantially delayed gastric emptying rate compared to foods typically consumed as part of the Western diet (white rice, boiled potatoes, and pasta) (Cisse et al., 2018). However, the underlying cause of the observed difference was not well understood. Previous research has identified the importance of rate of food breakdown in the stomach and suggested that foods which resist breakdown have a slower gastric emptying rate (Bornhorst, Chang, et al., 2013; Bornhorst, Kostlan, et al., 2013; Bornhorst, Roman, et al., 2013; Bornhorst, Ströbinger, et al., 2013). It is also hypothesized that a slow starch hydrolysis property of pearl millet-based foods, including couscous, plays a role in their slow gastric emptying through activation of the ileal brake feedback mechanism in the body (Fardet, 2015).

The emptying of food from the stomach is a complex process, as it depends on food breakdown, physical properties of digesta, and physiological regulation (Gallier et al., 2014; Gopirajah et al., 2016; G. Zhang et al., 2015). It has been found that food particles larger than approximately 2 mm in size are retained by the pyloric valve through a phenomenon called gastric sieving, which contributes to longer stomach retention times for foods that resist particle breakdown (Guo et al., 2015). Accordingly, foods which break down more slowly in the stomach have been found to delay gastric emptying (L. Marciani et al., 2001). However, gastric emptying rate is also controlled by the presence of macronutrients, including starch and partially hydrolysed starch in the distal small intestine, triggering the ileal brake feedback response (Hasek et al., 2018; Poppitt et al., 2017; Schirra et al., 1996).

The objective of this work was to determine how pearl millet couscous, which will hereafter be referred to as millet couscous, breaks down in a simulated gastric environment and whether it is resistant to breakdown; and to determine starch hydrolysis rate related to potential ileal brake activation. In both procedures, millet was compared to wheat couscous. Three types of millet couscous (self-made with large and small final particle sizes as well as a commercial type from Senegal) were studied along with two types of wheat couscous (self-made small and a

commercial type). Initial flour particle size was controlled and the final couscous particle size was matched in three types of couscous so that effects due to the differences in particle breakdown, and not differences in flour or initial particle size, could be elucidated. Starch fine structural features and rheological properties of initial couscous samples were analyzed.

### **3.3 Materials and Methods**

#### **3.3.1 Raw material preparation**

##### *Couscous materials*

Whole grain pearl millet (*Pennisetum glaucum*) grain was obtained as intact kernels (Alif Group, Dakar, Senegal) to be made into couscous. Commercially prepared millet couscous from Dakar, Senegal was also acquired and evaluated to represent couscous typically consumed in Western Africa (Mme. Deme of Free Work Services, Dakar, Senegal). Wheat flour was obtained from a commercial source (Bob's Red Mill, Milwaukie, OR, USA) and was made into wheat couscous. Commercial wheat couscous was purchased as a comparator (Riviana Foods Inc., Houston, TX, USA).

##### *Couscous pre-processing*

Millet grain was decorticated using an abrasive decorticator (15% loss in mass, resulting in bran removal). The kernels and bran were separated using a sieve shaker (Smico Corp., Oklahoma City, OK, USA) such that particles greater than approximately 1 mm were retained as decorticated kernels and were milled to flour using a pin mill operated at 5.5 rpm (Alpine, 160 Z, Augsburg, Germany). The millet flour was then separated into different particle size fractions using a sieve shaker (Model RX-24, W.S. Tyler Inc., Mentor, OH, USA). Millet flour particles between 300-495  $\mu\text{m}$  were used to make the millet couscous.

Flour for wheat couscous was obtained commercially, so no decortication or milling was necessary. Wheat flour was separated into the same particle size fractions as the millet flour using the procedure described above. Wheat flour particles between 300-495  $\mu\text{m}$  were used to make the wheat couscous.

### ***Couscous preparation***

Couscous was prepared according to a traditional West African method with the expertise of a Senegalese native with more than 15 years of experience preparing couscous. Briefly, flour (500 g wet weight) was weighed and water ( $283 \pm 11$  mL) was gradually added as the mixture was rolled continuously by hand into small couscous particulate spheres. These spheres were then passed through a 1.70 mm or 2.36 mm sieve to constitute the small and large couscous samples, respectively. All retained couscous spheres were sieved again before being steamed in a couscoussier for 14 min over boiling water (100-120°C). For uniformity and storage, samples were dried at 50°C for 240 min following steaming. Prior to simulated gastric digestion, all couscous samples were hydrated with water (2.5:1 g couscous: mL water, wet basis) and steamed 10 min, after which they were immediately used for simulated digestion. In total, five types of couscous were used in this study (Table 3.1).

### **3.3.2 Couscous characterization**

#### ***Rapid Visco Analyzer analysis***

Pasting profiles of couscous (small and large millet couscous combined, small wheat combined with an additional large wheat couscous treatment) without the second steaming step, and raw flours, were determined using a Rapid Visco Analyzer (RVA; model RVA-4, Perten Instruments Instrumentvägen 29, SE-126 53 Hägersten, Sweden) using the Standard 1 protocol supplied with the instrument. This protocol consists of holding at 50°C for 1 min, heating at a rate of 12°C/min to 95°C, equilibrating at 95°C for 2.5 min, cooling at a rate of 12°C/min to 50°C, and holding at 50°C for 2 min. The RVA mixing paddle speed was 960 rpm for the first 10 s and then 160 rpm for the remainder of the experiment. Slurries were made for each sample (3 g dry basis) with water (25 mL for millet flour and wheat flour; 15 mL for millet couscous and wheat couscous).

#### ***Starch fine structure***

Molecular size and unit chain length distribution of amylose and amylopectin (starch structure) were characterized for all couscous samples along with the flour starting materials for the self-made couscous by high performance size-exclusion chromatography (HPSEC) following the procedure of Roman et al. (Roman et al., 2017).

### ***Light microscopy***

Light microscopy was also performed as in Roman et al. (Roman et al., 2017) for all initial flour and couscous samples.

### **3.3.3 Simulated oral and gastric digestion**

#### ***Simulated saliva formulation***

Simulated saliva was prepared according to Bornhorst and Singh (Bornhorst & Singh, 2013). Briefly, mucin (1 g/L, Sigma-Aldrich, St. Louis, MO, USA),  $\alpha$ -amylase (from *Bacillus subtilis*, 1.18 g/L, MP Biomedicals, Catalog Number 100447, 160000 BAU/g activity, Santa Ana, CA, USA), NaCl (0.117 g/L, Avantor Performance Materials, Radnor, PA, USA), KCl (0.149 g/L, ThermoFisher Scientific, Waltham, MA, USA) and NaHCO<sub>3</sub> (2.10 g/L, ThermoFisher Scientific, Waltham, MA, USA) were mixed in deionized water. The concentration of  $\alpha$ -amylase was set to reflect its activity *in vivo* (Mackie & Pangborn, 1990).

#### ***Simulated gastric juice formulation***

Simulated gastric juice was prepared according to Mennah-Govela and Bornhorst (Mennah-Govela et al., 2015). Mucin (1.5 g/L, Sigma-Aldrich, St. Louis, MO, USA), NaCl (8.78 g/L, Sigma-Aldrich, St. Louis, MO, USA), and pepsin from porcine pancreas (1.0 g/L, Sigma-Aldrich, St. Louis, MO, USA) were mixed in deionized water (acidified to pH 1.8 using 3 M HCl). After all components were dissolved, pH was adjusted to 1.8 using 3 M HCl. Pepsin concentration was chosen to provide an activity of 2,000 U/mL in simulated gastric juice (Capuano et al., 2018; Minekus et al., 2014), and pH was set to 1.8 to simulate the fasted pH of gastric juice (Sams et al., 2016).

#### ***Simulated oral and gastric digestion procedure***

Following steaming, 300 g cooked couscous was weighed, and 60 mL of simulated saliva was added (0.2 mL/g) and mixed for 30 s to represent the oral phase (Ozvural & Bornhorst, 2018). Simulated gastric digestions were conducted using the HGS to simulate the peristaltic movement of the human stomach (Figure 3.1). The HGS has been described in detail previously (Dupont et

al., 2019; Phinney, 2013). Briefly, the HGS utilizes rollers to apply a simulated peristaltic wave (3 contractions/minute) to the food and simulated gastric juice (Hocke et al., 2009; L. Marciani et al., 2001; Swackhamer et al., 2019), which are contained in a flexible plastic bag. The temperature is maintained at 37°C.

Simulated gastric digestions were initiated immediately after the oral phase by placing the test meal into the HGS which was preloaded with 75 mL gastric juice preheated to 37°C. A peristaltic pump (Model 13-876-2, ThermoFisher Scientific, Waltham, MA, USA) was used to continuously secrete simulated gastric juice at 2.5 mL/min (Guo et al., 2014, 2015). Simulated gastric digestions were carried out for 180 min, with 90 mL samples of digesta (approximately 100 g wet weight) collected from the simulated pyloric valve every 30 min. The simulated pyloric valve consisted of a small opening (1 cm) in the antral region of the simulated stomach chamber, which released the sample at each predetermined time point. Due to the small initial size of the couscous particles (1.70-2.36 mm), the pyloric valve did not prevent the passage of larger particles. After collection, samples of digesta were analyzed for moisture content, pH, particle size, and reducing sugar content. Digestions were conducted in triplicate except for small millet couscous which was done in quadruplicate.

### **3.3.4 Moisture content**

Digesta was collected at each time point and 3 g, weighed into pre-dried aluminum pans, was dried in a vacuum oven (Lindberg Blue M, Thermo Scientific, Waltham, MA, USA) for 20 h at 120°C (AACCI Method 44-40.01).

### **3.3.5 pH measurement**

Digesta from each time point was placed in a 50 mL conical tube for pH measurement (IQ Scientific IQ150-77 ISFET, Cole-Parmer, Vernon Hills, IL, USA).

### **3.3.6 Particle size analysis**

Image analysis was used to determine the size distribution of couscous particles in the digesta according to a previously described method with minor modifications (Gebauer et al., 2016). Following collection of digesta from the HGS, an aliquot of  $0.48 \pm 0.01$  g was dispersed

into several petri dishes, each containing 20 mL deionized water. Multiple dishes were used for each sample in order to minimize particle overlap. Lugol's iodine solution (5-10  $\mu\text{L}$ ) was added to each petri dish to enhance the contrast between the light field and the particles. Petri dishes were illuminated from underneath using a lightbox (AGPtek HL0163, Brooklyn, NY, USA; color temperature 6000 K). A reference object (ABFO No. 2 photomacrographic standard reference scale) was included in all images for spatial calibration. One image of each dish was captured using a Canon EOS Rebel SL1 digital camera (18 Mega Pixels, APS-C CMOS sensor, Canon USA, INC. San Jose, CA, USA) that was fixed to a vertical support and triggered using a computer interface. The camera settings were: no flash, 35 mm focal length, aperture F8.0, ISO 100, and shutter speed 0.1 s. Images were analyzed using MATLAB (MathWorks, Natick, MA, USA) to determine the total number of particles in each image and the area of each particle. Particles per gram of dry mass was defined as the number of particles in a sample of digesta divided by the dry mass of the sample, as determined by moisture content analysis. The particle size distribution was analyzed by fitting the cumulative area percentage of the particles in each sample to the Rosin-Rammler model (Rosin & Rammler, 1933):

$$C_{area} = 1 - \exp\left(-\left(\frac{x}{x_{50}}\right)^b \ln(2)\right) \quad [1]$$

Where  $C_{area}$  is the cumulative area percentage of each particle (0 to 100%),  $x_{50}$  is the median particle area ( $\text{mm}^2$ ), and  $b$  is the distribution breadth constant (dimensionless). Smaller  $b$  values represent a broader distribution spread. This model has been used by previous researchers to describe the size changes of solid food particles during oral and gastric digestion using image analysis (Bornhorst, Kostlan, et al., 2013; Gebauer et al., 2016; Hedjazi et al., 2013).

### 3.3.7 Starch hydrolysis analysis

Aliquots of digesta samples from each time point were centrifuged at  $1000 \times g$ , upon which the supernatant was mixed with 0.3 M sodium carbonate (200  $\mu\text{L}$ ) and stored until analysis was performed. Reducing sugar content was then quantified using the dinitrosalicylic acid (DNS) method (G. L. Miller, 1959) and expressed as percent starch hydrolysis. Due to differences in surface area resulting from the different particle breakdown profiles observed during the simulated digestion experiments, percent starch hydrolysis at each time point was then divided by the total area of couscous particles from image analysis to obtain a value of starch hydrolysis per unit area

of digested particles (% starch hydrolysis/mm<sup>2</sup>), similar to the approach used by Ratanpaul et al. (Ratanpaul et al., 2018).

### 3.3.8 Relative gastric emptying of solids from the HGS

Samples of digesta were subjected to gravimetric moisture content analysis as described above to determine the solid matter content. The relative gastric emptying of solids was expressed as the remaining dry matter in the HGS at each time point divided by the initial dry matter. Since the overall emptying rate of digesta (90 mL every 30 min) was held constant for all types of couscous, the relative gastric emptying of solids reflected the solids content of digesta samples that were withdrawn from the HGS. For each type of couscous, the curve of relative gastric emptying of solids was fit to a modified power-exponential model used by previous researchers to fit gastric emptying data (Bornhorst, Chang, et al., 2013; Siegel et al., 1988; Urbain et al., 1989):

$$y(t) = 1 - (1 - e^{-kt})^\beta \quad [2]$$

Where  $y(t)$  is the percent of initial dry matter retained in the HGS at time  $t$ ,  $t$  is digestion time (min),  $k$  is the emptying rate parameter (min<sup>-1</sup>), and  $\beta$  is the extrapolated y-intercept from the terminal portion of the curve (dimensionless). The fit was conducted using nonlinear least squares in MATLAB (MathWorks, Natick, MA, USA). The half-time for relative gastric emptying of solids was estimated using Equation 3:

$$t_{1/2} = \frac{\ln(1-0.5^{1/\beta})}{-k} \quad [3]$$

Where  $t_{1/2}$  is the estimated time at which 50% of the dry mass present at time zero was emptied from the HGS (min), and the parameters  $k$  and  $\beta$  were from Equation 2.

### 3.3.9 Statistical analysis

Statistical analysis was conducted using SAS Enterprise Guide 7.1 (SAS Institute, Cary NC, USA). Initial properties of couscous were analyzed using a single factor ANOVA with type of couscous as the factor. Variables that were measured at each time point during simulated gastric digestion (median particle area, particles per gram, moisture content, pH, and starch hydrolysis per unit area) were analyzed using a two factor ANOVA with repeated measures (PROC MIXED). If the  $F$  value of the overall model was significant ( $p < 0.05$ ), post hoc tests were conducted using Tukey's HSD and significance was taken at  $p < 0.05$ .

## 3.4 Results

### 3.4.1 Couscous properties

#### *Rapid Visco Analyzer analysis*

To determine if initial material properties (i.e., viscosity) of couscous could help explain their behavior during simulated gastric digestion, analysis using the Rapid Visco Analyzer (RVA) was conducted. Viscosity profiles obtained using the RVA are shown in Figure 3.2. Wheat couscous exhibited an initial increase in viscosity before heating (0-250 s), referred to as cold swelling, while millet couscous did not. Peak viscosity (at ~320 s and 95°C) was lower for millet couscous than wheat couscous ( $2791 \pm 51$  cP and  $4084 \pm 137$  cP, respectively,  $p < 0.01$ ). The final viscosity measured during RVA was  $8206 \pm 116$  cP for wheat couscous,  $2761 \pm 28$  cP for wheat flour,  $5793 \pm 22$  cP for millet couscous, and  $3887 \pm 11$  cP for millet flour. All final viscosity values were statistically different from each other ( $p < 0.01$ ).

#### *Starch fine structure*

Starch fine structure was analyzed using HPSEC (Table 3.2). No significant differences were observed in amylose hydrodynamic radius, amylopectin hydrodynamic radius, or amylopectin chain lengths between wheat and millet samples. However, there were statistically significant differences in amylose chain length between the wheat and millet flours and couscous [degree of polymerization (DP),  $p < 0.05$ ]. Notably, wheat flour had the highest amylose chain length as represented by DP ( $1563.3 \pm 38.5$  DP), while small and large millet couscous samples had the lowest amylose chain lengths ( $839.0 \pm 42.2$  DP and  $865.8 \pm 24.9$  DP, respectively). All millet samples had smaller amylose chain lengths than wheat samples, although statistically significant differences were not observed across all samples (Table 3.2).

#### *Light microscopy*

Light micrographs of initial wheat and millet flour and couscous samples showed intact cell structures within the particles (Figure 3.3). Average millet cell diameter was estimated to be ~0.4 mm; wheat cells differed more in shape but were of a similar dimension.

### 3.4.2 Particle size analysis

The Rosin-Rammler model (Equation 1) was fit to the cumulative distribution of particle areas as measured using image analysis. It was found that the Rosin-Rammler function provided a good fit to the data as evidenced by a high coefficient of determination, with a minimum  $R^2$  of 0.945 across all types of couscous and gastric sampling time points, and the average  $R^2$  across all treatments of 0.980. Median particle area, as represented by Rosin-Rammler  $x_{50}$  ( $\text{mm}^2$ ), was significantly influenced by digestion time ( $p < 0.01$ ), type of couscous ( $p < 0.01$ ), and their interaction ( $p < 0.01$ ). The particle area of couscous experienced a large and statistically significant decrease throughout the simulated digestion for all types of couscous ( $p < 0.05$ ; Table 3.3). For example,  $x_{50}$  of commercial millet after 30 s of simulated oral phase was  $1.62 \text{ mm}^2$  and decreased to  $0.2 \text{ mm}^2$  for the sample that underwent 180 min of simulated gastric digestion in the HGS.

The spread of the particle size distribution is represented by Rosin-Rammler  $b$  (dimensionless), where a smaller value of  $b$  indicates a wider distribution of particle sizes and a larger value of  $b$  indicates a narrower distribution of particle sizes. Rosin-Rammler  $b$  was significantly influenced by digestion time ( $p < 0.01$ ), type of couscous ( $p < 0.01$ ), and their interaction ( $p < 0.01$ ; Table 3.3). Post-hoc tests showed that statistically significant differences in the value of  $b$  between different types of couscous were only present during the first two time points (after 30 s oral phase, and after 30 s oral phase followed by 30 min gastric digestion, respectively). This suggests that the spread of the particle size distribution was different between types of couscous at the beginning of simulated digestion, but that after 60 min of simulated digestion in the HGS the differences in distribution spread between different types of couscous were no longer significant.

Particle size analysis also allowed for quantification of the number of particles per gram of dry mass in the digesta. Particles per gram of dry mass in the digesta was significantly influenced by digestion time ( $p < 0.01$ ), type of couscous ( $p < 0.01$ ), and their interaction ( $p < 0.01$ ) (Figure 3.4). For all types of millet couscous there was a large and statistically significant increase in particles per gram of dry mass during simulated digestion. For example, small millet couscous had  $7.0 \times 10^3$  particles per gram after 30 s of simulated oral phase, but after 180 min in the HGS had  $88.8 \times 10^3$  particles per gram ( $p < 0.05$ ). Results showed that higher particle breakdown occurred during simulated gastric digestion of millet couscous leading to a substantial and statistically significant

increase in the number of particles per gram dry mass, whereas in wheat couscous there was not a statistically significant increase in the number of particles per gram of dry mass.

### **3.4.3 Starch hydrolysis in the HGS**

Reducing sugar content in the HGS was measured in the liquid phase of centrifuged digesta over the course of the simulated digestion and the percent of starch hydrolysis was divided by the total area of particles at the same time point; the resulting values were expressed as percent starch hydrolysis per unit area of digested particles. Expressing this data on a unit area basis was necessary due to the differences in surface area resulting from particle breakdown during simulated digestion. The percent starch hydrolysis values (without being expressed per unit area) are included in Table 3.4. Starch hydrolysis per unit area in the HGS was significantly influenced by digestion time ( $p < 0.01$ ) and type of couscous ( $p < 0.01$ ), but not their interaction ( $p > 0.05$ ) (Figure 3.5). There was a significant increase in percent starch hydrolysis in the total digestion time per unit area of digested particles for all types of couscous ( $p < 0.05$ ), except for small millet couscous ( $p > 0.05$ ). At the final time point of the simulated gastric digestion (180 min), percent starch hydrolysis per unit area for large millet couscous ( $16.8 \pm 5.0 \times 10^{-3} \% / \text{mm}^2$ ) and for small millet couscous ( $11.8 \pm 1.9 \times 10^{-3} \% / \text{mm}^2$ ) were significantly lower ( $p < 0.05$ ) than for commercial wheat couscous ( $26.3 \pm 3.9 \times 10^{-3} \% / \text{mm}^2$ ).

### **3.4.4 Moisture content**

Moisture content (dry basis) was significantly influenced by digestion time ( $p < 0.01$ ), but not by type of couscous ( $p > 0.05$ ) (Table 3.5). Moisture content of digesta was not significantly different between the five types of couscous from oral phase up to 150 min of simulated gastric digestion. Moisture content of digesta after 180 min ranged from  $4.09 \pm 0.58$  g moisture/g dry mass (wheat small) to  $7.62 \pm 1.79$  (millet small) g moisture/g dry mass.

### **3.4.5 pH**

pH of digesta was significantly influenced by digestion time ( $p < 0.01$ ), but not by type of couscous ( $p > 0.05$ ) (Table 3.5). The pH of digesta decreased throughout the simulated digestion due to the secretion of additional gastric juice. For example, the pH of small millet couscous was

$6.29 \pm 0.09$  after 30 s of simulated oral phase and decreased to  $2.91 \pm 0.32$  after 180 min simulated gastric digestion.

### 3.4.6 Relative gastric emptying of solids from the HGS

Relative gastric emptying of solids in the HGS was fit to Equation 2, and results are shown in Figure 3.6. The model provided a good fit to the data as evidenced by high coefficient of determination ( $R^2$  minimum = 0.997) (Table 3.6). The emptying rate parameter,  $k$  (min<sup>-1</sup>), was significantly influenced by couscous type ( $p < 0.05$ ). Large millet couscous had a significantly higher  $k$  value than commercial wheat couscous ( $p < 0.05$ ). The extrapolated y-intercept from the terminal portion of the curve,  $\beta$ , was not significantly influenced by type of couscous ( $p > 0.05$ ). The half-emptying time  $t_{1/2}$  (min) was significantly influenced by type of couscous ( $p < 0.01$ ). The highest half-emptying times were for commercial wheat couscous and small wheat couscous (240 min and 189 min, respectively). This reflects the slower emptying of solids from the HGS during simulated gastric digestions of commercial wheat couscous and small wheat couscous. It is important to note that these results indicate the emptying of solids as the overall gastric emptying rate of digesta was held constant at 3 mL/min for all types of couscous. The more rapid emptying of solids from millet couscous coincided with a greater degree of breakdown as described in the previous section, indicating that the HGS measures gastric emptying based on particle breakdown.

## 3.5 Discussion

In this study, the Human Gastric Simulator was used to quantify the physical and chemical breakdown of couscous samples during simulated gastric digestion. Previously, other starch-based carbohydrates, such as white and brown rice, have been studied for their physicochemical breakdown properties during gastric digestion (Bornhorst, Ferrua, et al., 2013; Bornhorst, Ströbinger, et al., 2013; Drechsler & Bornhorst, 2018). Millet couscous and other products made from millet have previously shown slow gastric emptying and digestion properties *in vivo* (Alyami, Ladd, et al., 2019; Cisse et al., 2018) and *in vitro* (Annor et al., 2015; Sandhu & Siroha, 2017), yet there is a lack of knowledge of the basis of this response. The objective of this work was to determine how pearl millet couscous breaks down in a simulated gastric environment and quantify the starch hydrolysis of the gastric breakdown products.

Initial properties of couscous samples and flour (for self-made couscous) were characterized by RVA analysis and HPSEC. RVA analysis is a rheological method to characterize suspensions containing starch and water during heating and cooling (Walker et al., 1988). Notable factors with impact on peak viscosity include the extent of amylose leaching, amylose-lipid complex formation, starch granule swelling, friction between swollen granules, and competition for free water between leached amylose and remaining ungelatinized granules (Almeida-Dominguez et al., 1997; Fitzgerald et al., 2003). For the current study, lower water amount was used for couscous samples than for flour samples (25 mL for flours, 15 mL for couscous), because couscous samples were pregelatinized and thus did not absorb water and swell like the intact starch granules in flours. Furthermore, millet couscous did not show a cold swelling property, which could be indicative of either immediate breakdown in the RVA or incomplete gelatinization of starch in millet couscous after the initial 14 min steaming period of preparation. However, it is important to note that for simulated digestions, all couscous samples were steamed an additional 10 min immediately prior to experimentation. Final viscosities from RVA results were compared due to relevance to foods prepared for consumption. Previous researchers found final viscosity to be the most sensitive measurement of intermolecular interactions in maize starch (Juhász & Salgó, 2008). Results indicated that final viscosity was higher for millet flour than for wheat flour ( $3887 \pm 11$  vs.  $2761 \pm 28$  cP,  $p < 0.01$ ). Given its higher viscosity, starch granules in millet flour exhibited greater amylose retrogradation than those in wheat flour (Juhász & Salgó, 2008). No significant amylose-lipid complex formation was evident for any of the samples as determined by differential scanning calorimetry (data not shown), so this would not have impacted the RVA profiles. In contrast to flour samples, wheat couscous exhibited higher final viscosity than millet couscous ( $8206 \pm 116$  vs.  $5793 \pm 22$  cP,  $p < 0.01$ ), indicating higher breakdown of millet couscous to smaller particles. Accordingly, millet couscous appeared paste-like, whereas wheat couscous particles remained intact.

HPSEC was used to determine starch fine structural features, as it was hypothesized that they could help explain the slower starch hydrolysis rate that was found for millet samples. Millet samples had smaller amylose chain length (839-963 DP) than wheat samples (1225-1563 DP;  $p < 0.05$ ; Table 3.2). Amylose of intermediate chain length (667 DP) was previously shown to exhibit a higher propensity to form intermolecular interactions (Jane & Chen, 1992). Although the amylose chain lengths measured for millet samples were somewhat larger than 667 DP, it can be

hypothesized that they also could exhibit increased intermolecular interactions, causing denser matrices that impede starch hydrolysis (B. Zhang et al., 2015). To the authors' knowledge, starch fine structural characteristics have not been previously elucidated for the particular type of pearl millet studied (grown in Senegal), however, the characteristics for wheat are similar to those found by Martinez et al. (Martinez et al., 2018).

Along with initial property measurements of couscous, the particle size of couscous in digesta emptied from the HGS was assessed. It was found that all types of couscous experienced a statistically significant reduction in particle size throughout simulated digestion, however, breakdown of millet couscous was substantial and significantly ( $p < 0.05$ ) higher than that of wheat couscous. For example, after 180 min simulated gastric digestion, large millet couscous particles had a median size of  $0.17 \text{ mm}^2$ , whereas commercial wheat couscous particles had a median size of  $1.06 \text{ mm}^2$  ( $p < 0.05$ ). A range of diameters of 0.37 to 0.59 mm was found for small, large, and commercial millet couscous after back-calculation from the obtained particle areas, assuming 2D circles, from 60 to 180 min in the HGS. This was similar to the initial millet cell diameter estimated from the light micrographs to be about 0.4 mm, suggesting that the simulator reduced the size of the millet couscous to that of individual cells. Additionally, the differences between breakdown of millet couscous and wheat couscous may be due to the presence of gluten in wheat (Delcour et al., 2012), which acts to provide structure in many gluten-containing foods, and may help wheat-based foods resist breakdown. Previous research has shown a decrease in particle size of white and brown rice during gastric processing *in vitro* (Kong & Singh, 2010) and *in vivo* (Bornhorst, Kostlan, et al., 2013). To the authors' knowledge, the particle breakdown of couscous has not previously been studied *in vitro* or *in vivo*.

Starch hydrolysis per unit area of digested particles increased over time for all types of couscous ( $p < 0.05$ ). To control for increases in surface area that occurred due to particle breakdown in the HGS, starch digestion was reported as percent starch hydrolysis per unit area of digested particles. Percent starch hydrolysis per unit area at the final time point in digestion was significantly lower ( $p < 0.05$ ) for large millet couscous ( $16.8 \pm 5.0 \times 10^{-3} \text{ \%}/\text{mm}^2$ ) and small millet couscous ( $11.8 \pm 1.9 \times 10^{-3} \text{ \%}/\text{mm}^2$ ) than for commercial wheat couscous ( $26.3 \pm 3.9 \times 10^{-3} \text{ \%}/\text{mm}^2$ ). Interestingly, starch hydrolysis per unit area increased by only 4% in the final hour of simulated gastric digestion for commercial wheat couscous, whereas there was an 88% increase over the same time period for large millet couscous and 85% increase for commercial millet couscous. This

suggests that the millet starch became more susceptible to hydrolysis in the last hour of digestion, whereas the wheat couscous starch was fully accessible by the end of the second hour of digestion. This finding suggests that changes to millet couscous resulting in an increased rate of starch hydrolysis occur only after two hours of simulated digestion. Previous researchers have found that millet has a slow starch hydrolysis property (Alyami, Ladd, et al., 2019; Annor et al., 2015; Sandhu & Siroha, 2017), lending support for the current results. Since pH profiles were not significantly different among the types of couscous, differences in hydrolysis between different types of couscous cannot be attributed to differences in residual salivary  $\alpha$ -amylase activity during simulated gastric digestion.

Differences in starch hydrolysis could have been due to retention of intact cells in millet couscous after breakdown as well as differences in chemical and/or structural composition of the couscous. The integrity of cell wall structure is a factor that could influence starch hydrolysis. Previous researchers have shown using wheat and sorghum that intact cells slow enzymatic hydrolysis to the inside starch due to hindered transport of enzyme through the cell walls (Bhattarai et al., 2018; Korompokis et al., 2019). Given that the millet couscous particle sizes obtained from 60 to 180 min of simulated digestion were in a similar size range as the initial intact cell, it seems plausible that the lower millet hydrolysis was affected by cell walls. However, cell wall structures were also observed in wheat flour particles that could affect starch hydrolysis. It is possible that millet cell wall structures are more rigid than wheat, thus impeding starch hydrolysis more. Another possibility is that intermediate amylose chain lengths (841-970 DP) for millet samples could have allowed for increased intermolecular interactions (Jane & Chen, 1992) which might have promoted the formation of denser matrices that are more resistant to hydrolysis (B. Zhang et al., 2015). Previous researchers have proposed that microstructural and starch granule features of starchy foods can influence starch hydrolysis (Roman, Sahagun, et al., 2019).

pH of the digesta decreased over time for all types of couscous due to the secretion of gastric juice during simulated digestion. Due to the constant secretion rate of gastric juice, the lack of significant differences in pH between the different couscous samples indicates that they had similar buffering capacity. The relatively high pH values (highest value among treatments at 30 min = 6.48; highest value at 180 min = 4.21) throughout gastric digestion create an environment where activity of salivary  $\alpha$ -amylase could be partially retained.

Relative gastric emptying of solids was greater for millet couscous than wheat couscous, as analyzed by calculating the percentage of initial dry matter that remained in the HGS at each time point. Since the overall emptying rate was held constant at 3 mL/min, differences in relative gastric emptying of solids reflected the solids content of samples withdrawn from the HGS and the relative breakdown of particles that occurred. It is hypothesized that the more rapid breakdown of millet couscous in comparison to wheat couscous led to increased packing density in the antral region of the simulated stomach chamber, allowing a greater amount of solids from millet couscous to be emptied at each time point. Curves representing relative emptying of solids were fit to a modified power-exponential model (Equations 2 and 3) which was used to describe the emptying profile in terms of a kinetic value,  $k$  ( $\text{min}^{-1}$ ), an extrapolated y intercept,  $\beta$ , and an emptying half-time,  $t_{1/2}$  (min). It was found that large millet couscous emptied the most rapidly, with  $k$  value of  $7.03 \text{ min}^{-1}$  and  $t_{1/2}$  of 122 min. Commercial wheat couscous emptied more slowly than large millet couscous, with  $k$  value of  $2.97 \text{ min}^{-1}$  and  $t_{1/2}$  of 146 min ( $p < 0.05$ ). Gastric emptying half-times in this study (122-240 min) were comparable in magnitude to those reported by previous researchers for *in vivo* gastric emptying of brown and white rice meals using the growing pig as a model for the adult human (229 and 227 min, respectively) (Bornhorst, Chang, et al., 2013). In our recent human study conducted in Mali, we found that millet couscous had very slow gastric half-emptying time (5.3 h) (Cisse et al., 2018). It appears that the discrepancy between gastric emptying times of millet couscous measured *in vivo* and in the HGS reflects that gastric emptying *in vivo* is affected by factors other than particle breakdown solely. In the HGS, millet couscous broke down into smaller, more numerous particles than wheat couscous and had a more rapid gastric emptying rate of solids. However, physiological feedback and control mechanisms of gastric emptying *in vivo* are not reproduced by current *in vitro* models. Thus, the results of this study lend support to the hypothesis that physiological controls of gastric emptying may better explain the slow gastric emptying of millet couscous *in vivo*, and that hydrolysis-resistant particles of millet couscous reaching the distal small intestine may activate the ileal brake. The ileal brake mechanism has been shown to delay gastric emptying rate in a dose-dependent manner (L. J. Miller et al., 1981) and when administered as a preload (Cisse et al., 2017). Of note, higher delay in gastric emptying has been related to greater length of small intestine exposure to glucose (Lin et al., 1989). In this study, percent starch hydrolysis of couscous was expressed per unit surface area of particles, and demonstrated that increased surface area by greater particle breakdown of millet

couscous still did not increase starch hydrolysis. Thus, millet particles exiting the stomach could reach the distal small intestine, potentially activating the ileal brake and contributing to the long gastric emptying times for these foods (Cisse et al., 2018). It is also possible that millet couscous, which broke down into smaller particles, could have experienced strong particle-particle interactions, forming a viscous paste in the stomach that slowed gastric emptying in the human study, but was not measured in the HGS. Meals higher in viscosity have been shown to delay gastric emptying rate *in vivo* (L Marciani et al., 2001; Luca Marciani et al., 2000). An area of future research is the measurement of viscosity of foods in the stomach as they undergo breakdown. This study indicates there are future opportunities to understand the mechanisms of gastric emptying and the means by which it is controlled by the body, which could be investigated using a combination of *in vivo* and *in vitro* methods.

### **3.6 Conclusions**

In this study, three types of millet couscous and two types of wheat couscous were digested using the Human Gastric Simulator, a device which simulates the peristaltic motion, continuous secretion of gastric juice, and intermittent emptying of the human stomach. It was found that millet couscous broke down into smaller and more numerous particles than wheat couscous. Millet couscous samples also showed lower percent starch hydrolysis per unit area of digested particles. It is hypothesized that the slow gastric emptying rate of millet couscous observed in humans may be explained by slow hydrolysis in the small intestines that activates the ileal brake mechanism. It was suggested that densely packed starch matrices with intact cell wall structure exist in gastric processed millet couscous particles that are slowly digesting to reach the ileum. This study provides new understanding of the slow gastric emptying of millet couscous, which could provide strategies to make processed foods with this quality for appetite control and extended nutrient (energy) delivery to the body after food consumption.

### **3.7 References**

Almeida-Dominguez, H. D., Suhendro, E. L., & Rooney, L. W. (1997). Factors affecting Rapid Visco Analyser curves for the determination of maize kernel hardness. *Journal of Cereal Science*, 25, 93–102. <https://doi.org/https://doi.org/10.1006/jcrs.1996.0072>

- Alyami, J., Ladd, N., Pritchard, S. E., Hoad, C. L., Sultan, A. A., Spiller, R. C., Gowland, P. A., Macdonald, I. A., Aithal, G. P., Marciani, L., & Taylor, M. A. (2019). Glycaemic, gastrointestinal and appetite responses to breakfast porridges from ancient cereal grains: A MRI pilot study in healthy humans. *Food Research International*, *118*, 49–57. <https://doi.org/10.1016/j.foodres.2017.11.071>
- Annor, G. A., Marcone, M., Corredig, M., Bertoft, E., & Seetharaman, K. (2015). Effects of the amount and type of fatty acids present in millets on their in vitro starch digestibility and expected glycemic index (eGI). *Journal of Cereal Science*, *64*, 76–81. <https://doi.org/10.1016/j.jcs.2015.05.004>
- Bhattacharai, R. R., Dhital, S., Mense, A., Gidley, M. J., & Shi, Y.-C. (2018). Intact cellular structure in cereal endosperm limits starch digestion in vitro. *Food Hydrocolloids*, *81*, 139–148. <https://doi.org/10.1016/j.foodhyd.2018.02.027>
- Bornhorst, G. M., Chang, L. Q., Rutherford, S. M., Moughan, P. J., & Singh, R. P. (2013). Gastric emptying rate and chyme characteristics for cooked brown and white rice meals in vivo. *Journal of the Science of Food and Agriculture*, *93*(12), 2900–2908. <https://doi.org/10.1002/jsfa.6160>
- Bornhorst, G. M., Ferrua, M. J., Rutherford, S. M., Heldman, D. R., & Singh, R. P. (2013). Rheological properties and textural attributes of cooked brown and white rice during gastric digestion in vivo. *Food Biophysics*, *8*(2), 137–150. <https://doi.org/10.1007/s11483-013-9288-1>
- Bornhorst, G. M., Kostlan, K., & Singh, R. P. (2013). Particle size distribution of brown and white rice during gastric digestion measured by image analysis. *Journal of Food Science*, *78*(9), E1383–E1391. <https://doi.org/10.1111/1750-3841.12228>
- Bornhorst, G. M., Roman, M. J., Rutherford, S. M., Burri, B. J., Moughan, P. J., & Singh, R. P. (2013). Gastric digestion of raw and roasted almonds in vivo. *Journal of Food Science*, *78*(11), H1807–H1813. <https://doi.org/10.1111/1750-3841.12274>
- Bornhorst, G. M., & Singh, R. P. (2013). Kinetics of in vitro bread bolus digestion with varying oral and gastric digestion parameters. *Food Biophysics*, *8*(1), 50–59. <https://doi.org/10.1007/s11483-013-9283-6>
- Bornhorst, G. M., Ströbinger, N., Rutherford, S. M., Singh, R. P., & Moughan, P. J. (2013). Properties of gastric chyme from pigs fed cooked brown or white rice. *Food Biophysics*, *8*(1), 12–23. <https://doi.org/10.1007/s11483-012-9277-9>
- Capuano, E., Pellegrini, N., Ntone, E., & Nikiforidis, C. V. (2018). In vitro lipid digestion in raw and roasted hazelnut particles and oil bodies. *Food & Function*, *9*(4), 2508–2516. <https://doi.org/10.1039/c8fo00389k>
- Cisse, F., Erickson, D. P., Hayes, A. M. R., Opekun, A. R., Nichols, B. L., & Hamaker, B. R. (2018). Traditional Malian solid foods made from sorghum and millet have markedly slower gastric emptying than rice, potato, or pasta. *Nutrients*, *10*(2), 124. <https://doi.org/10.3390/nu10020124>
- Cisse, F., Pletsch, E. A., Erickson, D. P., Chegeni, M., Hayes, A. M. R., & Hamaker, B. R. (2017). Preload of slowly digestible carbohydrate microspheres decreases gastric emptying rate of subsequent meal in humans. *Nutrition Research*, *45*, 46–51. <https://doi.org/10.1016/j.nutres.2017.06.009>
- Delcour, J. A., Joye, I. J., Pareyt, B., Wilderjans, E., Brijs, K., & Lagrain, B. (2012). Wheat gluten functionality as a quality determinant in cereal-based food products. *Annual Review of Food Science and Technology*, *3*, 469–492. <https://doi.org/10.1146/annurev-food-022811-101303>

- Drechsler, K. C., & Bornhorst, G. M. (2018). Modeling the softening of carbohydrate-based foods during simulated gastric digestion. *Journal of Food Engineering*, 222, 38–48. <https://doi.org/10.1016/j.jfoodeng.2017.11.007>
- Dupont, D., Alric, M., Blanquet-Diot, S., Bornhorst, G., Cueva, C., Deglaire, A., Denis, S., Ferrua, M., Havenaar, R., Lelieveld, J., Mackie, A. R., Marzorati, M., Menard, O., Minekus, M., Miralles, B., Recio, I., & Van den Abbeele, P. (2019). Can dynamic in vitro digestion systems mimic the physiological reality? *Critical Reviews in Food Science and Nutrition*, 59, 1546–1562. <https://doi.org/10.1080/10408398.2017.1421900>
- Fardet, A. (2015). A shift toward a new holistic paradigm will help to preserve and better process grain products' food structure for improving their health effects. *Food Funct.*, 6(2), 363–382. <https://doi.org/10.1039/C4FO00477A>
- Fitzgerald, M. A., Martin, M., Ward, R. M., Park, W. D., & Shead, H. J. (2003). Viscosity of rice flour: A rheological and biological study. *Journal of Agricultural and Food Chemistry*, 51, 2295–2299. <https://doi.org/10.1021/jf020574i>
- Gallier, S., Rutherford, S. M., Moughan, P. J., & Singh, H. (2014). Effect of food matrix microstructure on stomach emptying rate and apparent ileal fatty acid digestibility of almond lipids. *Food & Function*, 5, 2410–2419. <https://doi.org/10.1039/C4FO00335G>
- Gebauer, S. K., Novotny, J. A., Bornhorst, G. M., & Baer, D. J. (2016). Food processing and structure impact the metabolizable energy of almonds. *Food & Function*, 7(10), 4231–4238. <https://doi.org/10.1039/C6FO01076H>
- Gopirajah, R., Raichurkar, K. P., Wadhwa, R., & Anandharamakrishnan, C. (2016). Glycemic response to fibre rich foods and their relationship with gastric emptying and motor functions: An MRI Study. *Food Funct.*, 7, 3964–3972. <https://doi.org/10.1039/C6FO00659K>
- Guo, Q., Ye, A., Lad, M., Dalglish, D., & Singh, H. (2014). Effect of gel structure on the gastric digestion of whey protein emulsion gels. *Soft Matter*, 10(8), 1214–1223. <https://doi.org/10.1039/c3sm52758a>
- Guo, Q., Ye, A., Lad, M., Ferrua, M., Dalglish, D., & Singh, H. (2015). Disintegration kinetics of food gels during gastric digestion and its role on gastric emptying: An in vitro analysis. *Food and Function*, 6, 756–764. <https://doi.org/10.1039/c4fo00700j>
- Halawi, H., Camilleri, M., Acosta, A., Vazquez-Roque, M., Oduybo, I., Burton, D., Busciglio, I., & Zinsmeister, A. R. (2017). Relationship of gastric emptying or accommodation with satiation, satiety, and postprandial symptoms in health. *American Journal of Gastrointestinal and Liver Physiology*, 313, G442–G447. <https://doi.org/10.1152/ajpgi.00190.2017>
- Hasek, L. Y., Phillips, R. J., Zhang, G., Kinzig, K. P., Kim, C. Y., Powley, T. L., & Hamaker, B. R. (2018). Dietary slowly digestible starch triggers the gut-brain axis in obese rats with accompanied reduced food intake. *Molecular Nutrition & Food Research*, 62(5), 1700117. <https://doi.org/10.1002/mnfr.201700117>
- Hedjazi, L., Guessasma, S., Yven, C., Valle, G. Della, & Salles, C. (2013). Preliminary analysis of mastication dynamics and fragmentation during chewing of brittle cereal foods. *Food Research International*, 54, 1455–1462. <https://doi.org/https://doi.org/10.1016/j.foodres.2013.09.041>
- Hellström, P. M., & Näslund, E. (2001). Interactions between gastric emptying and satiety, with special reference to glucagon-like peptide-1. *Physiology & Behavior*, 74(4–5), 735–741.

- Hocke, M., Schöne, U., Richert, H., Görnert, P., Keller, J., Layer, P., & Stallmach, A. (2009). Every slow-wave impulse is associated with motor activity of the human stomach. *American Journal of Physiology-Gastrointestinal and Liver Physiology*, 296(4), G709–G716. <https://doi.org/10.1152/ajpgi.90318.2008>
- Jane, J.-L., & Chen, J.-F. (1992). Effect of amylose molecular size and amylopectin branch chain length on paste properties of starch. *Cereal Chemistry*, 69, 60–65.
- Juhász, R., & Salgó, A. (2008). Pasting Behavior of Amylose, Amylopectin and Their Mixtures as Determined by RVA Curves and First Derivatives. *Starch - Stärke*, 60(2), 70–78. <https://doi.org/10.1002/star.200700634>
- Kong, F., & Singh, R. P. (2010). A Human Gastric Simulator (HGS) to study food digestion in human stomach. *Journal of Food Science*, 75(9), E627–E635. <https://doi.org/10.1111/j.1750-3841.2010.01856.x>
- Korompokis, K., Brier, N. De, & Delcour, J. A. (2019). Differences in endosperm cell wall integrity in wheat (*Triticum aestivum* L.) milling fractions impact on the way starch responds to gelatinization and pasting treatments and its subsequent enzymatic in vitro digestibility. *Food & Function*, 10, 4674–4684. <https://doi.org/10.1039/c9fo00947g>
- Lin, H. C., Doty, J. E., Reedy, T. J., & Meyer, J. H. (1989). Inhibition of gastric emptying by glucose depends on length of intestine exposed to nutrient. *American Journal of Physiology*, 256, G404–G411.
- Mackie, D. A., & Pangborn, R. M. (1990). Mastication and its influence on human salivary flow and alpha-amylase secretion I. *Physiology & Behavior*, 47(801), 593–595.
- Marciani, L., Gowland, P. A., Fillery-Travis, A., Manoj, P., Wright, J., Smith, A., Young, P., Moore, R., & Spiller, R. C. (2001). Assessment of antral grinding of a model solid meal with echo-planar imaging. *American Journal of Physiology: Gastrointestinal and Liver Physiology*, 280, G844–G849.
- Marciani, L., Gowland, P. A., Spiller, R. C., Manoj, P., Moore, R. J., Young, P., & Fillery-Travis, A. J. (2001). Effect of meal viscosity and nutrients on satiety, intragastric dilution, and emptying assessed by MRI. *American Journal of Physiology. Gastrointestinal and Liver Physiology*, 280(6), G1227–G1233.
- Marciani, Luca, Gowland, P. A., Spiller, R. C., Manoj, P., Moore, R. J., Young, P., Al-Sahab, S., Bush, D., Wright, J., & Fillery-Travis, A. J. (2000). Gastric response to increased meal viscosity assessed by echo-planar magnetic resonance imaging in humans. *Journal of Nutrition*, 130, 122–127.
- Martinez, M. M., Li, C., Okoniewska, M., Mukherjee, I., Vellucci, D., & Hamaker, B. (2018). Slowly digestible starch in fully gelatinized material is structurally driven by molecular size and A and B1 chain lengths. *Carbohydrate Polymers*, 197, 531–539. <https://doi.org/10.1016/j.carbpol.2018.06.021>
- Mennah-Govela, Y. A., Bornhorst, G. M., & Singh, R. P. (2015). Acid diffusion into rice boluses is influenced by rice type, variety, and presence of  $\alpha$ -amylase. *Journal of Food Science*, 80(2), E316–E325. <https://doi.org/10.1111/1750-3841.12750>
- Miller, G. L. (1959). Use of dinitrosalicylic acid reagent for determination of reducing sugar. *Analytical Chemistry*, 31(3), 426–428. <https://doi.org/10.1021/ac60147a030>
- Miller, L. J., Malagelada, J. R., Taylor, W. F., & Go, V. L. (1981). Intestinal control of human postprandial gastric function: the role of components of jejunoileal chyme in regulating gastric secretion and gastric emptying. *Gastroenterology*, 80(4), 763–769.

- Minekus, M., Alming, M., Alvito, P., Ballance, S., Bohn, T., Bourlieu, C., Carrière, F., Boutrou, R., Corredig, M., Dupont, D., Dufour, C., Egger, L., Golding, M., Karakaya, S., Kirkhus, B., Le Feunteun, S., Lesmes, U., Macierzanka, A., Mackie, A., ... Brodkorb, A. (2014). A standardised static in vitro digestion method suitable for food - an international consensus. *Food & Function*, 5(6), 1113–1124. <https://doi.org/10.1039/c3fo60702j>
- Ozvural, E. B., & Bornhorst, G. M. (2018). Chemical and structural characteristics of frankfurters during in vitro gastric digestion as influenced by cooking method and severity. *Journal of Food Engineering*, 229, 102–108. <https://doi.org/10.1016/j.jfoodeng.2017.10.008>
- Phinney, D. M. (2013). *Design, construction, and evaluation of a reactor designed to mimic human gastric digestion*, University of California, Davis. 1548376.
- Poppitt, S. D., Shin, H. S., McGill, A. T., Budgett, S. C., Lo, K., Pahl, M., Duxfield, J., Lane, M., & Ingram, J. R. (2017). Duodenal and ileal glucose infusions differentially alter gastrointestinal peptides, appetite response, and food intake: A tube feeding study. *American Journal of Clinical Nutrition*, 106(3), 725–735. <https://doi.org/10.3945/ajcn.117.157248>
- Ratanpaul, V., Williams, B. A., Black, J. L., & Gidley, M. J. (2018). Apparent amylase diffusion rates in milled cereal grains determined in vitro: potential relevance to digestion in the small intestine of pigs. *Journal of Cereal Science*, 82, 42–48. <https://doi.org/10.1016/j.jcs.2018.05.007>
- Roman, L., Gomez, M., Li, C., Hamaker, B. R., & Martinez, M. M. (2017). Biophysical features of cereal endosperm that decrease starch digestibility. *Carbohydrate Polymers*, 165, 180–188. <https://doi.org/10.1016/j.carbpol.2017.02.055>
- Roman, L., Sahagun, M., Gomez, M., & Martinez, M. M. (2019). Nutritional and physical characterization of sugar-snap cookies: effect of banana starch in native and molten states. *Food & Function*, 10(2), 616–624. <https://doi.org/10.1039/C8FO02266F>
- Rosin, P., & Rammler, E. (1933). The laws governing the fineness of powdered coal. *Journal of the Institute of Fuel*, 7, 29–36.
- Sams, L., Paume, J., Giallo, J., & Carrière, F. (2016). Relevant pH and lipase for in vitro models of gastric digestion. *Food and Function*, 7(1), 30–45. <https://doi.org/10.1039/c5fo00930h>
- Sandhu, K. S., & Siroha, A. K. (2017). Relationships between physicochemical, thermal, rheological and in vitro digestibility properties of starches from pearl millet cultivars. *LWT - Food Science and Technology*, 83, 213–224. <https://doi.org/10.1016/j.lwt.2017.05.015>
- Schirra, J., Katschinski, M., Weidmann, C., Schäfer, T., Wank, U., Arnold, R., & Göke, B. (1996). Gastric emptying and release of incretin hormones after glucose ingestion in humans. *Journal of Clinical Investigation*, 97(1), 92–103. <https://doi.org/10.1172/JCI118411>
- Siegel, J. A., Urbain, J. L., Adler, L. P., Charkes, N. D., Maurer, A. H., Krevsky, B., Knight, L. C., Fisher, R. S., & Malmud, L. S. (1988). Biphasic nature of gastric emptying. *Gut*, 29, 85–89.
- Swackhamer, C., Zhang, Z., Taha, A. Y., & Bornhorst, G. M. (2019). Fatty acid bioaccessibility and structural breakdown from in vitro digestion of almond particles. *Food & Function*, 10(8), 5174–5187. <https://doi.org/10.1039/C9FO00789J>
- Urbain, J.-L., Siegel, J., Charkes, N. D., Maurer, A., Malmud, L., & Fisher, R. (1989). The two-component stomach: effects of meal particle size on fundal and antral emptying. *European Journal of Nuclear Medicine*, 15(5), 254–259. <https://doi.org/10.1007/BF00257543>
- Walker, C. W., Ross, A. S., Wrigley, C. W., & McMaster, G. J. (1988). Accelerated starch-paste characterization with the Rapid Visco-Analyzer. *Cereal Foods World*, 33, 491–494.

- Zhang, B., Dhital, S., & Gidley, M. J. (2015). Densely packed matrices as rate determining features in starch hydrolysis. *Trends in Food Science & Technology*, 43(1), 18–31. <https://doi.org/10.1016/j.tifs.2015.01.004>
- Zhang, G., Hasek, L. Y., Lee, B.-H., & Hamaker, B. R. (2015). Gut feedback mechanisms and food intake: a physiological approach to slow carbohydrate bioavailability. *Food Funct.*, 6(4), 1072–1089. <https://doi.org/10.1039/C4FO00803K>

Table 3.1 Types of couscous. Source of each couscous is given in addition to its initial (before digestion, dry) particle size as determined by sieving.

<b>Couscous type</b>	<b>Source</b>	<b>Initial particle size (mm)</b>
Wheat small	Flour from Bob's Red Mill, Milwaukie, OR, USA Couscous self-made at Purdue University, IN, USA	0.60 - 1.70
Wheat commercial	Riviana Foods Inc., Houston, TX, USA	0.60 - 2.36
Millet small	Grain from Alif Group, Dakar, Senegal Couscous self-made at Purdue University, IN, USA	0.60 - 1.70
Millet large	Grain from Alif Group, Dakar, Senegal Couscous self-made at Purdue University, IN, USA	1.70 - 2.36
Millet commercial	Mme. Deme of Free Work Services, Dakar, Senegal	0.30 - 2.36

Table 3.2 Starch structural characterization of initial (undigested) couscous as well as for flour starting materials used for self-made couscous types. Values in each column that do not share a letter (abc) represent significant differences ( $p < 0.05$ ) between different types of couscous or flour. DP = degree of polymerization. If no letter is shown, there were no statistically significant differences.

	<b>Amylose hydrodynamic radius (nm)</b>	<b>Amylopectin hydrodynamic radius (nm)</b>	<b>Amylopectin short chain length (DP)</b>	<b>Amylopectin long chain length (DP)</b>	<b>Amylose chain length (DP)</b>	<b>Molar ratio of long to short amylopectin chains</b>	<b>Amylose ratio (%)</b>
<b>Wheat flour</b>	43.1 ± 3.7	131.5 ± 0.4	13.1 ± 0.1	38.8 ± 0.5	1563.3 ± 38.5 <sup>a</sup>	0.541 ± 0.012	33.5 ± 2.6
<b>Millet flour</b>	28.9 ± 3.8	131.2 ± 1.1	14.7 ± 0.1	38.9 ± 0.2	962.6 ± 26.5 <sup>bc</sup>	0.532 ± 0.002	29.9 ± 2.7
<b>Small wheat couscous</b>	33.5 ± 0.4	130.1 ± 6.7	13.3 ± 0.2	39.1 ± 0.5	1224.9 ± 105.7 <sup>b</sup>	0.550 ± 0.004	34.7 ± 0.2
<b>Commercial wheat couscous</b>	27.5 ± 0.0	133.1 ± 0.0	16.1 ± 3.0	37.2 ± 2.4	1250.5 ± 123.2 <sup>ab</sup>	0.593 ± 0.042	35.6 ± 0.3
<b>Small millet couscous</b>	26.3 ± 7.0	131.9 ± 5.9	14.9 ± 0.1	38.7 ± 0.1	839.0 ± 42.2 <sup>c</sup>	0.540 ± 0.009	33.8 ± 4.1
<b>Large millet couscous</b>	25.0 ± 4.6	132.3 ± 7.4	14.9 ± 0.1	39.1 ± 0.3	865.8 ± 24.9 <sup>c</sup>	0.533 ± 0.004	32.6 ± 3.2
<b>Commercial millet couscous</b>	27.1 ± 0.5	128.2 ± 6.9	14.6 ± 0.2	38.0 ± 1.6	939.0 ± 47.1 <sup>bc</sup>	0.598 ± 0.122	38.2 ± 9.3

Table 3.3 Median particle size, quantified by Rosin-Rammler  $x_{50}$  (Equation 1), and particle size distribution spread parameter, quantified by Rosin-Rammler  $b$  (Equation 1), for particles in digesta withdrawn from the HGS at different time points and for different types of couscous. All values are means of multiple runs in the HGS ( $n=3$  runs, except for millet small which was  $n=4$ )  $\pm$  standard deviation. Values in each column that do not share a letter (abc) represent significant differences ( $p<0.05$ ) within a certain type of couscous across different digestion times. Values in each row that do not share a letter (zyx) represent significant differences ( $p<0.05$ ) within a certain time point across different types of couscous. If no letter is shown, there were no statistically significant differences.

Digestion time (min)	$x_{50}(mm^2)$					$b$ (dimensionless)				
	Wheat small	Wheat commercial	Millet small	Millet large	Millet commercial	Wheat small	Wheat commercial	Millet small	Millet large	Millet commercial
<b>0.5</b>	2.09 $\pm$ 0.73 <sup>a,yx</sup>	3.77 $\pm$ 0.11 <sup>a,z</sup>	1.45 $\pm$ 0.09 <sup>a,w</sup>	2.39 $\pm$ 0.30 <sup>a,y</sup>	1.62 $\pm$ 0.52 <sup>a,xw</sup>	1.33 $\pm$ 0.03 <sup>a,yx</sup>	1.72 $\pm$ 0.36 <sup>a,z</sup>	1.47 $\pm$ 0.12 <sup>a,zy</sup>	1.06 $\pm$ 0.26 <sup>x</sup>	1.09 $\pm$ 0.21 <sup>x</sup>
<b>30</b>	0.75 $\pm$ 0.19 <sup>b,y</sup>	2.27 $\pm$ 0.63 <sup>bc,z</sup>	0.15 $\pm$ 0.02 <sup>b,y</sup>	0.16 $\pm$ 0.02 <sup>b,y</sup>	0.42 $\pm$ 0.10 <sup>b,y</sup>	1.10 $\pm$ 0.15 <sup>ab,z</sup>	0.82 $\pm$ 0.02 <sup>b,zy</sup>	1.03 $\pm$ 0.05 <sup>b,zy</sup>	0.99 $\pm$ 0.04 <sup>zy</sup>	0.79 $\pm$ 0.01 <sup>y</sup>
<b>60</b>	0.56 $\pm$ 0.06 <sup>b,y</sup>	1.53 $\pm$ 0.41 <sup>de,z</sup>	0.14 $\pm$ 0.02 <sup>b,y</sup>	0.15 $\pm$ 0.03 <sup>b,y</sup>	0.25 $\pm$ 0.05 <sup>b,y</sup>	1.08 $\pm$ 0.14 <sup>ab</sup>	0.84 $\pm$ 0.07 <sup>b</sup>	1.09 $\pm$ 0.01 <sup>b</sup>	1.10 $\pm$ 0.05	0.88 $\pm$ 0.03
<b>90</b>	0.59 $\pm$ 0.03 <sup>b,y</sup>	1.61 $\pm$ 0.65 <sup>ce,z</sup>	0.16 $\pm$ 0.03 <sup>b,y</sup>	0.14 $\pm$ 0.03 <sup>b,y</sup>	0.23 $\pm$ 0.04 <sup>b,y</sup>	1.07 $\pm$ 0.07 <sup>ab</sup>	0.90 $\pm$ 0.17 <sup>b</sup>	1.02 $\pm$ 0.04 <sup>b</sup>	1.11 $\pm$ 0.03	0.90 $\pm$ 0.04
<b>120</b>	0.57 $\pm$ 0.09 <sup>b,y</sup>	2.50 $\pm$ 0.34 <sup>b,z</sup>	0.13 $\pm$ 0.03 <sup>b,y</sup>	0.12 $\pm$ 0.03 <sup>b,y</sup>	0.19 $\pm$ 0.01 <sup>b,y</sup>	1.11 $\pm$ 0.10 <sup>ab</sup>	0.86 $\pm$ 0.11 <sup>b</sup>	1.03 $\pm$ 0.05 <sup>b</sup>	1.10 $\pm$ 0.05	0.92 $\pm$ 0.05
<b>150</b>	0.76 $\pm$ 0.21 <sup>b,y</sup>	1.80 $\pm$ 0.84 <sup>bcd,e,z</sup>	0.27 $\pm$ 0.15 <sup>b,y</sup>	0.11 $\pm$ 0.03 <sup>b,y</sup>	0.19 $\pm$ 0.04 <sup>b,y</sup>	1.01 $\pm$ 0.10 <sup>ab</sup>	0.92 $\pm$ 0.33 <sup>b</sup>	0.90 $\pm$ 0.12 <sup>b</sup>	1.09 $\pm$ 0.08	0.89 $\pm$ 0.04
<b>180</b>	0.85 $\pm$ 0.19 <sup>b,zy</sup>	1.06 $\pm$ 0.76 <sup>de,z</sup>	0.18 $\pm$ 0.12 <sup>b,x</sup>	0.17 $\pm$ 0.07 <sup>b,x</sup>	0.20 $\pm$ 0.09 <sup>b,yx</sup>	0.98 $\pm$ 0.06 <sup>b</sup>	0.81 $\pm$ 0.08 <sup>b</sup>	1.02 $\pm$ 0.25 <sup>b</sup>	0.95 $\pm$ 0.09	0.85 $\pm$ 0.08

Table 3.4 Percent starch hydrolysis (%) of digesta withdrawn from the HGS at different time points and for different types of couscous (not expressed per unit area). All values are means of multiple runs in the HGS ( $n=3$  runs, except for millet small which was  $n=4$ )  $\pm$  standard deviation. Values in each column that do not share a letter (abc) represent significant differences ( $p<0.05$ ) within a certain type of couscous across different digestion times. Values in each row that do not share a letter (zyx) represent significant differences ( $p<0.05$ ) within a certain timepoint across different types of couscous. If no letter is shown, there were no statistically significant differences.

<b>Percent starch hydrolysis (%) in HGS</b>					
<b>Digestion time (min)</b>	<b>Wheat small</b>	<b>Wheat commercial</b>	<b>Millet small</b>	<b>Millet large</b>	<b>Millet commercial</b>
<b>30</b>	1.80 $\pm$ 0.11 <sup>d</sup>	1.64 $\pm$ 0.11 <sup>d</sup>	1.68 $\pm$ 0.01 <sup>c</sup>	1.75 $\pm$ 0.35 <sup>e</sup>	1.73 $\pm$ 0.06 <sup>d</sup>
<b>60</b>	2.39 $\pm$ 0.07 <sup>d</sup>	2.01 $\pm$ 0.34 <sup>cd</sup>	1.86 $\pm$ 0.22 <sup>c</sup>	1.87 $\pm$ 0.15 <sup>de</sup>	2.30 $\pm$ 0.12 <sup>d</sup>
<b>90</b>	3.00 $\pm$ 0.17 <sup>cd</sup>	3.10 $\pm$ 0.57 <sup>bc</sup>	2.22 $\pm$ 0.07 <sup>c</sup>	2.41 $\pm$ 0.25 <sup>de</sup>	2.78 $\pm$ 0.06 <sup>cd</sup>
<b>120</b>	3.94 $\pm$ 0.31 <sup>bc</sup>	3.62 $\pm$ 0.18 <sup>ab</sup>	2.69 $\pm$ 0.11 <sup>bc</sup>	3.01 $\pm$ 0.05 <sup>cd</sup>	3.74 $\pm$ 0.06 <sup>bc</sup>
<b>150</b>	4.44 $\pm$ 0.28 <sup>abc</sup>	4.55 $\pm$ 0.33 <sup>a</sup>	3.79 $\pm$ 0.60 <sup>ab</sup>	4.47 $\pm$ 0.45 <sup>ab</sup>	4.77 $\pm$ 0.18 <sup>ab</sup>
<b>180</b>	5.63 $\pm$ 0.00 <sup>ab,zy</sup>	4.74 $\pm$ 0.34 <sup>a,zy</sup>	4.23 $\pm$ 0.22 <sup>a,y</sup>	4.98 $\pm$ 1.24 <sup>a,zy</sup>	5.75 $\pm$ 0.24 <sup>a,z</sup>

Table 3.5 Moisture content (dry basis, g water/g dry mass) and pH of digesta withdrawn from the HGS at different time points and for different types of couscous. All values are means of multiple runs in the HGS ( $n=3$  runs, except for millet small which was  $n=4$ )  $\pm$  standard deviation. Values in each column that do not share a letter (abc) represent significant differences ( $p<0.05$ ) within a certain type of couscous across different digestion times. Values in each row that do not share a letter (zyx) represent significant differences ( $p<0.05$ ) within a certain time point across different types of couscous. If no letter is shown, there were no statistically significant differences.

Digestion time (min)	Moisture content (g moisture/g dry mass)					pH				
	Wheat small	Wheat commercial	Millet small	Millet large	Millet commercial	Wheat small	Wheat commercial	Millet small	Millet large	Millet commercial
<b>0.5</b>	0.84 $\pm$ 0.09 <sup>b</sup>	0.82 $\pm$ 0.03 <sup>b</sup>	0.80 $\pm$ 0.09 <sup>b</sup>	0.90 $\pm$ 0.10 <sup>c</sup>	0.89 $\pm$ 0.05 <sup>c</sup>	6.38 $\pm$ 0.51 <sup>a</sup>	6.44 $\pm$ 0.32 <sup>a</sup>	6.29 $\pm$ 0.09 <sup>a</sup>	6.48 $\pm$ 0.05 <sup>a</sup>	5.83 $\pm$ 0.17 <sup>a</sup>
<b>30</b>	2.66 $\pm$ 0.35 <sup>ab</sup>	2.93 $\pm$ 0.22 <sup>ab</sup>	1.80 $\pm$ 0.04 <sup>b</sup>	1.81 $\pm$ 0.04 <sup>c</sup>	1.86 $\pm$ 0.08 <sup>c</sup>	4.88 $\pm$ 0.17 <sup>bc</sup>	5.01 $\pm$ 0.15 <sup>bc</sup>	5.35 $\pm$ 0.13 <sup>b</sup>	5.23 $\pm$ 0.09 <sup>bc</sup>	4.98 $\pm$ 0.06 <sup>ab</sup>
<b>60</b>	2.36 $\pm$ 0.11 <sup>ab</sup>	2.83 $\pm$ 0.23 <sup>ab</sup>	1.70 $\pm$ 0.06 <sup>b</sup>	1.68 $\pm$ 0.05 <sup>c</sup>	1.74 $\pm$ 0.12 <sup>c</sup>	5.36 $\pm$ 0.16 <sup>b</sup>	5.14 $\pm$ 0.26 <sup>b</sup>	5.63 $\pm$ 0.10 <sup>ab</sup>	5.63 $\pm$ 0.11 <sup>ab</sup>	5.29 $\pm$ 0.07 <sup>ab</sup>
<b>90</b>	2.51 $\pm$ 0.18 <sup>ab</sup>	3.01 $\pm$ 0.09 <sup>ab</sup>	1.93 $\pm$ 0.60 <sup>b</sup>	1.76 $\pm$ 0.11 <sup>c</sup>	1.66 $\pm$ 0.07 <sup>c</sup>	5.30 $\pm$ 0.43 <sup>b</sup>	4.92 $\pm$ 0.32 <sup>bc</sup>	5.63 $\pm$ 0.24 <sup>ab</sup>	5.62 $\pm$ 0.06 <sup>ab</sup>	5.36 $\pm$ 0.10 <sup>a</sup>
<b>120</b>	2.92 $\pm$ 0.12 <sup>ab</sup>	3.45 $\pm$ 0.10 <sup>ab</sup>	2.26 $\pm$ 0.45 <sup>b</sup>	2.03 $\pm$ 0.20 <sup>c</sup>	2.41 $\pm$ 1.08 <sup>c</sup>	4.76 $\pm$ 0.80 <sup>bcd</sup>	4.58 $\pm$ 0.19 <sup>bcd</sup>	5.37 $\pm$ 0.22 <sup>b</sup>	5.43 $\pm$ 0.14 <sup>bc</sup>	4.96 $\pm$ 0.48 <sup>ab</sup>
<b>150</b>	3.61 $\pm$ 0.21 <sup>ab</sup>	4.21 $\pm$ 0.11 <sup>a</sup>	5.15 $\pm$ 1.83 <sup>a</sup>	3.24 $\pm$ 0.44 <sup>c</sup>	3.21 $\pm$ 0.31 <sup>bc</sup>	4.69 $\pm$ 0.38 <sup>bcd</sup>	4.18 $\pm$ 0.11 <sup>cd</sup>	3.88 $\pm$ 0.94 <sup>c</sup>	4.49 $\pm$ 0.41 <sup>c</sup>	4.37 $\pm$ 0.24 <sup>b</sup>
<b>180</b>	4.09 $\pm$ 0.58 <sup>a,y</sup>	5.16 $\pm$ 0.29 <sup>a,zy</sup>	7.62 $\pm$ 1.79 <sup>a,z</sup>	7.53 $\pm$ 1.82 <sup>b,z</sup>	6.14 $\pm$ 1.53 <sup>ab,zy</sup>	4.21 $\pm$ 0.25 <sup>cd</sup>	3.84 $\pm$ 0.25 <sup>d</sup>	2.91 $\pm$ 0.32 <sup>d</sup>	2.87 $\pm$ 0.39 <sup>d</sup>	3.24 $\pm$ 0.32 <sup>c</sup>

Table 3.6 Parameters of the modified power-exponential model (Equations 2 and 3) for gastric emptying. Values in each column that do not share a letter (abc) represent significant differences ( $p < 0.05$ ) between different types of couscous.

	$k \times 10^3 (\text{min}^{-1})$	$\beta$	$t_{1/2} (\text{min})$	$R^2$
<b>Wheat small</b>	$4.20 \pm 0.59^{\text{ab}}$	$1.14 \pm 0.07$	$189 \pm 25^{\text{ab}}$	$0.999 \pm 0.00$
<b>Wheat commercial</b>	$2.97 \pm 0.86^{\text{bc}}$	$0.99 \pm 0.07$	$240 \pm 49^{\text{a}}$	$0.999 \pm 0.00$
<b>Millet small</b>	$5.28 \pm 2.12^{\text{ab}}$	$1.06 \pm 0.19$	$146 \pm 29^{\text{bc}}$	$0.997 \pm 0.003$
<b>Millet large</b>	$7.03 \pm 0.60^{\text{a}}$	$1.25 \pm 0.06$	$122 \pm 6^{\text{bc}}$	$0.998 \pm 0.001$
<b>Millet commercial</b>	$5.76 \pm 1.09^{\text{ab}}$	$1.13 \pm 0.15$	$137 \pm 10^{\text{bc}}$	$0.998 \pm 0.001$

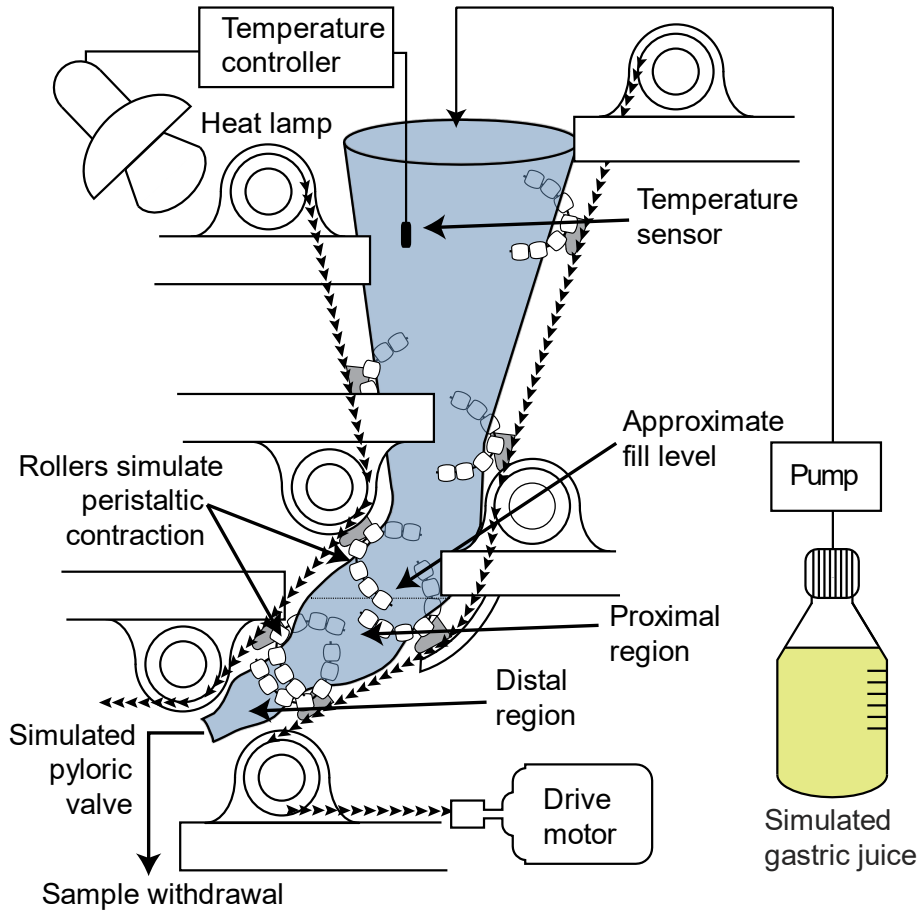


Figure 3.1 Diagram of the Human Gastric Simulator (HGS).

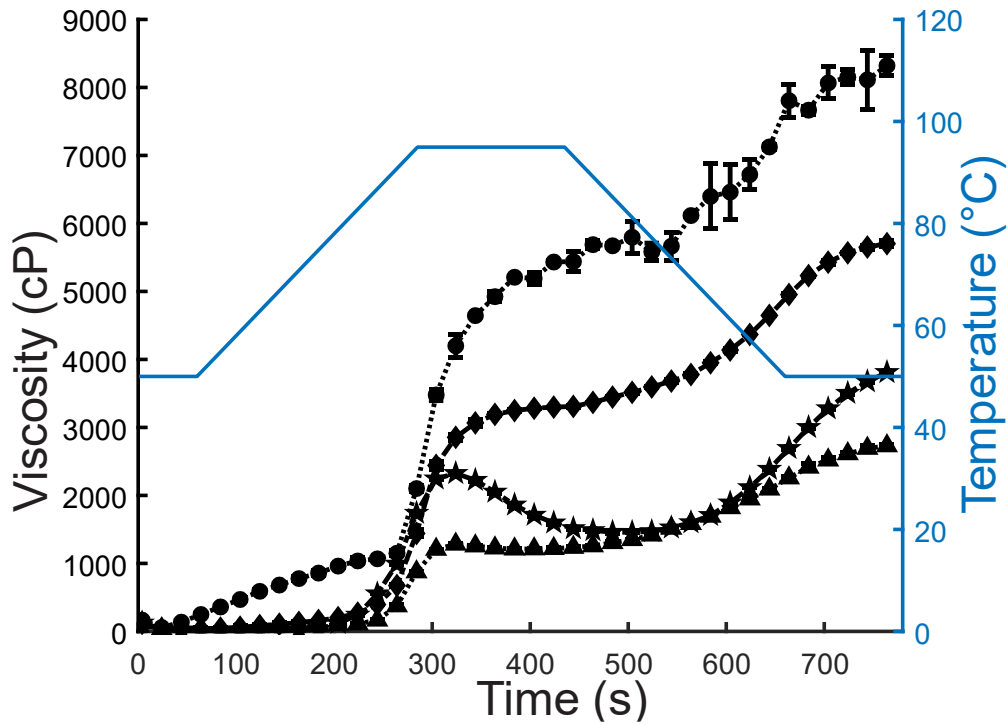


Figure 3.2 RVA profiles of wheat couscous (●), wheat flour (▲), millet couscous (◆), and millet flour (★). Error bars represent the standard deviation of two runs and in some cases may be too small to be seen. Viscosity was recorded every 4 seconds, but for clarity a symbol has been placed on every fifth data point (every 20 s).

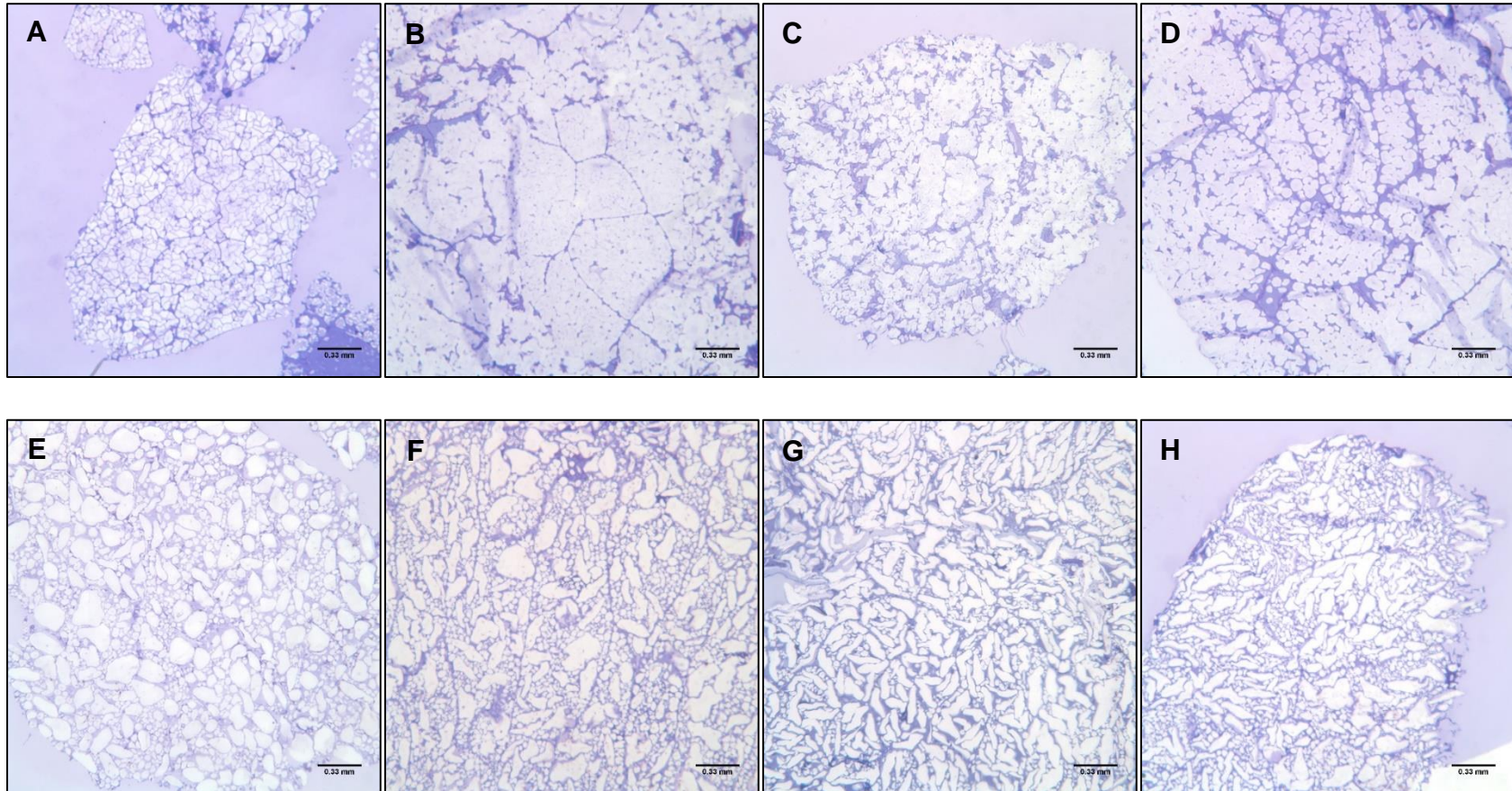


Figure 3.3 Light micrographs (A-H) of the initial flour and couscous samples: millet flour (A), small millet couscous (B), large millet couscous (C), commercial millet couscous (D), wheat flour (E), small wheat couscous (F), large wheat couscous (G), commercial wheat couscous (H).

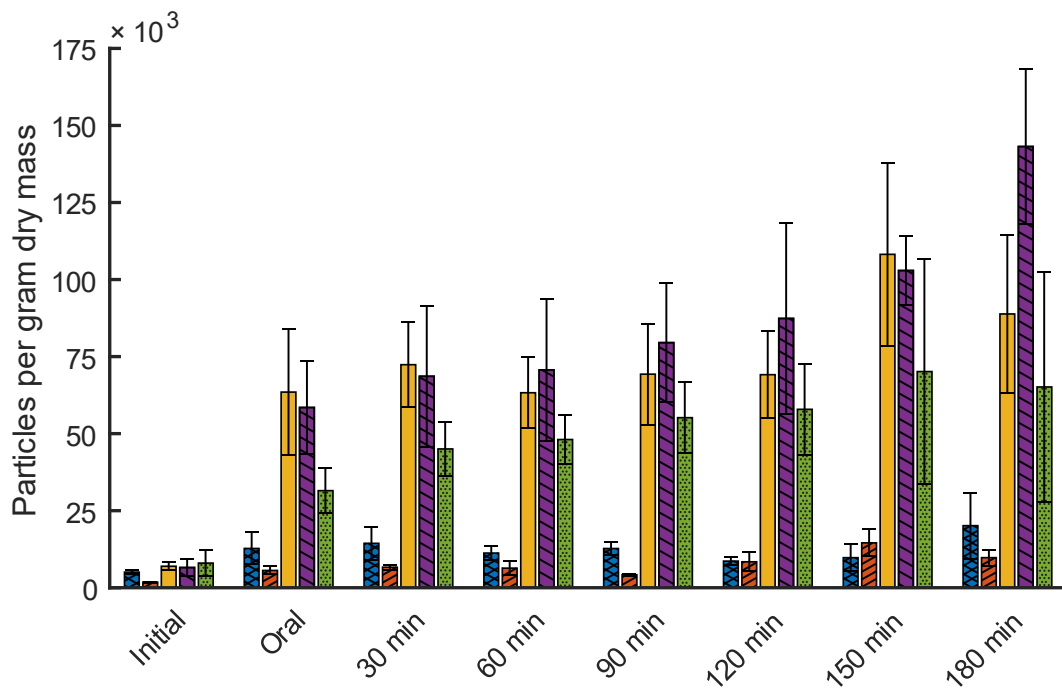


Figure 3.4 Particles per gram dry matter of for digesta of small wheat couscous (blue with white dots), commercial wheat couscous (orange with white dots), small millet couscous (yellow with white dots), large millet couscous (purple with white dots), and commercial millet couscous (green with white dots) during in vitro gastric digestion (initial = no digestion; oral = 30 s simulated oral digestion; 30-180 min = corresponding simulated gastric digestion time). Error bars represent standard deviation of either three or four digestions in the HGS.

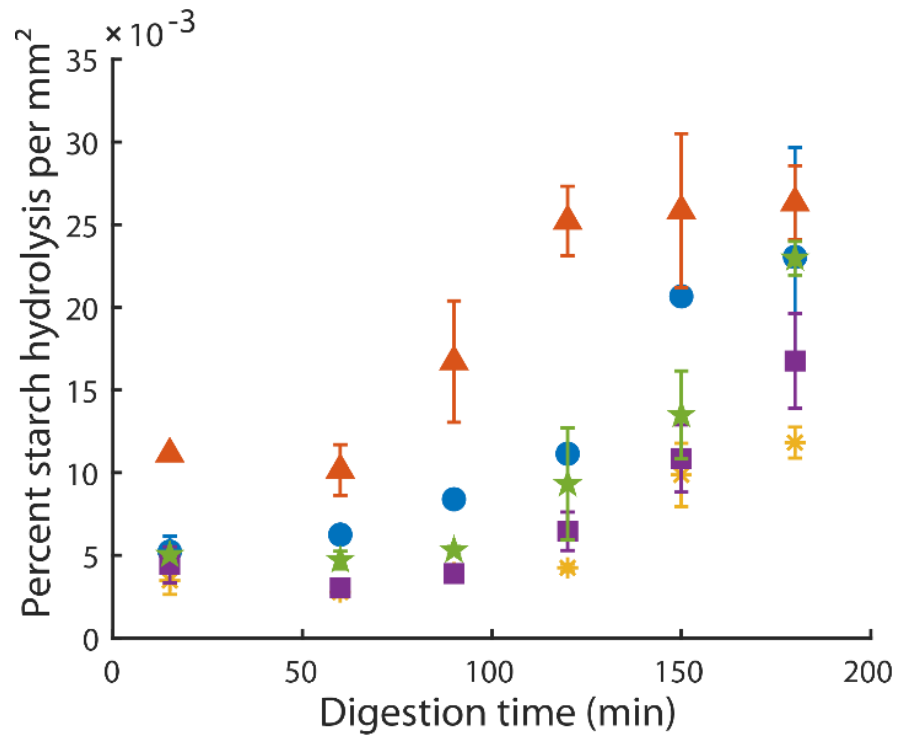


Figure 3.5 Percent starch hydrolysis per unit area of particles in the HGS for small wheat couscous (●), commercial wheat couscous (▲), small millet couscous (\*), large millet couscous (■), and commercial millet couscous (★). Error bars represent the standard error of three runs except for millet small (four runs).

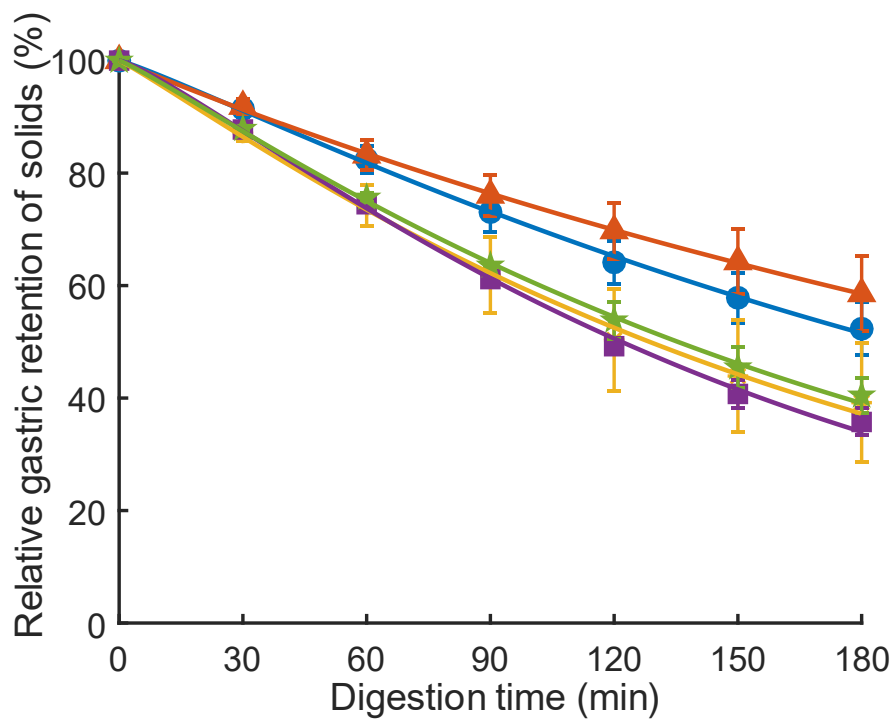


Figure 3.6 Relative solids remaining in the HGS (%), representative of relative gastric emptying, for small wheat couscous (●), commercial wheat couscous (▲), small millet couscous (\*), large millet couscous (■), and commercial millet couscous (★). Error bars represent the standard deviation of three digestions except for small millet couscous (four digestions). Lines represent the model fit (Equation 2).

## CHAPTER 4. SOME PEARL MILLET-BASED FOODS PROMOTE SATIETY OR REDUCE GLYCEMIC RESPONSE IN A CROSSOVER TRIAL

Reprinted with permission. Full citation:

Hayes, A. M. R., Gozzi, F., Diatta, A., Gorissen, T., Swackhamer, C., Bellmann, S., & Hamaker, B. R. (2020). Some pearl millet-based foods promote satiety or reduce glycaemic response in a crossover trial. *British Journal of Nutrition*. doi: 10.1017/S0007114520005036.

### 4.1 Abstract

In a previous trial in Mali, we showed traditional pearl millet couscous and thick porridge delayed gastric emptying (~5 h half-emptying times) in a normal weight population compared to non-traditional carbohydrate-based foods (pasta, potatoes, white rice; ~3 h half-emptying times), and in a gastric simulator we showed millet couscous had slower digestion than wheat couscous. In light of these findings, we tested the hypothesis in a normal weight U.S. population ( $n=14$ ) that millet foods would reduce glycemic response (continuous glucose monitor), improve appetitive sensations (Visual Analog Scale ratings), as well as reduce gastric emptying rate ( $^{13}\text{C}$  octanoic acid breath test). Five carbohydrate-based foods (millet couscous – commercial and self-made, millet thick porridge, wheat couscous, white rice) were fed in a crossover trial matched on available carbohydrate basis. Significantly lower overall glycemic response was observed for all millet-based foods and wheat couscous compared to white rice ( $p\leq 0.05$ ). Millet couscous (self-made) had significantly higher glycemic response than millet couscous (commercial) and wheat couscous ( $p<0.0001$ ), but as there were no differences in peak glucose values ( $p>0.05$ ) an extended glycemic response was indicated for self-made couscous. Millet couscous (self-made) had significantly lower hunger ratings ( $p<0.05$ ) and higher fullness ratings ( $p<0.01$ ) than white rice, millet thick porridge, and millet couscous (commercial). A normal gastric emptying rate (<3 h half-emptying times) was observed for all foods, with no significant differences among them ( $p>0.05$ ). In conclusion, some traditionally prepared pearl millet foods show the potential to reduce glycemic response and promote satiety.

Trial registration identifier: NCT03630458 (ClinicalTrials.gov).

## 4.2 Introduction

In the Sahelian region of West Africa, it is anecdotally known that people who consume foods made from pearl millet (*Pennisetum glaucum*) feel especially “full”, allowing them to go for a long period of time without feeling the need to eat. Thus, these millet foods appear to affect ingestive behavior by prolonging satiety. We previously conducted a human trial in Mali, West Africa, to assess the gastric emptying rate of traditional Sahelian West African foods (couscous and thick porridges made from millet and sorghum) compared to non-traditional carbohydrate foods (white rice, boiled potatoes, pasta) to determine if gastric emptying might be a physiological basis for this apparent satiety property (Cisse et al., 2018). Traditional viscous and non-viscous millet and sorghum foods [millet and sorghum thick porridges, and millet couscous (precooked agglomerated flour particles)] had markedly longer gastric half-emptying times compared to the Western foods (~5 vs. ~3 h, respectively). Viscosity might be one explanation for the slow gastric emptying times of the thick porridges, as high viscosity pudding in one study (Zhu et al., 2013) and a high viscosity locust bean gum paste in another (L Marciani et al., 2001) were shown to slow gastric emptying rate. For millet couscous, we further investigated the reason behind its slow gastric emptying rate using the Human Gastric Simulator, a dynamic model of human gastric digestion (Hayes et al., 2020). Breakdown and digestion properties of millet and wheat couscous were determined in relation to their physicochemical characteristics. Contrary to our thinking that millet couscous particles would be resistant to stomach breakdown and, in turn, slow gastric emptying, they instead broke down into smaller and more numerous particles than wheat couscous and produced a paste-like consistency, perhaps even generating viscosity in the stomach that could delay gastric emptying rate (Hayes et al., 2020). Moreover, the remaining smaller millet couscous particles were found to exhibit lower starch digestibility per unit surface area than wheat couscous particles, supporting that millet has a slow digestion property and may digest locationally into the distal small intestine to trigger the ileal brake (Jain et al., 1989; Poppitt et al., 2017). Related to this, we have found that slowly digestible carbohydrates activated the gut-brain axis and reduced food intake in rats (Hasek et al., 2018). Either one or both of these special properties of millet foods could explain the slower gastric emptying rates observed in the Mali trial.

Here, we examined the potential satiety and glycemic aspects of pearl millet in a U.S. population by testing primary outcomes of glycemic response and gastric emptying rate, and secondary outcomes of appetitive response and breath hydrogen following consumption of millet

couscous versus wheat couscous matched for particle size, along with millet thick porridge and white rice. We gained insight on the role of real-time viscosity of millet couscous in the stomach using the TIM-1 gastrointestinal digestion system equipped with the advanced gastric compartment (TIMagc). Our hypothesis tested, in a U.S. population, was whether millet couscous and/or millet thick porridge modulates postprandial glycemia and produces a satiety response, as well as slows gastric emptying rate.

## **4.3 Methods**

### **4.3.1 Participants and study design**

Participants were recruited from the Purdue University area (West Lafayette, IN, USA). Inclusion criteria were as follows: between 18 and 50 y in age, normal weight ( $18.5 \text{ kg/m}^2 \leq \text{BMI} \leq 25.0 \text{ kg/m}^2$ ), and normal fasting blood glucose ( $<100 \text{ mg/dL}$ ). Participants were excluded if they had any of the following: diabetes (any type); allergy to millet, wheat, and/or gluten allergy or sensitivity; history of or currently experiencing gastrointestinal diseases/disorders; or if pregnant or nursing. Interested potential participants underwent prescreening. Those that fit the inclusion criteria and agreed to participate gave written informed consent to be enrolled in the study. Participant recruitment and study participation proceeded as shown in Figure 4.1.

Following recruitment, enrolled participants participated in a crossover trial with five treatment arms, with one arm taking place per week to allow for a 5-7 day washout period. The order of the treatment arms was randomized to form one sequence, and all participants received the same sequence [millet couscous (self-made), white rice, wheat couscous, millet couscous (commercial), millet thick porridge]. Each arm consisted of two consecutive days. On day one, the continuous glucose monitors were equilibrated and, on day two, one test meal food was consumed as the morning meal with glycemic response, appetitive sensations, gastric emptying, and breath hydrogen measured over 4 h postprandially. The five test meal foods (one per arm) were millet couscous that had been self-made at Purdue University, a commercially available millet couscous from Senegal, wheat couscous that had been self-made at Purdue University, millet thick porridge, and white rice. Couscous were self-made to match for particle size. While participants' familiarity with the test meal foods was not formally assessed, it can be reasonably assumed that all were more familiar with rice and wheat couscous and less familiar with millet thick porridge and millet

couscous. Approximately 5-7 day washout periods were implemented between arms, and the order in which arms were assigned was determined using a random number generator (Microsoft Excel, version 1808). Neither participants nor experimenters were blinded due to the difficulty in masking the nature of the foods. This study was conducted according to the guidelines laid down in the Declaration of Helsinki and procedures involving human participants were approved by the Institutional Review Board at Purdue University under protocol #1706019348. Written informed consent was obtained from all participants. The study was registered at ClinicalTrials.gov with identifier NCT03630458.

#### **4.3.2 Pre-preparation of test meals foods**

Descriptions of the test meal foods are provided in Table 4.1. Whole millet grain (*Pennisetum glaucum*) as intact kernels and commercially available refined millet couscous were obtained from Senegal (grain from Alif Group, Dakar, Senegal; couscous from Mme. Deme of Free Work Services, Dakar, Senegal). Refined wheat flour (Bob's Red Mill, Milwaukie, OR, USA) and medium grain white rice (Nishiki Brand Rice, JFC International Inc., Los Angeles, CA, USA) were obtained commercially. The self-made millet and wheat couscous foods were processed and prepared as in Hayes et al. (2020), with minor modifications.

Briefly, for self-made millet couscous, millet grain was decorticated (15% mass removal by wet weight, indicating removal of bran) using an abrasive decorticator. The resulting kernels were milled into flour using a pin mill (6.5 rpm, Alpine, 160 Z, Augsburg, Germany). Millet flour particles between 0.3 and 0.5 mm were collected using a sieve shaker (Model RX-24, W.S. Tyler Inc., Mentor, OH, USA). Self-made millet couscous was prepared from the resulting flour as in Hayes et al. (2020), with the exception that couscous particles were made in the size range of 1.0 and 2.4 mm. Couscous was prepared via rolling and steaming, dried at 50°C for 4 h, vacuum sealed, and stored at -20°C until test day preparation.

Millet thick porridge was made from millet flour particles between 0.3 and 0.5 mm obtained from the same processing and collection techniques described above for self-made millet couscous. This resulting flour was reserved, vacuum sealed, and stored at -20°C until test day preparation.

For self-made wheat couscous, flour particles (obtained commercially) between 0.3 and 0.5 mm were collected via sieve shaker separation, and couscous (1.0 and 2.4 mm) was prepared

as described above for self-made millet couscous. Commercial millet couscous and white rice were acquired and stored until test day preparation. Available carbohydrate for each test meal food was based on total starch determination using an assay kit [Total Starch Assay Kit (AA/AMG), K-TSTA-50A, Megazyme, Wicklow, Ireland].

### **4.3.3 Test day preparation of test meal foods**

On the morning of the second test day of each arm, the final preparation steps were carried out for each test meal food. For all couscous samples, pre-hydration (0.9 g dry weight couscous:1 mL water) was achieved by gradual incorporation of water with mixing. Couscous samples were then steamed in a couscoussier for 14 min over boiling water (100°C) from a gas stove and weighed into individual portions.

Millet thick porridge was prepared from millet flour according to a traditional method (Cisse et al., 2018; Scheuring et al., 1981). Specifically, one portion of flour (690 g dry weight) was added to water (933 mL) and mixed to make a homogeneous slurry. The slurry was then gradually added to boiling water (2,555 mL; 100°C) on a gas stove and heated for 8 min with continuous stirring at reduced heat to make a thin porridge, traditionally referred to as “bouillie”. A portion (~500 g wet weight) of the resulting thin porridge was removed and reserved. Another portion of flour was gradually added to the remaining thin porridge with continuous stirring until completely incorporated, yielding thick porridge that was paste-like. Intermittent additions of the reserved thin porridge were also made as the dry flour was being added until it was all re-incorporated, in order to ensure the resulting porridge did not become too dry to mix. The final porridge was covered, cooked for 30 min, and then weighed into individual portions.

For the rice preparation, white rice (1116 g dry weight) and water (1674 mL) were placed in a pressure cooker (NESCO PC8-25, Two Rivers, WI, USA) and cooked for 10 min. Cooked rice was weighed into individual portions.

All test meals were served at 55-65°C. Total moisture content was held constant across all test meals by adjusting the amount of water served (130-150 mL) according to estimates of final moisture contents of cooked test meals (~290 mL total water content). Test meal sizes were based on 124 g dry weight available carbohydrate to approximately match the carbohydrate amount in the Mali study (Cisse et al., 2018). A small amount (0.5 g) of butter was added to each test meal before serving to increase palatability. The nutrient and caloric contents of the test meals are shown

in Table 4.1.  $^{13}\text{C}$ -octanoic acid (100 mg) was mixed into each test meal immediately prior to serving as a tracer for gastric emptying assessment.

#### **4.3.4 Test day procedures**

Participants arrived at the testing facilities at 8:00-8:30 a.m. on both consecutive test days per arm. On the first test day, a continuous glucose monitor (CGM) sensor (G4 Platinum, Dexcom, San Diego, CA, USA) was first inserted on the lower left abdomen of each participant. The CGM transmitter (G4 Platinum, Dexcom, San Diego, CA, USA) was then installed and the CGM receiver (G4 Platinum, Dexcom, San Diego, CA, USA) was turned on for an initial equilibration period during which participants were free to leave the testing facilities. Approximately 2 h later (10:00 a.m.), participants returned and two blood finger pricks (Microlet lancing device, Contour glucometer, and Contour blood glucose test strips; Ascensia Diabetes Care, Parsippany, NJ, USA; ReliOn Lancets, San Jose, CA, USA) were taken to calibrate the CGM. Participants were then free to leave the testing facilities for the remainder of the day. No test meal foods were provided on the first test day. Participants were instructed to consume similar foods that were low in fibre the evening of the first test day for each of the study arms as well as to maintain a consistent exercise level for the duration of the study.

On the second test day, participants arrived at the testing facilities after an overnight fast (>10 h). One finger prick blood sample was collected from each participant for CGM calibration. Thereafter, baseline breath samples for gastric emptying (two - 1.5 L bags, Cambridge Isotope Laboratories, Tewksbury, MA, USA) and breath hydrogen (one - 0.25 L bag, QuinTron Instrument Company, Inc., Milwaukee, WI, USA) were collected for each participant and each completed a baseline appetitive sensation survey (Visual Analog Scale [VAS], described below). Following completion of all initial steps, participants were provided one test meal and water, prepared as described above, according to the assigned arm of the study. Participants were instructed to consume the test meal in entirety within 20 min. No other food or drink was allowed for the remainder of the test session. Following test meal consumption, participants completed the following: 1) breathed into 0.30 L bags (Cambridge Isotope Laboratories, Tewksbury, MA, USA) every 15 min in the initial 2 h postprandial period and every 30 min in the 2-4 h postprandial period for assessment of gastric emptying, 2) breathed into 0.25 L bags (QuinTron Instrument Company, Inc., Milwaukee, WI, USA) every 15 min in the initial 2 h postprandial period and every 30 min

in the 2-4 h postprandial period for assessment of breath hydrogen, and 3) completed appetitive sensation surveys (VAS) every 30 min for the entire 4 h postprandial period. Glucose level was measured every 5 min by the CGM. Following completion of all breath collections and assessments during the 4 h postprandial period, CGMs were removed and participants were free to leave the testing facilities.

#### **4.3.5 Glycemic response**

Postprandial interstitial glycemia was measured as a primary outcome by CGM (G4 Platinum, Dexcom, San Diego, CA, USA) to represent glycemic response (Hall et al., 2019; Li et al., 2019). Glucose values during the 4 h postprandial period were corrected by subtracting each participant's baseline glucose value on test day 2 (for each study arm) from the following values to obtain change in glucose ( $\Delta$ Glucose) and then also expressed as glucose incremental area under the curve (iAUC,  $\text{mg}\times\text{min}/\text{dL}$ , including values below baseline). Glycemic response characteristics of peak glucose values ( $\text{mg}/\text{dL}$ ;  $\Delta$ Peak glucose value) and time of peak glucose value (min) were also calculated.

#### **4.3.6 Appetitive sensations**

VAS scales were used to assess participants' subjective feelings of hunger and fullness (in mm, secondary outcome) at baseline and every 30 min in the 4 h postprandial period using an online questionnaire (Qualtrics, Provo, Utah, USA). Participants were sent an email link to the questionnaire at each timepoint, which they promptly completed on the same interface (i.e. personal laptop or cell phone) for all arms of the study.

#### **4.3.7 Gastric emptying**

The  $^{13}\text{C}$  octanoic acid breath test was used to assess gastric emptying rate as has been previously done in our group (Cisse et al., 2018; Pletsch & Hamaker, 2018) according to the method from previous researchers (Braden et al., 1999; M Sanaka et al., 2007; Masaki Sanaka & Nakada, 2010; Schadewaldt et al., 1997; Schoeller et al., 1980), with adjustment for body surface area calculations from Haycock et al. (1978). Breath samples collected for gastric emptying assessment were analyzed within 48 h of collection using a  $^{13}\text{CO}_2$  breath analyser (POCone,

Otsuka Electronics Co., Ltd., Osaka, Japan). Gastric half-emptying time, the time required for half of the  $^{13}\text{C}$  dose to be metabolized (Perri et al., 2005), was calculated as a primary outcome.

Because millet is a C4 plant, it has a higher  $^{13}\text{C}$  to  $^{12}\text{C}$  ratio and possesses more endogenous  $^{13}\text{C}$  than C3 plants (e.g. wheat and rice) (Sage & Monson, 1999). Additional testing proceeded with a subgroup of participants ( $n=4$ ) to determine a corrective factor for  $^{13}\text{C}$  inherent to millet in a similar manner as in Cisse et al. (2018). On three separate test days, participants came to the testing facilities after an overnight fast (>10 h) and consumed one of three test meals (self-made millet couscous, self-made wheat couscous, white rice) that did not contain tracer. Breath samples for gastric emptying were collected in the same manner as above. The resulting values obtained from the breath samples for gastric emptying represented endogenous  $^{13}\text{C}$  in the foods at each timepoint. These values were averaged for the subgroup and subtracted from the corresponding timepoint values for each participant for test meals of the same grain source during the study (Table 4.2). Thereafter, the corrected values representing  $^{13}\text{C}$  at each timepoint were used for modelling percent dose recovery and cumulative percent dose recovery of the tracer, which were then used to calculate gastric half-emptying time (Figure 4.2, example of modelling).

Data for modelling the percent dose recovery and cumulative percent dose recovery of  $^{13}\text{C}$  (corrected for endogenous  $^{13}\text{C}$ ) are shown in Table 4.3. An  $R^2$  of 0.80 for the model fit for percent dose recovery of the  $^{13}\text{C}$  octanoic acid tracer was considered acceptable for data to be included. Lag phase and gastric emptying coefficient values were also calculated for the test meals (Table 4.4).

#### **4.3.8 Analysis of relationship between gastric emptying and glycemc response**

The relationships between gastric half-emptying time and three different glycemc response characteristics (glucose  $\text{iAUC}_{0-120 \text{ min}}$ ,  $\Delta\text{Peak}$  glucose value, and time of peak glucose value) were analyzed using one-way ANOVA with repeated measures per participant (PROC MIXED, SAS version 9.4, SAS Institute, Cary, NC, USA).

#### **4.3.9 Breath hydrogen**

Breath samples collected at baseline and in the 4 h postprandial period on test day 2 were analyzed for breath hydrogen within 24 h as in Pletsch and Hamaker (2018). A BreathTracker

Digital Microlyzer (Quintron Instrument Company, Milwaukee, WI, USA) was used to determine the hydrogen content (ppm), a secondary outcome, in each breath sample.

#### **4.3.10 *In vitro* gastric compartment pressure profiles**

To complement the trial in humans, *in vitro* experiments were performed using a multi-compartmental, computer-controlled gastrointestinal digestion system, TIM-1 (Minekus et al., 1995), equipped with the advanced gastric compartment (TIMagc) (Bellmann et al., 2016). Pressure profiles over time, related to real-time viscosity within the gastric compartment, were measured for millet couscous (self-made), millet thick porridge, wheat couscous, and white rice. Experiments for test meals (44 g dry weight available carbohydrate, based on a three-times down-scale) were conducted in duplicate for 6 h. Test meals were prepared immediately prior to experimentation in a similar manner as above. Experimental procedures followed those used by Bellmann et al. (2019).

#### **4.3.11 Statistical analysis**

A power calculation to determine sample size was conducted based on iAUC for glycemic response, because the calculated sample size was larger than for the gastric half-emptying time. The minimum detectable difference was set at 600 mg/dL with 414 mg/dL standard deviation as observed by Wolever et al. (2016). For five treatment arms and power of 0.8, it was determined that a minimum of 13 participants was required ( $n=13$ ).

Statistical analysis was conducted using SAS version 9.4 (SAS Institute, Cary, NC, USA). Two-way ANOVA (PROC MIXED) with test meal as a fixed effect and participant as a random effect was used to determine statistical significance of differences in glycemic response characteristics and gastric emptying parameters (iAUC<sub>0-120min</sub>, iAUC<sub>0-240min</sub>,  $\Delta$ Peak glucose value, time of peak glucose value, gastric half-emptying time, gastric lag phase, gastric emptying coefficient). Two-way ANOVA with repeated measures (PROC MIXED) with meal and time as fixed effects was conducted for glycemic response ( $\Delta$ Glucose), appetitive sensations (hunger and fullness), and breath hydrogen. For all repeated measures analyses ( $\Delta$ Glucose, hunger, fullness, breath hydrogen), baseline values were included as a covariate in the model according to Blundell et al. (2010). Residuals of all models were plotted and visually assessed for homoscedasticity and

normality using histograms and quantile-quantile plots. Breath hydrogen was not normally distributed and was transformed using Box-Cox ( $\lambda=-0.04$ ). All other data did not require transformation. Significance was considered at  $p<0.05$ , and Tukey's *post hoc* test for multiple comparisons were conducted when the overall model was significant ( $p<0.05$  for  $F$  value).

## 4.4 Results

### 4.4.1 Participant characteristics

Sixteen healthy participants were originally enrolled in the trial, and one participant withdrew after initial assignment to treatment arms, leaving 15 participants. Baseline participant characteristics ( $n=15$ ) are shown in Table 4.5. One enrolled male participant no longer wished to participate in the study after the third treatment and thus was withdrawn; this participant's data from the three completed treatment arms was included in the analyses. In the end, 14 participants (7 males, 7 females) completed the full trial (Figure 4.1).

### 4.4.2 Glycemic response

Glycemic response was expressed as mean changes in glucose from baseline over different timepoints in 5 min increments as assessed by CGM ( $\Delta$ Glucose; Figure 4.3). Statistical analysis revealed  $\Delta$ Glucose was significantly influenced by both time and test meal ( $p<0.001$ ) but not their interaction ( $p=0.90$ ). Overall, for the main effect of test meal, all millet foods as well as wheat couscous had significantly lower glycemic response than white rice [ $p<0.0001$  for millet couscous (commercial), millet thick porridge, wheat couscous vs. white rice;  $p=0.05$  for millet couscous (self-made) vs. white rice]. Millet thick porridge was also significantly lower than both types of millet couscous (commercial and self-made;  $p=0.01$  and  $p<0.0001$ , respectively) and wheat couscous ( $p<0.0001$ ). The significantly higher glycemic response of millet couscous (self-made) compared to millet couscous (commercial) and wheat couscous ( $p<0.0001$ ) may be explained by its visually blunted and extended  $\Delta$ Glucose profile (Figure 4.3), although a treatment-by-time interaction was not observed.

Glycemic response characteristics are shown in Table 4.6. For incremental area under the curve (iAUC) in the 0-240 min postprandial period (iAUC<sub>0-240 min</sub>), millet thick porridge was significantly lower than white rice (4755.7 vs. 6943.7 mg $\times$ min/dL;  $p=0.03$ ). iAUC between 0-120

min in the postprandial period (iAUC<sub>0-120 min</sub>) was also analyzed and significant differences were observed between test meal foods ( $p=0.03$ ). Again, millet thick porridge had significantly lower iAUC<sub>0-120 min</sub> than white rice (2296.3 vs. 4353.0 mg×min/dL;  $p=0.02$ ). Change in peak glucose values ( $\Delta$ Peak glucose) and mean peak times were also calculated for each test meal food (Table 4.6). For mean  $\Delta$ Peak glucose value, significant differences emerged between test meal foods ( $p=0.03$ ), with millet thick porridge exhibiting a significantly lower  $\Delta$ Peak glucose value than white rice (52.8 vs. 69.9 mg/dL;  $p=0.02$ ). For mean peak times, no statistically significant differences were observed between different test meal foods ( $p=0.24$ ).

#### 4.4.3 Appetitive sensations

Appetitive sensations were expressed as VAS ratings (Figures 4.4-4.5). Hunger was significantly influenced by both time and test meal food ( $p<0.0001$ ; Figure 4.4), but not their interaction ( $p=0.91$ ). Additionally, there were statistically significant differences between mean values of hunger in the postprandial period for different test meals (main effects). Notably, millet couscous (self-made) had significantly lower overall hunger ratings than white rice ( $p<0.0001$ ), wheat couscous ( $p=0.02$ ), millet thick porridge ( $p=0.008$ ), and millet couscous (commercial) ( $p=0.002$ ). Fullness was significantly influenced by both time and test meal foods ( $p<0.0001$ ; Figure 4.5), but not their interaction ( $p=0.90$ ). Statistically significant differences between mean values of fullness for different test meal foods in the postprandial period were also observed. Specifically, millet couscous (self-made) had significantly higher overall fullness ratings than white rice ( $p<0.0001$ ), millet thick porridge ( $p=0.0004$ ), and millet couscous (commercial) ( $p<0.0001$ ).

#### 4.4.4 Gastric emptying

Of the 73 <sup>13</sup>C octanoic acid breath tests measured, there were four gastric half-emptying times that were unusually high and did not work well with the established modelling approach (Braden et al., 1999; M Sanaka et al., 2007; Masaki Sanaka & Nakada, 2010; Schadewaldt et al., 1997) (modelling parameters shown in Table 4.3). In one other instance, the R<sup>2</sup> model fit for percent dose recovery was lower than the 0.80 cut-off (R<sup>2</sup>=0.69), and thus the accompanying gastric half-emptying value was not included in subsequent analysis. With this value excluded, the

average  $R^2$  for the model fit to percent dose recovery was  $0.94 \pm 0.04$ , and the average  $R^2$  for the model fit to cumulative percent dose recovery was  $0.9997 \pm 0.0003$ . When examined as a box-plot, a range in half-emptying times per test meal food was apparent (Figure 4.6). Gastric half-emptying times visualized by participant and averaged across all test meal foods revealed four instances of very long gastric half-emptying times (12.0, 13.8, 16.5 and 34.7 h) in a subset of three participants (Figure 4.7). These four instances were deemed to be outliers, because the percent dose recovery of the  $^{13}\text{C}$  tracer plateaued and did not decrease by more than 1% of its peak value during the monitoring period. Even though the model fit was good ( $R^2 \geq 0.93$  for percent dose recovery), the sustained elevation of  $^{13}\text{C}$  percent dose recovery resulted in an overestimation of gastric half-emptying times (see Figure 4.8 for an example of acceptable compared to excluded percent dose recovery curves).

In the end, no significant differences were found among mean gastric half-emptying times for the different test meal foods with outliers removed ( $p=0.18$ ; Figure 4.9). No significant differences were found for lag phase ( $p=0.89$ ). Millet thick porridge had a significantly higher gastric emptying coefficient than white rice ( $p=0.01$ ) and wheat couscous ( $p=0.02$ ). The gastric emptying coefficient parameter is an overall indicator of gastric emptying, though it is worth noting that it lacks a meaningful definition (Masaki Sanaka & Nakada, 2010).

#### **4.4.5 Analysis of relationship between gastric emptying and glycemic response**

No significant effects of gastric half-emptying time on glycemic response characteristics (iAUC<sub>0-120min</sub>,  $\Delta$ Peak glucose value, and time of peak glucose value) were observed, both with and without outliers included (without outliers:  $p=0.37$ ,  $p=0.38$ ,  $p=0.69$ , respectively; with outliers:  $p=0.39$ ,  $p=0.40$ ,  $p=0.73$ , respectively; Figure 4.10).

#### **4.4.6 Breath hydrogen**

Breath hydrogen, as an indicator of fermentation of indigestible carbohydrates in the large intestine (Simren & P-O, 2006), was measured during the postprandial period to determine if carbohydrate fermentation occurred, which could affect glycemic response and gastric emptying. As breath hydrogen values never rose above baseline for any of the treatments, it was concluded that fermentability was not a confounding factor in the study (Figure 4.11).

#### 4.4.7 *In vitro* gastric compartment pressure profiles

Gastric pressure profiles from *in vitro* experiments using the TIMagc showed millet couscous had an initial increase in pressure (~2.5 bar) that was reduced to nearly 0 bar within the first 1 h (Figure 4.12). Millet thick porridge exhibited high pressure (exceeding 10 bar at certain times) at later times than other test meal foods. Pressure profiles for wheat couscous and white rice showed slight initial increases in pressure and remained somewhat elevated (~1 bar) until about 1.5 and 2 h, respectively. All samples exhibited negligible pressure after 2.5 h, because the gastric compartment emptied over time. Pressure values are reflective of viscosity in the stomach.

#### 4.5 Discussion

Pearl millet foods had moderately low glycemic response compared to white rice, and millet couscous (self-made) had comparably high satiety relative to the other foods, with the exception of not having different fullness ratings from wheat couscous. This was despite a lack of difference in gastric half-emptying times that had been an original hypothesis of the study, since our previous work had shown very slow gastric emptying in millet foods in Malian participants. Nevertheless, millet foods may be a viable source of slowly digestible carbohydrates to moderate postprandial glycaemia and possibly food intake.

In the current trial, all millet-based foods and wheat couscous had significantly lower glycemic response than white rice ( $p \leq 0.05$ ). Our initial thinking was that high viscosity itself was the cause of the lower postprandial glycemia values for the two types of millet products, because the millet porridge was a thick, viscous one and, as mentioned above, millet couscous was shown in a gastric simulator to break down quickly and form a kind of paste. However, glycemic effects for viscous starchy foods like the millet thick porridge are different from the low glycemic response effect shown by other researchers for viscous soluble fibres (Repin et al., 2017, 2018), as starch is degraded fairly rapidly in the small intestine with a parallel drop in viscosity. Mlotha et al. (2016) indeed showed that thick maize porridge in Malawi had a high glycemic index. Thus, thick starchy porridges do not necessarily have low glycemic response. For the millet couscous, our postulate that its rapid breakdown in the stomach may result in formation of a viscous paste to slow starch digestion was not borne out in experiments using the TIMagc gastric compartment, where millet couscous had lower pressure at later timepoints than the other foods. Also, the idea

that thick pastes in the stomach would delay gastric emptying rate thereby lowering postprandial glycemia was not supported. We conclude that viscosity was unlikely to be the cause for the lower glycaemia of millet foods, and reasoned that it was caused by a slow carbohydrate digestion property, which has been reported in some millet foods related to retention of intact millet cell wall structures (Hayes et al., 2020), increased intermolecular interactions leading to formation of denser matrices (Hayes et al., 2020; Jane & Chen, 1992; B. Zhang et al., 2015), or the presence of phenolic compounds (Bora et al., 2019). Furthermore, previous studies have found that meal volume can affect gastric emptying rate (Doran et al., 1998; Hunt et al., 1985). Although not measured in this study, from observation, the couscous and rice samples were of a similar volume and the porridge had slightly less volume (though contained more water).

Notably, millet couscous (self-made) had overall lower hunger and higher fullness ratings compared to the other test meal foods (Figures 4.4 and 4.5), which supports the anecdotal feelings of “fullness” reported in West African populations consuming millet foods. However, why millet foods did not consistently promote higher satiety compared to other starchy foods matched in available carbohydrate remains unclear. Related to the anecdotal feeling of promoted satiety reported among individuals in the West African Sahel, it is possible that habitual consumption of millet impacts feelings of satiety through a physiological adaptation or cultural expectation of satiety.

No significant differences in gastric half-emptying times were observed among treatments, which was in contrast to our previous study in Mali showing millet couscous and thick porridge had much slower gastric emptying than non-traditional carbohydrate-based foods including white rice (Cisse et al., 2018) (Figure 4.9). Millet foods have been reported to have a slow carbohydrate digestion property (Annor et al., 2015; Hayes et al., 2020; Sandhu & Siroha, 2017), and we recently linked slow and ileal digestion of carbohydrates to slowed gastric emptying rate in rats (Hasek et al., 2020). Furthermore, we showed ileal digesting carbohydrate activated gut-brain axis signalling to decrease food intake in rats (Hasek et al., 2018). Although the digestive systems of rodents and humans differ in some ways (Dolenšek et al., 2015; Kararli, 1995), the small intestine has common structure and function features for the perception, digestion, and absorption of nutrients (Furness et al., 2015; Hryn et al., 2018). It was an unexpected result that millet foods did not have long gastric half-emptying times, even though this was a primary outcome hypothesis of the study. It is notable that half-emptying times for foods in the current trial were approximately 3 h, which is

comparable to times for white rice, potatoes, and pasta in the Mali study (Cisse et al., 2018). This suggests that the Malian population had the same “baseline” response to foods, but was more sensitive or prone to respond to millet. We speculate that usual consumption of millet-based foods may condition the body to respond by delaying gastric emptying rate, perhaps through a proliferation of ileal enteroendocrine L-cells, as has been observed in the colon in response to fermentable carbohydrates (Cani et al., 2007).

Our findings differ to some degree from two recent studies conducted with pearl millet porridge by Alyami et al. (2019; 2019) in populations in the United Kingdom. Notably, we observed differences in glycemic response but not gastric half-emptying time for pearl millet foods, whereas these previous studies did not find differences in glycemic response but instead observed differences in gastric volume as assessed by magnetic resonance imaging (MRI). However, both studies by Alyami et al. (2019; 2019) incorporated porridges with particle sizes that were not matched, while our study also involved couscous matched for particle size [millet couscous (self-made), wheat couscous (self-made)]; these differences may contribute to our different findings for glycemic response, as particle size of starch-based meals has been shown to affect postprandial glucose levels (Heaton et al., 1988). Lower hunger was reported in one of the previous pearl millet studies (Alyami, Ladd, et al., 2019), which aligns with our present findings. Intriguingly, Alyami et al. (2019) observed a marked decrease in glucose-dependent insulinotropic polypeptide for pearl millet porridge compared to oat porridge; investigating the hormonal responses for millet couscous may be a promising area of future research.

Our study had some strengths as well as limitations. We precisely controlled the preparation of the test meal foods in terms of matching particle sizes of couscous, and cooking and time of cooling prior to serving. Test meal were matched on the amount of available carbohydrate. We also did *in vitro* experiments to gain insight to the potential role of viscosity within the stomach. However, we did not collect blood to measure hormone levels (e.g. glucagon-like peptide 1; GLP-1) that would directly indicate whether or not the ileal brake or gut-brain axis feedback systems were triggered, and we also did not measure insulin. From the food side, although we were unable to obtain commercial millet couscous from exactly the same grain source as used for the self-made millet couscous, both millets were grown locally in Senegal and used in the Dakar market. Still, these different millet grain sources could have somewhat influenced differences in glycemic responses and appetitive sensations. The test meals differed in contents of fat, protein, and energy,

but these did not impact gastric half-emptying times. Other potential limitations include lack of blinding, randomization, and palatability measurements. Lastly, for the  $^{13}\text{C}$  octanoic acid breath test, an assumption made is that the tracer is emptying from the stomach at the same rate as the test meal.

In conclusion, pearl millet-based foods and wheat couscous had lower glycemic responses than white rice in a healthy normal weight U.S. population. In addition, millet couscous (self-made) had lower overall hunger ratings than white rice, millet thick porridge, millet couscous (commercial), and wheat couscous; as well as higher fullness ratings than white rice, millet thick porridge, and millet couscous (commercial). These findings demonstrate the potential of some millet-based foods to enhance satiety and aid in the control of blood glucose. Gastric half-emptying times did not differ among these foods, which was contrary to our previous finding that millet couscous and thick porridge markedly delayed gastric emptying rate in a Malian population (Cisse et al., 2018), and warrants further investigation. Overall, millet-based foods appear to be a source of slowly digestible carbohydrate.

#### 4.6 References

- Alyami, J., Ladd, N., Pritchard, S. E., Hoad, C. L., Sultan, A. A., Spiller, R. C., Gowland, P. A., Macdonald, I. A., Aithal, G. P., Marciani, L., & Taylor, M. A. (2019). Glycaemic, gastrointestinal and appetite responses to breakfast porridges from ancient cereal grains: A MRI pilot study in healthy humans. *Food Research International*, *118*, 49–57. <https://doi.org/10.1016/j.foodres.2017.11.071>
- Alyami, J., Whitehouse, E., Yakubov, G. E., Pritchard, S. E., Hoad, C. L., Blackshaw, E., Heissam, K., Cordon, S. M., Bligh, H. F. J., Spiller, R. C., Macdonald, I. A., Aithal, G. P., Gowland, P. A., Taylor, M. A., & Marciani, L. (2019). Glycaemic, gastrointestinal, hormonal and appetitive responses to pearl millet or oats porridge breakfasts: a randomised, crossover trial in healthy humans. *British Journal of Nutrition*, *122*(10), 1142–1154. <https://doi.org/10.1017/S0007114519001880>
- Annor, G. A., Marcone, M., Corredig, M., Bertoft, E., & Seetharaman, K. (2015). Effects of the amount and type of fatty acids present in millets on their in vitro starch digestibility and expected glycemic index (eGI). *Journal of Cereal Science*, *64*, 76–81. <https://doi.org/10.1016/j.jcs.2015.05.004>
- Bellmann, S., Krishnan, S., de Graaf, A., de Ligt, R. A., Pasman, W. J., Minekus, M., & Havenaar, R. (2019). Appetite ratings of foods are predictable with an in vitro advanced gastrointestinal model in combination with an in silico artificial neural network. *Food Research International*, *122*, 77–86. <https://doi.org/10.1016/j.foodres.2019.03.051>
- Bellmann, S., Lelieveld, J., Gorissen, T., Minekus, M., & Havenaar, R. (2016). Development of an advanced in vitro model of the stomach and its evaluation versus human gastric physiology. *Food Research International*, *88*, 191–198. <https://doi.org/10.1016/j.foodres.2016.01.030>

- Blundell, J., de Graaf, C., Hulshof, T., Jebb, S., Livingstone, B., Lluch, A., Mela, D., Salah, S., Schuring, E., van der Knaap, H., & Westerterp, M. (2010). Appetite control: methodological aspects of the evaluation of foods. *Obesity Reviews*, *11*(3), 251–270. <https://doi.org/10.1111/j.1467-789X.2010.00714.x>
- Bora, P., Ragaee, S., & Marcone, M. (2019). Effect of parboiling on decortication yield of millet grains and phenolic acids and in vitro digestibility of selected millet products. *Food Chemistry*, *274*, 718–725. <https://doi.org/10.1016/j.foodchem.2018.09.010>
- Braden, B., Caspary, W. F., & Lembcke, B. (1999). Nondispersive infrared spectrometry for <sup>13</sup>CO<sub>2</sub>/<sup>12</sup>CO<sub>2</sub>-measurements: a clinically feasible analyzer for stable isotope breath tests in gastroenterology. *Zeitschrift Fur Gastroenterologie*, *37*(6), 477–481. <http://www.ncbi.nlm.nih.gov/pubmed/10427653>
- Cani, P. D., Hoste, S., Guiot, Y., & Delzenne, N. M. (2007). Dietary non-digestible carbohydrates promote L-cell differentiation in the proximal colon of rats. *British Journal of Nutrition*, *98*(1), 32–37. <https://doi.org/10.1017/S0007114507691648>
- Cisse, F., Erickson, D. P., Hayes, A. M. R., Opekun, A. R., Nichols, B. L., & Hamaker, B. R. (2018). Traditional Malian solid foods made from sorghum and millet have markedly slower gastric emptying than rice, potato, or pasta. *Nutrients*, *10*(2), 124. <https://doi.org/10.3390/nu10020124>
- Dolenšek, J., Rupnik, M. S., & Stožer, A. (2015). Structural similarities and differences between the human and the mouse pancreas. *Islets*, *7*(1), e1024405. <https://doi.org/10.1080/19382014.2015.1024405>
- Doran, S., Jones, K. L., Andrews, J. M., & Horowitz, M. (1998). Effects of meal volume and posture on gastric emptying of solids and appetite. *American Journal of Physiology*, *275*(5 Pt 2), R1712–R1718.
- Furness, J. B., Cottrell, J. J., & Bravo, D. M. (2015). COMPARATIVE GUT PHYSIOLOGY SYMPOSIUM: Comparative physiology of digestion1. *Journal of Animal Science*, *93*(2), 485–491. <https://doi.org/10.2527/jas.2014-8481>
- Hall, K. D., Ayuketah, A., Brychta, R., Cai, H., Cassimatis, T., Chen, K. Y., Chung, S. T., Costa, E., Courville, A., Darcey, V., Fletcher, L. A., Forde, C. G., Gharib, A. M., Guo, J., Howard, R., Joseph, P. V., McGehee, S., Ouwkerk, R., Raising, K., ... Zhou, M. (2019). Ultra-processed diets cause excess Calorie intake and weight gain: an inpatient randomized controlled trial of ad libitum food intake. *Cell Metabolism*, *30*, 1–11. <https://doi.org/10.1016/j.cmet.2019.05.008>
- Hasek, L. Y., Phillips, R. J., Hayes, A. M. R., Kinzig, K., Zhang, G., Powley, T. L., & Hamaker, B. R. (2020). Carbohydrates designed with different digestion rates modulate gastric emptying response in rats. *International Journal of Food Sciences and Nutrition*. <https://doi.org/10.1080/09637486.2020.1738355>
- Hasek, L. Y., Phillips, R. J., Zhang, G., Kinzig, K. P., Kim, C. Y., Powley, T. L., & Hamaker, B. R. (2018). Dietary slowly digestible starch triggers the gut-brain axis in obese rats with accompanied reduced food intake. *Molecular Nutrition & Food Research*, *62*(5), 1700117. <https://doi.org/10.1002/mnfr.201700117>
- Haycock, G. B., Schwartz, G. J., & Wisotsky, D. H. (1978). Geometric method for measuring body surface area: A height-weight formula validated in infants, children, and adults. *The Journal of Pediatrics*, *93*(1), 62–66. [https://doi.org/10.1016/S0022-3476\(78\)80601-5](https://doi.org/10.1016/S0022-3476(78)80601-5)

- Hayes, A. M. R., Swackhamer, C., Mennah-Govela, Y. A., Martinez, M. M., Diatta, A., Bornhorst, G. M., & Hamaker, B. R. (2020). Pearl millet (*Pennisetum glaucum*) couscous breaks down faster than wheat couscous in the Human Gastric Simulator, though has slower starch hydrolysis. *Food & Function*, *11*(1), 111–122. <https://doi.org/10.1039/C9FO01461F>
- Heaton, K. W., Marcus, S. N., Emmett, P. M., & Bolton, C. H. (1988). Particle size of wheat, maize, and oat test meals: effects on plasma glucose and insulin responses and on the rate of starch digestion in vitro. *The American Journal of Clinical Nutrition*, *47*(4), 675–682. <https://doi.org/10.1093/ajcn/47.4.675>
- Hryn, V. H., Kostylenko, Y. P., Yushchenko, Y. P., Lavrenko, A. V., & Ryabushko, O. B. (2018). General comparative anatomy of human and white rat digestive systems: a bibliographic analysis. *Wiadomosci Lekarskie*, *71*(8), 1599–1602. <http://www.ncbi.nlm.nih.gov/pubmed/30684346>
- Hunt, J. N., Smith, J. L., & Jiang, C. L. (1985). Effect of meal volume and energy density on the gastric emptying of carbohydrates. *Gastroenterology*, *89*(6), 1326–1330. [https://doi.org/10.1016/0016-5085\(85\)90650-X](https://doi.org/10.1016/0016-5085(85)90650-X)
- Jain, N. K., Boivin, M., Zinsmeister, A. R., Brown, M. L., Malagelada, J.-R. R., & DiMagno, E. P. (1989). Effect of Ileal Perfusion of Carbohydrates and Amylase Inhibitor on Gastrointestinal Hormones and Emptying. *Gastroenterology*, *96*(2), 377–387. [https://doi.org/10.1016/0016-5085\(89\)91561-8](https://doi.org/10.1016/0016-5085(89)91561-8)
- Jane, J.-L., & Chen, J.-F. (1992). Effect of amylose molecular size and amylopectin branch chain length on paste properties of starch. *Cereal Chemistry*, *69*, 60–65.
- Kararli, T. T. (1995). Comparison of the gastrointestinal anatomy, physiology, and biochemistry of humans and commonly used laboratory animals. *Biopharmaceutics & Drug Disposition*, *16*(5), 351–380. <https://doi.org/10.1002/bdd.2510160502>
- Li, M., George, J., Hunter, S., Hamaker, B., Mattes, R., & Ferruzzi, M. G. (2019). Potato product form impacts: In vitro starch digestibility and glucose transport but only modestly impacts 24 h blood glucose response in humans. *Food and Function*, *10*(4), 1846–1855. <https://doi.org/10.1039/c8fo02530d>
- Marciani, L., Gowland, P. A., Spiller, R. C., Manoj, P., Moore, R. J., Young, P., & Fillery-Travis, A. J. (2001). Effect of meal viscosity and nutrients on satiety, intragastric dilution, and emptying assessed by MRI. *American Journal of Physiology. Gastrointestinal and Liver Physiology*, *280*(6), G1227–G1233.
- Mattei, J., Malik, V., Wedick, N. M., Hu, F. B., Spiegelman, D., Willett, W. C., & Campos, H. (2015). Reducing the global burden of type 2 diabetes by improving the quality of staple foods: The Global Nutrition and Epidemiologic Transition Initiative. *Globalization and Health*, *11*(1), 23. <https://doi.org/10.1186/s12992-015-0109-9>
- Minekus, M., Marteau, P., Havenaar, R., & Huis in 't Veld, J. (1995). A multi compartmental dynamic computer-controlled model simulating the stomach and small intestine. *Alternatives to Laboratory Animals (ATLA)*, *23*, 197–209.
- Mlotha, V., Mwangwela, A. M., Kasapila, W., Siyame, E. W. P., & Masamba, K. (2016). Glycemic responses to maize flour stiff porridges prepared using local recipes in Malawi. *Food Science & Nutrition*, *4*(2), 322–328. <https://doi.org/10.1002/fsn3.293>
- Perri, F., Pastore, M. R., & Annese, V. (2005). 13C-octanoic acid breath test for measuring gastric emptying of solids. *European Review for Medical and Pharmacological Sciences*, *9*(5 Suppl 1), 3–8.

- Pletsch, E. A., & Hamaker, B. R. (2018). Brown rice compared to white rice slows gastric emptying in humans. *European Journal of Clinical Nutrition*, 72(3), 367–373. <https://doi.org/10.1038/s41430-017-0003-z>
- Poppitt, S. D., Shin, H. S., McGill, A. T., Budgett, S. C., Lo, K., Pahl, M., Duxfield, J., Lane, M., & Ingram, J. R. (2017). Duodenal and ileal glucose infusions differentially alter gastrointestinal peptides, appetite response, and food intake: A tube feeding study. *American Journal of Clinical Nutrition*, 106(3), 725–735. <https://doi.org/10.3945/ajcn.117.157248>
- Repin, N., Cui, S. W., & Goff, H. D. (2018). Impact of dietary fibre on in vitro digestibility of modified tapioca starch: viscosity effect. *Bioactive Carbohydrates and Dietary Fibre*, 15(October), 2–11. <https://doi.org/10.1016/j.bcdf.2016.11.002>
- Repin, N., Kay, B. A., Cui, S. W., Wright, A. J., Duncan, A. M., & Douglas Goff, H. (2017). Investigation of mechanisms involved in postprandial glycemia and insulinemia attenuation with dietary fibre consumption. *Food & Function*, 8(6), 2142–2154. <https://doi.org/10.1039/C7FO00331E>
- Sage, R. F., & Monson, R. K. (Eds.). (1999). *C4 Plant Biology*. Academic Press.
- Sanaka, M., Yamamoto, T., Anjiki, H., Nagasawa, K., & Kuyama, Y. (2007). Effects of agar and pectin on gastric emptying and post-prandial glycaemic profiles in healthy human volunteers. *Clinical and Experimental Pharmacology and Physiology*, 34(11), 1151–1155.
- Sanaka, Masaki, & Nakada, K. (2010). Stable isotope breath tests for assessing gastric emptying: A comprehensive review. *Journal of Smooth Muscle Research*, 46(6), 267–280.
- Sandhu, K. S., & Siroha, A. K. (2017). Relationships between physicochemical, thermal, rheological and in vitro digestibility properties of starches from pearl millet cultivars. *LWT - Food Science and Technology*, 83, 213–224. <https://doi.org/10.1016/j.lwt.2017.05.015>
- Schadewaldt, P., Schommartz, B., Wienrich, G., Brösicke, H., Piolot, R., & Ziegler, D. (1997). Application of isotope-selective nondispersive infrared spectrometry (IRIS) for evaluation of [<sup>13</sup>C]octanoic acid gastric-emptying breath tests: comparison with isotope ratio–mass spectrometry (IRMS). *Clinical Chemistry*, 43(3), 518–522.
- Scheuring, S., Sidibe, S., & Kante, A. (1981). Sorghum alkali to quality considerations. *Proceedings of the International Symposium on Sorghum Grain Quality; International Crops Research Institute for the Semi-Arid Tropics*.
- Schoeller, D. A., Klein, P. D., Watkins, J. B., Heim, T., & MacLean Jr, W. C. (1980). <sup>13</sup>C abundances of nutrients and the effect of variations in <sup>13</sup>C isotopic abundances of test meals formulated for <sup>13</sup>CO<sub>2</sub> breath tests. *The American Journal of Clinical Nutrition*, 33(11), 2375–2385.
- Simren, M., & P-O, S. (2006). Use and abuse of hydrogen breath tests. *Gut*, 55(3), 297–303. <https://doi.org/10.1136/gut.2005.075127>
- Wolever, T. M., van Klinken, B. J.-W., Bordenave, N., Kaczmarczyk, M., Jenkins, A. L., Chu, Y., & Harkness, L. (2016). Reformulating cereal bars: high resistant starch reduces in vitro digestibility but not in vivo glucose or insulin response; whey protein reduces glucose but disproportionately increases insulin. *The American Journal of Clinical Nutrition*, 104(4), 995–1003. <https://doi.org/10.3945/ajcn.116.132431>
- Zhang, B., Dhital, S., & Gidley, M. J. (2015). Densely packed matrices as rate determining features in starch hydrolysis. *Trends in Food Science & Technology*, 43(1), 18–31. <https://doi.org/10.1016/j.tifs.2015.01.004>

Zhu, Y., Hsu, W. H., & Hollis, J. H. (2013). The Impact of Food Viscosity on Eating Rate, Subjective Appetite, Glycemic Response and Gastric Emptying Rate. *PLoS ONE*, 8(6), e67482. <https://doi.org/10.1371/journal.pone.0067482>

Table 4.1 Test meal foods.

Test meal food	Source	Initial particle size (mm)	Test meal size (g, wet weight)	Protein per test meal (g, dry weight)	Fat per test meal (g, dry weight) <sup>1</sup>	Energy per test meal (kcal) <sup>2</sup>	Available carbohydrate per test meal (g, dry weight)
White rice	Nishiki Brand Rice, JFC International Inc., Los Angeles, CA, USA	Medium grain (~5-6 mm in length)	250.4	10.9	0.7	547.7	124.2
Millet thick porridge	Grain from Alif Group, Dakar, Senegal Processed to flour (0.300-0.495 mm) at Purdue University, IN, USA	0.300-0.495	281.1	17.0	7.2	633.9	124.2
Millet couscous (self-made)	Grain from Alif Group, Dakar, Senegal Couscous self-made from flour (0.300-0.495 mm) at Purdue University, IN, USA	1.70-2.36	253.4	15.9	6.5	623.3	124.2
Millet couscous (commercial)	Mme. Deme of Free Work Services, Dakar, Senegal	<2.36	253.4	16.9	4.7	617.2	124.2
Wheat couscous (self-made)	Flour from Bob's Red Mill, Milwaukie, OR, USA Couscous self-made from flour (0.300-0.495 mm) at Purdue University, IN, USA	1.00-2.36	260.6	27.0	1.0	616.1	124.2

<sup>1</sup>Including 0.5 g butter. <sup>2</sup>Including kcal from 0.5 g butter.

Table 4.2 Values used for correction of endogenous  $^{13}\text{C}$  for percent dose recovery per timepoint for gastric emptying assessment of millet-based meals. Values are means from testing with a subgroup of 4 participants (n=4). Values shown were used for the millet thick porridge, millet couscous (self-made), and millet couscous (commercial) test meals. Endogenous  $^{13}\text{C}$  for white rice and wheat couscous were nearly negligible.

Time (min)	Millet $^{13}\text{C}$ (DOB, ‰)
0	-0.16
15	0.46
30	0.66
45	1.06
60	0.84
75	1.04
90	1.62
105	2.02
120	2.62
150	3.22
180	3.80
210	3.56
240	3.92

DOB, delta over baseline.

Table 4.3 Parameters from modelling percent dose recovery (PDR) and cumulative percent dose recovery (CPDR) of  $^{13}\text{C}$  (corrected for endogenous  $^{13}\text{C}$ ) for each participant. These parameters were used for calculating gastric half-emptying time, lag phase, and gastric emptying coefficient.

Test meal	Parti- pant number	PDR model				CPDR model				tHalf (h)
		a	b	c	R <sup>2</sup>	m	k	$\beta$	R <sup>2</sup>	
White rice	19	15.66	0.62	0.48	0.88	45.65	0.42	1.77	1.00	2.70
	20	18.40	0.70	0.40	0.97	80.39	0.32	1.75	1.00	3.51
	32	12.41	0.68	0.25	0.95	142.61	0.16	1.66	1.00	6.57
	39	16.57	0.01	0.38	0.95	40.67	0.45	1.25	1.00	1.89
	43	19.51	0.54	0.58	0.91	39.29	0.53	1.74	1.00	2.09
	48	17.75	0.60	0.61	0.97	34.18	0.53	1.73	1.00	2.09
	56	21.16	0.57	0.55	0.95	48.72	0.47	1.71	1.00	2.34
	61	19.41	0.17	0.47	0.99	40.15	0.53	1.41	1.00	1.80
	65 <sup>a</sup>	6.89	0.16	0.00	0.93 <sup>a</sup>	566.58	0.02	1.25	1.00	34.69 <sup>a</sup>
	71	16.99	0.32	0.48	0.96	37.76	0.50	1.54	1.00	2.05
	80	15.34	0.44	0.32	0.93	62.33	0.33	1.61	1.00	3.14
	85	20.90	0.65	0.42	0.90	79.53	0.35	1.77	1.00	3.18
	93	18.27	0.32	0.37	0.98	56.72	0.39	1.50	1.00	2.56
95	16.40	0.52	0.45	0.97	50.58	0.37	1.60	1.00	2.80	
Millet thick porridge	19	58.77	2.19	1.53	0.99	37.98	0.88	3.41	1.00	1.92
	20	33.34	0.93	0.76	0.99	55.39	0.57	2.00	1.00	2.16
	25	14.95	0.43	0.32	0.98	67.53	0.29	1.52	1.00	3.50
	32	15.68	0.52	0.27	0.91	117.36	0.21	1.57	1.00	5.01
	39	26.52	0.63	0.73	0.91	38.83	0.66	1.88	1.00	1.78
	43	39.54	1.37	1.62	0.96	15.04	1.24	2.82	1.00	1.23
	48	24.44	0.69	0.63	0.96	47.16	0.54	1.84	1.00	2.14
	56	21.20	1.16	0.95	0.98	26.48	0.66	2.23	1.00	2.00
	65	10.62	0.47	0.20	0.89	95.71	0.19	1.59	1.00	5.41
	71	10.25	0.75	0.81	0.97	13.82	0.65	1.89	1.00	1.82
	80	30.64	1.02	0.83	0.95	46.55	0.60	2.11	1.00	2.12
	85	23.00	1.56	0.88	0.94	48.33	0.53	2.53	1.00	2.70
	93	17.44	0.36	0.35	0.90	64.59	0.33	1.49	1.00	3.02
95	27.00	0.53	0.59	0.99	53.48	0.52	1.67	1.00	2.09	
Millet couscous (self-made)	19	19.17	0.64	0.55	0.96	46.57	0.45	1.72	1.00	2.47
	20	17.94	0.83	0.42	0.96	85.91	0.31	1.88	1.00	3.75
	25	19.66	0.44	0.43	0.89	57.25	0.40	1.58	1.00	2.59
	32 <sup>a</sup>	9.64	0.16	0.01	0.93 <sup>a</sup>	344.40	0.05	1.30	1.00	16.54 <sup>a</sup>
	43 <sup>a</sup>	10.20	0.10	0.00	0.94 <sup>a</sup>	275.75	0.06	1.25	1.00	13.79 <sup>a</sup>
	48	15.90	0.53	0.36	0.94	69.32	0.31	1.63	1.00	3.47

Table 4.3 continued

56	22.42	0.47	0.44	0.98	63.63	0.41	1.63	1.00	2.55	
61	24.53	0.70	0.80	0.89	31.96	0.71	1.98	1.00	1.72	
65	12.73	0.25	0.31	0.94	47.29	0.32	1.40	1.00	2.92	
71	18.01	0.55	0.47	0.94	51.60	0.41	1.67	1.00	2.64	
80	15.08	0.50	0.38	0.85	54.27	0.36	1.67	1.00	2.97	
85	17.09	0.91	0.56	0.94	51.92	0.42	2.00	1.00	2.92	
93 <sup>b</sup>	17.32	0.22	0.29	0.69 <sup>b</sup>	66.18	0.33	1.43	1.00	2.91 <sup>b</sup>	
95	18.37	0.40	0.37	0.96	61.64	0.37	1.55	1.00	2.78	
<hr/>										
19	21.09	0.73	0.67	0.86	40.46	0.53	1.86	1.00	2.22	
20	18.78	1.01	0.52	0.97	76.10	0.35	2.01	1.00	3.49	
25	15.90	0.51	0.35	0.94	66.15	0.33	1.65	1.00	3.28	
32	18.82	0.62	0.44	0.99	62.82	0.37	1.72	1.00	2.95	
39	19.72	0.51	0.44	0.92	59.05	0.40	1.65	1.00	2.68	
43	18.86	0.75	0.57	0.95	45.35	0.47	1.87	1.00	2.48	
48	20.70	0.60	0.46	0.97	63.15	0.39	1.70	1.00	2.78	
Millet couscous (commercial)	56	22.50	0.59	1.21	0.96	14.07	1.16	2.00	1.00	1.06
65 <sup>a</sup>	8.64	0.22	0.07	0.93 <sup>a</sup>	191.60	0.07	1.29	1.00	11.98 <sup>a</sup>	
71	8.40	0.38	0.60	0.98	14.77	0.57	1.58	1.00	1.81	
80	21.02	0.55	0.98	0.92	19.53	0.81	1.72	1.00	1.35	
85	26.56	0.74	0.63	0.98	53.71	0.53	1.88	1.00	2.24	
93	33.10	1.24	0.97	0.96	40.33	0.69	2.37	1.00	2.00	
95	18.92	0.81	0.49	0.96	64.53	0.39	1.90	1.00	3.06	
<hr/>										
19	19.82	0.56	0.46	0.91	55.99	0.43	1.73	1.00	2.58	
20	15.23	0.64	0.36	0.98	76.39	0.29	1.70	1.00	3.82	
25	9.40	0.48	0.39	0.89	31.65	0.39	1.69	1.00	2.79	
32	11.35	0.39	0.16	0.95	116.80	0.16	1.50	1.00	6.03	
39	20.27	0.45	0.37	0.96	74.45	0.35	1.60	1.00	3.00	
43	26.27	0.87	0.76	0.84	39.46	0.64	2.06	1.00	1.94	
48	16.65	0.65	0.48	0.97	50.30	0.41	1.77	1.00	2.78	
Wheat couscous (self-made)	56	19.43	0.52	0.80	0.99	23.76	0.70	1.67	1.00	1.54
61	25.15	0.45	0.87	0.97	25.56	0.87	1.76	1.00	1.30	
65	12.25	0.37	0.21	0.93	89.10	0.21	1.50	1.00	4.75	
71	18.22	0.52	0.61	0.93	32.31	0.58	1.72	1.00	1.90	
80	15.83	0.50	0.48	0.91	39.42	0.47	1.69	1.00	2.34	
85	17.87	0.82	0.55	0.90	50.52	0.44	1.95	1.00	2.76	
93	22.75	0.37	0.51	0.95	49.08	0.51	1.59	1.00	2.04	
95	14.33	0.45	0.29	0.93	79.42	0.25	1.55	1.00	4.04	

CPDR, cumulative percent dose recovery; PDR, percent dose recovery; tHalf, gastric half-emptying time. <sup>a</sup>Instances in which the PDR did not decrease by more than 1% of its peak value during the monitoring period and thus these values were deemed outliers. <sup>b</sup>tHalf value excluded from further analyses because R<sup>2</sup> for PDR was less than 0.80.

Table 4.4 Mean lag phase and gastric emptying coefficient values ( $n=14$ )<sup>a</sup>.

Test meal	Mean gastric emptying parameter	
	Lag phase	GEC
White rice	1.29 ± 0.18	2.86 ± 0.04 <sup>b</sup>
Millet thick porridge	1.36 ± 0.12	3.12 ± 0.13 <sup>a</sup>
Millet couscous (self-made)	1.33 ± 0.09	2.89 ± 0.05 <sup>ab</sup>
Millet couscous (commercial)	1.25 ± 0.11	2.97 ± 0.09 <sup>ab</sup>
Wheat couscous (self-made)	1.36 ± 0.13	2.83 ± 0.07 <sup>b</sup>

<sup>a</sup> ± SEM, Standard error of the mean. GEC, gastric emptying coefficient. Means (with outliers removed) not sharing the same letter are significantly different ( $p<0.05$ ). No statistically significant differences were found for lag phase ( $p=0.89$ ).

Table 4.5 Participant baseline characteristics ( $n=15$ )<sup>a</sup>.

Characteristic	Mean $\pm$ SEM <sup>b</sup>
Age (y)	26.6 $\pm$ 1.2
Height (m)	1.7 $\pm$ 0.0
Weight (kg)	67.6 $\pm$ 2.9
Body mass index (kg/m <sup>2</sup> )	22.8 $\pm$ 0.7
Fasting blood glucose (mg/dL)	87.3 $\pm$ 2.9
Sex <sup>c</sup>	8 M <sup>d</sup> ; 7 F

<sup>a</sup>One participant withdrew after completion of the third treatment arm, but this participant's characteristics have still been included.

<sup>b</sup>SEM, Standard error of the mean.

<sup>c</sup>M, male; F, female.

<sup>d</sup>One male participant withdrew after completion of the third treatment arm, leaving a final of 7 males completing the entire trial.

Table 4.6 Glycemic response characteristics<sup>a</sup>.

Test meal food	Mean glucose iAUC <sub>0-240 min</sub> (mg×min/dL)	Mean glucose iAUC <sub>0-120 min</sub> (mg×min/dL)	Mean ΔPeak glucose value (mg/dL)	Mean peak glucose time (min)
White rice	6943.7 ± 779.9 <sup>a</sup>	4353.0 ± 400.8 <sup>a</sup>	69.9 ± 5.9 <sup>a</sup>	61.3 ± 3.8 <sup>a</sup>
Millet thick porridge	4755.7 ± 546.8 <sup>b</sup>	2296.3 ± 302.0 <sup>b</sup>	52.8 ± 4.5 <sup>b</sup>	66.1 ± 3.9 <sup>a</sup>
Millet couscous (self-made)	5912.0 ± 997.7 <sup>ab</sup>	3596.3 ± 479.2 <sup>ab</sup>	59.5 ± 5.8 <sup>ab</sup>	62.5 ± 4.4 <sup>a</sup>
Millet couscous (commercial)	5535.7 ± 708.4 <sup>ab</sup>	3740.9 ± 492.4 <sup>ab</sup>	58.6 ± 6.0 <sup>ab</sup>	59.3 ± 4.0 <sup>a</sup>
Wheat couscous (self-made)	5686.1 ± 397.1 <sup>ab</sup>	3399.8 ± 263.0 <sup>ab</sup>	56.4 ± 3.9 <sup>ab</sup>	56.4 ± 2.9 <sup>a</sup>

<sup>a</sup> ± SEM, Standard error of the mean. iAUC, incremental area under the curve; ΔPeak glucose value, change in peak glucose value from baseline. Means not sharing the same letter are significantly different ( $p < 0.05$ ).

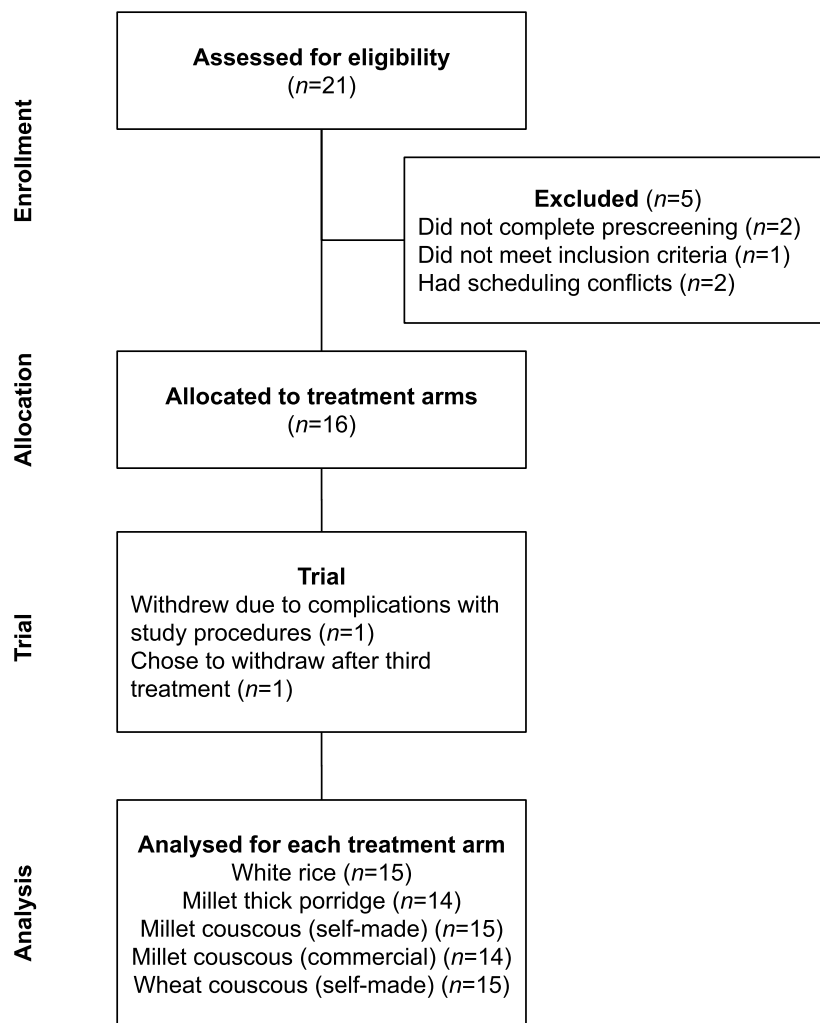


Figure 4.1 Participant recruitment and participation flow diagram.

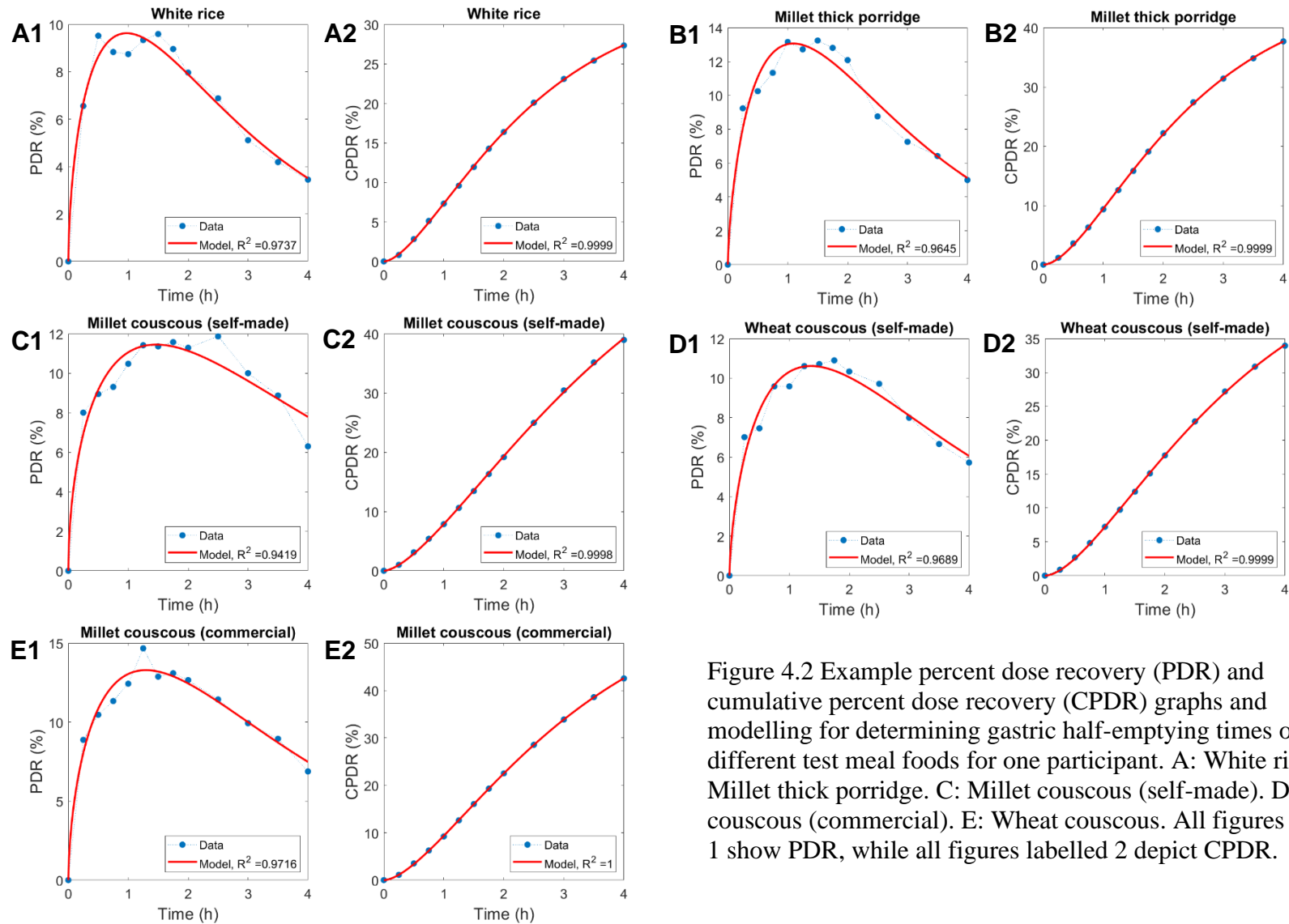


Figure 4.2 Example percent dose recovery (PDR) and cumulative percent dose recovery (CPDR) graphs and modelling for determining gastric half-emptying times of the different test meal foods for one participant. A: White rice. B: Millet thick porridge. C: Millet couscous (self-made). D: Millet couscous (commercial). E: Wheat couscous. All figures labelled 1 show PDR, while all figures labelled 2 depict CPDR.

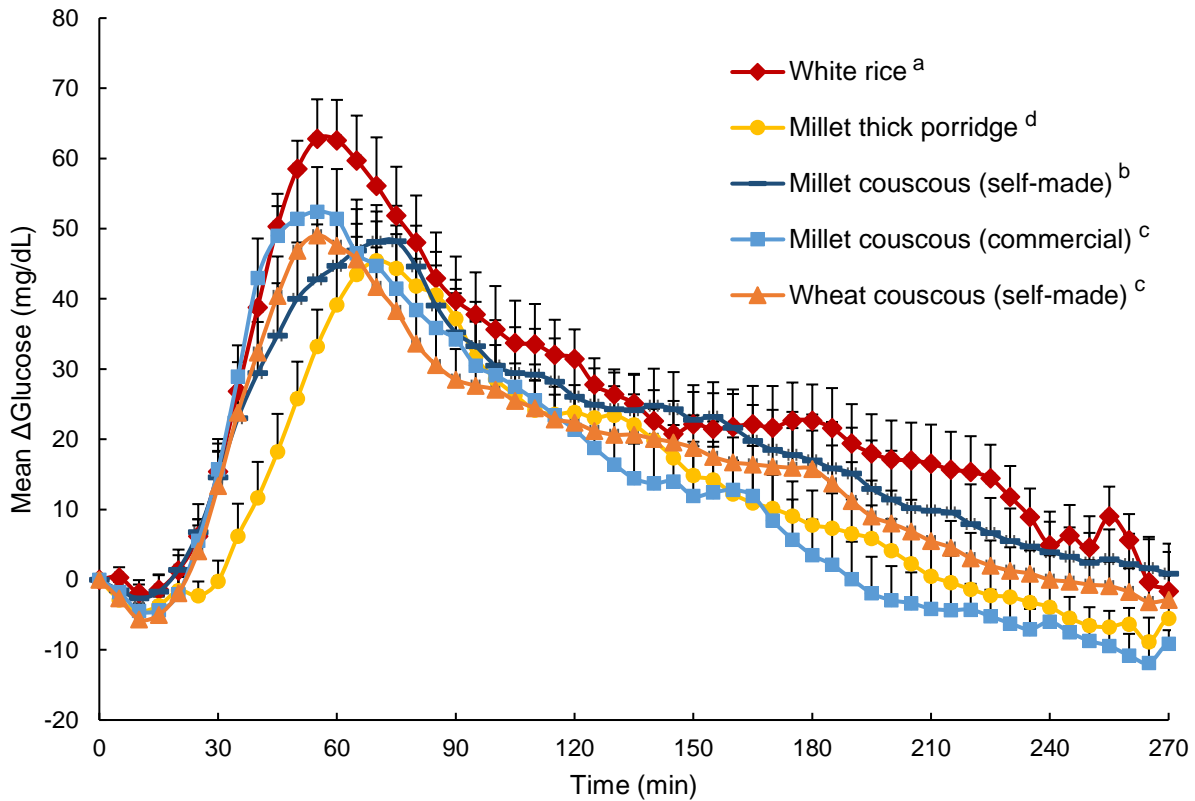


Figure 4.3 Mean glucose expressed as mean  $\Delta$ Glucose (glucose difference from baseline) for carbohydrate-based test meals. Error bars represent standard error of the mean (SEM). Means not sharing the same letter are significantly different ( $p < 0.05$ ) in main effects: All millet foods and wheat couscous had significantly lower glycemic response than white rice [ $p < 0.0001$  for millet couscous (commercial), millet thick porridge, wheat couscous vs. white rice;  $p = 0.05$  for millet couscous (self-made) vs. white rice]. Millet thick porridge had significantly lower glycemic response than both types of millet couscous (commercial and self-made;  $p = 0.01$  and  $p < 0.0001$ , respectively) and wheat couscous ( $p < 0.0001$ ). Millet couscous (self-made) also had significantly higher glycemic response than millet couscous (commercial) and wheat couscous ( $p < 0.0001$ ). A significant effect for time was also evident ( $p < 0.0001$ ).

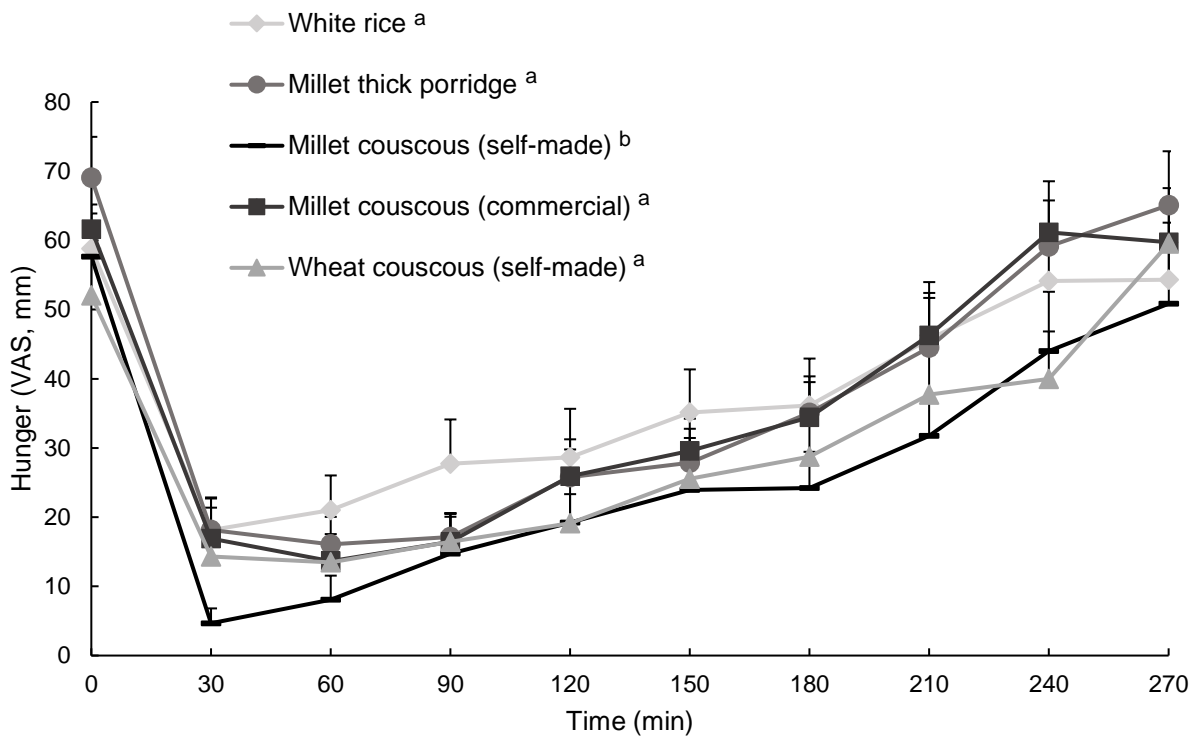


Figure 4.4 Mean hunger ratings (Visual Analog Scale) immediately prior to and 4 h following consumption of carbohydrate-based test meal foods. Error bars represent standard error of the mean (SEM). Means not sharing the same letter are significantly different ( $p < 0.05$ ) in main effects: Millet couscous (self-made) was significantly lower than white rice ( $p < 0.0001$ ), wheat couscous ( $p = 0.02$ ), millet thick porridge ( $p = 0.008$ ), and millet couscous (commercial) ( $p = 0.002$ ). A significant effect for time was also evident ( $p < 0.0001$ ).

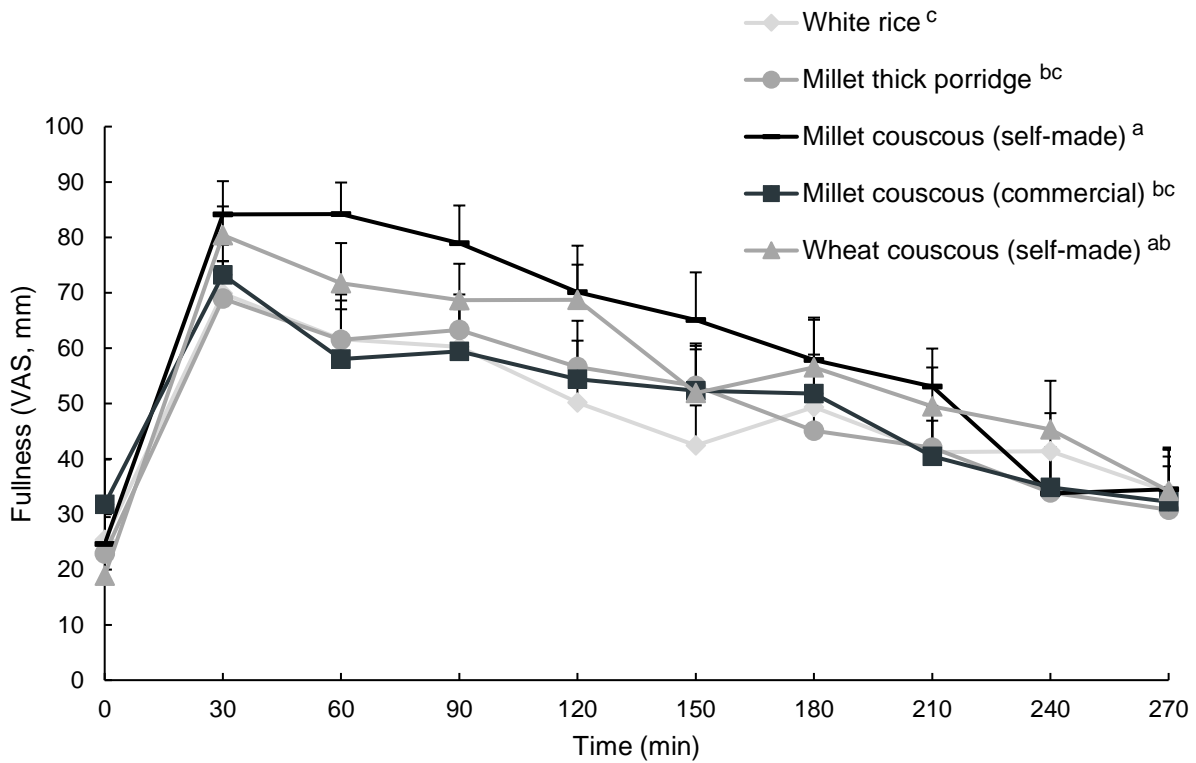


Figure 4.5 Mean fullness ratings (Visual Analog Scale) immediately prior to and 4 h following consumption of carbohydrate-based test meal foods. Error bars represent standard error of the mean (SEM). Means not sharing the same letter are significantly different ( $p < 0.05$ ) in main effects: Millet couscous (self-made) was significantly higher than white rice ( $p < 0.0001$ ), millet couscous (commercial) ( $p < 0.0001$ ), and millet thick porridge ( $p = 0.0004$ ). A significant effect for time was also evident ( $p < 0.0001$ ).

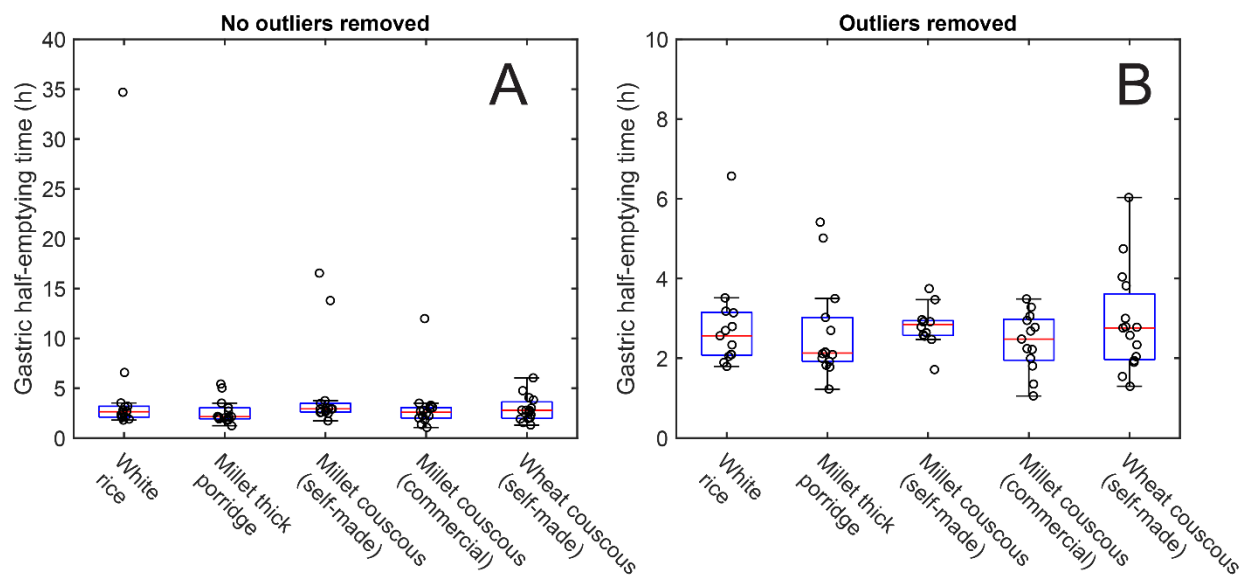


Figure 4.6 Mean gastric half-emptying times for each carbohydrate-based test food displayed as a box-plot, with either all values (A) or outliers removed (B) ( $n=14$ ). No statistically significant differences were found ( $p=0.15$ ). Circles represent values from individual participants per test meal. Central red marks indicate the median. Bottom and top edges of the blue box represent the 25<sup>th</sup> and 75<sup>th</sup> percentiles, respectively. Note that instances for which the percent dose recovery of the tracer did not decrease by more than 1% of its peak value during the monitoring period were deemed outliers (4 values greater than 10 h).

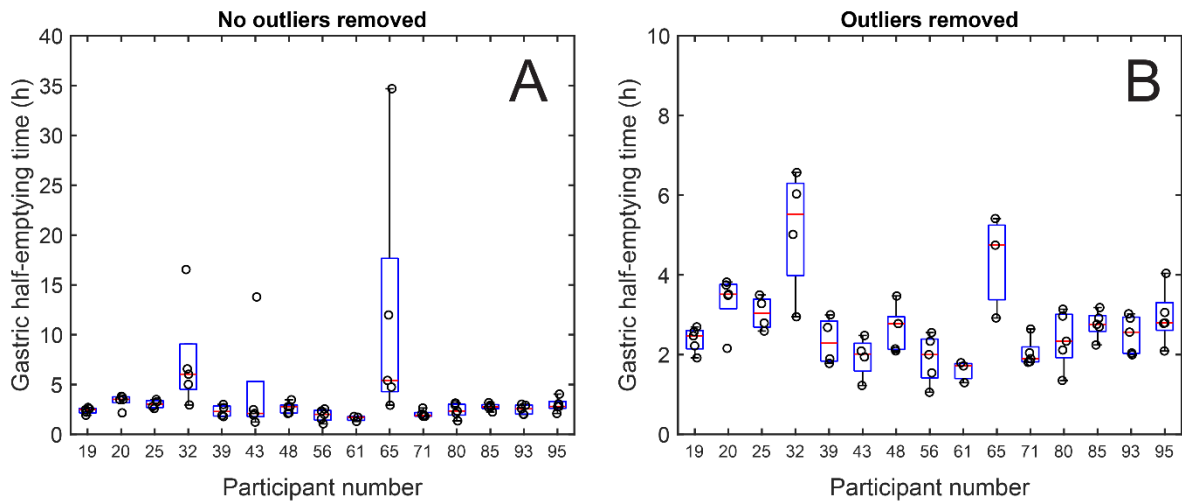


Figure 4.7 Gastric half-emptying times by participant averaged across all test meal foods ( $n=15$ , includes participant 61 who withdrew during the study). Exploratory data visualization, so no statistical analysis was conducted. Circles represent values for individual test meal foods per participant. Central red mark indicates the median. Bottom and top edges of the blue box represent the 25<sup>th</sup> and 75<sup>th</sup> percentiles, respectively. Note that instances for which the percent dose recovery of the tracer did not decrease by more than 1% of its peak value during the monitoring period were deemed outliers (4 values greater than 10 h).

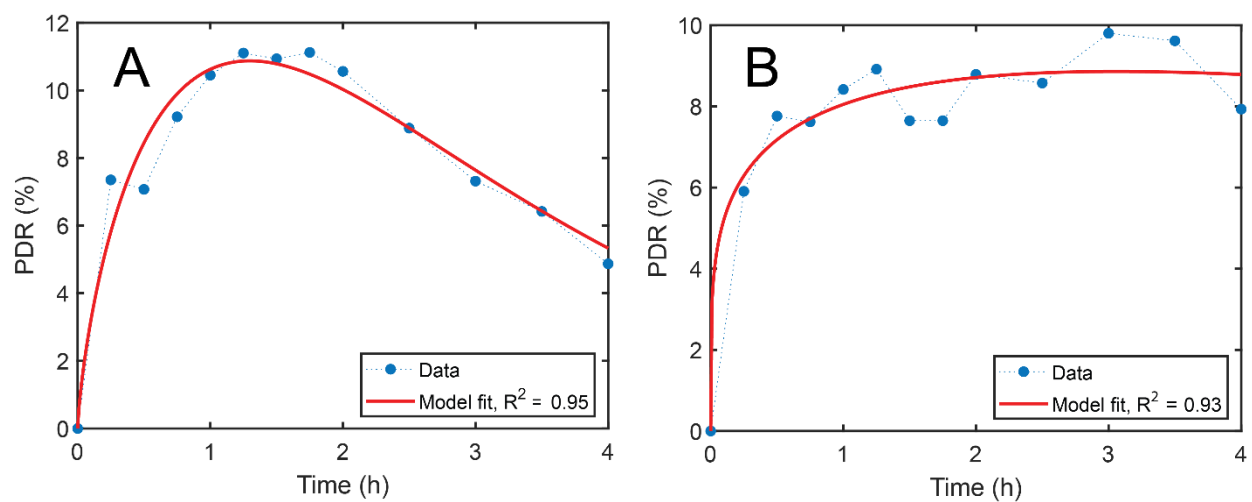


Figure 4.8 Example of included (A) and excluded (B) percent dose recovery (PDR) modelling curves for gastric half-emptying time. Excluded modelling curves (and therefore gastric half-emptying times) did not decrease by more than 1% of their peak value during the monitoring period, such as the curve seen in (B), were deemed outliers.

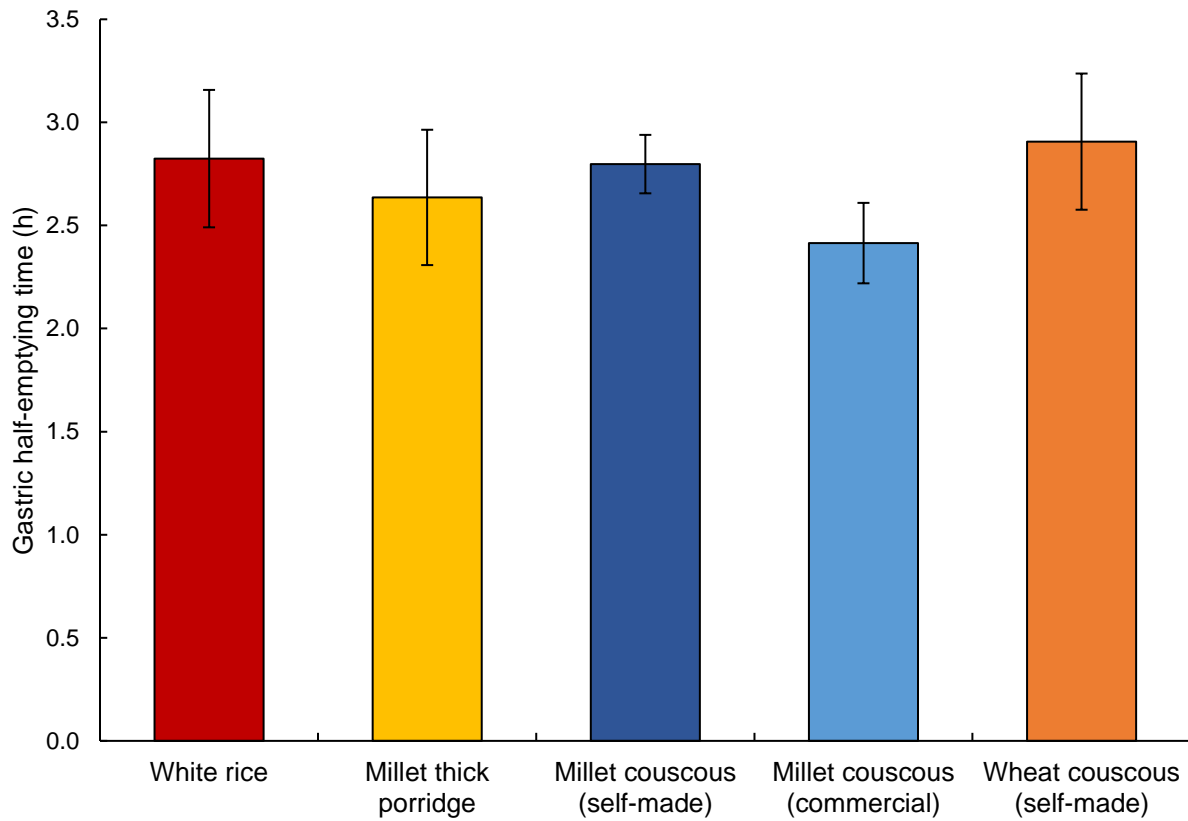


Figure 4.9 Mean gastric half-emptying time for each carbohydrate-based test food (excluding 4 outlier values) as determined using the  $^{13}\text{C}$  octanoic breath test. Error bars represent  $\pm$  standard error of the mean (SEM). No statistically significant differences were found ( $p=0.18$ ).

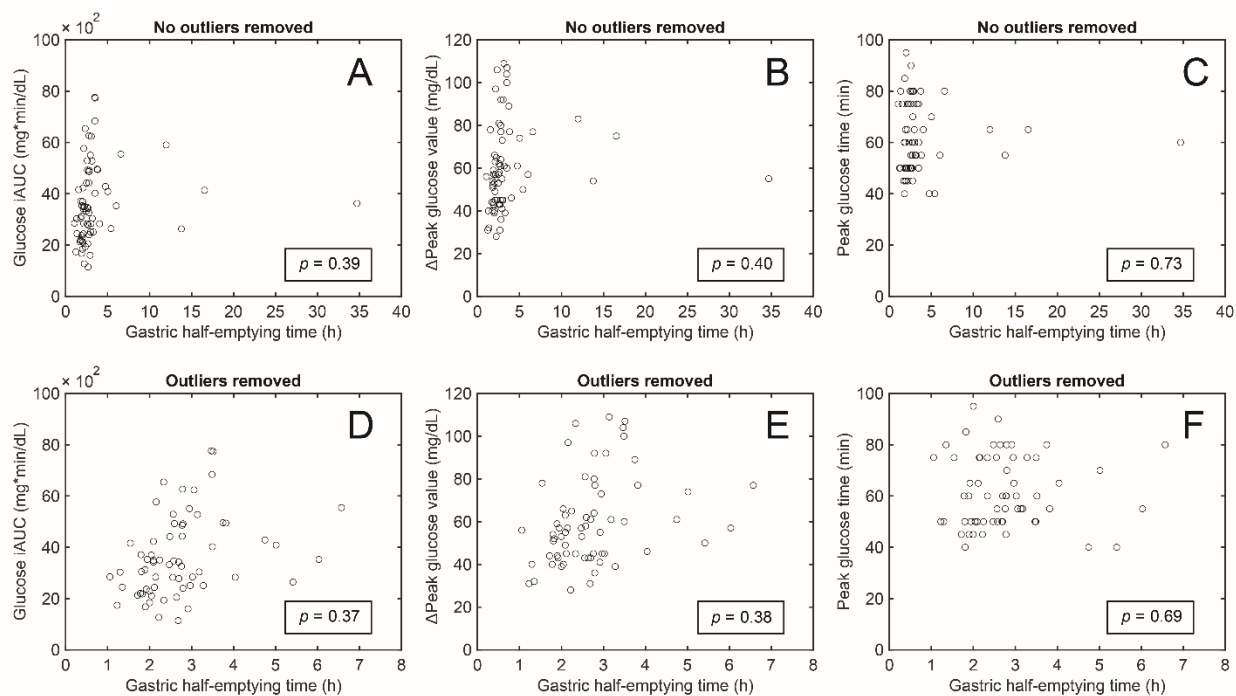


Figure 4.10 Relationship between gastric half-emptying time (h) and glucose incremental area under the curve from 0-120 min (iAUC<sub>0-120min</sub>; mg×min/dL; A, D), ΔPeak glucose value (mg/dL; B, E), and peak glucose time (min; C, F) ( $n=14$ ). Analyses in two instances of inclusion of gastric half-emptying time values are shown. A-C: no values removed. D-F: outliers removed. Note that instances in which the percent dose recovery of the tracer did not decrease by more than 1% of its peak value during the monitoring period were deemed outliers.

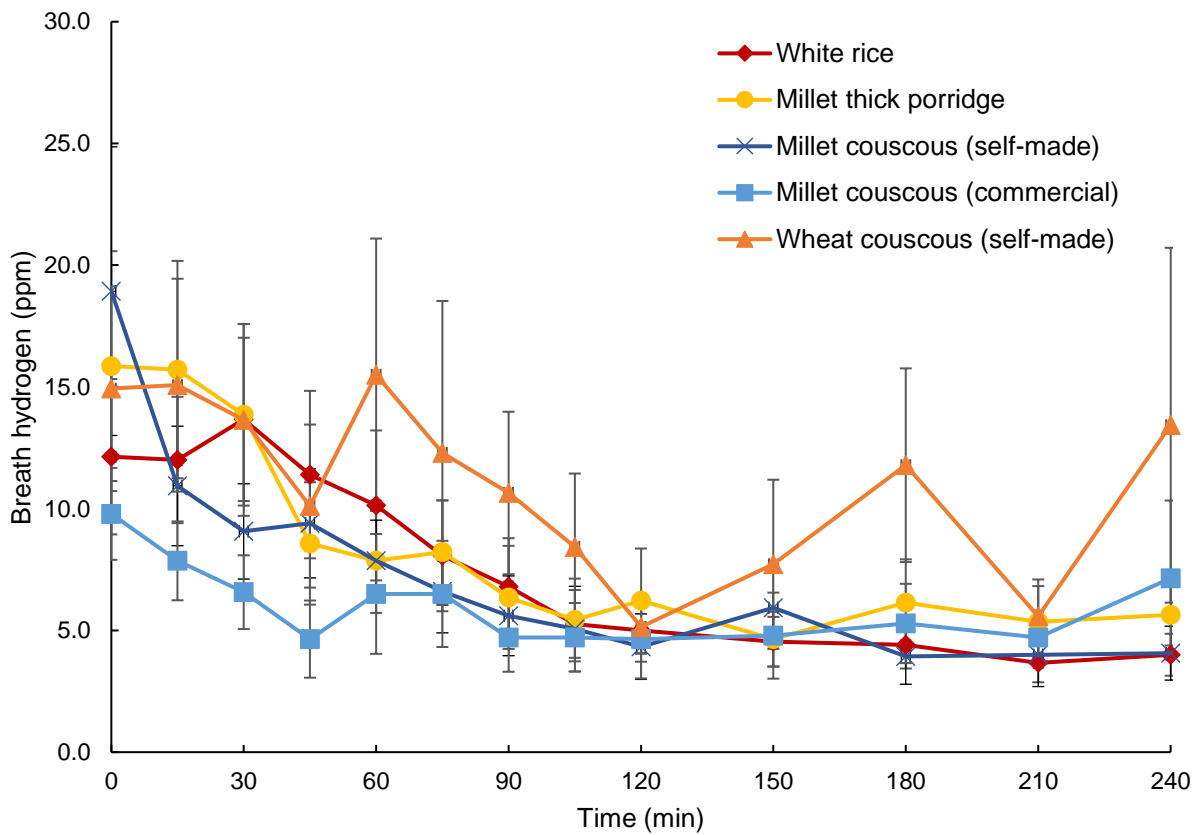


Figure 4.11 Mean breath hydrogen during the 4 h postprandial period for each test meal ( $n=14$ , excluding one participant due to outlier values and one additional outlier value) as a general indicator of potential fermentation of the test meals. As breath hydrogen values never rose above baseline for any of the treatments, it was concluded that fermentability was not a confounding factor in the study.

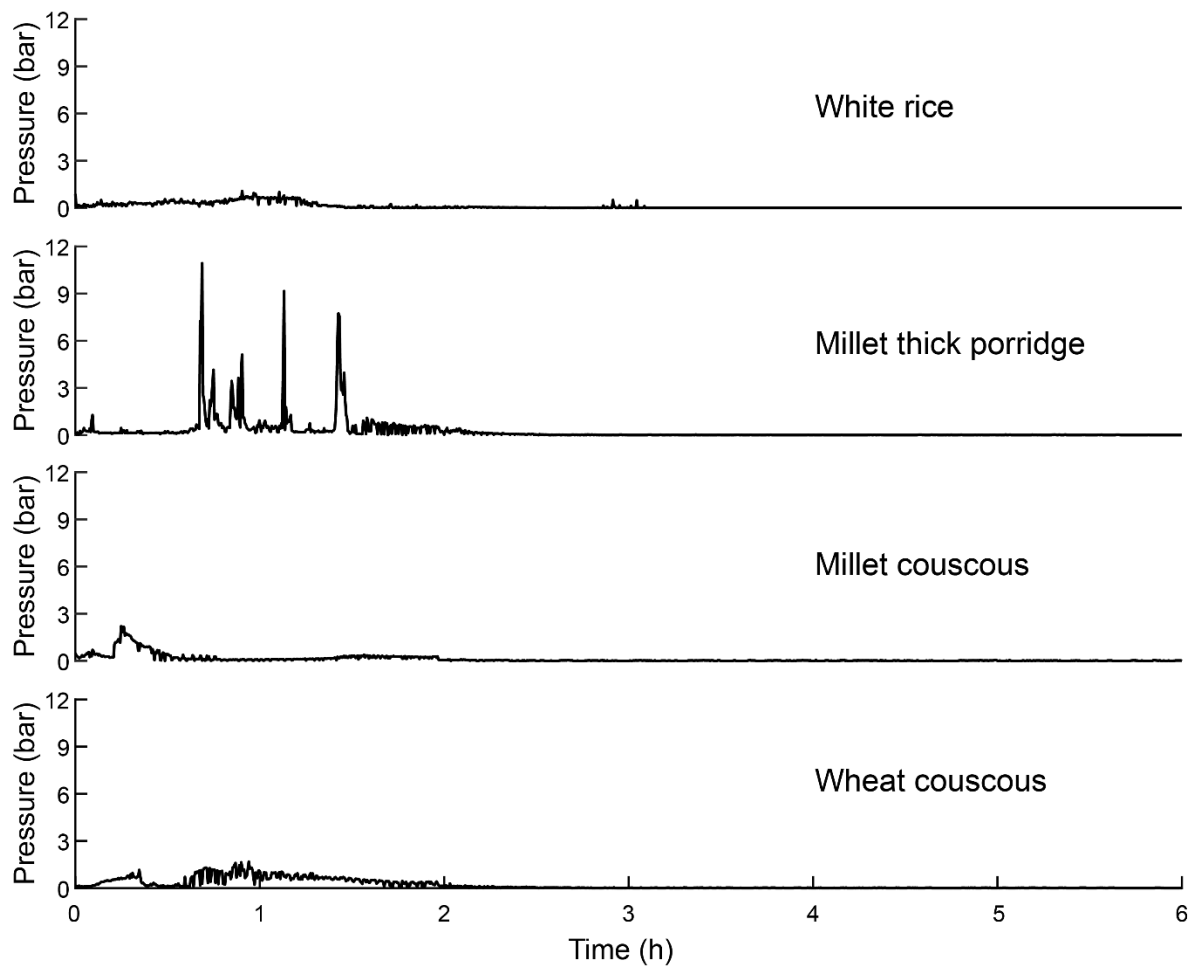


Figure 4.12 Mean pressure values within the gastric compartment during *in vitro* gastrointestinal experiments for white rice, millet thick porridge, millet couscous (self-made), and wheat couscous. Means represent values from duplicate runs from experiments lasting 6 h.

## CHAPTER 5. MODERATING CARBOHYDRATE DIGESTION PROMOTES FAT OXIDATION AND MAY ENHANCE METABOLIC FLEXIBILITY

### 5.1 Abstract

The impact of carbohydrate digestion rate on its utilization for energy by the body is incompletely understood but may have implications on insulin sensitivity, adipose tissue deposition, and weight status as they influence overall health. In this study, we investigated dietary conditions with different degrees of carbohydrate digestion and specific metabolic consequences that relate to energy expenditure. A key focus was on metabolic flexibility, or the ability of the body to efficiently switch between carbohydrate and fat oxidation. Our overall hypothesis was that reduced carbohydrate digestion rate decreases the utilization of carbohydrate as a substrate for energy (i.e. carbohydrate oxidation) and increases metabolic flexibility. Respiratory exchange ratio (RER), representing the ratio of carbohydrate oxidation to fat oxidation, was measured during four 24 h cycles through indirect calorimetry in mice lacking the mucosal maltase-glucoamylase enzyme (null) [n=8] and wild-type mice [n=8] fed six different diets (53% Conventional starch [raw corn starch], 53% Resistant starch [high-amylose corn starch, Novelose 260], 35% Resistant starch [Novelose 260], 18% Resistant starch [Novelose 260], 65% Sucrose, and High-fat [42% fat]). During the final two cycles in the chamber for each diet, fungal amyloglucosidase (AMG, 0.5%) was supplemented in drinking water to increase carbohydrate digestion in both the null and wild-type mice treatment groups. Characteristics of RER were determined through modeling using the sine equation as well as percent relative cumulative frequency (PRCF) analyses coupled with modeling using the Weibull and Mixed Weibull Cumulative Distribution functions. Results showed that null mice did not consistently exhibit lower carbohydrate oxidation than wild-type mice, but they tended to have higher metabolic flexibility ( $b_2$ ). The Conventional starch diet promoted greater fat oxidation ( $x_{50,1}$ ) in both null and wild-type mice but did not increase carbohydrate oxidation ( $x_{50,2}$ ) compared to the other diets, yet it tended to promote metabolic flexibility (sine  $c$ ,  $b_1$ ), suggesting slow carbohydrate digestion (as seen with raw corn starch) has greater effect on these aspects of metabolism than low carbohydrate digestion (as seen with high-amylose corn starch). The Sucrose diet had the highest carbohydrate oxidation and the High-fat diet had the lowest carbohydrate oxidation ( $p < 0.05$  for  $x_{50,2}$ ), validating the modeling approaches

employed, and dysregulated metabolism was suggested for the High-fat diet (since  $a$ ,  $c$ ,  $x_{50_1}$ ,  $x_{50_2}$ ,  $b_2$ ). AMG generally increased carbohydrate oxidation for all but the Sucrose and High-fat diets ( $x_{50_2}$ ) and caused more rapid shifts to carbohydrate oxidation (since  $c$ ,  $b_2$ ), yet it blunted fat oxidation ( $x_{50_1}$ ). The application of the novel approaches used in this study may help reveal how diets can have distinct effects on substrate oxidation and energy metabolism despite lack of differences in energy expenditure. Overall, given these findings, we propose that moderating carbohydrate digestion provides the ideal combination of balancing carbohydrate and fat oxidation while promoting metabolic flexibility.

## 5.2 Introduction

As the prevalence of obesity and type 2 diabetes continues to increase worldwide, there are persistent concerns about dietary carbohydrates and public health (Kroemer et al. 2018; AlEissa et al. 2018). Dietary carbohydrates constitute the main source of energy in most diets (Shan et al. 2019), and thus determining how carbohydrates can be used to help prevent or reduce the detrimental side effects of obesity and type 2 diabetes, or complications thereof, could be key for combating these public health challenges. The issue is carbohydrate quality. Basic differences in the types of carbohydrates – such as sugar (sucrose), starch, and fiber – are widely recognized. Yet – within these types – not all sugars, starches, or fibers are the same. For starches, differences in botanical source (E.-S. Lee et al. 2018; Martinez et al. 2018); macro-, micro-, or fine structure (Roman et al. 2017; Zhang, Venkatachalam, and Hamaker 2006; Ao et al. 2007; Roman et al. 2020); food form (Li et al. 2019; Barkeling et al. 1995); processing and preparation (Wu et al. 2019; Borah, Deka, and Duary 2017; Vinoy et al. 2013); and other factors can give rise to different post-ingestive (acute) effects on the body, which may lead to other impacts in the long term (Ludwig and Ebbeling 2018; Santiago et al. 2015; AlEissa et al. 2018). These mainly relate to starch digestion rate and location of digestion in the small intestine (Zhang and Hamaker 2009; Zhang et al. 2015; B.-H. Lee et al. 2013).

The digestion of starch-based glucose polymers to absorbable free glucose is termed  $\alpha$ -glucogenesis (Diaz-Sotomayor et al. 2013), involving six starch-degrading enzymes: salivary  $\alpha$ -amylase, pancreatic  $\alpha$ -amylase, two types of maltase-glucoamylase (Mgam; N-terminal and C-terminal), and two types of sucrase-isomaltase (Si; N-terminal and C-terminal). A general proposition is that these six enzymes complement each other and may be adaptive to evolutionary

and cultural variations in food and feeding. Substantial research has been conducted to better understand the catalytic sites, activities, and substrate specificities of these enzymes from humans and other animal species (Diaz-Sotomayor et al. 2013; Simsek et al. 2015; Quezada-Calvillo, Robayo-Torres, Opekun, et al. 2007; Nichols et al. 2009; Brás et al. 2018; Quezada-Calvillo, Robayo-Torres, Ao, et al. 2007; Lin, Hamaker, and Nichols 2012; Chegeni et al. 2018; Frandsen and Svensson 1998; Santos, Goda, and Koldovsky 1992). However, it remains incompletely understood how  $\alpha$ -glucogenesis related to differences in starch digestion rate and amount impacts carbohydrate metabolism and energy partitioning.

One key question surrounding carbohydrates, digestion, and health is how consumption of carbohydrates ultimately affects body weight. Although body weight is affected by many complex factors, in a basic sense it is the interchange between the amount of energy consumed and the amount of energy expended. Different foods can affect both sides of this interchange, and the rate and extent of digestion may play a pivotal role. In the present study, we investigated specific metabolic consequences that relate to energy expenditure of diets containing carbohydrates with different digestibilities. For the carbohydrates of focus, we selected a starch that is in part resistant to digestion in the small intestine (Novelose 260, high-amylose corn starch) and a conventional starch that is more digestible (normal corn starch). Resistant starch passes into the large intestine to undergo fermentation, producing short chain fatty acids (SCFAs), while conventional starch is digested and absorbed in the small intestine to more directly affect glycemic response and carbohydrate metabolism. Our study is focused on oxidation, but implicit to this is a “togglng” between oxidation of absorbed glucose and fermentation for resistant starch generating SCFAs, which requires further investigation. We also studied diets that contained sucrose (highly available carbohydrate (Sun and Empie 2012)) and that were high in fat (low in carbohydrate) as comparators. Intriguingly, our initial findings showed that mice fed the carbohydrate-based diets did not exhibit differences in energy expenditure (Supplementary Figure A.1). These findings were surprising because the extents of carbohydrate digestibility differed markedly among the diets, and thus suggest that the mice possessed some form of metabolic adaptability. Such adaptability likely involves changes in utilization of carbohydrate vs. fat as substrates for energy and thus relates to metabolic flexibility, or the ability of an organism to adjust substrate oxidation (i.e. fat or carbohydrate) according to its availability (J. M. S. Fernández-Calleja, Bouwman, Swarts, Oosting, et al. 2019). Having poor metabolic flexibility (i.e. metabolic inflexibility) is thought to be rooted

in a rigidity in mitochondrial substrate selection, such that mitochondria have hindered ability to freely switch fuel choice according to nutritional circumstances (Muoio 2014). Having a high degree of metabolic flexibility is associated with good health and, conversely, a low degree of metabolic flexibility is linked with poor health, such as the obese state and type 2 diabetes (Goodpaster and Sparks 2017; Muoio 2014; Meex et al. 2010; van de Weijer et al. 2013). Although good health and proper weight balance are not the same, they are often linked. Metabolic flexibility has generally been studied in the context of disease states (Stull et al. 2010; Kelley and Mandarino 2000; van de Weijer et al. 2013), exercise (Meex et al. 2010; Malin et al. 2013), and fasting (Reichenbach et al. 2018; van de Weijer et al. 2013), though very few studies relate to diet (Begaye et al. 2020; Duivenvoorde et al. 2015; Gribok et al. 2016) and even further to carbohydrate digestibility (J. Fernández-Calleja et al. 2018).

Given our findings that energy expenditure was the same for carbohydrates differing in digestion characteristics, we hypothesized that dietary carbohydrates with different digestibilities would have distinct effects on the utilization of absorbed glucose as a substrate for energy (i.e. carbohydrate oxidation) and the ability to switch between utilization of carbohydrate versus fat for metabolism (i.e. metabolic flexibility). Namely, we reasoned that dietary carbohydrates with slower digestion would decrease the utilization of carbohydrate as a substrate for energy (i.e. carbohydrate oxidation) and increase metabolic flexibility. To thoroughly probe these hypotheses, we altered carbohydrate digestibility/digestion in three ways and examined the impacts of these alterations on respiratory exchange ratio (RER), or the ratio of carbohydrate oxidation to fat oxidation, in mice. These three alterations were as follows:

- 1) Eliminating a starch-degrading enzyme complex through use of Mgam knockout (null) mice
- 2) Feeding diets with different *in vitro* carbohydrate digestion profiles
- 3) Supplementing a starch-degrading enzyme (amyloglucosidase, AMG) (Warren et al. 2015) that is key to digesting starch; this restored the missing Mgam activity in null mice

Effectively, we decreased carbohydrate digestion through Mgam knockout (null) mice and diets with different levels of resistant starch, and we increased carbohydrate digestion by providing AMG in efforts to determine how carbohydrate digestion impacts the utilization of carbohydrates

for energy (i.e. substrate partitioning and metabolic flexibility). In alignment with the three means of altering carbohydrate digestion, we hypothesized the following:

- 1) Mgam knockout (null) mice would have reduced RER and higher metabolic flexibility compared to wild-type mice
- 2) Reduced carbohydrate digestion rate would reduce RER and lead to greater metabolic flexibility
- 3) Supplementation with AMG to increase carbohydrate digestion would result in higher RER and decreased metabolic flexibility

To test these hypotheses, we measured RER as a primary outcome through indirect calorimetry, which represents the ratio of carbohydrate oxidation to fat oxidation. However, the existing approaches for analyzing RER data did not allow for optimal conclusions to be drawn about substrate partitioning and metabolic flexibility. Therefore, we developed two new approaches for examining specific characteristics of carbohydrate oxidation through RER:

- 1) Modeling with the sine equation to describe diurnal patterns of RER and gain insight to metabolic flexibility
- 2) Percent relative cumulative frequency (PRCF) analysis as proposed by Riachi et al. (2004), plus modeling with the Weibull and Mixed Weibull Cumulative Distribution function to differentiate carbohydrate vs. fat oxidation as well as impacts on metabolic flexibility

These approaches involve parameters that describe specific characteristics of RER which enable more insights to be gained, especially related to carbohydrate vs. fat oxidation and the efficiency of switching between these two oxidation modes. The application of such approaches for the present study and in future research may help reveal how very different diets can have distinct effects on carbohydrate oxidation, especially despite lack of differences in energy expenditure.

### **5.3 Materials and Methods**

This study was performed in Mgam knockout and wild-type mice. All study procedures were conducted with full approval from the Baylor College of Medicine Institutional Animal Care and Use Committee (IACUC; protocol AN-1577).

### 5.3.1 Animals

Equal groups of Mgam knockout (null) and wild-type mice were used ( $n=8$  per group; 8 males in null group, 7 males and 2 females in wild-type group). Both groups were Sv/129 mice (The Jackson Laboratory, Bar Harbor, ME). For the null mice, the Mgam gene was ablated as reported previously (Quezada-Calvillo, Robayo-Torres, Opekun, et al. 2007) and genotyping proceeded using quantitative polymerase chain reaction (PCR) of tail DNA as described in Nichols et al. (2009). For the wild-type mice, the Mgam gene was not ablated. All mice were weaned at least 42 days before initiation of experimentation. Mice were housed in rooms maintained at  $22 \pm 2^\circ\text{C}$  with a 12:12 h dark:light cycle (18:00-06:00 dark).

### 5.3.2 Experimental diets

Mice were fed six different diets *ad libitum* over time in the following sequence: **1)** 53% Conventional starch diet (Envigo-Teklad TD.01629; Envigo, Indianapolis, IN), **2)** 53% Resistant starch diet (Envigo-Teklad TD.02130), **3)** 65% Sucrose diet (Envigo-Teklad TD.02129), **4)** 35% Resistant starch diet (Envigo-Teklad TD.02129), **5)** 18% Resistant starch diet (Envigo-Teklad TD.02130), **6)** High-fat diet (21.2% fat, or 42% kcal from fat; Envigo-Teklad TD.88137). With the exception of the High-fat diet, the only difference among the diets was in the carbohydrate portion (Table 5.1). Novelose 260 was donated and used as the resistant starch in the three resistant starch-based diets (Ingredion, Westchester, IL). The % kcal and % by weight from protein, carbohydrate, and fat were matched for all but the High-fat diet. Further, all diets had an energy density of 3.6 kcal/g with the exception of the High-fat diet, which had 4.5 kcal/g. When the mice were not on an experimental diet, they were fed a chow lab diet (PicoLab Rodent Diet 20, 5053; 62% kcal from carbohydrate, 25% kcal from protein, 13% kcal from fat; LabDiet, St. Louis, MO). Total starch in each diet was determined using a total starch analysis kit (amyloglucosidase/alpha-amylase method; Total Starch Assay Kit [AA/AMG], K-TSTA-50A, Megazyme, Wicklow, Ireland). Starch and moisture contents of all diets are shown in Table 5.2. Amounts of rapidly digestible starch, slowly digestible starch, and resistant starch were determined using the Englyst assay (H. N. Englyst, Kingman, and Cummings 1992; K. N. Englyst et al. 1999), and percent amylose within the carbohydrate component of each diet was calculated (considering that normal corn starch contains 28% amylose and Novelose 260 contains 70% amylose). Furthermore, food

quotients (macronutrient oxidation ratio for food or, in this case, for different diets) were calculated for all of the diets assuming a quotient of oxidation of 1.0 for carbohydrates, 0.70 for fats, and 0.825 for proteins. According to IACUC requirements, diets were stored for no longer than 6 weeks before being provided to animals.

For experimentation, animals were initially subjected to the diets and indirect calorimetry chambers for 4 cycles (24 h per cycle) prior to data collection as a means of acclimation (Figure 5.1). Due to the nature of these experiments, one animal was housed per chamber/cage. Following these 4 cycles, data collection proceeded for 4 more cycles (24 h per cycle) in the indirect calorimetry chambers as described below. Animals were weighed before and after being housed in the chambers. At least 10 day/night cycles served as a washout period between diets. Mice were also given free access to drinking water at all times (either with or without AMG supplementation for data collection, see section 5.2.3).

### **5.3.3 Amyloglucosidase (AMG) supplementation**

During the latter two cycles of the data collection period in the indirect calorimetry chambers (cycles 3 and 4), each animal's drinking water was replaced by drinking water supplemented with 0.5% amyloglucosidase (AMG) from *Aspergillus niger* (2 mL AMG/400 mL drinking water; AMG 300 L, AMP30095, activity 300 U/mL; Novo Nordisk BioChem, North America, Inc., Franklinton, NC). This supplementation level was determined considering a standard AMG activity of 0.2 U/g digestible starch in mice, and by assuming animals would consume 2.5 g starch/d; taken together, these factors indicated a level of 0.5 U/d was desired, which was then incorporated with the activity level of the AMG per mL (3000 U/mL) to indicate 2 mL AMG per 400 mL drinking water was required (0.5%). Following the termination of cycle 4 for each diet data collection period, the drinking water was switched back to the unsupplemented version.

### **5.3.4 Indirect calorimetry – Respiratory Exchange Ratio (RER)**

The respiratory exchange ratio (RER) of each mouse for the 4-cycle data collection period was determined using an open-circuit indirect calorimeter (version 5.61, Oxymax, Columbus Instruments, Columbus, OH) designed to measure consumption of oxygen ( $V_{O_2}$ ) and production

of carbon dioxide ( $V_{CO_2}$ ). This 4-cycle data collection period was initiated following the 4-cycle acclimation period (Figure 5.1). With 16 separate chambers, this system had the capacity to house 16 mice simultaneously. Calibration of the  $V_{O_2}$  and  $V_{CO_2}$  sensors as well as flow meters was performed immediately prior to the data collection period for each diet. Sampling of inlet air from each chamber ensued every 43 min during the data collection period, with a 30 s measure time and 120 s settle time (referencing method 2, interval 1). Using equations derived from mass balance across the chamber,  $V_{O_2}$  and  $V_{CO_2}$  were calculated. The Weir equation (Weir 1949) was used to internally calculate energy expenditure for each mouse, with adjustments made for individual mouse body weight (before being placed in indirect calorimetry chamber for each diet) and RER. RER values were averaged per 24 h separately for cycles 2 and 3 per treatment group (factors: diet  $\times$  genotype  $\times$  cycle), as well as analyzed and modeled for pooled treatment groups overall or per individual mice as described below (sections 5.2.5-5.2.7).

### 5.3.5 Modeling of RER using sine equation

To more readily characterize the impact of starch digestion on RER, the RER data for individual mice was fit to curves using the sine equation (Eq. 1):

$$y = a \sin(bx + c) + d \quad [1]$$

Where  $a$  indicates the amplitude,  $b$  indicates the period (breadth or width),  $c$  indicates the horizontal shift on the  $x$ -axis, and  $d$  indicates the vertical shift on the  $y$ -axis for the sinusoidal curve. We would expect that smaller  $a$  value for amplitude (smaller range in RER), smaller  $b$  value for period (less swift fluctuation in RER), and smaller value for  $d$  (lower RER values overall) would be indicative of less carbohydrate oxidation. Meanwhile, smaller/more negative  $c$  value would represent increased susceptibility to carbohydrate oxidation, or greater metabolic flexibility, because this indicates an earlier rise in RER. Modeling was conducted by first converting time from hh:min to numeral form (using the VALUE function in Excel; Microsoft Corporation, Redmond, WA) and then converting it to fraction of day by subtracting the integer from each number (using the INT function in Excel). This allowed for comparison of RER values per 24 h cycle. Furthermore, RER values were transformed by subtracting the minimum value observed in cycles 2 and 3 per mouse by the range in RER values for that same mouse and time period. Essentially, this “stretched” the  $y$ -axis so that values ranged from 0 to 1, which helped create better curve fitting to the sine equation (otherwise, the range in untransformed RER values was very

small, which did not work well with the sine curve fitting). Following transformation, the 24 h periods for cycle 2 (without AMG) and cycle 3 (with AMG) were modeled using the “fit” function with nonlinear least squares method option in MATLAB (R2020a, Update 5, 9.8.0.1451342, The MathWorks, Inc., Natick, MA). Each cycle in this analysis began at 18:00 because this was the beginning of the dark period. Cycles 2 and 3 were selected for analysis in order to capture the exact transition from without AMG supplementation to with AMG supplementation.

### 5.3.6 Calculation of Percent Relative Cumulative Frequency (PRCF) of RER

Untransformed RER data for individual mice was used to calculate RER percent relative cumulative frequency (PRCF) per mouse genotype, diet, and cycle (cycle 2 [without AMG] vs. cycle 3 [with AMG]) according to the method of Riachi et al. (2004). Briefly, this involved the following steps: (1) the RER data was sorted in ascending order, (2) an interval of increment was selected (i.e. 0.01), (3) the frequency of observations per interval within the range of all values was calculated, (4) the cumulative frequency was calculated, and (5) the cumulative frequency was expressed as a percentile curve. The analysis was performed for individual mice per diet, genotype, and cycle, as well as for pooled data from all mice per diet, genotype, and cycle.

### 5.3.7 Modeling of PRCF

Following calculation of PRCF, plots of RER (ascending order) vs. PRCF were fit to the Weibull Cumulative Distribution function (Eq. 2) and the Mixed Weibull Cumulative Distribution function (Eq. 3). The key difference between these two model functions is that the Weibull Cumulative Distribution function (Eq. 2) represents a unimodal distribution, whereas the Mixed Weibull Cumulative Distribution function represents a bimodal distribution (Eq. 3).

$$y = 1 - \exp\left(-\left[\frac{x}{x_{50}}\right]^b \ln(2)\right) \quad [2]$$

$$y = \alpha \left(1 - \exp\left(-\left[\frac{x}{x_{50,1}}\right]^{b,1}\right)\right) + (1 - \alpha) \left(1 - \exp\left(-\left[\frac{x}{x_{50,2}}\right]^{b,2}\right)\right) \quad [3]$$

Where for Eq. 2:

$y$  = percent relative cumulative frequency (PRCF; 0 to 100%);

$x_{50}$  = median respiratory exchange ratio (median RER);

$b$  = distribution breadth constant (dimensionless), indicative of slope;

And for Eq. 3:

$y$  = percent relative cumulative frequency (PRCF; 0 to 100%);

$\alpha$  = mixing weight parameter that represents the proportion of the first mode;

$x_{50\_1}$  = median respiratory exchange ratio (median RER) for the first mode;

$b\_1$  = distribution breadth constant for first mode (dimensionless), indicative of slope for the first mode;

$x_{50\_2}$  = median respiratory exchange ratio (median RER) for the second mode;

$b\_2$  = distribution breadth constant for the second mode (dimensionless), indicative of slope for the second mode.

Modeling was done using the “fitnlm” function with the nonlinear least squares method option in MATLAB (R2020a, Update 5, 9.8.0.1451342, The MathWorks, Inc., Natick, MA). The Weibull Cumulative Distribution function (Eq. 2) was used as in Hayes et al. (2020) and Swackhamer et al. (2019) (although in these papers it was referred to by an alternative name, the “Rosin-Rammler Distribution”), whereas the Mixed Weibull Cumulative Distribution function (Eq. 3) was used as in Drechsler and Ferrua (2016). Bounds were placed on the  $x_{50}$ ,  $x_{50\_1}$ , and  $x_{50\_2}$  model parameters to restrict them to the range of RER values for each individual dataset, and  $\alpha$  was restricted to the range of 0 to 1. An iterative modeling approach was used in which 5 initial “best guess” fits were attempted in order to achieve the best fit per each parameter for each curve. An F-test using the F ratio for goodness of fit was used as in Ludden et al. (1994) to assess how using the simpler Weibull Cumulative Distribution compared to using the more complex Mixed Weibull Cumulative Distribution for each individual curve (for curves representing RER from individual mice and pooled from all mice). Examples of the model comparison for two curves from individual mice are shown in Supplementary Figure A.2.

### 5.3.8 Mean RER per 24 h

Mean RER per 24 h cycle was calculated for each group (diet  $\times$  genotype  $\times$  cycle [without/with AMG]) by taking averages of the RER values for cycles 2 and 3.

### **5.3.9 Body weight**

The body weight of each mouse was measured prior to its placement into the indirect calorimetry chamber for each diet acclimation/experimental period for adjustment of the RER calculation (i.e. 6 times total, once before for each of the 6 diets). Additionally, body weight of each mouse was measured at the termination of each diet experimental period in the indirect calorimetry chamber system (i.e. after cycle 4).

### **5.3.10 *Ex vivo* assay of jejunal enzyme activities**

Following experimentation with all the diets, a subset of null and wild-type mice were subjected to one of 6 dietary conditions for 4 additional 24 h cycles ( $n=4$  per condition per genotype): 1) Conventional starch diet, 2) 53% Resistant starch diet, 3) Conventional starch diet with AMG, 4) Conventional starch diet containing 0.5 g/kg acarbose [enzyme inhibitor], 5) Sucrose diet, or 6) fasting [for 12 h only]. Following these exposures, mice were euthanized by decapitation at 24:00 for all conditions except fasting (which was done at 12:00). The abdomen of each mouse was opened and the small intestine was dissected. The intestinal lumen was flushed immediately with 0.01%  $\text{CaCl}_2$  in PBS at 4°C (10 mmol/L phosphate, 0.15 mol/L NaCl, pH 6.8) in order to clean and chill the luminal tissue. The intestine was transferred to a chilled glass plate and mid-jejunal segments were isolated, placed into capped tubes, snap frozen in liquid nitrogen, and stored at -70°C until assaying. Jejunal enzyme activities were assessed for sucrase and  $\alpha$ -glucosidase using the Dahlqvist method (Dahlqvist and Borgstrom 1961; Dahlqvist 1962; Dahlqvist and Telenius 1969). Briefly, sucrase activity involved 60-min incubations at 37°C with 16 mmol/L sucrose as substrate. Assay of  $\alpha$ -glucosidase activity followed procedures previously reported (Quezada-Calvillo, Robayo-Torres, Opekun, et al. 2007; Quezada-Calvillo, Robayo-Torres, Ao, et al. 2007; Nichols et al. 2009) with 20 g/L maltodextrin as substrate. International enzyme units (U/g protein; 1 U = 1  $\mu\text{mol}$  glucose released/min reaction) were used to express activity.

### **5.3.11 Statistical analysis**

To determine the appropriate sample size of mice to use (diet  $\times$  genotype  $\times$  cycle; 24 treatment groups total [with 6 diets, 2 genotypes, and 2 cycles]), a power calculation was conducted

based on average RER over a 24 h period (G\*Power v.3.1.9.7) (Faul et al. 2007). The effect size was set at 0.34 (effect size  $F$ , ratio of population standard deviations) using the G\*Power built-in determination tool by inputting the results of Fernández-Calleja et al. (2018) for RER over a 24 h period. For six diets split into 24 treatment groups and power of 0.8, it was determined that a minimum of 5 mice was required per treatment group ( $n=5$ ). Eight mice were used per treatment group ( $n=8$ ). Note that, because each mouse received each treatment, a total of 16 mice were used.

SAS version 9.4 (SAS Institute, Cary, NC) was used to conduct all statistical analyses. Three-way ANOVA (PROC MIXED) with diet, mouse genotype, and cycle (with or without AMG) as fixed effects was used to determine differences in sine equation parameters (i.e.  $a$ ,  $b$ ,  $c$ ,  $d$ ) as well as in Weibull and Mixed Weibull function parameters (i.e.  $x_{50}$  and  $b$  for Weibull;  $\alpha$ ,  $x_{50_1}$ ,  $b_1$ ,  $x_{50_2}$ , and  $b_2$  for Mixed Weibull). Residuals of all models were plotted and visually assessed for homoscedasticity and normality using histograms and quantile-quantile plots. Statistically significant differences were considered at  $p<0.05$ , and Tukey's *post hoc* test for multiple comparisons was performed when the overall model was significant ( $p<0.05$  for  $F$  value).

For the pooled PRCF analyses, the data from all mice was pooled together and thus there were no replicates. For statistical analysis of this data, 95% confidence intervals were determined for the Weibull and Mixed Weibull parameters (i.e.  $x_{50}$ ,  $b$ ,  $\alpha$ ,  $x_{50_1}$ ,  $b_1$ ,  $x_{50_2}$ ,  $b_2$ ), an approach that has been used previously with modeling (Gardner and Altman 1986; Kreutz, Raue, and Timmer 2012). If the confidence intervals did not overlap, the parameter estimates were considered significantly different at  $p<0.05$ .

## **5.4 Results and Discussion**

### **5.4.1 Starch digestibility, percent amylose, and food quotient of experimental diets**

According to the results from the Englyst assay, the Conventional starch diet had the highest amount of rapidly digestible starch and a negligible amount of resistant starch relative to the other diets (Table 5.3). The Resistant starch diets contained incrementally increasing amounts of resistant starch according to the level of Novelose 260 inclusion in each (18%, 35%, and 53% Resistant starch diets had 10.2, 15.3, and 28.5% resistant starch, respectively; Table 5.3). It is important to note that Novelose 260 is not entirely comprised by resistant starch, which accounts for the discrepancies between the Novelose 260 inclusion levels and actual amounts of resistant

starch in these diets. Additionally, Novelose 260 contains a fraction of pre-treated/pre-gelatinized starch that is likely very highly digestible. Although technically the diets containing Novelose 260 had lower percentages of rapidly digestible starch compared to the Conventional starch diet, the rapidly digestible starch they did contain may have been very highly digestible *in vivo* – in such a manner that is not accurately reflected *in vitro*. This speaks to one of the limitations of the Englyst assay (Zhang and Hamaker 2009). The Sucrose, High-fat, and PicoLab (non-experimental) diets contained negligible amounts of resistant starch. The PicoLab diet contained the highest amount of slowly digestible starch among all the diets, which may be attributed to the inclusion of ground raw corn in this diet instead of corn starch (as was used for the experimental diets). Additionally, the corn starch used in the experimental diets was in the raw state. Raw corn starch has a well-characterized slow digestion property (Zhang, Ao, and Hamaker 2006), and, accordingly, the Conventional starch diet had a relatively high amount of slowly digestible starch according to the Englyst assay.

The 42% fat diet was designed to mimic the average U.S. adult human diet in terms of macronutrient percentage and general composition. Its inclusion in these experiments not only served as a means to “calibrate” our results but also to add context for other studies using this diet.

A portion of maltodextrin was included in each of the diets because it improved their pelletization. This contributed to the fairly large fractions of rapidly digestible starch (55.1% to 74.0%, dry starch basis; Table 5.3) in the diets. Additionally, the High-fat diet contained more sucrose than starch (341.5 g/kg vs. 150 g/kg) and no maltodextrin; sucrose improves pelletization of the diet as well and thus no maltodextrin was required in the High-fat diet.

When percent amylose within the digestible carbohydrate component of each diet was calculated, the diets fell in the following order based on highest to lowest amylose percentage: 53% Resistant starch diet > 35% Resistant starch diet > 18% Resistant starch diet > Conventional starch diet > PicoLab diet (non-experimental) > High-fat diet > Sucrose diet (Table 5.3). The spread in amylose percentages ranged from 0 to 57% of the carbohydrate component, and it is worth noting that not all amylose constitutes resistant starch (Cairns et al. 1995), as there are numerous other chemical, structural, and physical factors that affect resistant starch content.

Food quotients were calculated based on the percent of each macronutrient by weight in each of the diets and were very similar among the diets, ranging from 0.73 to 0.79 (Table 5.3). These calculations are solely based on macronutrient compositions (i.e. percentages of

carbohydrate, protein, and fat) and thus were similar for all the diets. Such quotients may benefit from factoring in additional aspects of the diets, such as carbohydrate digestibility.

#### 5.4.2 Effect of diet, genotype, and AMG supplementation on RER

The mean parameters  $a$ ,  $b$ ,  $c$ , and  $d$  from the sine equation curve fitting for individual mice, along with the corresponding  $R^2$  values as indications of goodness of fit, are shown in Table 5.4. Because of variations observed in mice activity level (though not measured quantitatively), values that were 2 standard deviations from the mean ( $\pm 2$  standard deviations) were excluded in calculating the means per parameter (note that this was not done for the means for  $R^2$  though). Statistical analyses were conducted both with and without outliers. Figures 5.2-5.7 show the mean parameter equations per group plotted as smooth curves per diet. Figures 5.8 and 5.9 depict the mean parameter equations plotted as smooth curves per null and wild-type mice, respectively. Figures 5.10 and 5.11 illustrate mean parameter equations plotted as smooth curves for both genotypes but with AMG only and without AMG only, respectively. Figure 5.12 shows the mean parameter equations split by diet. A sine function visualization tool may aid the reader in interpreting these results (e.g. <https://www.geogebra.org/m/znb4GNk7>).

Results from three-way ANOVA showed that there was a main effect of diet for the  $a$  and  $c$  parameters ( $p < 0.0001$  for both). *Post hoc* tests revealed that the High-fat diet had significantly lower  $a$  parameter than all the other diets (Tables 5.4 and 5.5; Figure 5.12), which suggests such diet had lower metabolic flexibility because the fluctuation in RER values (indicated by the amplitude,  $a$ ) was smaller (Muoio 2014). This also corroborates previous research indicating that high-fat diets impair the diurnal rhythm of RER (Small et al. 2019). For the  $c$  parameter, the High-fat diet had significantly higher values (i.e. values that were less negative) than all the other diets, and the 53% Resistant starch diet had significantly higher values than the 18% Resistant starch diet. In other words, RER values for the High-fat diet shifted to the right and had a less swift rise in RER, signifying a slower transition to carbohydrate oxidation. The 53% Resistant starch diet had a less swift shift to carbohydrate oxidation than the 18% Resistant starch diet, potentially due to lower digestion, and thus higher fermentation, of the high amount of resistant starch and ensuing fatty acid oxidation. In general, RER for all the carbohydrate diets became higher earlier in time compared to the High-fat diet, which corresponds with the higher amount of carbohydrate in these diets. Furthermore, higher digestible carbohydrate amount resulted in an earlier shift to

carbohydrate oxidation. This effect was also observed for the  $c$  parameter when outliers were included ( $p=0.0002$ ). This novel finding suggests a more efficient switch to carbohydrate oxidation for carbohydrates that are more digestible, though it is important to note that the Conventional starch diet contained raw corn starch and had a high proportion of slowly digestible starch. We postulate that moderating carbohydrate digestion by feeding slowly digestible starch may optimize the efficiency of switching between fat and carbohydrate oxidation.

An intriguing pattern can be observed in Figure 5.12A for null mice fed the Conventional starch diet and all three resistant starch-based diets: there is an incremental shift of the  $c$  parameter according to the level of resistant starch. Namely, the curves appear to shift according to their  $c$  parameter values in the following order: Conventional starch diet (-10.47), 18% Resistant starch diet (-10.30), 35% Resistant starch diet (-10.07), [Sucrose diet is next for an unknown reason (-9.56)], and 53% Resistant starch diet (-9.04). A smaller (i.e. more negative)  $c$  value represents an earlier rise in carbohydrate oxidation and, although only significant differences in  $c$  were observed between the 53% Resistant starch diet and 18% Resistant starch diet, a later shift toward carbohydrate oxidation was observed by increasing the resistant starch content in the diet. An exploratory linear regression analysis of this data revealed that there were trending direct relationships between both amylose percentage and resistant starch amount (separately) vs. the  $c$  parameter from the sine equation curve fitting for the three resistant starch diets and the Conventional starch diet ( $r=0.91$ ,  $p=0.09$  for amylose percentage vs.  $c$ ;  $r=0.94$ ,  $p=0.06$  for resistant starch amount vs.  $c$ ; Figure 5.13). Lower percent amylose and resistant starch amount were associated with earlier rise in RER (i.e. earlier shift to carbohydrate oxidation as indicated by lower  $c$  value). No other relationships or trending relationships were found for null mice with AMG or wild-type mice either with or without AMG ( $p>0.05$ ), which suggests Mgam has larger influence over digesting resistant starches than Si. These results suggest that faster and higher carbohydrate digestion promotes earlier switching to carbohydrate oxidation and thus may indicate enhanced metabolic flexibility. However, in this case, the Conventional starch diet also contained a substantial amount of slowly digestible starch and thus further investigation is needed to determine if the more efficient switching is due to rapidly digestible starch or slowly digestible starch.

There was only an effect of genotype for the  $d$  parameter, such that null mice had higher  $d$  than wild-type ( $p=0.01$ ; Tables 5.4 and 5.5; Figures 5.8 and 5.9), which may mean that carbohydrate oxidation was increased in null mice (because higher  $d$  indicates RER values were

shifted higher on the  $y$ -axis). This finding was surprising because we expected the null mice to have reduced carbohydrate oxidation compared to the wild-type mice because they were lacking Mgam enzyme activity. However, this effect was not observed when outliers were included in the analysis ( $p=0.21$ ).

As for the effect of AMG supplementation, statistical analysis showed that there was a main effect of cycle (i.e. with vs. without AMG) for the parameters  $a$ ,  $c$ , and  $d$ , such that  $a$  was lower with AMG ( $p=0.03$ ),  $c$  was lower with AMG ( $p<0.0001$ ), and  $d$  was higher with AMG ( $p<0.0001$ ) (Table 5.5; Figures 5.10 and 5.11). This effect for the  $c$  parameter was also observed when outliers were included ( $p=0.04$ ; Table 5.5). These results show that AMG made the amplitude of the curve smaller, shifted the curve to the left (on the  $x$ -axis), and shifted the curve up (on the  $y$ -axis). Fundamentally, they demonstrate that AMG increased the affinity for and utilization of carbohydrate for oxidation, which further supports that notion that increased carbohydrate digestion promotes carbohydrate oxidation ( $d$  parameter) and switch to carbohydrate oxidation ( $c$  parameter). Yet, the lower  $a$  parameter in the context of a high  $d$  parameter signifies a blunted lower range of RER values, which may be detrimental because this suggests less fat oxidation was occurring. We propose that moderated carbohydrate digestion may allow for better switching between both high carbohydrate oxidation and high fat oxidation (i.e. high RER and low RER).

### **5.4.3 Effect of diet, genotype, and AMG supplementation on PRCF of RER**

#### ***Data analyzed per individual mice***

PRCF of RER was analyzed per individual mice and fit to both the Weibull Cumulative Distribution (Eq. 2) and Mixed Weibull Cumulative Distribution (Eq. 3). An F-test was conducted to examine which model would be superior to use for each individual mouse per diet, genotype, and cycle ( $n=190$  total); this analysis indicated that the Weibull was only superior to the Mixed Weibull in one instance ( $p=0.09$ ), whereas the Mixed Weibull was better for all 189 others ( $p<0.05$ ), noting that only 10 instances had F-tests with  $p$ -values between 0.0001 and 0.0500 and the rest were lower than 0.0001. For the purposes of this investigation, we decided to move forward using the Mixed Weibull Cumulative Distribution for analyzing the PRCF data of individual mice. We included the one instance that technically had a better fit to the Weibull Cumulative

Distribution by the F-test (with  $p=0.09$ ) because its  $R^2$  was still high ( $R^2=0.99$  for the Mixed Weibull Cumulative Distribution). In a similar manner to what was done with the sine equation parameters, we excluded values that were 2 standard deviations from the mean ( $\pm 2$  standard deviations) in calculating the means for each parameter ( $\alpha$ ,  $x_{50\_1}$ ,  $b\_1$ ,  $x_{50\_2}$ ,  $b\_2$ ) per treatment group. Statistical analyses were conducted excluding these outliers. All mean parameter estimates are shown in Table 5.6, with  $x_{50\_1}$  and  $x_{50\_2}$  also shown in Figure 5.14, and  $b\_1$  and  $b\_2$  also shown in Figure 5.15.

To aid in interpretation of the parameters from both the Weibull Cumulative Distribution (even though we are not reporting the data from this analysis) and the Mixed Weibull Cumulative Distribution, visual representations of each with theoretical curves are included in Supplementary Figures A.3 and A.4 for the Weibull and in Supplementary Figures A.5-A.9 for the Mixed Weibull. In each of these figures, one parameter is altered while all others are held constant in order to examine how one parameter affects the shape of the curve and therefore relates to RER.

The PRCF curves of the RER data generally appeared bimodal, with one mode generally ranging from approximately 0.65 to 0.85 RER and the other mode ranging from approximately 0.95 to 1.03 RER. Because an RER of 0.70 indicates fat is being used as the predominant fuel source, and an RER of 1.00 indicates carbohydrate is being used as the predominant fuel source, we propose that the two modes in our PRCF curves represent fat oxidation and carbohydrate oxidation, respectively. Using this interpretation, the  $x_{50\_1}$  value is suggested to represent the median RER of the fat oxidation mode, and the  $x_{50\_2}$  value is suggested to represent the median RER of the carbohydrate oxidation mode. Furthermore, the  $b\_1$  and  $b\_2$  values describe the fat oxidation and carbohydrate oxidation modes, respectively.

Using the Mixed Weibull Cumulative Distribution, three-way ANOVA indicated a main effect of diet for the  $x_{50\_1}$ ,  $x_{50\_2}$ , and  $b\_2$  parameters ( $p<0.0001$ ,  $p<0.0001$ , and  $p=0.01$ , respectively; Table 5.6, Figures 5.14 and 5.15). *Post-hoc* analyses revealed that the Conventional starch and 18% Resistant starch diets had significantly lower  $x_{50\_1}$  values than 53% Resistant starch, Sucrose, and High-fat diets, indicating that this diet had lower median RER values for the first mode, which we propose is the mode representing fat oxidation. A lower RER value for the fat oxidation mode suggests greater degree of fat oxidation. The explanation as to why the Conventional starch and 18% Resistant starch diets would have greater fat oxidation than diets containing larger amounts of resistant starch is unclear, but the greater amount of raw corn starch

in these diets likely had a slow digestion property and may have played a role (Zhang, Ao, and Hamaker 2006). Furthermore, oxidation of fat within the body is generally not driven by the amount of fat consumed but instead by the lack of carbohydrate consumed (i.e. displacement of carbohydrate consumed); this is further affected by body weight, body composition, and level of activity (Flatt 1995; Kevin D. Hall 2012; Longo et al. 2010). In our case, the mice were similar in body weight (see “Body Weight” section below) and body composition (data not shown); however, we did not measure their activity. The High-fat diet had higher  $x_{50_1}$  than anticipated, but it is important to note that this diet also contained a relatively high amount of sucrose. Specific to the null mice, these mice have been shown to have enhanced activity of sucrase-isomaltase (Si) as partial compensation for the lack of Mgam (Quezada-Calvillo, Robayo-Torres, Opekun, et al. 2007), and this Si may have a preferential ability to hydrolyze sucrose and thereby affect RER. For  $x_{50_2}$ , diets ranked as follows (highest to lowest  $x_{50_2}$ , or median RER for the second mode): Sucrose diet > 53% Resistant starch diet = 18% Resistant starch diet > 35% Resistant starch diet = Conventional starch diet > High-fat diet (Table 5.6; Figure 5.14). Because  $x_{50_2}$  represents the median RER of the second mode, which we propose describes carbohydrate oxidation, these findings suggest greater carbohydrate oxidation was observed for the carbohydrate-predominant diets compared to the High-fat diet. Specifically, the Sucrose diet contained a large portion of readily available carbohydrate (and note the different absorption pathway for fructose (Sun and Empie 2012) that contributes to carbohydrate oxidation), and thus it had the highest carbohydrate oxidation, with mean values of 1.11-1.12. Because de novo lipogenesis may increase RER (Crescenzo et al. 2013; Glamour et al. 1995), such values suggest carbohydrates were being oxidized and stored as fat for the Sucrose diet feeding. The 53% Resistant starch diet may have had a portion of very rapidly digestible carbohydrate from the Novelose 260 to drive carbohydrate oxidation, as described above. The reason the 18% Resistant starch diet had similar mean carbohydrate oxidation to the 53% Resistant starch diet is rather perplexing, but it may also be that the 35% Resistant starch diet has an optimized ratio of resistant starch to raw corn starch to exert an effect on RER. The meaning of the effect size of these differences (values from 1.04-1.08 for 53% Resistant starch diet compared to 1.00-1.04 for 35% Resistant starch diet) is also worthy of consideration. As the Conventional starch diet also had relatively low  $x_{50_2}$  (carbohydrate oxidation) compared to the other carbohydrate-dominant diets, the raw corn starch in this diet could have been more slowly delivered to the body to affect carbohydrate oxidation or processes

that ultimately impact carbohydrate oxidation. Most of the *in vivo* work on slowly digestible carbohydrates to date has focused on glycemic response or physiological/hormonal responses, and the work on resistant carbohydrates has generally focused on glycemic response, fermentation, and the gut microbiome. Aside from one study by Fernández-Calleja et al. (2018) showing a more pronounced carbohydrate oxidation response in female mice compared to male mice fed a high-amylose diet (diet with 60% of carbohydrate component from amylose), to our knowledge little is known about how the amount or type of slowly digestible or resistant carbohydrate can affect metabolism and partitioning of carbohydrate for energy. Sophisticated tools have been developed that allow for simultaneous, continuous, and prolonged measurement of RER,  $^{13}\text{CO}_2$ , and fermentation indicators (i.e.  $\text{H}_2$  and  $\text{CH}_4$ ) using an enhanced indirect calorimetry system (J. M. S. Fernández-Calleja et al. 2018; J. Fernández-Calleja et al. 2018; J. M. S. Fernández-Calleja, Bouwman, Swarts, Billecke, et al. 2019; J. M. S. Fernández-Calleja, Bouwman, Swarts, Oosting, et al. 2019), which makes investigations of carbohydrate partitioning for oxidation as well as metabolic flexibility promising areas for future research. For  $b_2$ , the High-fat diet had significantly higher values than the Sucrose diet, but all other diets did not differ (Table 5.6; Figure 5.15). This finding suggests there was a narrower spread in RER values for the second mode (representing carbohydrate oxidation) for the High-fat diet than for the Sucrose diet (Supplementary Figure A.8). A key concept in metabolic flexibility is how substrate utilization changes during the transition from fed to fasted states (Goodpaster and Sparks 2017). A narrowing in the range of RER values in either the carbohydrate or fat oxidation modes could be indicative of a swift and more complete change in substrate utilization (as opposed to a gradual change, as would be characteristic of a wider range of values in the mode). From this perspective, a narrower range of RER values, or higher  $b_1$  or  $b_2$  values, may be indicative of enhanced metabolic flexibility.

A main effect of genotype was observed for the  $x_{50_1}$  and  $b_2$  parameters ( $p=0.0004$  and  $p=0.02$ , respectively), such that null mice had significantly higher  $x_{50_1}$  and  $b_2$  than wild-type mice (Table 5.6, Figures 5.14 and 5.15). The higher  $x_{50_1}$  (representing the fat oxidation mode) for null mice suggests that altered ability to digest carbohydrate also reduced fat metabolism, aligning with the concept that fat oxidation levels change more as a function of carbohydrate intake and energy expenditure (Flatt 1995); however, in this line of thinking, hindered or slowed carbohydrate digestion (as is the case for null mice) would theoretically lead to increased fat

oxidation instead of the decreased oxidation observed, so this requires further investigation. Yet, this finding corroborates the increased  $d$  values observed for null mice from the sine equation approach. Considering that null mice likely had increased levels of resistant starch due to their lack of Mgam, it appears that slow carbohydrate digestion (but not low carbohydrate digestion as seen for resistant starch) promotes fat oxidation. The higher  $b_2$  suggests that null mice had a narrow spread in RER values for the second mode (representing carbohydrate oxidation), which suggests a more complete switch to carbohydrate oxidation and thus increased metabolic flexibility. In the end, null mice burned less fat as fuel compared to wild-type mice, yet null mice had a higher degree of metabolic flexibility in the carbohydrate oxidation mode. These differences were overall minor compared to what we anticipated for mice lacking a complete set of enzymes, but they support the previous findings that Si is able to handle the digestion of most types of starch, such as those used here, while Mgam has wider versatility for hydrolyzing more difficult to digest starches and other  $\alpha$ -glucans (B.-H. Lee et al. 2016).

Regarding AMG supplementation, there was a main effect of cycle (i.e. with AMG vs. without AMG) for the  $x_{50_1}$ ,  $x_{50_2}$ , and  $b_2$  parameters ( $p=0.002$ ,  $p<0.0001$ , and  $p=0.03$ , respectively; Table 5.6, Figures 5.14 and 5.15). For  $x_{50_1}$ , values were significantly higher with AMG compared to without AMG, which suggests that adding AMG had an impact on the fat oxidation mode despite AMG acting on carbohydrates [aligning with the carbohydrate displacement theory of Flatt (1995)]. These results agree with the sine equation results described above, and we reason that the apparent lower degree of fat oxidation observed with AMG supplementation may be undesirable. For  $x_{50_2}$ , adding AMG also increased  $x_{50_2}$  values, signifying supplementation of the diets with AMG increased median RER of the second mode (representing carbohydrate oxidation). This suggests AMG increased partitioning of carbohydrates to be used for metabolism and energy use or storage. AMG supplementation also somewhat increased  $b_2$ , indicating that it decreased the spread of RER values in the second (carbohydrate oxidation) mode and increased metabolic flexibility. However, it appears that the effect was most pronounced for the High-fat diet, though the diet  $\times$  cycle interaction was not significant. These findings do not support our hypothesis related to AMG. Yet, the blunted fat oxidation observed with AMG (generally higher  $x_{50_1}$  values) may not be ideal, and we speculate that rapidly digestible carbohydrates may similarly impede fat oxidation. It is intriguing to note that the Conventional starch and 18% Resistant starch diets, both which have greater amounts of slowly

digestible starch, had lower  $x_{50,1}$  values (Figure 5.14), suggesting that slowly digestible starch may have optimal digestibility to enable a greater amount of fat oxidation.

An interaction effect was found for  $\alpha$  such that genotype  $\times$  cycle was significant ( $p=0.03$ ), but *post hoc* tests corrected for multiple comparisons revealed there were no statistically significant differences between any genotype  $\times$  cycle treatment groups (there was only a trending difference between wild-type mice without AMG and wild-type mice with AMG,  $p=0.10$ ). No other interactions were significant ( $p>0.05$ ).

### ***Data analyzed as pooled from all mice***

#### *Weibull Cumulative Distribution*

For the pooled PRCF analysis, the Weibull Cumulative Distribution yielded a good fit for the 24 treatment groups (minimum  $R^2$  of 0.94, mean  $R^2$  of  $0.97 \pm 0.00$ ), but the Mixed Weibull Cumulative Distribution significantly improved the fit for 19 of the 24 groups ( $p<0.05$  for F-test comparing the two models, mean  $R^2$  of  $0.99 \pm 0.00$ ). We examined the data using both approaches and included all 24 treatment groups in both.

PRCF curves of the pooled data are depicted separately per diet in Figure 5.16, split by genotype in Figure 5.17, and split by cycle (with AMG vs. without AMG) in Figure 5.18. Because these analyses were of pooled data and no measures of variation could be calculated from the data itself, 95% confidence intervals were determined through modeling and used to identify statistically significant differences among parameters. Weibull parameters of  $x_{50}$  and  $b$  are shown in Tables 5.7 and 5.8, respectively. Mixed Weibull parameters of  $\alpha$ ,  $x_{50,1}$ ,  $b_1$ ,  $x_{50,2}$ , and  $b_2$  are shown in Tables 5.9-5.13, respectively. The tables include arrows in separate columns for genotype and AMG to more readily visualize the effects of these two factors within each diet.

For  $x_{50}$  from the Weibull Cumulative Distribution, the Sucrose diet was significantly highest with the exception that wild-type mice consuming this diet with AMG did not significantly differ from wild-type mice consuming the 53% Resistant starch diet with AMG (Table 5.7). This is consistent with the previous PRCF approach (Mixed Weibull with curve fitting for data from individual mice) and the idea that greater carbohydrate oxidation is observed for diets containing more highly available carbohydrate (e.g. sucrose). As mentioned above, the relatively high carbohydrate oxidation for the 53% Resistant starch diet could possibly be related to the supposed

fraction of very highly digestible carbohydrate in Novelose 260, also noting that the raw crystalline regions of high-amylose corn starch are digested simultaneously with the amorphous regions (Man et al. 2012; Zhang, Ao, and Hamaker 2006). The null and wild-type mice fed Conventional starch diet without AMG had the lowest values overall, with null mice fed the High-fat diet having a similarly low value. Because the effect observed for the Conventional starch diet was lost when AMG was provided, it appears that the corn starch in this diet may have exerted an effect due to a slow digestion property, which appears to be beneficial for optimizing the switching between fat oxidation and carbohydrate oxidation, although this requires further investigation. Low  $x_{50}$  for the High-fat diet can be expected because this diet had a lower percentage of carbohydrate. The remaining diets'  $x_{50}$  values fell between the Sucrose and High-fat/Conventional starch diets (without AMG). Genotype differences emerged for the 53% Resistant starch and High-fat diets, with additional minor differences for the 35% and 18% Resistant starch diets fed to null mice with AMG (Table 5.7). A lower  $x_{50}$  for null mice than wild-type mice fed the 53% Resistant starch diet suggests hindered carbohydrate oxidation overall, as fermentation of the high amount of resistant starch was likely occurring in the large intestine to a greater degree in the null mice than wild-type mice because they lacked Mgam. The lower  $x_{50}$  for null mice compared to wild-type mice when fed High-fat diet may seem surprising because of the large portion of fat in this diet compared to the other diets. However, as noted above, the High-fat diet contained a relatively high amount of sucrose, and the enhanced activity of Si in null mice may have partially compensated for the lack of Mgam (Quezada-Calvillo, Robayo-Torres, Opekun, et al. 2007) to hydrolyze sucrose and increase RER. AMG supplementation generally increased  $x_{50}$  when both null and wild-type mice were fed the Conventional starch and 53% Resistant starch diets, and only null mice when fed the 35% Resistant starch and 18% Resistant starch, and High-fat diets. These findings suggest increasing carbohydrate digestion through AMG supplementation resulted in increased carbohydrate oxidation. Overall, instances that increased  $x_{50}$  suggest that the median RER shifted toward more carbohydrate oxidation (Supplementary Figure A.3). However, this approach involves only the overall median RER and thus distinctions in the distribution of the first and second RER modes were not captured using this set of analyses (see Figure 5.16A-E, for visualization of the bimodal distributions for most of the groups per diet).

For  $b$  from the Weibull Cumulative Distribution, only subtle differences were observed. The key difference was that the High-fat diet caused  $b$  values to increase relative to the other diets,

and this is readily apparent in comparing Figure 5.16F to Figure 5.16A-E, as well as in Figures 5.17 and 5.18. According to the rationale described above, this may signify enhanced metabolic flexibility for the High-fat diet compared to the other diets. However, the High-fat diet also had a blunted upper limit of RER, suggesting the High-fat diet enhanced switching of RER for a lower range of values, which is not beneficial (Muio 2014). We propose that the High-fat diet caused a dysregulation of RER as opposed to improved metabolic flexibility. The Sucrose and 18% Resistant starch diets had the lowest overall  $b$  values, ranging between 6.36 and 7.28, but they were not consistently significantly different from the other diets. Such low  $b$  values indicate wider spread of RER values (Supplementary Figure A.4), which could be interpreted as decreased metabolic flexibility. For the effect of genotype, null mice fed the High-fat diet without AMG had significantly higher  $b$  value than wild-type mice fed the same diet without AMG, but, this effect was not observed when AMG was supplemented. Because a higher  $b$  value signifies a narrower spread of RER values, this suggests null mice had higher metabolic flexibility, and this effect was likely due to limited carbohydrate digestion because supplementation with AMG negated the effect. Overall, the higher  $b$  values for the High-fat diet show a narrower spread of RER values was observed for this diet compared to the other diets (Supplementary Figure A.3, Figures 5.16-5.18), while genotype and AMG had minimal effect on the spread of RER according to this approach.

#### *Mixed Weibull Cumulative Distribution*

The Mixed Weibull Cumulative Distribution is advantageous over the Weibull Cumulative Distribution in that it can more readily characterize the bimodal distributions that were observed for a majority of the PRCF curves for RER (e.g. Figure 5.16). In the Mixed Weibull Cumulative Distribution, the  $\alpha$  parameter is an indicator of relative partitioning between fat and carbohydrate oxidation, as it designates the split between the two modes (note that we propose the first mode represents fat oxidation and the second mode represents carbohydrate oxidation, as described in section 5.3.3.1). A smaller  $\alpha$  indicates more of the distribution is partitioned to carbohydrate oxidation, and a larger  $\alpha$  indicates more of the distribution is partitioned to fat oxidation (Supplementary Figure A.5). Using the pooled data approach with 95% confidence intervals for the mean parameter values, in general the three resistant starch diets had larger  $\alpha$  values than the Conventional starch diet (Table 5.9 and Figure 5.19), which is reasonable considering resistant starch is not as easily digested and absorbed in the small intestine and may prompt greater fatty

acid oxidation as it passes into the large intestine where it is fermented to produce short chain fatty acids. This would limit the amount of carbohydrate available for digestion, absorption, and metabolism. Oddly, the High-fat diet had  $\alpha$  values that varied greatly (from 0.126 to 0.712), which suggests dysregulated metabolism and may be partially attributed to the fact that the RER data for this diet visually appeared to be more unimodal rather than bimodal (Figure 5.16). Yet, the F-test indicated the Mixed Weibull Cumulative Distribution significantly improved the fit compared to the Weibull Cumulative Distribution for the High-fat diet using this pooled data approach. There were inconsistencies in the impact of genotype. Namely, there were no differences between null and wild-type mice for the Conventional starch or 18% Resistant starch diets, but there were differences for the 53% Resistant starch diet with AMG, the Sucrose diet without AMG, the High-fat diet without AMG, and the 35% Resistant starch diet both with and without AMG (Table 5.9 and Figure 5.19). In the 53% Resistant starch diet with AMG and Sucrose diet without AMG, null mice had lower  $\alpha$  than wild-type mice. These results suggest greater partitioning of carbohydrates for energy when: (1) the diet with the greatest amount of resistant starch (least digestible starch) was given in combination with the AMG to increase digestion and (2) the diet with the most amount of sucrose was provided, potentially indicating overexpression of Si in null mice. For the High-fat diet without AMG, the null mice had higher  $\alpha$  than wild-type mice, which may be due to the lower/slower ability of null mice to digest starch in combination with the low portion of carbohydrate in the diet. Within the 35% Resistant starch diet, null mice had higher  $\alpha$  than wild-type when they were not given the AMG supplement, but with AMG the effect switched – the null mice had lower  $\alpha$  than wild-type mice. This switch in impact suggests the combination of 35% Resistant starch diet and AMG gave null mice an increased affinity to oxidize carbohydrate compared to wild-type mice. Regardless, AMG either decreased  $\alpha$  or had no effect for both genotypes for all diets. It had the most pronounced effect for the 53% Resistant starch diet. This effect of AMG supports that a smaller  $\alpha$  signifies more of the distribution is partitioned to carbohydrate oxidation because AMG increases carbohydrate digestion. However, it is curious that this effect was not observed using the Mixed Weibull approach with curve fitting to individual mice.

The  $x_{50,1}$  parameter ranged from 0.739 to 0.876 RER among the 24 treatment groups (diet  $\times$  genotype  $\times$  cycle; Table 5.10). Wild-type mice consuming the High-fat diet with AMG had the highest  $x_{50,1}$  value overall (0.876 RER; Figure 5.18B), which was significantly higher than all

other groups ( $p < 0.05$ ; Table 5.10). Null mice under the same conditions had the second highest value (0.849 RER), although this was not significantly different from the null mice fed the Sucrose diet (both with and without AMG). These findings seem to suggest that lower oxidation of fat was observed – at least in the fat oxidation RER mode – when mice were fed a High-fat diet, regardless of whether or not Mgam was present, which may suggest that mice fed this diet were experiencing smaller alterations in fat oxidation and storage than when fed the other diets. In a previous study, blunted RER values (values going both not very high or very low) were observed for mice fed a normal chow diet for 17 wk and then fed a high-fat diet for 4 days compared to lean mice fed the normal chow diet the entire study, and this effect was further blunted for mice fed a high-fat diet for 17 wk (Longo et al. 2010). Previous research has shown that high-fat diets impair the diurnal rhythm of RER (Small et al. 2019), and in the present study aberrations in RER are apparent through the sine equation approach (Table 5.4; Figures 5.7-5.12) as well as PRCF approaches (Figures 5.16-5.18), especially for the  $\alpha$  parameter calculation for pooled data noted above. Both null and wild-type mice fed the Conventional starch diet without AMG had the lowest  $x_{50,1}$  values among the groups, although these did not differ from null mice fed 53% Resistant starch without AMG or wild-type mice fed 18% Resistant starch without AMG (Table 5.10). As stated above, we hypothesize that the slowly digestible starch present in the raw corn starch for this diet may have enabled more efficient switching to low RER values, promoting greater fat oxidation. The null mice fed 53% Resistant starch without AMG were expected to have a low  $x_{50,1}$  value (i.e. greater fat oxidation) because this diet contained the largest amount of resistant starch (which would pass into the large intestine to undergo fermentation and fatty acid oxidation), the mice lacked the Mgam enzyme, and no supplement was given to increase carbohydrate digestion; in essence, this treatment group had the lowest level of possible carbohydrate digestion among the carbohydrate-predominant diets. As for genotype, there was a genotype effect for the 53% Resistant starch, Sucrose, and High-fat diets, although it was inconsistent among them (e.g. null mice had consistently lower  $x_{50,1}$  than wild-type mice for the 53% Resistant starch diet both with and without AMG, but they had consistently higher  $x_{50,1}$  for the Sucrose diet; Figure 5.17). A lower  $x_{50,1}$  for null mice fed the 53% Resistant starch diet suggests greater fat oxidation; in this treatment group, less carbohydrate digestion would be occurring due to the high amount of resistant starch, and such resistant starch may be more readily fermented because of the lack of Mgam enzyme. Conversely, the higher  $x_{50,1}$  for null mice fed the Sucrose diet may have resulted in part because

sucrase-isomaltase is upregulated to partially compensate for the lack of Mgam in these mice (Quezada-Calvillo, Robayo-Torres, Opekun, et al. 2007); higher sucrose digestion prompted by Si could increase carbohydrate oxidation and in turn reduce fat oxidation. AMG significantly increased  $x_{50,1}$  for both genotypes of mice fed the Conventional starch diet, 53% Resistant starch diet, and High-fat diet, but AMG only increased  $x_{50,1}$  for null mice fed the 35% Resistant starch diet (Figure 5.18). It appears that inhibiting the activity of a small intestinal  $\alpha$ -glucosidase enzyme (i.e. knocking out Mgam) may decrease fat oxidation for starch-dominant diets, or adding a carbohydrate-degrading enzyme (i.e. providing AMG) may increase fat oxidation. This supports that slower (but not lower) starch digestion may help promote fat oxidation, which suggests enhanced ability to shift between carbohydrate and fat oxidation.

Although 95% confidence intervals indicated statistically significant differences in the  $b_1$  parameter among diets, there did not appear to be a consistent clustering per diet type, with the exception that the Sucrose diet generally had intermediate-low values (14.3-19.6, unitless) considering the overall range (12.3-42.0, unitless; Table 5.11; Figure 5.16E). Null mice fed the 53% Resistant starch diet without AMG had higher  $b_1$  than wild-type mice under the same conditions, and null mice fed the 35% Resistant starch diet with AMG had lower  $b_1$  than wild-type mice (Figure 5.17). Such results suggest metabolic flexibility (i.e. the spread in RER values for the fat oxidation mode) was enhanced for null mice compared to wild-type mice at the lowest level of carbohydrate digestion (i.e. 53% Resistant starch diet [lowest digestibility], without AMG to augment digestion]. Aside from these differences, there were no other effects of genotype on  $b_1$ . As for effects of AMG, although not always significantly different, AMG tended to decrease  $b_1$ . The only exceptions to this were that AMG increased  $b_1$  for wild-type mice fed the 53% Resistant starch and the 35% Resistant starch diets (Table 5.11). These results should be interpreted with caution because there were no differences in the  $b_1$  values using the Mixed Weibull approach with curve fitting for individual mice.

The spread in  $x_{50,2}$  values, which represent the median RER for the carbohydrate oxidation mode, was 0.945-1.12 RER (Table 5.12). The Sucrose diet groups had significantly larger  $x_{50,2}$  than all other groups (1.11-1.12 RER; Figures 5.16-5.18), which is consistent with the other PRCF approaches and could be expected because this diet provided the most readily available carbohydrate among all the diets. The  $x_{50,2}$  for the High-fat diet groups was generally very low, with the exception of the wild-type mice fed the High-fat diet with AMG; this group had a median

RER ( $x_{50,2}$ ) of 1.00 RER, while the values for the other 3 High-fat diet groups ranged from 0.945-0.978 RER. These findings build upon previous evidence indicating high-fat diet blunts the diurnal patterns of RER and decreases carbohydrate oxidation (Small et al. 2019), yet it is unclear why the of High-fat diet with AMG in wild-type mice would differ from other High-fat diet treatment groups (or at least the null mice fed the High-fat diet with AMG). Interestingly, the null and wild-type mice fed the Conventional starch diet without AMG had considerably low  $x_{50,2}$  values (both 0.988 RER); this could also be related to the raw corn starch in the Conventional starch diet. However, it may be that a value above 1.0 RER is less desirable because it suggests de novo lipogenesis (Crescenzo et al. 2013; Glamour et al. 1995). A previous study with human participants that were either healthy or had type 2 diabetes found a decrease in total carbohydrate oxidation in the participants with type 2 diabetes when 50 g of a slowly digestible starch (46:54 ratio of raw tapioca and maize starches) was fed compared to 50 g of a more rapidly digestible starch (raw maize starch), although no effect was found in healthy participants (Seal et al. 2003); such findings suggest that slowly digestible starches impact carbohydrate metabolism but also that factors such as insulin sensitivity/action should also be considered. Related to the present study, the null mice (Mgam knockout) had impaired insulin action due to the lack of Mgam (Nichols et al. 2009), but the wild-type mice reportedly had proper insulin action. Further investigations of the relationship among slowly digestible starch and resistant starch, insulin action, and carbohydrate oxidation are needed to elucidate the mechanism(s) at play, especially because insulin resistance has been linked with impaired metabolic flexibility (Muoio 2014; Goodpaster and Sparks 2017; Stull et al. 2010). As for an effect of genotype, null mice had significantly lower  $x_{50,2}$  than wild-type mice when fed the 53% Resistant starch diet, the 18% Resistant starch diet without AMG, and the High-fat diet, and (Figure 5.17). However, the AMG supplement increased  $x_{50,2}$  for null mice fed the 35% Resistant starch diet compared to the other 35% Resistant starch diet groups, and null mice fed the 18% Resistant starch diet with AMG had higher  $x_{50,2}$  than wild-type mice under the same conditions. Such findings suggest AMG compensated for the lack of Mgam in null mice to increase their propensity to oxidize carbohydrate for these diets. As for a generalized effect of AMG, this supplement increased  $x_{50,2}$  for mice fed the Conventional starch, 53% Resistant starch, and High-fat diets (Figure 5.18). AMG increased  $x_{50,2}$  in null mice only when they were fed the 18% Resistant starch and Sucrose diets. These findings suggest that providing a starch digesting enzyme can directly influence carbohydrate oxidation and at least partially compensate for the lack of

Mgam in the null mice. We initially thought that the AMG may have had some sucrase activity, which could partially account for the shift observed in the sine  $c$  parameter and the increase in  $x_{50,2}$  for the null mice, yet an analysis of enzyme activity for this supplement indicated there was very minimal sucrase activity (0.5 U/mL sucrose-degrading activity vs. 979.7 U/mL maltodextrin-degrading activity; other data not shown). Overall, greater carbohydrate availability/digestion appeared to result in higher carbohydrate oxidation, and slowly digestible starch (i.e. raw corn starch in the Conventional starch diet) may enable a moderate carbohydrate oxidation.

$b_2$  represents the spread of data within the second mode (describing carbohydrate oxidation; Supplementary Figure A.8). Using the pooled data approach, diets did not have consistent effects on  $b_2$  (Table 5.13). For example, the wild-type mice fed the High-fat diet without AMG had the lowest  $b_2$  value (10.6, unitless), which we propose is indicative of poor metabolic flexibility, but for the same diet with AMG, wild-type mice had the highest value among all the groups, which would represent improved metabolic flexibility (33.3, unitless; Table 5.13; Figure 5.16). As for the effect of genotype, null mice tended to have higher  $b_2$  values for all but the 53% Resistant starch and High-fat diets, suggesting that they had increased metabolic flexibility in the circumstances when they had more non-resistant starch or carbohydrate available to digest, respectively. As such, null mice had significantly higher  $b_2$  values than wild-type when fed the 35% Resistant starch diet with AMG, 18% Resistant starch diet with AMG, Sucrose diet without AMG, and High-fat diet without AMG, but they had lower  $b_2$  value than wild-type mice when fed the 53% Resistant starch diet (suggesting decreased metabolic flexibility within the carbohydrate oxidation mode for this diet) (Figure 5.17). As for the impact of AMG, AMG decreased  $b_2$  for wild-type mice fed the 53% Resistant starch diet, but increased  $b_2$  for wild-type mice fed the High-fat diet (Figure 5.18). As increases in  $b_2$  indicate decreased spread of RER values (narrowed spread) within the carbohydrate oxidation mode, these results demonstrate a generally narrower spread for the High-fat diet compared to the carbohydrate-based diets (Figures 5.16-5.18). When visually examining the pooled PRCF curves split by cycle (Figure 5.18), it appears that AMG supplementation (i.e. cycle 3) tended to make the curves for carbohydrate-based diets more similar (especially in the second mode) compared to no AMG (i.e. cycle 2). This suggests that PRCF curves of the RER distribution for carbohydrate-based diets with that are more digestible may approach a distinct shape. It is worth noting that the pooled data analysis with 95% confidence intervals does not allow for the use of statistical approaches, such as general linear or

mixed models, that would otherwise more readily reveal the potential role(s) of certain fixed effects (e.g. diet, genotype) and interactions.

### ***Notable differences among PRCF approaches***

Three different approaches were reported to examine the RER data analyzed with PRCF: (1) Mixed Weibull Cumulative Distribution modeling for data from individual mice, (2) Weibull [not Mixed Weibull] Cumulative Distribution modeling for data pooled from all mice, and (3) Mixed Weibull Cumulative Distribution modeling for data pooled from all mice. As described above, the statistical assessments for these approaches differed. However, several consistent findings suggested through each approach allow us to gain deeper insight into the metabolic consequences of carbohydrate digestion and lend support to the potential use of these three approaches. For one, the differences among treatment groups were similar for the  $x_{50\_1}$ ,  $x_{50\_2}$ , and  $b_2$  values from the Mixed Weibull approaches. Notably, consistencies were evident in both by the relatively high  $x_{50\_1}$  values for the High-fat diet, relatively low  $x_{50\_1}$  and  $x_{50\_2}$  values for the Conventional starch diet, relatively low  $x_{50\_1}$  values for the 53% Resistant starch diet, high  $x_{50\_2}$  values for the Sucrose diet, low  $x_{50\_2}$  values for the High-fat diet, non-incremental effects for the 3 resistant starch diets (inconsistent effects for the 35% Resistant starch diet), effects of genotype on  $b_2$ , and general increases in  $x_{50\_1}$ ,  $x_{50\_2}$ , and  $b_2$  observed for AMG with most diets. One notable difference between these two Mixed Weibull approaches is that the pooled data approach revealed large differences in  $\alpha$ , while the individual mouse approach did not yield any differences at all. The reason(s) for this are unknown, but we can speculate that there was high variability in the estimates for this term among individual mice that, upon pooling the data, were diminished to reveal an overall effect. With this in mind, it is important to note that the pooled data approach does not allow for statistical adjustments for multiple comparisons, which may inflate the likelihood of type II errors (i.e. false positives), and may be evident by the statistical differences observed for  $\alpha$  and  $b_1$  using this approach that were not observed for the other Mixed Weibull approach. Regarding the Weibull approach, this may be useful for determining overall differences in RER, but it suffers from poorer fits to the data and does not characterize the two modes that we propose represent carbohydrate and fat oxidation. However, this type of model may be useful for analyzing unimodal data as originally described by Riachi et al. (2004).

As an additional consideration, in the originally proposed PRCF approach by Riachi et al. (2004), the need for 1000 RER data points was specified in order to achieve the representative “metabolic signature” of the group of mice being studied. For one, Riachi et al. (2004) emphasized that 1000 RER data points are required in order to achieve a “smooth curve” with an  $R^2$  that exceeds 0.98 using their curve fitting equation (which is a different equation from the Weibull and Mixed Weibull Cumulative Distribution equations we used). Secondly, Riachi et al. (2004) stated that at least 1000 data points are required in order to achieve a normally distributed dataset. In our analyses, we had only 272-280 RER data points for each PRCF analysis of pooled data from all mice and only 34-35 RER data points for each PRCF analysis of data for individual mice. However, given the approaches we took to analyze the PRCF data with the Weibull and Mixed Weibull Cumulative Distribution functions, we believe these numbers of data points were still adequate, especially considering such functions have been used with as few as 20 data points (Rinne 2008; Razali and Al-Wakeel 2013). Furthermore, using our Weibull and Mixed Weibull approaches, the  $R^2$  values were very high: for the Mixed Weibull approach with curve fitting per individual mice, the mean overall  $R^2$  was  $0.99 \pm 0.00$ ; for the Weibull approach with data pooled from all mice, the mean overall  $R^2$  was  $0.97 \pm 0.00$ ; and for the Mixed Weibull approach with data pooled from all mice, the mean overall  $R^2$  was  $0.997 \pm 0.00$ . Although our  $R^2$  for the Weibull approach with pooled data is lower than the 0.98 cutoff proposed by Riachi et al. (2004), we have noted the limitations in using this type of distribution above and we do feel that the Mixed Weibull approach is superior. As for the concern about a normal distribution, we believe it is possible that the RER distribution from *in vivo* data is in fact bimodal due to the values of 0.70 and 1.00 for fat vs. carbohydrate oxidation, respectively; a large number of data points (>1000) may be needed to obtain a normally distributed dataset merely due to this bimodal distribution. In the end, we propose that our approaches with at least the Mixed Weibull Cumulative Distribution are a means to describe the partitioning between oxidation of carbohydrate and fat as substrates and to characterize metabolic flexibility with as few as 34 data points. Additionally, our approach for curve fitting per individual mice allows more robust statistical analyses to be conducted, which would otherwise be challenging if 1000 data points were required for each mouse.

#### 5.4.4 Mean RER per 24 h

Three-way ANOVA conducted on the mean RER values per 24 h cycle for the groups (diet × genotype × cycle [without/with AMG]) revealed main effects for diet and cycle ( $p < 0.0001$  for both). The interaction term for diet × genotype × cycle was also significant ( $p = 0.0001$ ), so *post hoc* comparisons were made among the 24 groups (Table 5.14). Sucrose diet had the highest mean RER values, with null mice (both with and without AMG) having significantly higher RER than all other groups and wild-type mice having significantly higher RER than all other groups except the wild-type mice fed the 53% Resistant starch diet when given AMG and the null mice fed the Sucrose diet. This suggests that the Sucrose diet yielded a greater extent of carbohydrate oxidation, as also concluded from the PRCF approaches. As mentioned above, the relatively high amount of rapidly digestible carbohydrate contributed by Novelose 260 may have given rise to the high mean RER for the 53% Resistant starch diet, and the relatively high amount of slowly digestible carbohydrate contributed by raw corn starch may have resulted in the low mean RER for the Conventional starch diet. AMG supplementation also had a clear effect for both genotypes fed the Conventional starch diet and the null mice fed the 53% Resistant starch diet, which is in agreement with the sine and PRCF analyses.

#### 5.4.5 Body weight

Mice maintained stable body weight during their periods in the indirect calorimetry chambers for each diet ( $p = 0.87$ ; data not shown), which indicates that weight gain or loss were not contributing to differences in RER. There are a number of previous studies and reviews that take thorough approaches to modeling metabolism and body weight dynamics in mice and humans (Guo and Hall 2009; K.D. Hall 2010; K. D. Hall, Bain, and Chow 2007). For the current study, we decided to reduce the scope to specifically examine RER as an indication of substrate utilization in the body, especially given body weight did not change during the experimental periods.

#### 5.4.6 *Ex vivo* assay of jejunal enzyme activities

Maltodextrin and sucrose substrate-induced jejunal enzyme activities are shown in Table 5.15 for six different dietary conditions in both null and wild-type mice. This subset of experiments was conducted to determine if the null and wild-type mice exhibited differences in enzyme

activities (as a form of validation). The results showed that there were robust differences between maltodextrin-induced enzyme activities in null and wild-type mice under the Fasting, Conventional starch diet, 53% Resistant starch diet, Conventional starch diet with AMG, and Sucrose diet conditions ( $p=0.001$ ,  $p=0.013$ ,  $p=0.005$ ,  $p=0.004$ , and  $p<0.0001$ , respectively). There was a trending difference for the Conventional starch diet with acarbose ( $p=0.063$ ). Therefore, the lack of Mgam enzyme in null mice clearly inhibited the ability of these mice to digest starch degradation products (partially digested starch). Conversely, there was only a statistically significant difference in sucrose substrate-induced enzyme activity between null and wild-type mice for the 53% Resistant starch diet ( $p<0.0001$ ), although there was also a borderline difference for the Conventional starch diet ( $p=0.05$ ). These findings suggest the null mice, which lacked Mgam, generally had adequate sucrase activity (with the exception of the 53% Resistant starch diet condition). However, we only measured enzyme activities in the jejunum and it is possible that  $\alpha$ -glucosidase activities may have varied to a greater degree in the duodenum or ileum. It is also curious that despite these differences in enzyme activities, there were minimal differences in RER for null and wild-type mice. This suggests Si is a more dominant starch digesting enzyme than Mgam, which is in agreement with previous research (Diaz-Sotomayor et al. 2013; Quezada-Calvillo, Robayo-Torres, Ao, et al. 2007; Nichols et al. 2017).

#### **5.4.7 Strengths and potential limitations**

This study took novel approaches to examine how alterations in carbohydrate digestion affected carbohydrate oxidation in mice. Diets incorporating carbohydrate components with varying digestibilities were used, mice lacking one of the  $\alpha$ -glucosidases that hydrolyzes starch degradation products were used (compared to wild-type mice that possessed the complete set of starch digestion enzymes), and AMG was used to augment starch digestion. Including an acclimation period (four 24-h cycles) to the diet and indirect calorimetry chamber for each diet treatment ensured any differences observed were not due to initial exposure to the experimental conditions imposed. Integrating previously proposed approaches for analyzing RER with new approaches has provided an innovative means to study dynamics in RER to examine the effects of different conditions on metabolism.

As for limitations, one notable constraint is that food intake was not measured. However, previous studies found that mice food intake in home cages vs. indirect calorimetry chambers did

not differ (Duivenvoorde et al. 2015), and in a previous experiment the food intake between the same type of null mice in this study (Mgam knockout) and wild-type mice did not differ for a carbohydrate-predominant diet (data not shown). It is possible that mice consumed more food for certain diets (e.g. Sucrose diet, High-fat diet) than others (e.g. 53% Resistant starch diet) because of diet palatability or appetite. We also did not measure activity level of the mice while they were in the indirect calorimetry chambers (the system used was not equipped to do so). We believe differences in activity level for individual mice may have contributed to some of the variation observed within treatment groups, and to partially account for this we excluded values that were  $\pm 2$  standard deviations from the mean for certain analyses as described above (i.e. sine parameter estimates, Weibull and Mixed Weibull parameter estimates for data modeled per individual mouse). Two assumptions tied into our interpretation of these experimental findings are that there were no changes in mitochondrial number or function for the different treatments and that the mouse is an appropriate model for human starch digestion. As indicated in the Methods and Results sections above, another limitation in this work is that we did not feed a treatment of gelatinized starch, especially considering that humans regularly consume gelatinized starch as opposed to raw starch. As the diets tested contained substantial amounts of slowly digestible and resistant carbohydrate, incorporating a diet containing a greater proportion of rapidly digestible carbohydrate (e.g. maltodextrin) would also strengthen future research. Furthermore, additional research is required to better understand the “togglng” between oxidation and fermentation, which may be especially relevant for resistant starch and the null mice (Mgam knockout).

## 5.5 Conclusion

The objective of this study was to determine how altering carbohydrate digestion affects the utilization of carbohydrate as a substrate for energy and the ensuing impact on metabolic flexibility between oxidation of carbohydrate and fat. We devised and carried out novel applications of mathematical modeling approaches to help explore this objective.

Although null mice exhibited PRCF distributions of RER that had more pronounced visual spread than wild-type mice, they generally did not have lower carbohydrate oxidation (as would have been shown through low  $x_{50,2}$  values), which did not support the first part of our first hypothesis. They also had higher  $x_{50,1}$  values, suggesting lower fat oxidation, than wild-type mice. Given this finding, we reason that slower, but not lower, carbohydrate digestion promotes fat

oxidation. AMG supplement appeared to at least partially restore digestion to increase carbohydrate oxidation in null mice. Null mice did appear to have increased metabolic flexibility as signified by higher  $b_1$  and  $b_2$  values, which supported the second part of our first hypothesis. Furthermore, in null mice a greater level of amylose and resistant starch in the diet was associated with slower shift to carbohydrate oxidation (sine  $c$ ) – a relationship not observed for wild-type mice. There was some evidence that sucrase-isomaltase may have been upregulated in null mice, perhaps as compensation for the lack of maltase-glucoamylase. Despite these findings, the observed differences between null and wild-type mice were minor overall, considering that the null mice lacked a complete set of starch digesting enzymes. Because the null mice with only sucrase-isomaltase generally performed as well as wild-type mice, this suggests sucrase-isomaltase is a more dominant starch digesting enzyme than maltase-glucoamylase, which corroborates previous research (Diaz-Sotomayor et al. 2013; Quezada-Calvillo, Robayo-Torres, Ao, et al. 2007; Nichols et al. 2017).

As for diet-related differences, although the extents of carbohydrate oxidation were inconsistent for the diets containing three different levels of high-amylose corn starch (53%, 35%, and 18% Resistant starch diets), it appears that the Conventional starch diet, which had the highest amount of slowly digestible starch among the experimental diets, had superior ability to promote fat oxidation (lower  $x_{50_1}$ ) and may have enhanced metabolic flexibility to a relatively high degree. This supports our second hypothesis (that reduced carbohydrate digestion rate would result in lower RER and greater metabolic flexibility), and it is apparent that slow digestion, but not reduced digestion, had the greatest impact. The Conventional starch diet did not promote carbohydrate oxidation (i.e. increase  $x_{50_2}$ ), although it is possible that the high  $x_{50_2}$  values observed for the other diets may be detrimental because they exceeded 1.00 RER. In addition, the Sucrose diet had the highest carbohydrate oxidation and the High-fat diet had the lowest carbohydrate oxidation, lending support for this idea and helping to validate our modeling approaches. Hindered metabolic flexibility was suggested for the High-fat diet by a high  $b_2$  (narrowed spread in RER for the carbohydrate oxidation mode) compared to the Sucrose diet, and other metabolic perturbations were suggested by results from the sine equation curve fitting for the High-fat diet (sine  $a$  and  $c$ ).

AMG generally increased carbohydrate oxidation, as indicated by  $x_{50_2}$  values, for all but the Sucrose and High-fat diets, which supported the first part of our third hypothesis – that supplementation with AMG to increase carbohydrate digestion would result in higher RER (i.e.

greater carbohydrate oxidation). AMG caused more rapid shifts to carbohydrate oxidation as shown by higher  $c$  parameter values from the sine equation curve fitting, which appear to suggest increased shift to carbohydrate oxidation. In agreement with this, the results from PRCF suggested AMG somewhat increased metabolic flexibility in the carbohydrate oxidation mode (represented by increased  $b_2$ ), though this was more pronounced and consistent for the High-fat diet, which also had a blunted level of carbohydrate oxidation. Additionally, results from the PRCF approach for pooled data from all mice (but not the PRCF approach for data from individual mice) showed AMG increased the partitioning of substrate utilization from fat to carbohydrate for the three resistant starch diets (except wild-type mice fed the 35% Resistant starch diet) as well as null mice fed the High-fat diet. One potential concern with the AMG supplement is that it seemed to shift substrate utilization toward carbohydrate, but not back toward fat (as indicated by the higher  $x_{50,1}$  values and lack of differences in  $b_2$ ).

In the end, the results of this study generally support that moderated or slow carbohydrate digestion, as observed for the Conventional starch diet tested here, promotes fat oxidation and may enable an optimal ability to switch between high carbohydrate oxidation and high fat oxidation. This improvement in metabolic flexibility between utilization of substrates may have implications on deposition of adipose tissue, insulin sensitivity, and mitochondrial function in the body (Goodpaster and Sparks 2017; Muoio 2014), even in the absence of differences in energy expenditure, and indicates a new potential role of slowly digestible carbohydrates in the control of weight management.

## **5.6 Acknowledgements**

I would like to thank Buford L. Nichols and his collaborative research team – Roberto Quezada-Calvillo, Firoz A. Vohra, Stephen E. Avery, Nancy F. Butte, Erwin E. Sterchi, and Ursi Lugenbuhl – for the contributions to the experiments described in this chapter. I was fortunate to be able to analyze the data they collected using the innovative approaches described.

## 5.7 References

- AlEsa, H. B., Cohen, R., Malik, V. S., Adebamowo, S. N., Rimm, E. B., Manson, J. A. E., Willett, W. C., & Hu, F. B. (2018). Carbohydrate quality and quantity and risk of coronary heart disease among US women and men. *American Journal of Clinical Nutrition*, *107*(2), 257–267. <https://doi.org/10.1093/ajcn/nqx060>
- Ao, Z., Simsek, S., Zhang, G., Venkatachalam, M., Reuhs, B. L., & Hamaker, B. R. (2007). Starch with a slow digestion property produced by altering its chain length, branch density, and crystalline structure. *Journal of Agricultural and Food Chemistry*, *55*(11), 4540–4547. <https://doi.org/10.1021/jf063123x>
- Barkeling, B., Granfelt, Y., Bjorck, I., & Rossner, S. (1995). Effects of carbohydrates in the form of pasta and bread on food intake and satiety in man. *Nutrition Research*, *15*(4), 467–476.
- Begaye, B., Vinales, K. L., Hollstein, T., Ando, T., Walter, M., Bogardus, C., Krakoff, J., & Piaggi, P. (2020). Impaired metabolic flexibility to high-fat overfeeding predicts future weight gain in healthy adults. *Diabetes*, *69*(2), 181–192. <https://doi.org/10.2337/db19-0719>
- Borah, P. K., Deka, S. C., & Duary, R. K. (2017). Effect of repeated cycled crystallization on digestibility and molecular structure of glutinous Bora rice starch. *Food Chemistry*, *223*, 31–39. <https://doi.org/10.1016/j.foodchem.2016.12.022>
- Brás, N. F., Santos-Martins, D., Fernandes, P. A., & Ramos, M. J. (2018). Mechanistic Pathway on Human  $\alpha$ -Glucosidase Maltase-Glucoamylase Unveiled by QM/MM Calculations. *Journal of Physical Chemistry B*, *122*(14), 3889–3899. <https://doi.org/10.1021/acs.jpcc.8b01321>
- Cairns, P., Sun, L., Morris, V. J., & Ring, S. G. (1995). Physicochemical studies using amylose as an in vitro model for resistant starch. *Journal of Cereal Science*, *21*(1), 37–47. [https://doi.org/10.1016/S0733-5210\(95\)80006-9](https://doi.org/10.1016/S0733-5210(95)80006-9)
- Chegeni, M., Amiri, M., Nichols, B. L., Naim, H. Y., & Hamaker, B. R. (2018). Dietary starch breakdown product sensing mobilizes and apically activates  $\alpha$ -glucosidases in small intestinal enterocytes. *FASEB Journal*, *32*(7), 3903–3911. <https://doi.org/10.1096/fj.201701029R>
- Crescenzo, R., Bianco, F., Falcone, I., Coppola, P., Liverini, G., & Iossa, S. (2013). Increased hepatic de novo lipogenesis and mitochondrial efficiency in a model of obesity induced by diets rich in fructose. *European Journal of Nutrition*, *52*(2), 537–545. <https://doi.org/10.1007/s00394-012-0356-y>
- Dahlqvist, A. (1962). Specificity of the human intestinal disaccharidases and implications for hereditary disaccharide intolerance. *Journal of Clinical Investigation*, *41*(3), 463–470.
- Dahlqvist, A., & Borgstrom, B. (1961). Digestion and absorption of disaccharides in man. *Biochemical Journal*, *81*(2), 411–418. <https://doi.org/10.1042/bj0810411>
- Dahlqvist, A., & Telenius, U. (1969). Column chromatography of human small-intestinal maltase, isomaltase and invertase activities. *Biochemical Journal*, *111*(2), 139–146. <https://doi.org/10.1042/bj1110139>
- Diaz-Sotomayor, M., Quezada-Calvillo, R., Avery, S. E., Chacko, S. K., Yan, L., Lin, A. H.-M., Ao, Z., Hamaker, B. R., & Nichols, B. L. (2013). Maltase-Glucoamylase Modulates Gluconeogenesis and Sucrase-Isomaltase Dominates Starch Digestion Glucogenesis. *Journal of Pediatric Gastroenterology and Nutrition*, *57*(6), 704–712. <https://doi.org/10.1097/MPG.0b013e3182a27438>
- Drechsler, K. C., & Ferrua, M. J. (2016). Modelling the breakdown mechanics of solid foods during gastric digestion. *Food Research International*, *88*, 181–190. <https://doi.org/10.1016/j.foodres.2016.02.019>

- Duivenvoorde, L. P. M., van Schothorst, E. M., Swarts, H. M., Kuda, O., Steenbergh, E., Termeulen, S., Kopecky, J., & Keijer, J. (2015). A Difference in Fatty Acid Composition of Isocaloric High-Fat Diets Alters Metabolic Flexibility in Male C57BL/6JOLA<sub>Hsd</sub> Mice. *PLOS ONE*, *10*(6), e0128515. <https://doi.org/10.1371/journal.pone.0128515>
- Englyst, H. N., Kingman, S. M., & Cummings, J. H. (1992). Classification and measurement of nutritionally important starch fractions. *European Journal of Clinical Nutrition*, *46 Suppl 2*, S33-50. <http://www.ncbi.nlm.nih.gov/pubmed/1330528>
- Englyst, K. N., Englyst, H. N., Hudson, G. J., Cole, T. J., & Cummings, J. H. (1999). Rapidly available glucose in foods: An in vitro measurement that reflects the glycemic response. *American Journal of Clinical Nutrition*, *69*(3), 448–454.
- Faul, F., Erdfelder, E., Lang, A.-G., & Buchner, A. (2007). G\*Power 3: A flexible statistical power analysis program for the social, behavioral, and biomedical sciences. *Behavior Research Methods*, *39*(2), 175–191.
- Fernández-Calleja, J., Bouwman, L., Swarts, H., Oosting, A., Keijer, J., & van Schothorst, E. (2018). Direct and Long-Term Metabolic Consequences of Lowly vs. Highly-Digestible Starch in the Early Post-Weaning Diet of Mice. *Nutrients*, *10*(11), 1788. <https://doi.org/10.3390/nu10111788>
- Fernández-Calleja, J. M. S., Bouwman, L. M. S., Swarts, H. J. M., Billecke, N., Oosting, A., Keijer, J., & van Schothorst, E. M. (2019). A Lowly Digestible-Starch Diet after Weaning Enhances Exogenous Glucose Oxidation Rate in Female, but Not in Male, Mice. *Nutrients*, *11*(9), 2242. <https://doi.org/10.3390/nu11092242>
- Fernández-Calleja, J. M. S., Bouwman, L. M. S., Swarts, H. J. M., Oosting, A., Keijer, J., & van Schothorst, E. M. (2019). Extended indirect calorimetry with isotopic CO<sub>2</sub> sensors for prolonged and continuous quantification of exogenous vs. total substrate oxidation in mice. *Scientific Reports*, *9*(1), 11507. <https://doi.org/10.1038/s41598-019-47977-w>
- Fernández-Calleja, J. M. S., Konstanti, P., Swarts, H. J. M., Bouwman, L. M. S., Garcia-Campayo, V., Billecke, N., Oosting, A., Smidt, H., Keijer, J., & van Schothorst, E. M. (2018). Non-invasive continuous real-time in vivo analysis of microbial hydrogen production shows adaptation to fermentable carbohydrates in mice. *Scientific Reports*, *8*(1), 15351. <https://doi.org/10.1038/s41598-018-33619-0>
- Flatt, J. P. (1995). Use and storage of carbohydrate and fat. *The American Journal of Clinical Nutrition*, *61*(4), 952S-959S. <https://doi.org/10.1093/ajcn/61.4.952S>
- Frandsen, T. P., & Svensson, B. (1998). Plant  $\alpha$ -glucosidases of the glycoside hydrolase family 31. Molecular properties, substrate specificity, reaction mechanism, and comparison with family members of different origin. *Plant Molecular Biology*, *37*(1), 1–13.
- Gardner, M. J., & Altman, D. G. (1986). Confidence intervals rather than P values: estimation rather than hypothesis testing. *BMJ*, *292*(6522), 746–750. <https://doi.org/10.1136/bmj.292.6522.746>
- Glamour, T. S., McCullough, A. J., Sauer, P. J. J., & Kalhan, S. C. (1995). Quantification of carbohydrate oxidation by respiratory gas exchange and isotopic tracers. *American Journal of Physiology-Endocrinology and Metabolism*, *268*(4), E789–E796. <https://doi.org/10.1152/ajpendo.1995.268.4.E789>
- Goodpaster, B. H., & Sparks, L. M. (2017). Metabolic Flexibility in Health and Disease. *Cell Metabolism*, *25*(5), 1027–1036. <https://doi.org/10.1016/j.cmet.2017.04.015>

- Gribok, A., Leger, J. L., Stevens, M., Hoyt, R., Buller, M., & Rumpler, W. (2016). Measuring the short-term substrate utilization response to high-carbohydrate and high-fat meals in the whole-body indirect calorimeter. *Physiological Reports*, 4(12), e12835. <https://doi.org/10.14814/phy2.12835>
- Guo, J., & Hall, K. D. (2009). Estimating the Continuous-Time Dynamics of Energy and Fat Metabolism in Mice. *PLoS Computational Biology*, 5(9), e1000511. <https://doi.org/10.1371/journal.pcbi.1000511>
- Hall, K. D., Bain, H. L., & Chow, C. C. (2007). How adaptations of substrate utilization regulate body composition. *International Journal of Obesity*, 31(9), 1378–1383. <https://doi.org/10.1038/sj.ijo.0803608>
- Hall, K.D. (2010). Mechanisms of Metabolic Fuel Selection: Modeling Human Metabolism and Body-Weight Change. *IEEE Engineering in Medicine and Biology Magazine*, 29(1), 36–41. <https://doi.org/10.1109/MEMB.2009.935465>
- Hall, Kevin D. (2012). Modeling Metabolic Adaptations and Energy Regulation in Humans. *Annual Review of Nutrition*, 32(1), 35–54. <https://doi.org/10.1146/annurev-nutr-071811-150705>
- Hayes, A. M. R., Swackhamer, C., Mennah-Govela, Y. A., Martinez, M. M., Diatta, A., Bornhorst, G. M., & Hamaker, B. R. (2020). Pearl millet (*Pennisetum glaucum*) couscous breaks down faster than wheat couscous in the Human Gastric Simulator, though has slower starch hydrolysis. *Food & Function*, 11(1), 111–122. <https://doi.org/10.1039/C9FO01461F>
- Kelley, D. E., & Mandarino, L. J. (2000). Fuel selection in human skeletal muscle in insulin resistance: a reexamination. *Diabetes*, 49(5), 677–683. <https://doi.org/10.2337/diabetes.49.5.677>
- Kreutz, C., Raue, A., & Timmer, J. (2012). Likelihood based observability analysis and confidence intervals for predictions of dynamic models. *BMC Systems Biology*, 6(1), 120. <https://doi.org/10.1186/1752-0509-6-120>
- Kroemer, G., López-Otín, C., Madeo, F., & de Cabo, R. (2018). Carbotoxicity—Noxious Effects of Carbohydrates. *Cell*, 175(3), 605–614. <https://doi.org/10.1016/j.cell.2018.07.044>
- Lee, B.-H., Bello-Pérez, L. A., Lin, A. H.-M., Kim, C. Y., & Hamaker, B. R. (2013). Importance of Location of Digestion and Colonic Fermentation of Starch Related to Its Quality. *Cereal Chemistry*, 90(4), 335–343. <https://doi.org/10.1094/CCHEM-05-13-0095-FI>
- Lee, B.-H., Rose, D. R., Lin, A. H.-M., Quezada-Calvillo, R., Nichols, B. L., & Hamaker, B. R. (2016). Contribution of the Individual Small Intestinal  $\alpha$ -Glucosidases to Digestion of Unusual  $\alpha$ -Linked Glycemic Disaccharides. *Journal of Agricultural and Food Chemistry*, 64(33), 6487–6494. <https://doi.org/10.1021/acs.jafc.6b01816>
- Lee, E.-S., Shin, H., Seo, J.-M., Nam, Y.-D., Lee, B.-H., & Seo, D.-H. (2018). Effects of raw potato starch on body weight with controlled glucose delivery. *Food Chemistry*, 256, 367–372. <https://doi.org/10.1016/j.foodchem.2018.02.150>
- Li, M., George, J., Hunter, S., Hamaker, B., Mattes, R., & Ferruzzi, M. G. (2019). Potato product form impacts: In vitro starch digestibility and glucose transport but only modestly impacts 24 h blood glucose response in humans. *Food and Function*, 10(4), 1846–1855. <https://doi.org/10.1039/c8fo02530d>
- Lin, A. H. M., Hamaker, B. R., & Nichols, B. L. (2012). Direct starch digestion by sucrase-isomaltase and maltase-glucoamylase. *Journal of Pediatric Gastroenterology and Nutrition*, 55(SUPPL.2), 43–45. <https://doi.org/10.1097/01.mpg.0000421414.95751.be>

- Longo, K. A., Charoenthongtrakul, S., Giuliana, D. J., Govek, E. K., McDonagh, T., DiStefano, P. S., & Geddes, B. J. (2010). The 24-hour respiratory quotient predicts energy intake and changes in body mass. *American Journal of Physiology-Regulatory, Integrative and Comparative Physiology*, 298(3), R747–R754. <https://doi.org/10.1152/ajpregu.00476.2009>
- Ludden, T. M., Beal, S. L., & Sheiner, L. B. (1994). Comparison of the Akaike Information Criterion, the Schwarz criterion and the F test as guides to model selection. *Journal of Pharmacokinetics and Biopharmaceutics*, 22(5), 431–445. <https://doi.org/10.1007/BF02353864>
- Ludwig, D. S., & Ebbeling, C. B. (2018). The Carbohydrate-Insulin Model of Obesity. *JAMA Internal Medicine*, 178(8), 1098. <https://doi.org/10.1001/jamainternmed.2018.2933>
- Malin, S. K., Haus, J. M., Solomon, T. P. J., Blaszcak, A., Kashyap, S. R., & Kirwan, J. P. (2013). Insulin sensitivity and metabolic flexibility following exercise training among different obese insulin-resistant phenotypes. *American Journal of Physiology-Endocrinology and Metabolism*, 305(10), E1292–E1298. <https://doi.org/10.1152/ajpendo.00441.2013>
- Man, J., Yang, Y., Zhang, C., Zhou, X., Dong, Y., Zhang, F., Liu, Q., & Wei, C. (2012). Structural changes of high-amylose rice starch residues following in vitro and in vivo digestion. *Journal of Agricultural and Food Chemistry*, 60(36), 9332–9341. <https://doi.org/10.1021/jf302966f>
- Martinez, M. M., Li, C., Okoniewska, M., Mukherjee, I., Vellucci, D., & Hamaker, B. (2018). Slowly digestible starch in fully gelatinized material is structurally driven by molecular size and A and B1 chain lengths. *Carbohydrate Polymers*, 197, 531–539. <https://doi.org/10.1016/j.carbpol.2018.06.021>
- Meex, R. C. R., Schrauwen-Hinderling, V. B., Moonen-Kornips, E., Schaart, G., Mensink, M., Phielix, E., van de Weijer, T., Sels, J.-P., Schrauwen, P., & Hesselink, M. K. C. (2010). Restoration of Muscle Mitochondrial Function and Metabolic Flexibility in Type 2 Diabetes by Exercise Training Is Paralleled by Increased Myocellular Fat Storage and Improved Insulin Sensitivity. *Diabetes*, 59(3), 572–579. <https://doi.org/10.2337/db09-1322>
- Muoio, D. M. (2014). Metabolic inflexibility: When mitochondrial indecision leads to metabolic gridlock. *Cell*, 159(6), 1253–1262. <https://doi.org/10.1016/j.cell.2014.11.034>
- Nichols, B. L., Avery, S. E., Quezada-Calvillo, R., Kilani, S. B., Lin, A. H. M., Burrin, D. G., Hodges, B. E., Chacko, S. K., Opekun, A. R., Hindawy, M. El, Hamaker, B. R., & Oda, S. I. (2017). Improved Starch Digestion of Sucrase-deficient Shrews Treated with Oral Glucoamylase Enzyme Supplements. *Journal of Pediatric Gastroenterology and Nutrition*, 65(2), e35–e42. <https://doi.org/10.1097/MPG.0000000000001561>
- Nichols, B. L., Quezada-Calvillo, R., Robayo-Torres, C. C., Ao, Z., Hamaker, B. R., Butte, N. F., Marini, J., Jahoor, F., & Sterchi, E. E. (2009). Mucosal Maltase-Glucoamylase Plays a Crucial Role in Starch Digestion and Prandial Glucose Homeostasis of Mice. *The Journal of Nutrition*, 139(4), 684–690. <https://doi.org/10.3945/jn.108.098434>
- Quezada-Calvillo, R., Robayo-Torres, C. C., Ao, Z., Hamaker, B. R., Quaroni, A., Brayer, G. D., Sterchi, E. E., Baker, S. S., & Nichols, B. L. (2007). Luminal Substrate “Brake” on Mucosal Maltase-glucoamylase Activity Regulates Total Rate of Starch Digestion to Glucose. *Journal of Pediatric Gastroenterology and Nutrition*, 45(1), 32–43. <https://doi.org/10.1097/MPG.0b013e31804216fc>

- Quezada-Calvillo, R., Robayo-Torres, C. C., Opekun, A. R., Sen, P., Ao, Z., Hamaker, B. R., Quaroni, A., Brayer, G. D., Wattler, S., Nehls, M. C., Sterchi, E. E., & Nichols, B. L. (2007). Contribution of Mucosal Maltase-Glucoamylase Activities to Mouse Small Intestinal Starch  $\alpha$ -Glucogenesis. *The Journal of Nutrition*, *137*(7), 1725–1733. <https://doi.org/10.1093/jn/137.7.1725>
- Razali, A. M., & Al-Wakeel, A. A. (2013). Mixture Weibull distributions for fitting failure times data. *Applied Mathematics and Computation*, *219*(24), 11358–11364. <https://doi.org/10.1016/j.amc.2013.05.062>
- Reichenbach, A., Stark, R., Mequinion, M., Denis, R. R. G., Goularte, J. F., Clarke, R. E., Lockie, S. H., Lemus, M. B., Kowalski, G. M., Bruce, C. R., Huang, C., Schittenhelm, R. B., Mynatt, R. L., Oldfield, B. J., Watt, M. J., Luquet, S., & Andrews, Z. B. (2018). AgRP Neurons Require Carnitine Acetyltransferase to Regulate Metabolic Flexibility and Peripheral Nutrient Partitioning. *Cell Reports*, *22*(7), 1745–1759. <https://doi.org/10.1016/j.celrep.2018.01.067>
- Riachi, M., Himmis-Hagen, J., & Harper, M. E. (2004). Percent relative cumulative frequency analysis in indirect calorimetry: Application to studies of transgenic mice. *Canadian Journal of Physiology and Pharmacology*, *82*(12), 1075–1083. <https://doi.org/10.1139/y04-117>
- Rinne, H. (2008). *The Weibull Distribution - A Handbook*. CRC Press.
- Roman, L., Gomez, M., Li, C., Hamaker, B. R., & Martinez, M. M. (2017). Biophysical features of cereal endosperm that decrease starch digestibility. *Carbohydrate Polymers*, *165*, 180–188. <https://doi.org/10.1016/j.carbpol.2017.02.055>
- Roman, L., Yee, J., Hayes, A. M. R., Hamaker, B. R., Bertoft, E., & Martinez, M. M. (2020). On the role of the internal chain length distribution of amylopectins during retrogradation: Double helix lateral aggregation and slow digestibility. *Carbohydrate Polymers*, *246*, 116633. <https://doi.org/10.1016/j.carbpol.2020.116633>
- Santiago, S., Zazpe, I., Bes-Rastrollo, M., Sánchez-Tainta, A., Sayón-Orea, C., de la Fuente-Arrillaga, C., Benito, S., Martínez, J. a, & Martínez-González, M. Á. (2015). Carbohydrate quality, weight change and incident obesity in a Mediterranean cohort: the SUN Project. *European Journal of Clinical Nutrition*, *69*(3), 297–302. <https://doi.org/10.1038/ejcn.2014.187>
- Santos, B. K. S.-D., Goda, T., & Koldovsky, O. (1992). Dietary-induced increases of disaccharidase activities in rat jejunum. *British Journal of Nutrition*, *67*(2), 267–278. <https://doi.org/10.1079/BJN19920030>
- Seal, C. J., Daly, M. E., Thomas, L. C., Bal, W., Birkett, A. M., Jeffcoat, R., & Mathers, J. C. (2003). Postprandial carbohydrate metabolism in healthy subjects and those with type 2 diabetes fed starches with slow and rapid hydrolysis rates determined in vitro. *British Journal of Nutrition*, *90*(5), 853–864. <https://doi.org/10.1079/BJN2003972>
- Shan, Z., Rehm, C. D., Rogers, G., Ruan, M., Wang, D. D., Hu, F. B., Mozaffarian, D., Zhang, F. F., & Bhupathiraju, S. N. (2019). Trends in Dietary Carbohydrate, Protein, and Fat Intake and Diet Quality Among US Adults, 1999-2016. *JAMA*, *322*(12), 1178. <https://doi.org/10.1001/jama.2019.13771>
- Simsek, M., Quezada-Calvillo, R., Ferruzzi, M. G., Nichols, B. L., & Hamaker, B. R. (2015). Dietary Phenolic Compounds Selectively Inhibit the Individual Subunits of Maltase-Glucoamylase and Sucrase-Isomaltase with the Potential of Modulating Glucose Release. *Journal of Agricultural and Food Chemistry*, *63*(15), 3873–3879. <https://doi.org/10.1021/jf505425d>

- Small, L., Brandon, A. E., Parker, B. L., Deshpande, V., Samsudeen, A. F., Kowalski, G. M., Reznick, J., Wilks, D. L., Preston, E., Bruce, C. R., James, D. E., Turner, N., & Cooney, G. J. (2019). Reduced insulin action in muscle of high fat diet rats over the diurnal cycle is not associated with defective insulin signaling. *Molecular Metabolism*, 25(April), 107–118. <https://doi.org/10.1016/j.molmet.2019.04.006>
- Stull, A. J., Galgani, J. E., Johnson, W. D., & Cefalu, W. T. (2010). The contribution of race and diabetes status to metabolic flexibility in humans. *Metabolism*, 59(9), 1358–1364. <https://doi.org/10.1016/j.metabol.2009.12.020>
- Sun, S. z., & Empie, M. W. (2012). Fructose metabolism in humans--what isotopic tracer studies tell us. *Nutrition and Metabolism*, 9(1), 89.
- Swackhamer, C., Zhang, Z., Taha, A. Y., & Bornhorst, G. M. (2019). Fatty acid bioaccessibility and structural breakdown from in vitro digestion of almond particles. *Food & Function*, 10(8), 5174–5187. <https://doi.org/10.1039/C9FO00789J>
- van de Weijer, T., Sparks, L. M., Phielix, E., Meex, R. C., van Herpen, N. A., Hesselink, M. K. C., Schrauwen, P., & Schrauwen-Hinderling, V. B. (2013). Relationships between Mitochondrial Function and Metabolic Flexibility in Type 2 Diabetes Mellitus. *PLoS ONE*, 8(2), e51648. <https://doi.org/10.1371/journal.pone.0051648>
- Vinoy, S., Normand, S., Meynier, A., Sothier, M., Louche-Pelissier, C., Peyrat, J., Maitrepierre, C., Nazare, J. A., Brand-Miller, J., & Laville, M. (2013). Cereal Processing Influences Postprandial Glucose Metabolism as Well as the GI Effect. *Journal of the American College of Nutrition*, 32(2), 79–91. <https://doi.org/10.1080/07315724.2013.789336>
- Warren, F. J., Zhang, B., Waltzer, G., Gidley, M. J., & Dhital, S. (2015). The interplay of  $\alpha$ -amylase and amyloglucosidase activities on the digestion of starch in in vitro enzymic systems. *Carbohydrate Polymers*, 117, 192–200. <https://doi.org/10.1016/j.carbpol.2014.09.043>
- Weir, J. B. de V. (1949). New methods for calculating metabolic rate with special reference to protein metabolism. *The Journal of Physiology*, 109(1–2), 1–9. <https://doi.org/10.1113/jphysiol.1949.sp004363>
- Wu, W., Qiu, J., Wang, A., & Li, Z. (2019). Impact of whole cereals and processing on type 2 diabetes mellitus: a review. *Critical Reviews in Food Science and Nutrition*, 0(0), 1–28. <https://doi.org/10.1080/10408398.2019.1574708>
- Zhang, G., Ao, Z., & Hamaker, B. R. (2006). Slow digestion property of native cereal starches. *Biomacromolecules*, 7(11), 3252–3258. <https://doi.org/10.1021/bm060342i>
- Zhang, G., & Hamaker, B. R. (2009). Slowly Digestible Starch: Concept, Mechanism, and Proposed Extended Glycemic Index. *Critical Reviews in Food Science and Nutrition*, 49(10), 852–867. <https://doi.org/10.1080/10408390903372466>
- Zhang, G., Hasek, L. Y., Lee, B.-H., & Hamaker, B. R. (2015). Gut feedback mechanisms and food intake: a physiological approach to slow carbohydrate bioavailability. *Food Funct.*, 6(4), 1072–1089. <https://doi.org/10.1039/C4FO00803K>
- Zhang, G., Venkatachalam, M., & Hamaker, B. R. (2006). Structural basis for the slow digestion property of native cereal starches. *Biomacromolecules*, 7(11), 3259–3266. <https://doi.org/10.1021/bm060343a>

Table 5.1 Experimental diet compositions.

Component	Conventional starch TD.01629	53% Resistant starch TD.02130	35% Resistant starch TD.02130	18% Resistant starch TD.02129	Sucrose TD.02129	High-fat TD.88137
g/kg						
Casein	200	200	200	200	200	195
DL-Methionine	3	3	3	3	3	3
Maltodextrin	120	120	120	120	0	0
Corn starch	530	0	177	353	0	150
Resistant starch (Novelose 260)	0	530	353	177	0	0
Sucrose	0	0	0	0	650	342
Anhydrous milkfat	0	0	0	0	0	210
Cholesterol	0	0	0	0	0	1.5
Soybean Oil	50	50	50	50	50	0
Cellulose	50	50	50	50	50	50
Mineral mix <sup>a</sup>	35	35	35	35	35	35
Calcium carbonate	0	0	0	0	0	4
Vitamin mix <sup>b</sup>	10	10	10	10	10	10
Choline bitartrate	2.5	2.5	2.5	2.5	2.5	0
TBHQ (antioxidant)	0.01	0.01	0.01	0.01	0.01	0
Ethoxyquin	0	0	0	0	0	0.04
% kcal						
Protein	19.6	19.6	19.6	19.6	19.6	15.2
Carbohydrate	67.4	67.4	67.4	67.4	67.4	42.7
Fat	13.0	13.0	13.0	13.0	13.0	42.0
% by weight						
Protein	17.7	17.7	17.7	17.7	17.7	17.3
Carbohydrate	60.9 <sup>c</sup>	60.9 <sup>c</sup>	60.9	60.9	60.9	48.5
Fat	5.2	5.2	5.2	5.2	5.2	21.2
Energy density (kcal/g)	3.6	3.6	3.6	3.6	3.6	4.5

*Footnotes for Table 5.1*

<sup>a</sup>Mineral mix composition (g/kg; AIN-93G-MX, TD.94046): calcium carbonate, 357.0; potassium phosphate (monobasic), 196.0; potassium citrate (monohydrate), 70.78; sodium chloride, 74.0; potassium sulfate, 46.6; magnesium oxide, 24.3; ferric citrate, 6.06; zinc carbonate, 1.65; manganous carbonate, 0.63; cupric carbonate, 0.31; potassium iodate, 0.01; sodium selenate, 0.0103; ammonium paramolybdate (tetrahydrate), 0.008; sodium meta-silicate (nonahydrate), 1.45; chromium potassium sulfate (dodecahydrate), 0.275; lithium chloride, 0.0174; boric acid, 0.0815; sodium fluoride, 0.0635; nickel carbonate hydroxide (tetrahydrate), 0.0318; ammonium meta-vanadate, 0.0066; sucrose (fine ground), 220.7. Note that these values are the g/kg amounts within the mineral mix, and only 35 g/kg of this mix was used within the diet.

<sup>b</sup>Vitamin mix composition (g/kg; AIN-93-VX, TD.94047): niacin, 3.0; calcium pantothenate, 1.6; pyridoxine hydrochloric acid, 0.7; thiamin (81%), 0.6; riboflavin, 0.6; folic acid, 0.2; biotin, 0.02; vitamin B<sub>12</sub> (0.1% in mannitol), 2.5; vitamin E (DL-alpha tocopheryl acetate, 500 IU/g), 15.0; vitamin A palmitate (500,000 IU/g), 0.8; vitamin D<sub>3</sub> (cholecalciferol, 500,000 IU/g), 0.2; vitamin K<sub>1</sub> (phylloquinone), 0.075; sucrose (fine ground), 974.7. Note that these values are the g/kg amounts within the mineral mix, and only 10 g/kg of this mix was used within the diet.

<sup>c</sup>53% of which was experimental carbohydrate (Conventional starch [corn starch], 53% Resistant starch [Novelose 260]).

Table 5.2 Starch contents in different diets<sup>a</sup>.

Diet	Moisture (%)	Starch content (% , d.w.b.)
Conventional starch diet	10.4 ± 0.1	51.8 ± 0.6
53% Resistant starch diet	10.5 ± 0.1	54.1 ± 1.3
35% Resistant starch diet	12.3 ± 0.1	51.6 ± 1.1
18% Resistant starch diet	10.6 ± 0.2	56.1 ± 0.6
Sucrose diet	3.5 ± 0.1	0.0 ± 0.0
High-fat diet	n.d.	n.d.
PicoLab diet 5053 (non-experimental)	11.0 ± 0.8	32.6 ± 1.1

d.w.b., dry weight basis; n.d., not determined.

<sup>a</sup>Analyzed using a total starch analysis kit (amyloglucosidase/alpha-amylase method; Total Starch Assay Kit [AA/AMG], K-TSTA-50A, Megazyme, Wicklow, Ireland).

Table 5.3 Contents of rapidly digestible, slowly digestible, and resistant starches in different diets (% , dry starch basis).<sup>a</sup> Mean values shown with  $\pm$  standard deviation as applicable.

Diet	Rapidly digestible starch (%)	Slowly digestible starch (%)	Resistant starch (%)	Percent amylose <sup>b</sup> (%)	Food quotient <sup>c</sup>
Conventional starch diet	74.0 $\pm$ 4.8	26.9 $\pm$ 5.4	-0.9	23	0.79
53% Resistant starch diet	55.1 $\pm$ 2.8	16.4 $\pm$ 3.0	28.5	57	0.79
35% Resistant starch diet	59.5 $\pm$ 3.7	25.2 $\pm$ 6.5	15.3	46	0.79
18% Resistant starch diet	64.7 $\pm$ 2.7	25.1 $\pm$ 2.4	10.2	34	0.79
Sucrose diet <sup>d</sup>	32.2 <sup>b</sup>	32.7 <sup>b</sup>	0.0	0	0.79
High-fat diet	n.d.	n.d.	n.d.	9	0.78
PicoLab diet 5053 (non-experimental)	58.7 $\pm$ 4.7	43.7 $\pm$ 3.1	-2.4	18	0.73

n.d., not determined.

<sup>a</sup>Analyzed using the Englyst assay (K. N. Englyst et al. 1999; H. N. Englyst, Kingman, and Cummings 1992).

<sup>b</sup>Calculated as percent of amylose within the digestible carbohydrate component of each diet, considering normal corn starch contains 28% amylose and Novelose 260 contains 70% amylose.

<sup>c</sup>Food quotient of oxidation per diet: calculated according to macronutrient ratio by weight, assuming a quotient of oxidation of 1.0 for carbohydrates, 0.70 for fats, and 0.825 for proteins.

<sup>d</sup>Glucose contents of the sample incubated after 20 and 120 min were 32.2 and 32.7%, respectively. This is due to the invertase in the Englyst assay, noting that the other carbohydrate components of this diet are fructose and cellulose and thus would not be detected using the Englyst assay.

Table 5.4 Sine equation parameters for curve fitting of respiratory exchange ratio (RER) for individual mice, per diet type, per cycle (with vs. without AMG). Value are means  $\pm$  standard error the mean. Groups not sharing the same letters or symbols are significantly different ( $p < 0.05$ ).

Group	<i>a</i>	<i>b</i>	<i>c</i>	<i>d</i>	<i>R</i> <sup>2</sup>
Conventional starch   Null   without AMG	0.37 $\pm$ 0.01 <sup>a,x</sup>	6.53 $\pm$ 0.20	-10.47 $\pm$ 0.30 <sup>bc,x</sup>	0.48 $\pm$ 0.02 <sup>†,y</sup>	0.80 $\pm$ 0.03
Conventional starch   Wild-type   without AMG	0.37 $\pm$ 0.01 <sup>a,x</sup>	6.05 $\pm$ 0.24	-10.40 $\pm$ 0.36 <sup>bc,x</sup>	0.45 $\pm$ 0.02 <sup>‡,y</sup>	0.83 $\pm$ 0.02
Conventional starch   Null   with AMG	0.39 $\pm$ 0.02 <sup>a,y</sup>	5.83 $\pm$ 0.29	-15.56 $\pm$ 0.84 <sup>bc,y</sup>	0.57 $\pm$ 0.02 <sup>†,x</sup>	0.81 $\pm$ 0.03
Conventional starch   Wild-type   with AMG	0.37 $\pm$ 0.03 <sup>a,y</sup>	5.88 $\pm$ 0.36	-15.82 $\pm$ 1.06 <sup>bc,y</sup>	0.54 $\pm$ 0.02 <sup>‡,x</sup>	0.75 $\pm$ 0.05
53% Resistant starch   Null   without AMG	0.47 $\pm$ 0.08 <sup>a,x</sup>	5.41 $\pm$ 0.51	-9.04 $\pm$ 0.98 <sup>b,x</sup>	0.47 $\pm$ 0.01 <sup>†,y</sup>	0.84 $\pm$ 0.02
53% Resistant starch   Wild-type   without AMG	0.41 $\pm$ 0.04 <sup>a,x</sup>	5.49 $\pm$ 0.43	-9.27 $\pm$ 0.83 <sup>b,x</sup>	0.46 $\pm$ 0.04 <sup>‡,y</sup>	0.80 $\pm$ 0.04
53% Resistant starch   Null   with AMG	0.41 $\pm$ 0.02 <sup>a,y</sup>	5.26 $\pm$ 0.39	-13.88 $\pm$ 1.11 <sup>b,y</sup>	0.56 $\pm$ 0.03 <sup>†,x</sup>	0.83 $\pm$ 0.02
53% Resistant starch   Wild-type   with AMG	0.39 $\pm$ 0.03 <sup>a,y</sup>	5.32 $\pm$ 0.52	-14.27 $\pm$ 1.53 <sup>b,y</sup>	0.56 $\pm$ 0.03 <sup>‡,x</sup>	0.76 $\pm$ 0.03
35% Resistant starch   Null   without AMG	0.44 $\pm$ 0.01 <sup>a,x</sup>	5.89 $\pm$ 0.10	-10.07 $\pm$ 0.19 <sup>bc,x</sup>	0.50 $\pm$ 0.02 <sup>†,y</sup>	0.86 $\pm$ 0.04
35% Resistant starch   Wild-type   without AMG	0.42 $\pm$ 0.03 <sup>a,x</sup>	6.14 $\pm$ 0.25	-10.47 $\pm$ 0.46 <sup>bc,x</sup>	0.48 $\pm$ 0.03 <sup>‡,y</sup>	0.81 $\pm$ 0.03
35% Resistant starch   Null   with AMG	0.43 $\pm$ 0.02 <sup>a,y</sup>	5.25 $\pm$ 0.33	-13.86 $\pm$ 0.98 <sup>bc,y</sup>	0.52 $\pm$ 0.02 <sup>†,x</sup>	0.84 $\pm$ 0.02
35% Resistant starch   Wild-type   with AMG	0.39 $\pm$ 0.02 <sup>a,y</sup>	6.03 $\pm$ 0.37	-16.08 $\pm$ 1.09 <sup>bc,y</sup>	0.50 $\pm$ 0.02 <sup>‡,x</sup>	0.78 $\pm$ 0.04
18% Resistant starch   Null   without AMG	0.39 $\pm$ 0.02 <sup>a,x</sup>	6.08 $\pm$ 0.33	-10.30 $\pm$ 0.62 <sup>c,x</sup>	0.48 $\pm$ 0.02 <sup>†,y</sup>	0.82 $\pm$ 0.03
18% Resistant starch   Wild-type   without AMG	0.42 $\pm$ 0.02 <sup>a,x</sup>	6.32 $\pm$ 0.18	-10.84 $\pm$ 0.31 <sup>c,x</sup>	0.50 $\pm$ 0.01 <sup>‡,y</sup>	0.86 $\pm$ 0.03
18% Resistant starch   Null   with AMG	0.43 $\pm$ 0.01 <sup>a,y</sup>	5.72 $\pm$ 0.27	-17.05 $\pm$ 0.93 <sup>c,y</sup>	0.52 $\pm$ 0.02 <sup>†,x</sup>	0.86 $\pm$ 0.03
18% Resistant starch   Wild-type   with AMG	0.41 $\pm$ 0.01 <sup>a,y</sup>	6.05 $\pm$ 0.18	-17.57 $\pm$ 1.02 <sup>c,y</sup>	0.50 $\pm$ 0.01 <sup>‡,x</sup>	0.85 $\pm$ 0.02

Table 5.4, continued.

Group	<i>a</i>	<i>b</i>	<i>c</i>	<i>d</i>	<i>R</i> <sup>2</sup>
Sucrose   Null   without AMG	0.43 ± 0.02 <sup>a,x</sup>	5.69 ± 0.44	-9.56 ± 0.84 <sup>bc,x</sup>	0.50 ± 0.02 <sup>†,y</sup>	0.79 ± 0.03
Sucrose   Wild-type   without AMG	0.43 ± 0.03 <sup>a,x</sup>	5.60 ± 0.54	-9.38 ± 1.02 <sup>bc,x</sup>	0.46 ± 0.04 <sup>‡,y</sup>	0.76 ± 0.02
Sucrose   Null   with AMG	0.38 ± 0.03 <sup>a,y</sup>	5.35 ± 0.66	-14.15 ± 1.98 <sup>bc,y</sup>	0.52 ± 0.03 <sup>†,x</sup>	0.70 ± 0.05
Sucrose   Wild-type   with AMG	0.43 ± 0.05 <sup>a,y</sup>	5.26 ± 0.71	-14.55 ± 2.30 <sup>bc,y</sup>	0.46 ± 0.04 <sup>‡,x</sup>	0.70 ± 0.07
High-fat   Null   without AMG	0.32 ± 0.02 <sup>b,x</sup>	7.06 ± 0.32	-7.75 ± 0.66 <sup>a,x</sup>	0.52 ± 0.01 <sup>†,y</sup>	0.60 ± 0.09
High-fat   Wild-type   without AMG	0.35 ± 0.02 <sup>b,x</sup>	5.47 ± 0.98	-4.80 ± 1.83 <sup>a,x</sup>	0.49 ± 0.01 <sup>‡,y</sup>	0.69 ± 0.08
High-fat   Null   with AMG	0.23 ± 0.09 <sup>b,y</sup>	5.61 ± 0.82	-9.66 ± 1.77 <sup>a,y</sup>	0.56 ± 0.03 <sup>†,x</sup>	0.63 ± 0.06
High-fat   Wild-type   with AMG	0.12 ± 0.11 <sup>b,y</sup>	5.77 ± 0.97	-10.47 ± 2.25 <sup>a,y</sup>	0.49 ± 0.04 <sup>‡,x</sup>	0.61 ± 0.09

AMG, amyloglucosidase.

<sup>abc</sup>Superscript letters a-c indicate statistically significant differences among diets.

<sup>xy</sup>Superscript letters x and y indicate statistically significant differences between cycles 2 and 3 (without vs. with AMG).

<sup>†‡</sup>Symbols † and ‡ indicate statistically significant differences between genotypes (null vs. wild-type).

Table 5.5 Statistical analysis for sine equation parameters for curve fitting of respiratory exchange ratio (RER) for individual mice, per diet type, genotype (null vs. wild-type), per cycle (with vs. without AMG).

Factor	<i>p-value</i>							
	<i>a</i>	<i>b</i>	<i>c</i>	<i>d</i>	<i>a</i> – no outliers <sup>a</sup>	<i>b</i> – no outliers <sup>a</sup>	<i>c</i> – no outliers <sup>a</sup>	<i>d</i> – no outliers <sup>a</sup>
Diet	0.9985	0.7487	0.0002*	0.9726	<0.0001*	0.1661	<0.0001*	0.5246
Genotype	0.1641	0.4824	0.1484	0.2056	0.3969	0.8993	0.5523	0.0098*
Cycle	0.1967	0.0360*	<0.0001*	0.2141	0.0262*	0.0655	<0.0001*	<0.0001*
<i>Interaction p-values</i>								
Diet × genotype	0.0916	0.0211*	0.8510	0.1202	0.8640	0.5928	0.9324	0.6297
Diet × cycle	0.2123	0.6544	0.7707	0.1353	0.0355*	0.9953	0.5229	0.0406*
Genotype × cycle	0.6018	0.0535	0.2292	0.6658	0.5002	0.2252	0.3297	0.5174
Diet × genotype × cycle	0.9194	0.5270	0.5370	0.9401	0.5767	0.8088	0.9544	0.9680

<sup>a</sup>Outliers determined as > 2 standard deviations from the mean for each group (diet × mouse genotype × cycle).

\*Statistically significant.

Table 5.6 Mixed Weibull Cumulative Distribution parameter estimates ( $\alpha$ ,  $x_{50\_1}$ ,  $b\_1$ ,  $x_{50\_2}$ ,  $b\_2$ ) for respiratory exchange ratio (RER) from individual percent relative cumulative frequency (PRCF) analyses.  $R^2$  is also shown as an indicator of goodness of fit. Values are means  $\pm$  standard error of the mean. Groups not sharing the same letters or symbols are significantly different ( $p < 0.05$ ).

Group	$\alpha^*$	$x_{50\_1}$	$b\_1$	$x_{50\_2}$	$b\_2$	$R^2$
Conventional starch   Null   without AMG	0.53 $\pm$ 0.04	0.80 $\pm$ 0.02 <sup>d,y†</sup>	18.23 $\pm$ 2.88	0.99 $\pm$ 0.01 <sup>c,y</sup>	24.43 $\pm$ 3.11 <sup>bc,y†</sup>	0.99 $\pm$ 0.00
Conventional starch   Wild-type   without AMG	0.41 $\pm$ 0.07	0.74 $\pm$ 0.01 <sup>d,y‡</sup>	27.82 $\pm$ 5.24	0.99 $\pm$ 0.01 <sup>c,y</sup>	23.76 $\pm$ 2.88 <sup>bc,y‡</sup>	0.99 $\pm$ 0.00
Conventional starch   Null   with AMG	0.46 $\pm$ 0.07	0.78 $\pm$ 0.01 <sup>d,x†</sup>	32.55 $\pm$ 6.42	1.02 $\pm$ 0.01 <sup>c,x</sup>	26.25 $\pm$ 5.62 <sup>bc,x†</sup>	0.99 $\pm$ 0.00
Conventional starch   Wild-type   with AMG	0.57 $\pm$ 0.08	0.79 $\pm$ 0.01 <sup>d,x‡</sup>	19.12 $\pm$ 1.79	1.02 $\pm$ 0.01 <sup>c,x</sup>	23.69 $\pm$ 2.27 <sup>bc,x‡</sup>	0.99 $\pm$ 0.00
53% Resistant starch   Null   without AMG	0.56 $\pm$ 0.07	0.83 $\pm$ 0.03 <sup>abc,y†</sup>	17.77 $\pm$ 4.16	1.02 $\pm$ 0.01 <sup>b,y</sup>	31.59 $\pm$ 7.55 <sup>bc,y†</sup>	0.99 $\pm$ 0.00
53% Resistant starch   Wild-type   without AMG	0.52 $\pm$ 0.07	0.78 $\pm$ 0.02 <sup>abc,y‡</sup>	27.90 $\pm$ 3.64	1.04 $\pm$ 0.01 <sup>b,y</sup>	22.06 $\pm$ 2.75 <sup>bc,y‡</sup>	0.99 $\pm$ 0.00
53% Resistant starch   Null   with AMG	0.51 $\pm$ 0.07	0.86 $\pm$ 0.03 <sup>abc,x†</sup>	18.85 $\pm$ 5.04	1.06 $\pm$ 0.01 <sup>b,x</sup>	31.78 $\pm$ 9.04 <sup>bc,x†</sup>	0.99 $\pm$ 0.00
53% Resistant starch   Wild-type   with AMG	0.62 $\pm$ 0.05	0.80 $\pm$ 0.01 <sup>abc,x‡</sup>	22.21 $\pm$ 3.93	1.07 $\pm$ 0.01 <sup>b,x</sup>	21.62 $\pm$ 2.69 <sup>bc,x‡</sup>	0.99 $\pm$ 0.00
35% Resistant starch   Null   without AMG	0.59 $\pm$ 0.06	0.78 $\pm$ 0.01 <sup>cd,y†</sup>	24.39 $\pm$ 3.84	1.01 $\pm$ 0.01 <sup>c,y</sup>	25.60 $\pm$ 5.01 <sup>bc,y†</sup>	0.99 $\pm$ 0.00
35% Resistant starch   Wild-type   without AMG	0.50 $\pm$ 0.07	0.79 $\pm$ 0.01 <sup>cd,y‡</sup>	27.43 $\pm$ 3.40	1.01 $\pm$ 0.01 <sup>c,y</sup>	20.50 $\pm$ 3.65 <sup>bc,y‡</sup>	0.99 $\pm$ 0.00
35% Resistant starch   Null   with AMG	0.47 $\pm$ 0.05	0.83 $\pm$ 0.02 <sup>cd,x†</sup>	21.77 $\pm$ 5.82	1.04 $\pm$ 0.00 <sup>c,x</sup>	33.13 $\pm$ 7.03 <sup>bc,x†</sup>	0.99 $\pm$ 0.00
35% Resistant starch   Wild-type   with AMG	0.54 $\pm$ 0.07	0.78 $\pm$ 0.01 <sup>cd,x‡</sup>	18.13 $\pm$ 2.70	1.00 $\pm$ 0.01 <sup>c,x</sup>	25.63 $\pm$ 3.50 <sup>bc,x‡</sup>	0.99 $\pm$ 0.00

Table 5.6, continued.

Group	$\alpha^*$	$x_{50\_1}$	$b\_1$	$x_{50\_2}$	$b\_2$	$R^2$
18% Resistant starch   Null   without AMG	$0.47 \pm 0.07$	$0.76 \pm 0.01^{d,y}\ddagger$	$32.64 \pm 4.20$	$1.02 \pm 0.01^{b,y}$	$22.19 \pm 2.87^{bc,y}\ddagger$	$0.99 \pm 0.00$
18% Resistant starch   Wild-type   without AMG	$0.42 \pm 0.03$	$0.75 \pm 0.01^{d,y}\ddagger$	$23.15 \pm 5.42$	$1.04 \pm 0.01^{b,y}$	$21.63 \pm 2.96^{bc,y}\ddagger$	$0.99 \pm 0.00$
18% Resistant starch   Null   with AMG	$0.52 \pm 0.06$	$0.79 \pm 0.02^{d,x}\ddagger$	$16.95 \pm 2.36$	$1.06 \pm 0.01^{b,x}$	$39.62 \pm 6.84^{bc,x}\ddagger$	$0.99 \pm 0.00$
18% Resistant starch   Wild-type   with AMG	$0.58 \pm 0.05$	$0.77 \pm 0.01^{d,x}\ddagger$	$14.64 \pm 1.48$	$1.04 \pm 0.01^{b,x}$	$21.97 \pm 2.83^{bc,x}\ddagger$	$0.99 \pm 0.00$
Sucrose   Null   without AMG	$0.47 \pm 0.06$	$0.84 \pm 0.02^{abc,y}\ddagger$	$18.69 \pm 3.59$	$1.12 \pm 0.00^{a,y}$	$26.14 \pm 4.97^{c,y}\ddagger$	$0.99 \pm 0.00$
Sucrose   Wild-type   without AMG	$0.56 \pm 0.07$	$0.81 \pm 0.01^{abc,y}\ddagger$	$18.99 \pm 1.84$	$1.11 \pm 0.01^{a,y}$	$15.58 \pm 1.97^{c,y}\ddagger$	$0.99 \pm 0.00$
Sucrose   Null   with AMG	$0.45 \pm 0.09$	$0.83 \pm 0.01^{abc,x}\ddagger$	$21.80 \pm 3.12$	$1.11 \pm 0.01^{a,x}$	$15.24 \pm 1.57^{c,x}\ddagger$	$0.99 \pm 0.00$
Sucrose   Wild-type   with AMG	$0.54 \pm 0.06$	$0.82 \pm 0.01^{abc,x}\ddagger$	$16.03 \pm 2.30$	$1.11 \pm 0.01^{a,x}$	$20.99 \pm 3.57^{c,x}\ddagger$	$0.99 \pm 0.00$
High-fat   Null   without AMG	$0.55 \pm 0.07$	$0.82 \pm 0.02^{a,y}\ddagger$	$23.08 \pm 2.85$	$0.96 \pm 0.01^{d,y}$	$30.48 \pm 3.89^{ab,y}\ddagger$	$0.99 \pm 0.00$
High-fat   Wild-type   without AMG	$0.53 \pm 0.10$	$0.81 \pm 0.02^{a,y}\ddagger$	$21.60 \pm 4.15$	$0.98 \pm 0.02^{d,y}$	$23.22 \pm 4.01^{ab,y}\ddagger$	$0.99 \pm 0.00$
High-fat   Null   with AMG	$0.55 \pm 0.08$	$0.86 \pm 0.01^{a,x}\ddagger$	$19.73 \pm 2.18$	$0.97 \pm 0.02^{d,x}$	$40.00 \pm 7.46^{ab,x}\ddagger$	$0.99 \pm 0.00$
High-fat   Wild-type   with AMG	$0.59 \pm 0.08$	$0.85 \pm 0.02^{a,x}\ddagger$	$27.77 \pm 7.85$	$0.98 \pm 0.01^{d,x}$	$42.65 \pm 13.07^{ab,x}\ddagger$	$0.99 \pm 0.00$

<sup>abc</sup>Superscript letters a-d indicate statistically significant differences among diets.

<sup>xy</sup>Superscript letters x and y indicate statistically significant differences between cycles 2 and 3 (without vs. with AMG).

$\ddagger$  Symbols  $\ddagger$  and  $\ddagger$  indicate statistically significant differences between genotypes (null vs. wild-type).

\*An interaction effect was found for  $\alpha$  such that genotype  $\times$  cycle was significant ( $p=0.03$ ), but *post hoc* tests revealed no differences.

Table 5.7 Parameter estimates, confidence intervals, statistical groupings, and visualization of genotype and amyloglucosidase (AMG) effects for median respiratory exchange ratio ( $x_{50}$  RER) from pooled percent relative cumulative frequency (PRCF) using the Weibull Cumulative Distribution function.

Group	Median ( $x_{50}$ )	Median ( $x_{50}$ ) confidence interval	Median ( $x_{50}$ ) statistical groupings	Genotype	AMG
Conventional starch   Null   without AMG	0.890	[0.880, 0.899]	ij	↔	↓
Conventional starch   Wild-type   without AMG	0.890	[0.880, 0.899]	ij	↔	↓
Conventional starch   Null   with AMG	0.933	[0.925, 0.940]	def	↔	↑
Conventional starch   Wild-type   with AMG	0.935	[0.928, 0.941]	d	↔	↑
53% Resistant starch   Null   without AMG	0.918	[0.911, 0.926]	efg	↓	↓
53% Resistant starch   Wild-type   without AMG	0.949	[0.939, 0.960]	cd	↑	↓
53% Resistant starch   Null   with AMG	0.964	[0.958, 0.970]	c	↓	↑
53% Resistant starch   Wild-type   with AMG	0.980	[0.972, 0.988]	b	↑	↑
35% Resistant starch   Null   without AMG	0.917	[0.908, 0.927]	fgh	↔	↔
35% Resistant starch   Wild-type   without AMG	0.916	[0.910, 0.923]	gh	↔	↔
35% Resistant starch   Null   with AMG	0.933	[0.925, 0.942]	de	↑	↑
35% Resistant starch   Wild-type   with AMG	0.912	[0.905, 0.918]	gh	↔	↔

Table 5.7, continued.

Group	Weibull $x_{50}$	Weibull $x_{50}$ confidence interval	Weibull $x_{50}$ statistical groupings	Genotype	AMG
18% Resistant starch   Null   without AMG	0.918	[0.908, 0.927]	efgh	↔	↓
18% Resistant starch   Wild-type   without AMG	0.917	[0.907, 0.928]	efgh	↔	↔
18% Resistant starch   Null   with AMG	0.942	[0.931, 0.953]	d	↑	↑
18% Resistant starch   Wild-type   with AMG	0.919	[0.911, 0.927]	efg	↔	↔
Sucrose   Null   without AMG	1.005	[0.996, 1.015]	a	↔	↔
Sucrose   Wild-type   without AMG	1.000	[0.992, 1.009]	a	↔	↔
Sucrose   Null   with AMG	1.005	[0.997, 1.012]	a	↔	↔
Sucrose   Wild-type   with AMG	0.996	[0.988, 1.003]	ab	↔	↔
High-fat   Null   without AMG	0.887	[0.884, 0.891]	j	↓	↓
High-fat   Wild-type   without AMG	0.909	[0.906, 0.912]	gh	↑	↔
High-fat   Null   with AMG	0.900	[0.896, 0.904]	i	↓	↑
High-fat   Wild-type   with AMG	0.907	[0.904, 0.910]	h	↑	↔

AMG, amyloglucosidase.

Table 5.8 Parameter estimates, confidence intervals, statistical groupings, and visualization of genotype and amyloglucosidase (AMG) effects for the distribution breadth constant ( $b$ ) of respiratory exchange ratio (RER) from pooled percent relative cumulative frequency (PRCF) using the Weibull Cumulative Distribution function.

Group	Weibull $b$	Weibull $b$ confidence interval	Weibull $b$ statistical groupings	Genotype	AMG
Conventional starch   Null   without AMG	7.069	[6.359, 7.780]	cdefgh	↔	↔
Conventional starch   Wild-type   without AMG	7.069	[6.359, 7.780]	cdefgh	↔	↔
Conventional starch   Null   with AMG	8.156	[7.406, 8.907]	bcdf	↔	↔
Conventional starch   Wild-type   with AMG	8.062	[7.480, 8.644]	bc	↔	↔
53% Resistant starch   Null   without AMG	7.577	[6.929, 8.225]	cdefg	↔	↔
53% Resistant starch   Wild-type   without AMG	7.511	[6.632, 8.391]	cdefgh	↔	↔
53% Resistant starch   Null   with AMG	7.872	[7.316, 8.428]	cdefg	↔	↔
53% Resistant starch   Wild-type   with AMG	7.894	[7.175, 8.614]	bcdfg	↔	↔
35% Resistant starch   Null   without AMG	7.724	[6.902, 8.546]	bcdefg	↔	↔
35% Resistant starch   Wild-type   without AMG	7.797	[7.220, 8.374]	cdefg	↔	↔
35% Resistant starch   Null   with AMG	8.060	[7.258, 8.862]	bcdfg	↔	↔
35% Resistant starch   Wild-type   with AMG	7.637	[7.076, 8.197]	cdefg	↔	↔

Table 5.8, continued.

Group	Weibull <i>b</i>	Weibull <i>b</i> confidence interval	Weibull <i>b</i> statistical groupings	Genotype	AMG
18% Resistant starch   Null   without AMG	6.874	[6.199, 7.548]	cdefgh	↔	↔
18% Resistant starch   Wild-type   without AMG	6.269	[5.668, 6.870]	h	↔	↔
18% Resistant starch   Null   with AMG	6.733	[6.012, 7.454]	fgh	↔	↔
18% Resistant starch   Wild-type   with AMG	6.364	[5.860, 6.867]	h	↔	↔
Sucrose   Null   without AMG	6.701	[6.072, 7.331]	gh	↔	↔
Sucrose   Wild-type   without AMG	6.819	[6.275, 7.363]	defgh	↔	↔
Sucrose   Null   with AMG	7.281	[6.757, 7.805]	cdefgh	↔	↔
Sucrose   Wild-type   with AMG	6.784	[6.300, 7.268]	efgh	↔	↔
High-fat   Null   without AMG	11.388	[10.743, 12.034]	a	↑	↔
High-fat   Wild-type   without AMG	8.829	[8.499, 9.159]	b	↓	↔
High-fat   Null   with AMG	11.461	[10.732, 12.189]	a	↔	↔
High-fat   Wild-type   with AMG	11.126	[10.566, 11.687]	a	↔	↔

AMG, amyloglucosidase.

Table 5.9 Parameter estimates, confidence intervals, statistical groupings, and visualization of genotype and amyloglucosidase (AMG) effects for the  $\alpha$  parameter from modeling of respiratory exchange ratio (RER) from pooled percent relative cumulative frequency (PRCF) using the Mixed Weibull Cumulative Distribution function.

Group	Mixed Weibull $\alpha$	Mixed Weibull $\alpha$ confidence interval	Mixed Weibull $\alpha$ statistical groupings	Genotype	AMG
Conventional starch   Null   without AMG	0.341	[0.326, 0.357]	f	↔	↔
Conventional starch   Wild-type   without AMG	0.341	[0.326, 0.357]	f	↔	↔
Conventional starch   Null   with AMG	0.322	[0.305, 0.399]	gh	↔	↓
Conventional starch   Wild-type   with AMG	0.329	[0.300, 0.357]	fh	↔	↔
53% Resistant starch   Null   without AMG	0.736	[0.714, 0.758]	a	↔	↑
53% Resistant starch   Wild-type   without AMG	0.698	[0.680, 0.716]	abc	↔	↑
53% Resistant starch   Null   with AMG	0.217	[0.194, 0.240]	j	↓	↓
53% Resistant starch   Wild-type   with AMG	0.276	[0.262, 0.289]	i	↑	↓
35% Resistant starch   Null   without AMG	0.666	[0.643, 0.688]	bcd	↑	↑
35% Resistant starch   Wild-type   without AMG	0.333	[0.306, 0.360]	fh	↓	↔
35% Resistant starch   Null   with AMG	0.301	[0.280, 0.322]	hi	↓	↓
35% Resistant starch   Wild-type   with AMG	0.409	[0.352, 0.465]	ef	↑	↔

Table 5.9, continued.

Group	Mixed Weibull $\alpha$	Mixed Weibull $\alpha$ confidence interval	Mixed Weibull $\alpha$ statistical groupings	Genotype	AMG
18% Resistant starch   Null   without AMG	0.657	[0.638, 0.675]	d	↔	↑
18% Resistant starch   Wild-type   without AMG	0.646	[0.625, 0.668]	d	↔	↑
18% Resistant starch   Null   with AMG	0.343	[0.322, 0.363]	f	↔	↓
18% Resistant starch   Wild-type   with AMG	0.367	[0.345, 0.390]	ef	↔	↓
Sucrose   Null   without AMG	0.636	[0.610, 0.661]	d	↓	↓
Sucrose   Wild-type   without AMG	0.694	[0.680, 0.708]	bc	↑	↔
Sucrose   Null   with AMG	0.694	[0.678, 0.711]	bc	↔	↔
Sucrose   Wild-type   with AMG	0.697	[0.682, 0.712]	bc	↔	↔
High-fat   Null   without AMG	0.712	[0.642, 0.781]	ab	↑	↑
High-fat   Wild-type   without AMG	0.126	[0.096, 0.155]	k	↓	↓
High-fat   Null   with AMG	0.476	[0.366, 0.586]	e	↔	↓
High-fat   Wild-type   with AMG	0.369	[0.285, 0.453]	efg	↔	↓

AMG, amyloglucosidase.

Table 5.10 Parameter estimates, confidence intervals, statistical groupings, and visualization of genotype and amyloglucosidase (AMG) effects for the median RER ( $x_{50,1}$ ) parameter from modeling of respiratory exchange ratio (RER) from pooled percent relative cumulative frequency (PRCF) using the Mixed Weibull Cumulative Distribution function.

Group	Mixed Weibull $x_{50,1}$	Mixed Weibull $x_{50,1}$ confidence interval	Mixed Weibull $x_{50,1}$ statistical groupings	Genotype	AMG
Conventional starch   Null   without AMG	0.739	[0.735, 0.744]	j	↔	↓
Conventional starch   Wild-type   without AMG	0.739	[0.735, 0.744]	j	↔	↓
Conventional starch   Null   with AMG	0.787	[0.782, 0.792]	f	↓	↑
Conventional starch   Wild-type   with AMG	0.800	[0.793, 0.808]	de	↑	↑
53% Resistant starch   Null   without AMG	0.747	[0.741, 0.753]	j	↓	↓
53% Resistant starch   Wild-type   without AMG	0.765	[0.756, 0.774]	hi	↑	↓
53% Resistant starch   Null   with AMG	0.770	[0.762, 0.779]	gh	↓	↑
53% Resistant starch   Wild-type   with AMG	0.794	[0.788, 0.800]	ef	↑	↑
35% Resistant starch   Null   without AMG	0.770	[0.763, 0.776]	gh	↔	↔
35% Resistant starch   Wild-type   without AMG	0.782	[0.775, 0.789]	fg	↔	↔
35% Resistant starch   Null   with AMG	0.820	[0.801, 0.839]	cd	↑	↑
35% Resistant starch   Wild-type   with AMG	0.775	[0.771, 0.779]	g	↓	↔

Table 5.10, continued.

Group	Mixed Weibull $x_{50_1}$	Mixed Weibull $x_{50_1}$ confidence interval	Mixed Weibull $x_{50_1}$ statistical groupings	Genotype	AMG
18% Resistant starch   Null   without AMG	0.760	[0.755, 0.766]	hi	↔	↔
18% Resistant starch   Wild-type   without AMG	0.750	[0.744, 0.756]	ij	↔	↓
18% Resistant starch   Null   with AMG	0.768	[0.760, 0.775]	h	↔	↔
18% Resistant starch   Wild-type   with AMG	0.770	[0.764, 0.777]	gh	↔	↔
Sucrose   Null   without AMG	0.835	[0.825, 0.846]	b	↑	↔
Sucrose   Wild-type   without AMG	0.813	[0.808, 0.818]	d	↓	↔
Sucrose   Null   with AMG	0.830	[0.824, 0.836]	bc	↑	↔
Sucrose   Wild-type   with AMG	0.810	[0.805, 0.816]	d	↓	↔
High-fat   Null   without AMG	0.805	[0.796, 0.813]	de	↑	↓
High-fat   Wild-type   without AMG	0.765	[0.759, 0.771]	hi	↓	↓
High-fat   Null   with AMG	0.849	[0.838, 0.861]	b	↓	↑
High-fat   Wild-type   with AMG	0.876	[0.863, 0.888]	a	↑	↑

AMG, amyloglucosidase.

Table 5.11 Parameter estimates, confidence intervals, statistical groupings, and visualization of genotype and amyloglucosidase (AMG) effects for the median RER  $b_1$  parameter from modeling of respiratory exchange ratio (RER) from pooled percent relative cumulative frequency (PRCF) using the Mixed Weibull Cumulative Distribution function.

Group	Mixed Weibull $b_1$	Mixed Weibull $b_1$ confidence interval	Mixed Weibull $b_1$ statistical groupings	Genotype	AMG
Conventional starch   Null   without AMG	25.0	[20.6, 29.4]	abce	↔	↔
Conventional starch   Wild-type   without AMG	25.0	[20.6, 29.4]	abce	↔	↔
Conventional starch   Null   with AMG	24.2	[20.6, 27.7]	abce	↔	↔
Conventional starch   Wild-type   with AMG	18.3	[15.5, 21.1]	efghij	↔	↔
53% Resistant starch   Null   without AMG	29.3	[22.1, 36.6]	abc	↑	↔
53% Resistant starch   Wild-type   without AMG	13.2	[10.8, 15.5]	jk	↓	↓
53% Resistant starch   Null   with AMG	23.0	[16.6, 29.3]	abcdeghi	↔	↔
53% Resistant starch   Wild-type   with AMG	18.2	[15.7, 20.7]	efghi	↔	↑
35% Resistant starch   Null   without AMG	25.6	[19.6, 31.6]	abcde	↔	↑
35% Resistant starch   Wild-type   without AMG	19.8	[16.5, 23.0]	bcdeghi	↔	↓
35% Resistant starch   Null   with AMG	12.3	[9.5, 15.1]	k	↓	↓
35% Resistant starch   Wild-type   with AMG	30.0	[25.0, 34.9]	a	↑	↑

Table 5.11, continued.

Group	Mixed Weibull $b_1$	Mixed Weibull $b_1$ confidence interval	Mixed Weibull $b_1$ statistical groupings	Genotype	AMG
18% Resistant starch   Null   without AMG	23.4	[19.3, 27.5]	abcde	↔	↔
18% Resistant starch   Wild-type   without AMG	23.7	[19.0, 28.4]	abcdeg	↔	↔
18% Resistant starch   Null   with AMG	22.5	[17.4, 27.6]	abcdegh	↔	↔
18% Resistant starch   Wild-type   with AMG	17.1	[14.8, 19.5]	fghijk	↔	↔
Sucrose   Null   without AMG	14.3	[11.9, 16.6]	ijk	↔	↔
Sucrose   Wild-type   without AMG	17.3	[15.3, 19.2]	fghij	↔	↔
Sucrose   Null   with AMG	16.3	[14.4, 18.2]	hijk	↔	↔
Sucrose   Wild-type   with AMG	19.6	[17.0, 22.2]	cdegh	↔	↔
High-fat   Null   without AMG	22.6	[18.3, 26.8]	abcdeg	↔	↔
High-fat   Wild-type   without AMG	42.0	[22.6, 61.3]	ab	↔	↑
High-fat   Null   with AMG	18.5	[16.5, 20.6]	dfghi	↔	↔
High-fat   Wild-type   with AMG	15.4	[14.1, 16.7]	ijk	↔	↓

AMG, amyloglucosidase.

Table 5.12 Parameter estimates, confidence intervals, statistical groupings, and visualization of genotype and amyloglucosidase (AMG) effects for the median RER ( $x_{50,2}$ ) parameter from modeling of respiratory exchange ratio (RER) from pooled percent relative cumulative frequency (PRCF) using the Mixed Weibull Cumulative Distribution function.

Group	Mixed Weibull $x_{50,2}$	Mixed Weibull $x_{50,2}$ confidence interval	Mixed Weibull $x_{50,2}$ statistical groupings	Genotype	AMG
Conventional starch   Null   without AMG	0.988	[0.985, 0.991]	j	↔	↓
Conventional starch   Wild-type   without AMG	0.988	[0.985, 0.991]	j	↔	↓
Conventional starch   Null   with AMG	1.020	[1.017, 1.023]	h	↔	↑
Conventional starch   Wild-type   with AMG	1.026	[1.021, 1.030]	gh	↔	↑
53% Resistant starch   Null   without AMG	1.003	[0.999, 1.006]	i	↓	↓
53% Resistant starch   Wild-type   without AMG	1.036	[1.033, 1.039]	ef	↑	↓
53% Resistant starch   Null   with AMG	1.042	[1.038, 1.046]	e	↓	↑
53% Resistant starch   Wild-type   with AMG	1.065	[1.062, 1.067]	c	↑	↑
35% Resistant starch   Null   without AMG	1.009	[1.005, 1.013]	i	↔	↔
35% Resistant starch   Wild-type   without AMG	1.009	[1.005, 1.013]	i	↔	↔
35% Resistant starch   Null   with AMG	1.029	[1.023, 1.035]	fg	↑	↑
35% Resistant starch   Wild-type   with AMG	1.002	[0.999, 1.005]	i	↔	↔

Table 5.12, continued.

Group	Mixed Weibull $x_{50.2}$	Mixed Weibull $x_{50.2}$ confidence interval	Mixed Weibull $x_{50.2}$ statistical groupings	Genotype	AMG
18% Resistant starch   Null   without AMG	1.023	[1.020, 1.027]	gh	↓	↓
18% Resistant starch   Wild-type   without AMG	1.036	[1.032, 1.041]	ef	↑	↔
18% Resistant starch   Null   with AMG	1.051	[1.047, 1.056]	d	↑	↑
18% Resistant starch   Wild-type   with AMG	1.040	[1.036, 1.044]	e	↓	↔
Sucrose   Null   without AMG	1.122	[1.118, 1.127]	a	↑	↑
Sucrose   Wild-type   without AMG	1.108	[1.105, 1.110]	b	↔	↔
Sucrose   Null   with AMG	1.107	[1.104, 1.110]	b	↔	↔
Sucrose   Wild-type   with AMG	1.105	[1.102, 1.108]	b	↔	↔
High-fat   Null   without AMG	0.945	[0.938, 0.952]	l	↓	↓
High-fat   Wild-type   without AMG	0.964	[0.960, 0.968]	k	↑	↓
High-fat   Null   with AMG	0.978	[0.966, 0.990]	jk	↓	↑
High-fat   Wild-type   with AMG	1.003	[0.995, 1.012]	i	↑	↑

AMG, amyloglucosidase.

Table 5.13 Parameter estimates, confidence intervals, statistical groupings, and visualization of genotype and amyloglucosidase (AMG) effects for the median RER  $b_2$  parameter from modeling of respiratory exchange ratio (RER) from pooled percent relative cumulative frequency (PRCF) using the Mixed Weibull Cumulative Distribution function.

Group	Mixed Weibull $b_2$	Mixed Weibull $b_2$ confidence interval	Mixed Weibull $b_2$ statistical groupings	Genotype	AMG
Conventional starch   Null   without AMG	18.4	[16.9, 19.9]	bce	↔	↔
Conventional starch   Wild-type   without AMG	18.4	[16.9, 19.9]	bce	↔	↔
Conventional starch   Null   with AMG	18.7	[17.2, 20.1]	bc	↔	↔
Conventional starch   Wild-type   with AMG	16.6	[14.9, 18.4]	cdfg	↔	↔
53% Resistant starch   Null   without AMG	14.4	[13.1, 15.6]	fgh	↓	↔
53% Resistant starch   Wild-type   without AMG	21.3	[19.5, 23.2]	ab	↑	↑
53% Resistant starch   Null   with AMG	13.5	[12.4, 14.5]	h	↓	↔
53% Resistant starch   Wild-type   with AMG	17.9	[16.8, 19.0]	ce	↑	↓
35% Resistant starch   Null   without AMG	19.5	[17.2, 21.8]	bc	↔	↔
35% Resistant starch   Wild-type   without AMG	16.5	[14.8, 18.2]	cdfg	↔	↔
35% Resistant starch   Null   with AMG	25.1	[19.4, 30.8]	ab	↑	↔
35% Resistant starch   Wild-type   with AMG	14.0	[13.0, 15.1]	gh	↓	↔

Table 5.13, continued.

Group	Mixed Weibull $b_2$	Mixed Weibull $b_2$ confidence interval	Mixed Weibull $b_2$ statistical groupings	Genotype	AMG
18% Resistant starch   Null   without AMG	17.0	[15.4, 18.6]	cdf	↔	↔
18% Resistant starch   Wild-type   without AMG	15.3	[13.7, 17.0]	defgh	↔	↔
18% Resistant starch   Null   with AMG	18.5	[16.3, 20.7]	bcd	↑	↔
18% Resistant starch   Wild-type   with AMG	14.7	[13.3, 16.1]	fgh	↓	↔
Sucrose   Null   without AMG	19.4	[17.0, 21.8]	bc	↑	↑
Sucrose   Wild-type   without AMG	15.3	[14.4, 16.2]	dfgh	↓	↔
Sucrose   Null   with AMG	15.6	[14.6, 16.6]	dfg	↔	↔
Sucrose   Wild-type   with AMG	14.3	[13.4, 15.2]	gh	↔	↔
High-fat   Null   without AMG	17.2	[14.6, 19.8]	cdfg	↑	↔
High-fat   Wild-type   without AMG	10.6	[10.0, 11.3]	i	↓	↓
High-fat   Null   with AMG	20.9	[15.0, 26.8]	abc	↔	↔
High-fat   Wild-type   with AMG	33.3	[22.2, 44.5]	a	↔	↑

AMG, amyloglucosidase.

Table 5.14 Mean RER per 24 h for each group (diet × genotype × cycle [without/with AMG]). Mean values shown with ± standard error of the mean. Values not sharing the same letter are significantly different ( $p < 0.05$ ; diet × genotype × cycle was significant [ $p = 0.0001$ ], so *post hoc* comparisons were made among the 24 groups). Arrows in columns for genotype and AMG breakdown the effects of these two factors *within* each diet.

Diet	Mean RER per 24 h	Genotype	AMG
Conventional starch   Null   without AMG	0.883 ± 0.007 <sup>f</sup>	↔	↓
Conventional starch   Wild-type   without AMG	0.886 ± 0.007 <sup>f</sup>	↔	↓
Conventional starch   Null   with AMG	0.925 ± 0.007 <sup>de</sup>	↔	↑
Conventional starch   Wild-type   with AMG	0.929 ± 0.007 <sup>de</sup>	↔	↑
53% Resistant starch   Null   without AMG	0.910 ± 0.007 <sup>ef</sup>	↔	↓
53% Resistant starch   Wild-type   without AMG	0.935 ± 0.008 <sup>cde</sup>	↔	↔
53% Resistant starch   Null   with AMG	0.954 ± 0.008 <sup>bcd</sup>	↔	↑
53% Resistant starch   Wild-type   with AMG	0.967 ± 0.008 <sup>abc</sup>	↔	↔
35% Resistant starch   Null   without AMG	0.911 ± 0.007 <sup>ef</sup>	↔	↔
35% Resistant starch   Wild-type   without AMG	0.912 ± 0.007 <sup>ef</sup>	↔	↔
35% Resistant starch   Null   with AMG	0.927 ± 0.007 <sup>de</sup>	↔	↔
35% Resistant starch   Wild-type   with AMG	0.910 ± 0.007 <sup>ef</sup>	↔	↔
18% Resistant starch   Null   without AMG	0.912 ± 0.008 <sup>ef</sup>	↔	↔
18% Resistant starch   Wild-type   without AMG	0.912 ± 0.009 <sup>ef</sup>	↔	↔
18% Resistant starch   Null   with AMG	0.934 ± 0.008 <sup>cde</sup>	↔	↔
18% Resistant starch   Wild-type   with AMG	0.916 ± 0.008 <sup>def</sup>	↔	↔
Sucrose   Null   without AMG	0.994 ± 0.009 <sup>a</sup>	↔	↔
Sucrose   Wild-type   without AMG	0.990 ± 0.009 <sup>ab</sup>	↔	↔
Sucrose   Null   with AMG	0.996 ± 0.008 <sup>a</sup>	↔	↔
Sucrose   Wild-type   with AMG	0.989 ± 0.009 <sup>ab</sup>	↔	↔
High-fat   Null   without AMG	0.884 ± 0.005 <sup>f</sup>	↔	↔
High-fat   Wild-type   without AMG	0.906 ± 0.007 <sup>ef</sup>	↔	↔
High-fat   Null   with AMG	0.898 ± 0.005 <sup>ef</sup>	↔	↔
High-fat   Wild-type   with AMG	0.905 ± 0.005 <sup>ef</sup>	↔	↔

AMG, amyloglucosidase; RER, respiratory exchange ratio.

Table 5.15 Effect of dietary condition and genotype on *ex vivo* jejunal enzyme activities (U/gm protein) for maltodextrin and sucrose substrates sampled by military time (MT),  $n=4$  per group. Mean values are shown  $\pm$  standard error of the mean.  $p$ -values indicate statistical comparisons between genotype per diet for the two substrates.

Condition	MT	Maltodextrin substrate-induced enzyme activity (U/gm protein)			Sucrose substrate-induced enzyme activity (U/gm protein)		
		Wild-type	Null	$p$	Wild-type	Null	$p$
Fasting	12:00	180.35 $\pm$ 8.37	87.12 $\pm$ 9.41	0.001	116.7 $\pm$ 6.82	153.4 $\pm$ 17.6	0.147
Conventional starch diet	24:00	230.7 $\pm$ 25.5	68.93 $\pm$ 3.30	0.013	145.2 $\pm$ 18.7	87.12 $\pm$ 9.41	0.050
53% Resistant starch diet	24:00	193.3 $\pm$ 16.2	77.1 $\pm$ 12.2	0.005	117.47 $\pm$ 3.71	68.93 $\pm$ 3.3	0.000
Conventional starch with AMG	24:00	159.40 $\pm$ 6.01	70.86 $\pm$ 8.44	0.004	108.87 $\pm$ 4.55	94.94 $\pm$ 8.9	0.235
Conventional starch with acarbose	24:00	96.00 $\pm$ 2.01	92.31 $\pm$ 5.74	0.063	104.2 $\pm$ 18.4	99.78 $\pm$ 7.81	0.845
Sucrose diet	24:00	187.52 $\pm$ 8.14	90.7 $\pm$ 11.3	0.000	158.24 $\pm$ 6.85	142.59 $\pm$ 3.85	0.117

AMG, amyloglucosidase; MT, military time.

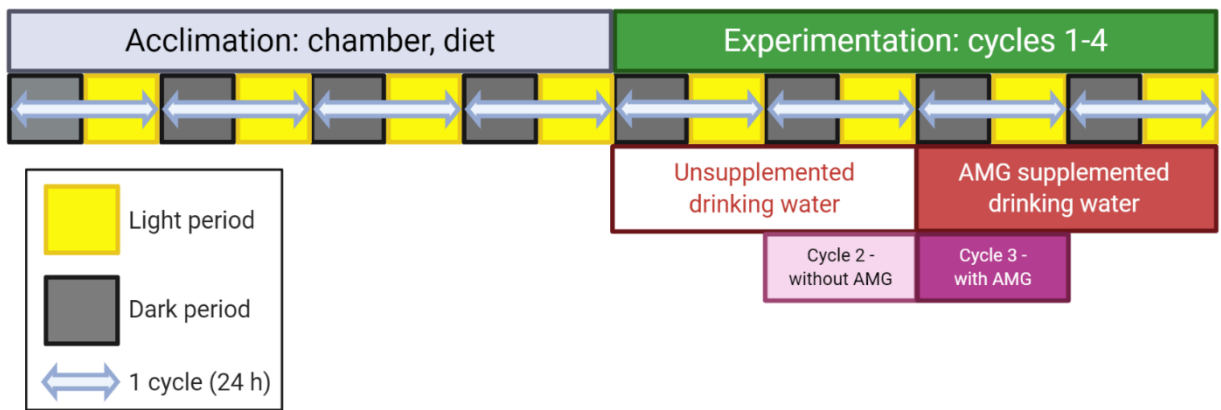


Figure 5.1 Diagram of indirect calorimetry experiments protocol per diet. Figure made using BioRender. AMG, amyloglucosidase.

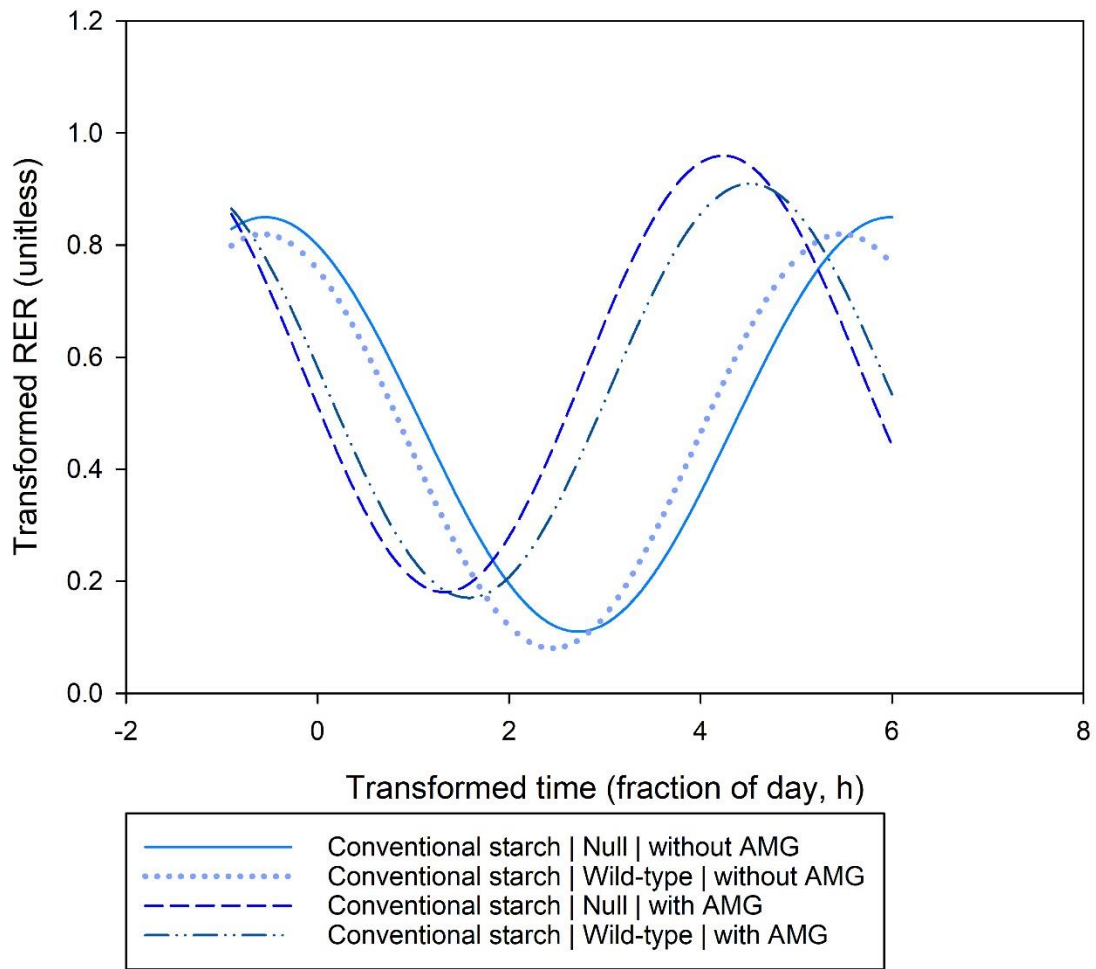


Figure 5.2 Modeled respiratory exchange ratio (RER) for Conventional starch diet. AMG, amyloglucosidase.

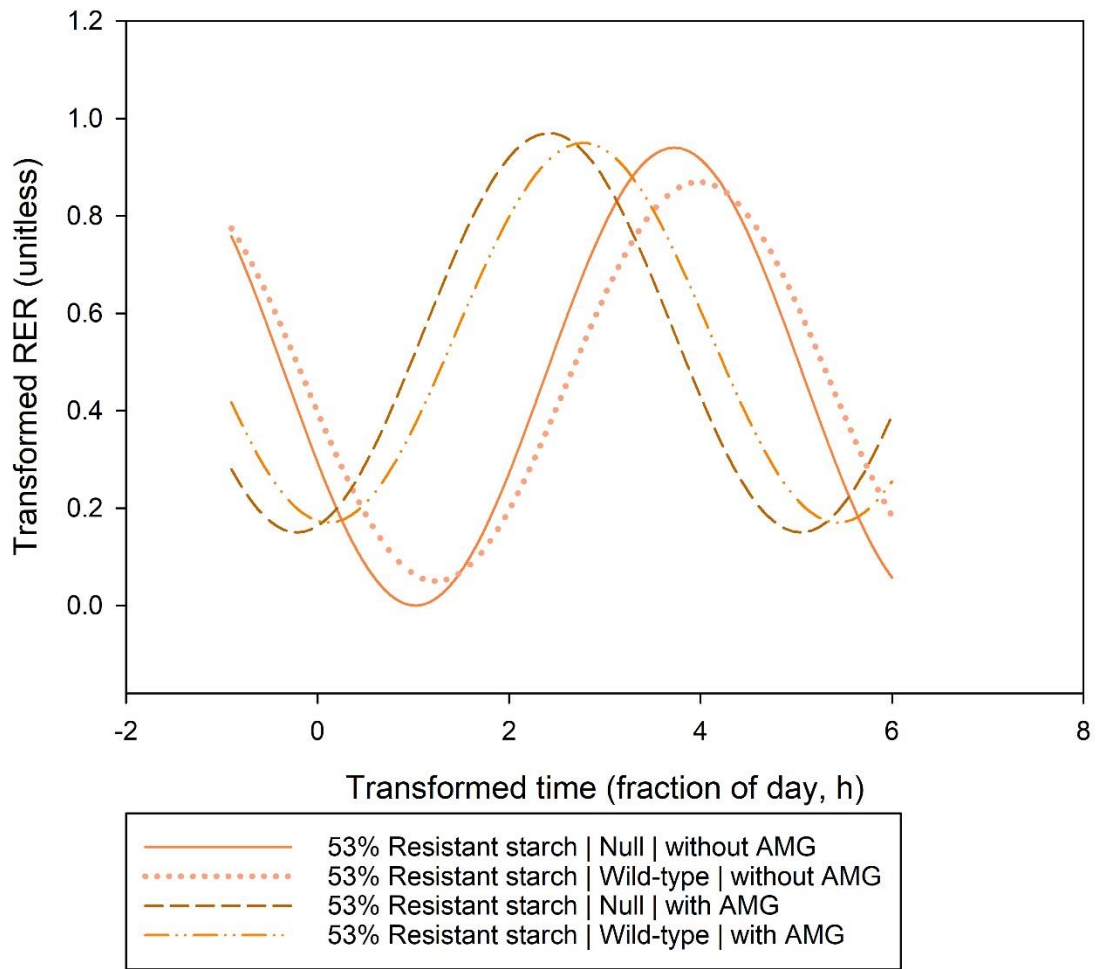


Figure 5.3 Modeled respiratory exchange ratio (RER) for 53% Resistant starch diet. AMG, amyloglucosidase.

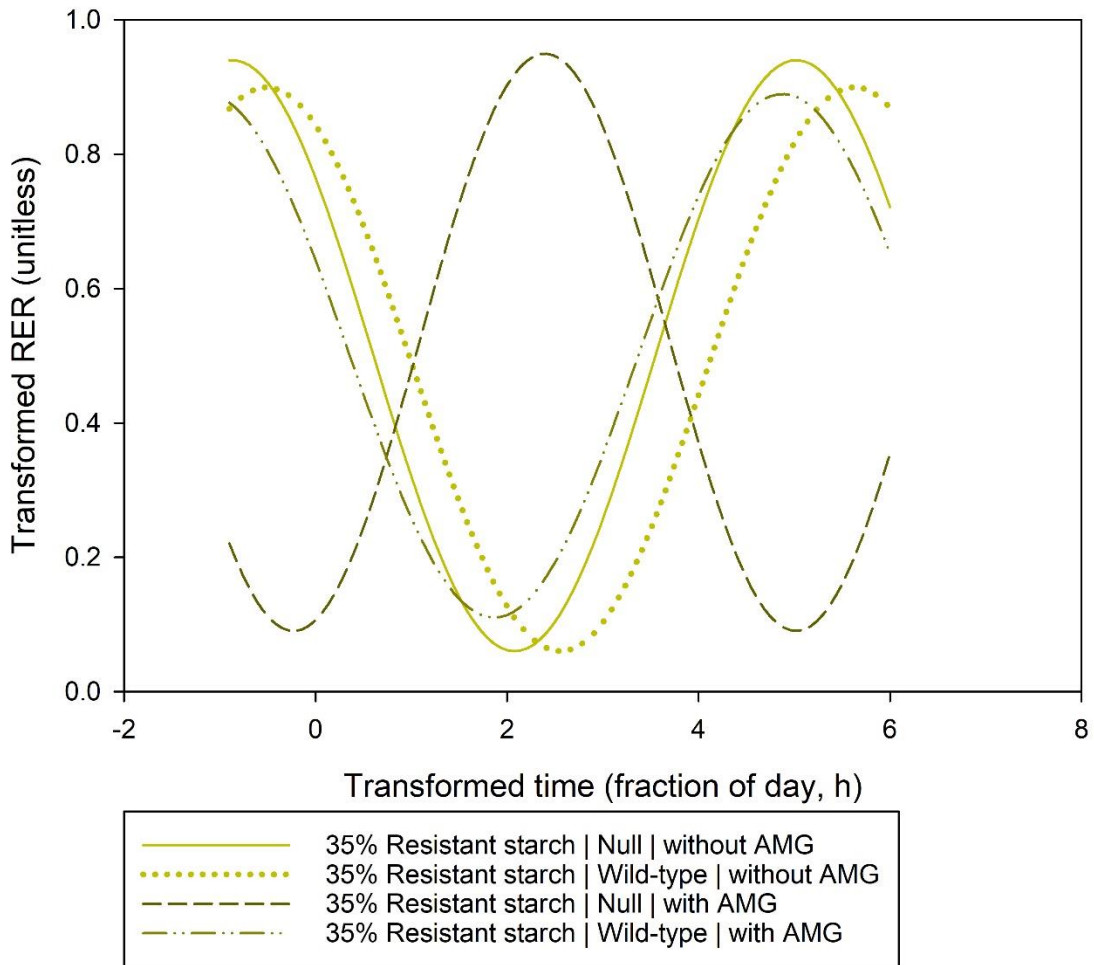


Figure 5.4 Modeled respiratory exchange ratio (RER) for 35% Resistant starch diet. AMG, amyloglucosidase.

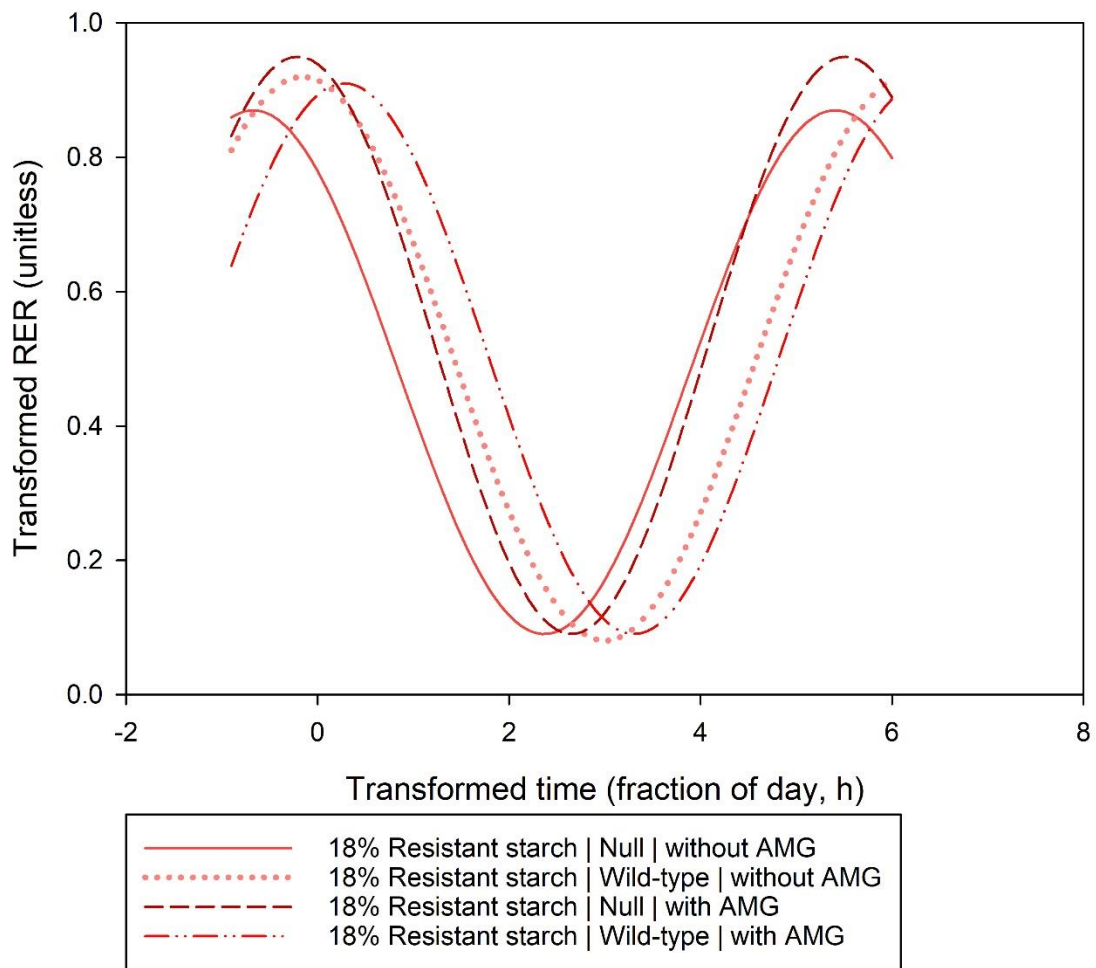


Figure 5.5 Modeled respiratory exchange ratio (RER) for 18% Resistant starch diet. AMG, amyloglucosidase.

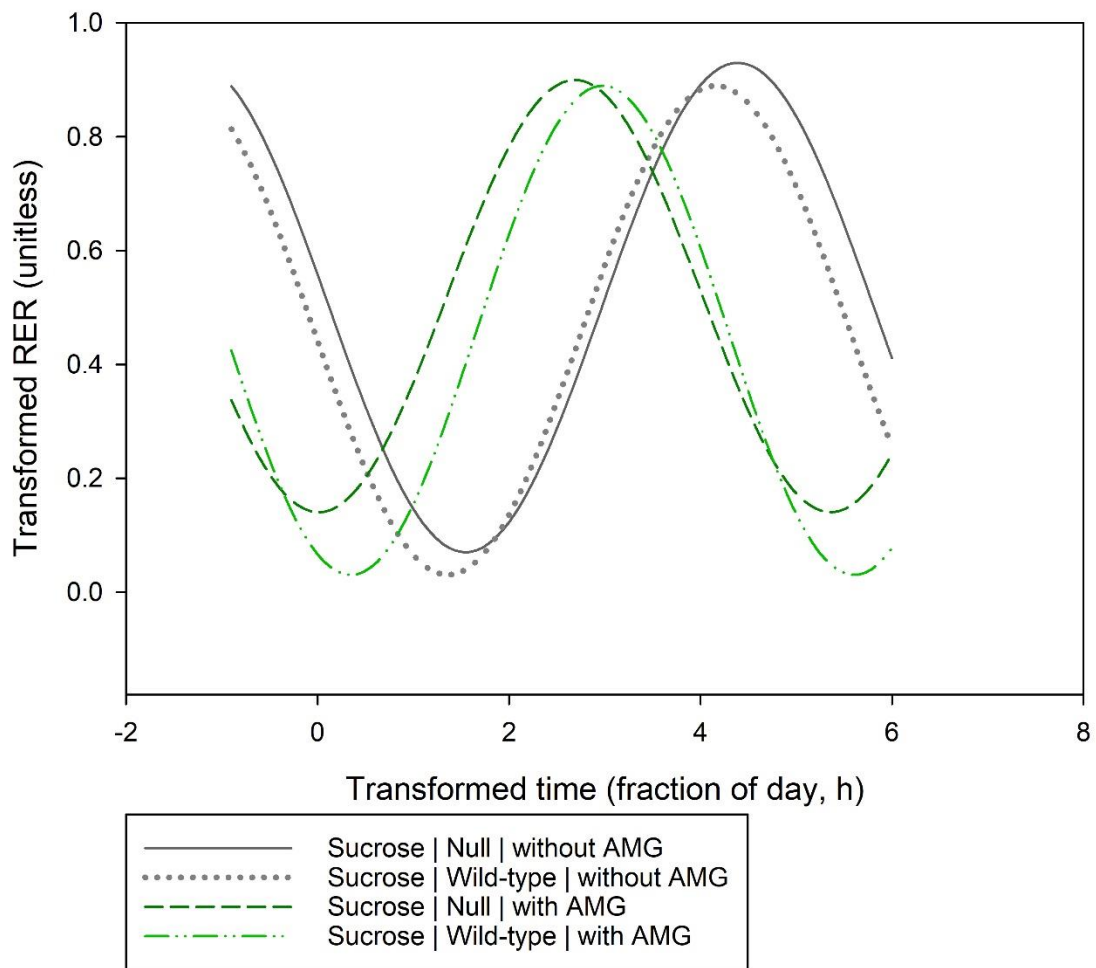


Figure 5.6 Modeled respiratory exchange ratio (RER) for Sucrose diet. AMG, amyloglucosidase.

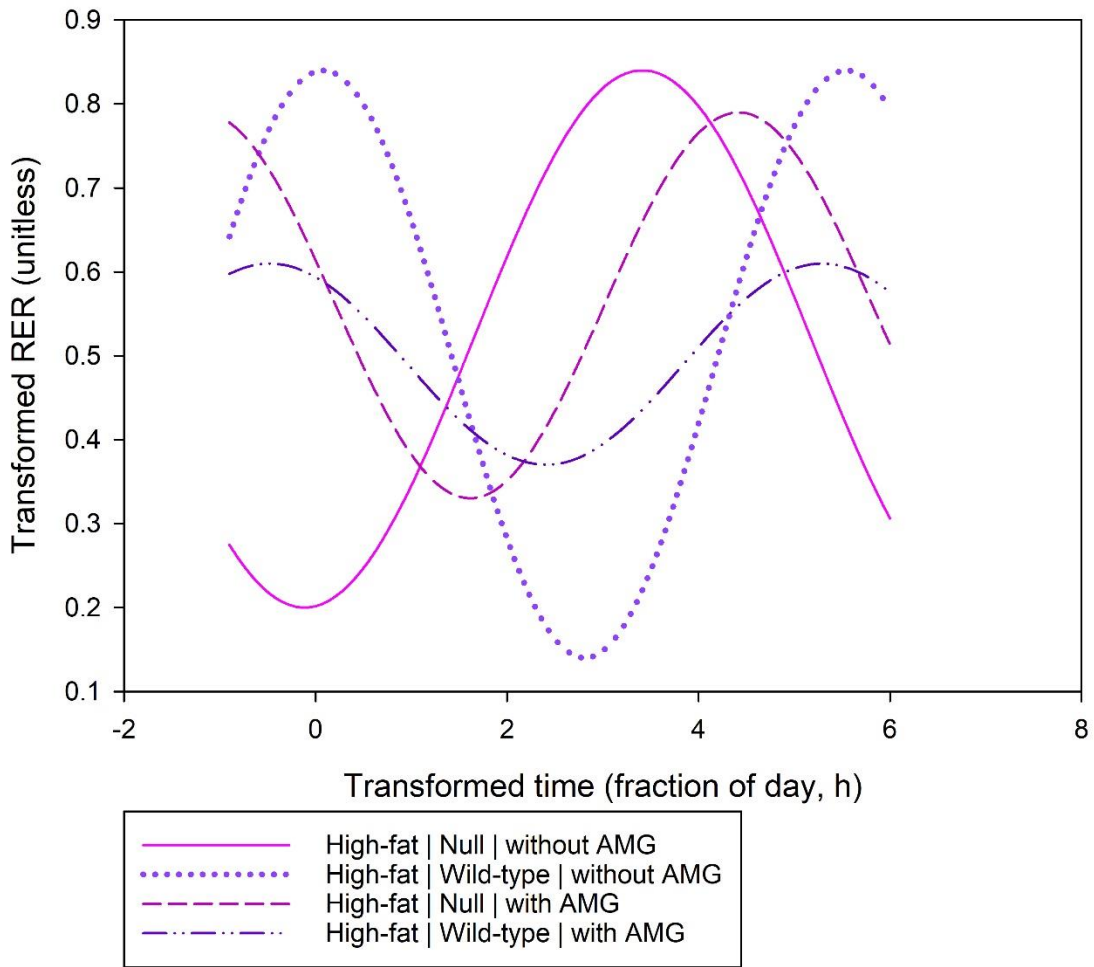


Figure 5.7 Modeled respiratory exchange ratio (RER) for High-fat diet. AMG, amyloglucosidase.

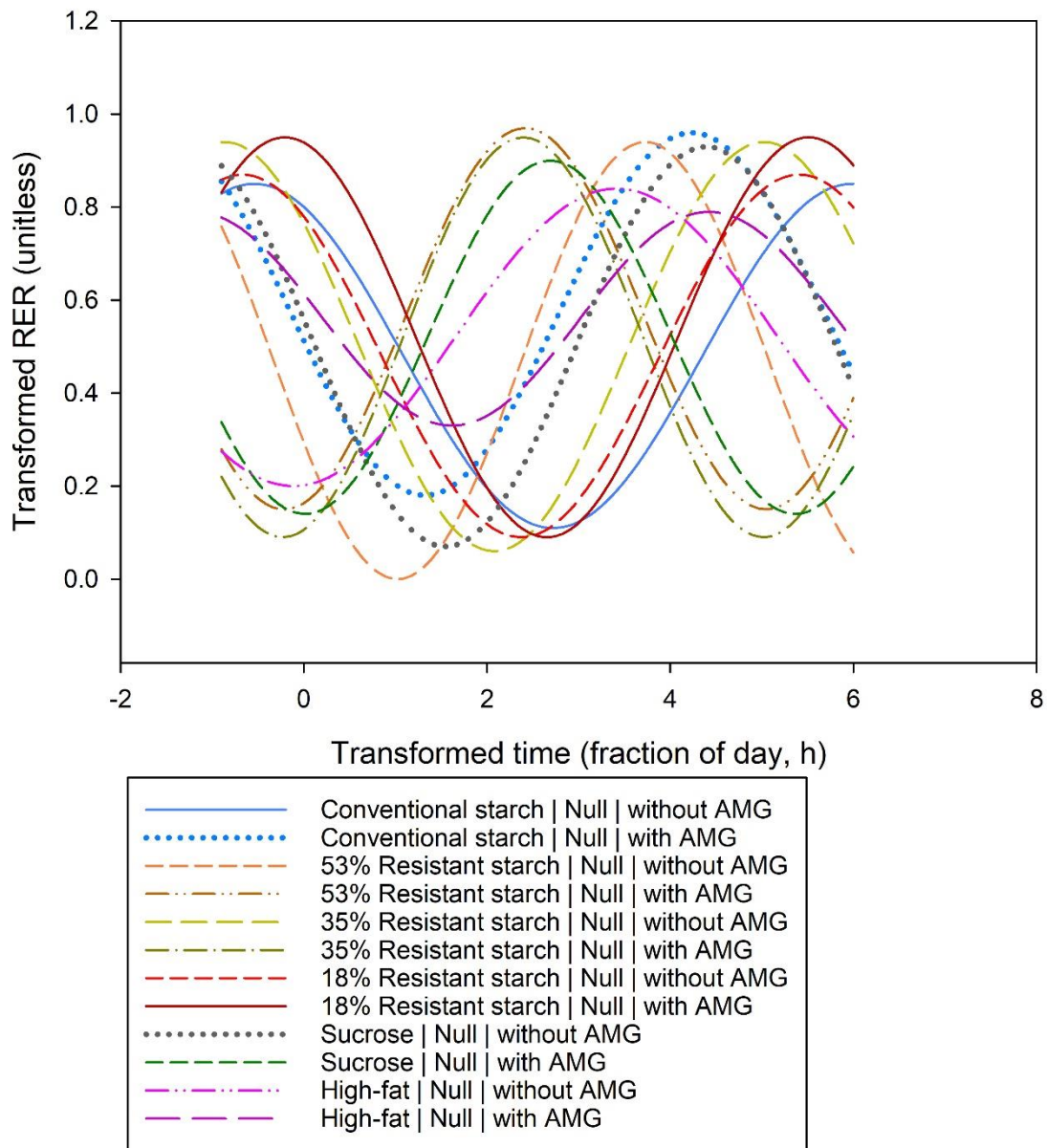


Figure 5.8 Sine curves for average sine parameters from RER data fit for all null mice per diet (diet  $\times$  mouse genotype [null]  $\times$  cycle). AMG, amyloglucosidase.

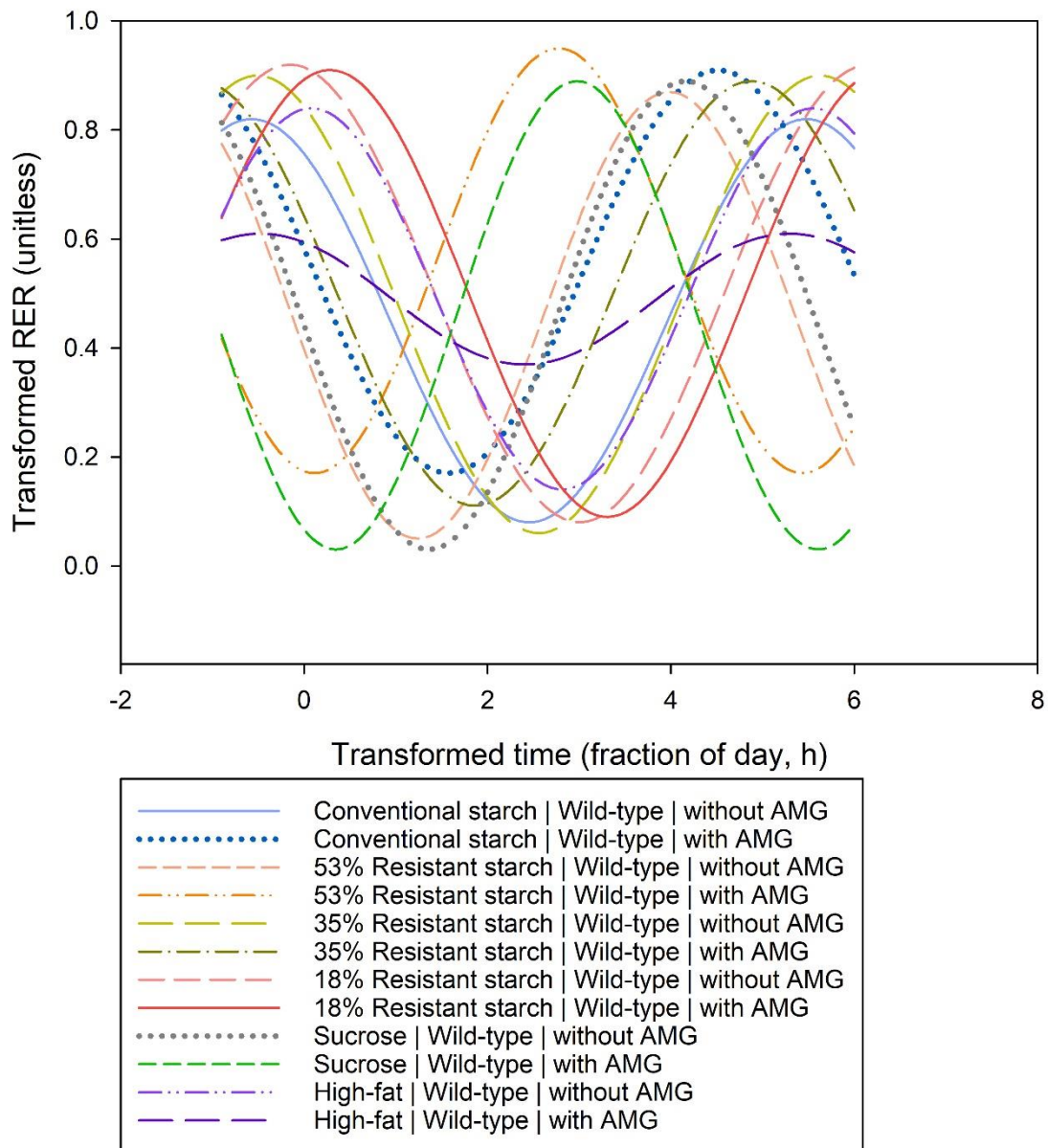


Figure 5.9 Sine curves for average sine parameters from RER data fit for all wild-type mice per diet (diet  $\times$  mouse genotype [wild-type]  $\times$  cycle). AMG, amyloglucosidase.

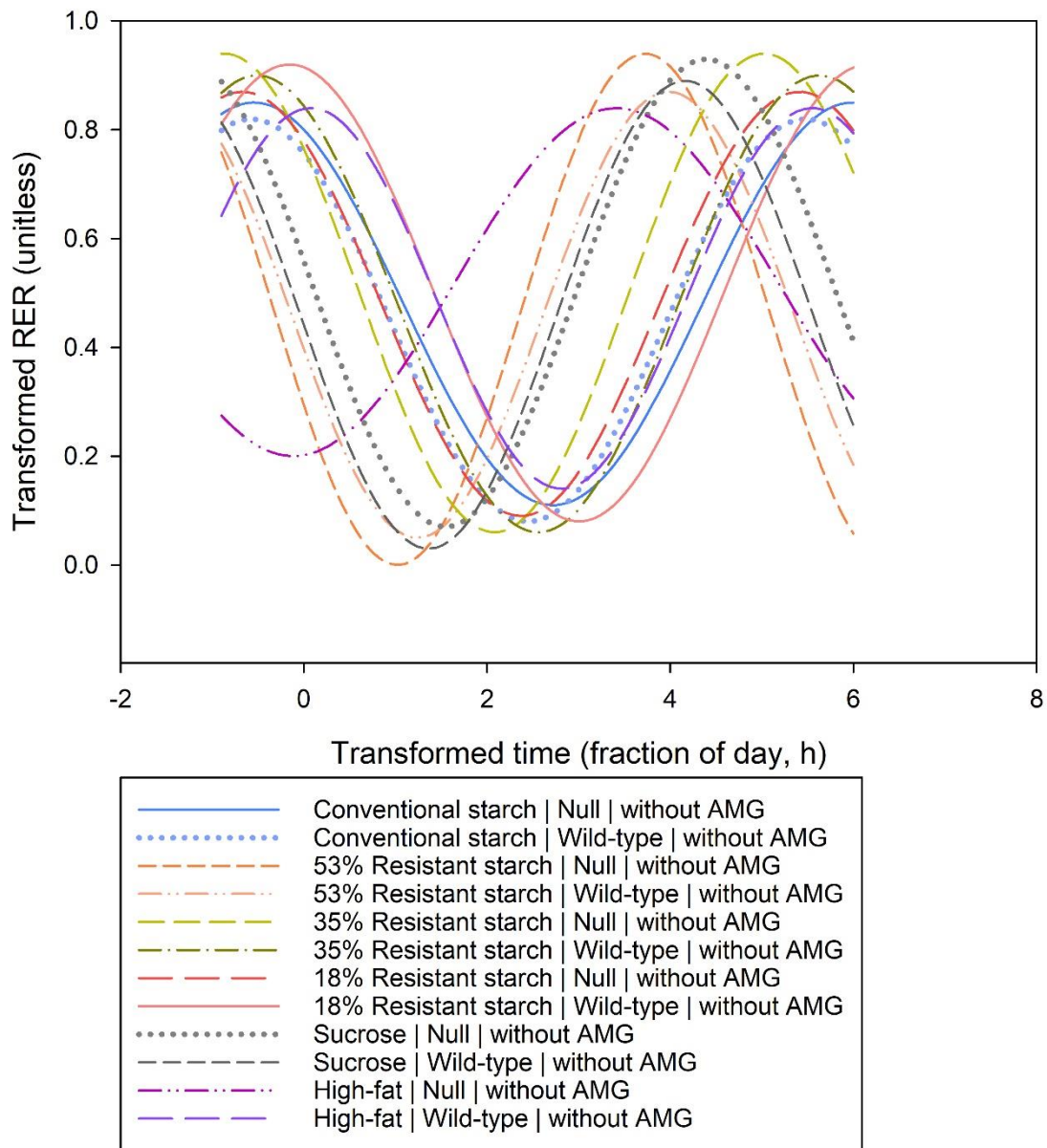


Figure 5.10 Sine curves for average sine parameters from RER data fit for all mice per diet (diet  $\times$  mouse genotype  $\times$  cycle), illustrated without AMG only [cycle 2]. AMG, amyloglucosidase.

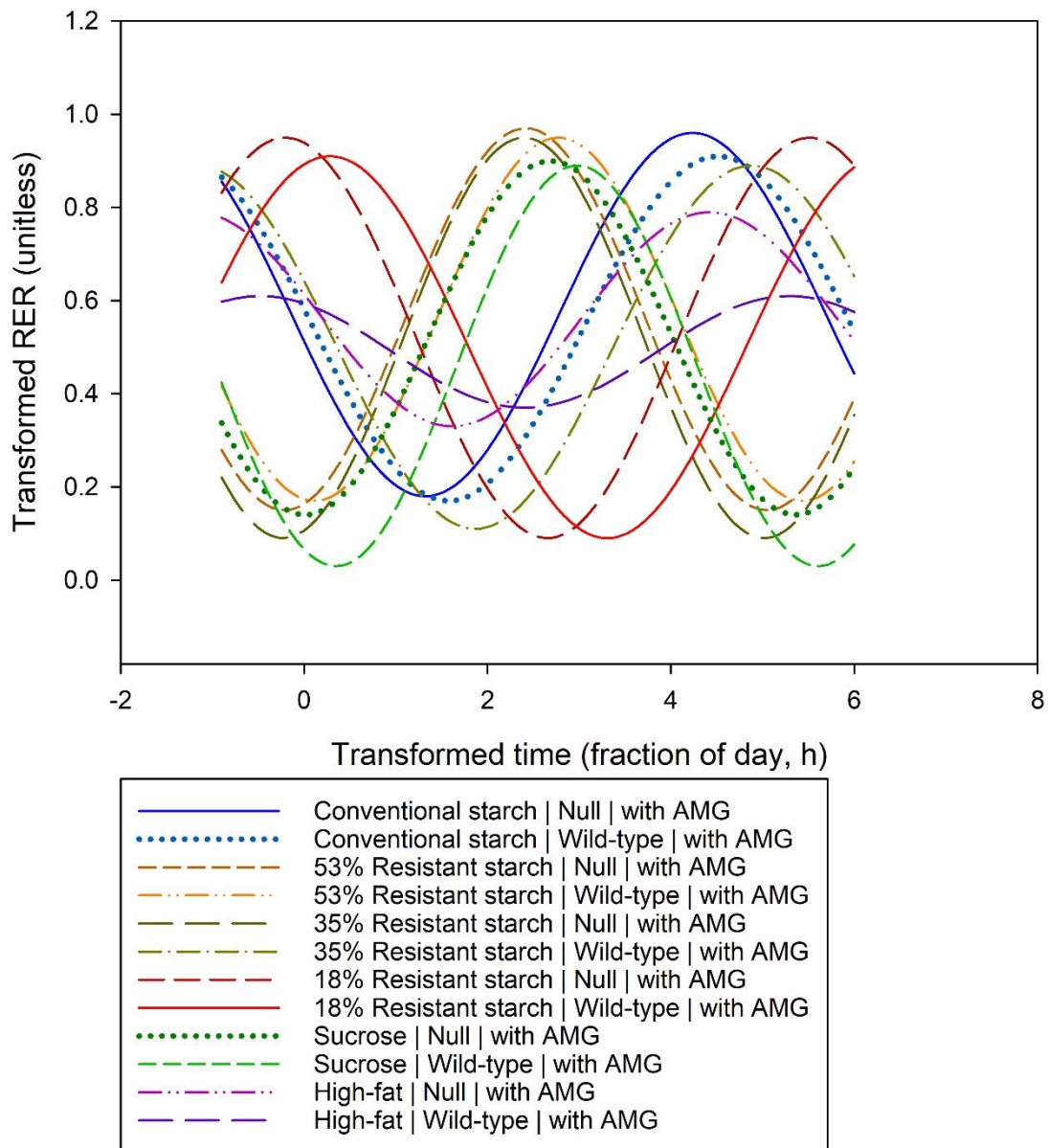


Figure 5.11 Sine curves for average sine parameters from RER data fit for all mice per diet (diet  $\times$  mouse genotype  $\times$  cycle), illustrated with AMG only [cycle 3]. AMG, amyloglucosidase.

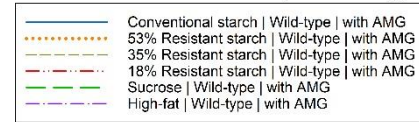
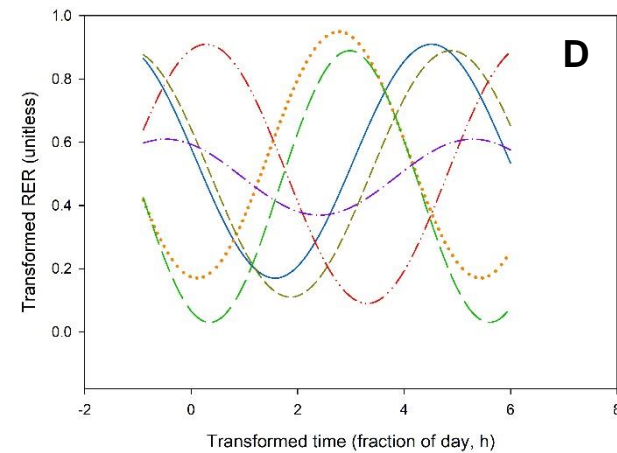
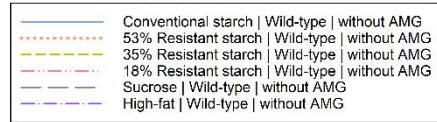
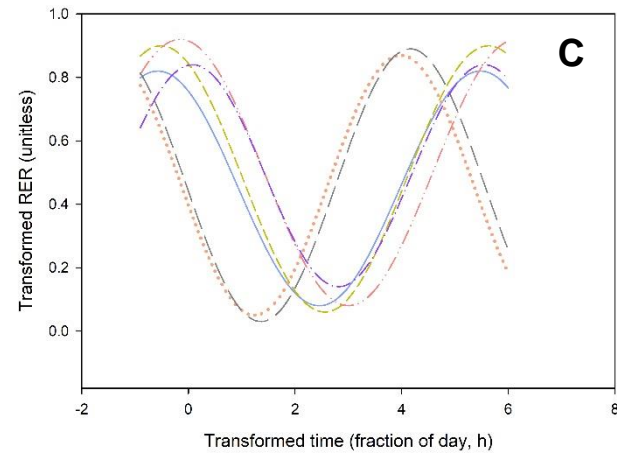
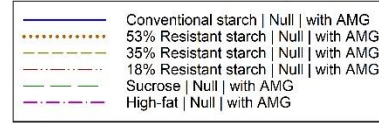
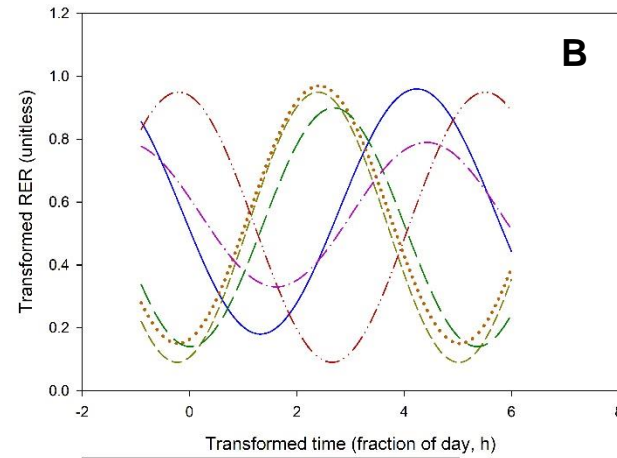
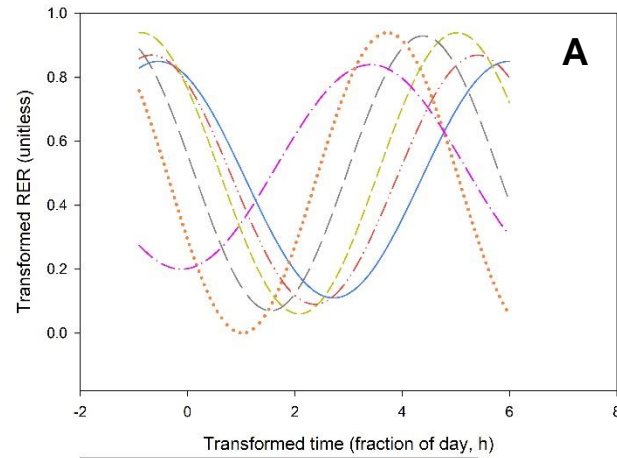


Figure 5.12 Sine curves for average sine parameters from RER data fit for all mice per diet (diet  $\times$  mouse genotype  $\times$  cycle). Split per genotype and cycle: null cycle 2 [without AMG] (A), null cycle 3 [without AMG] (B), wild-type cycle 2 [without AMG] (C), wild-type cycle 3 [with AMG] (D). AMG, amyloglucosidase.

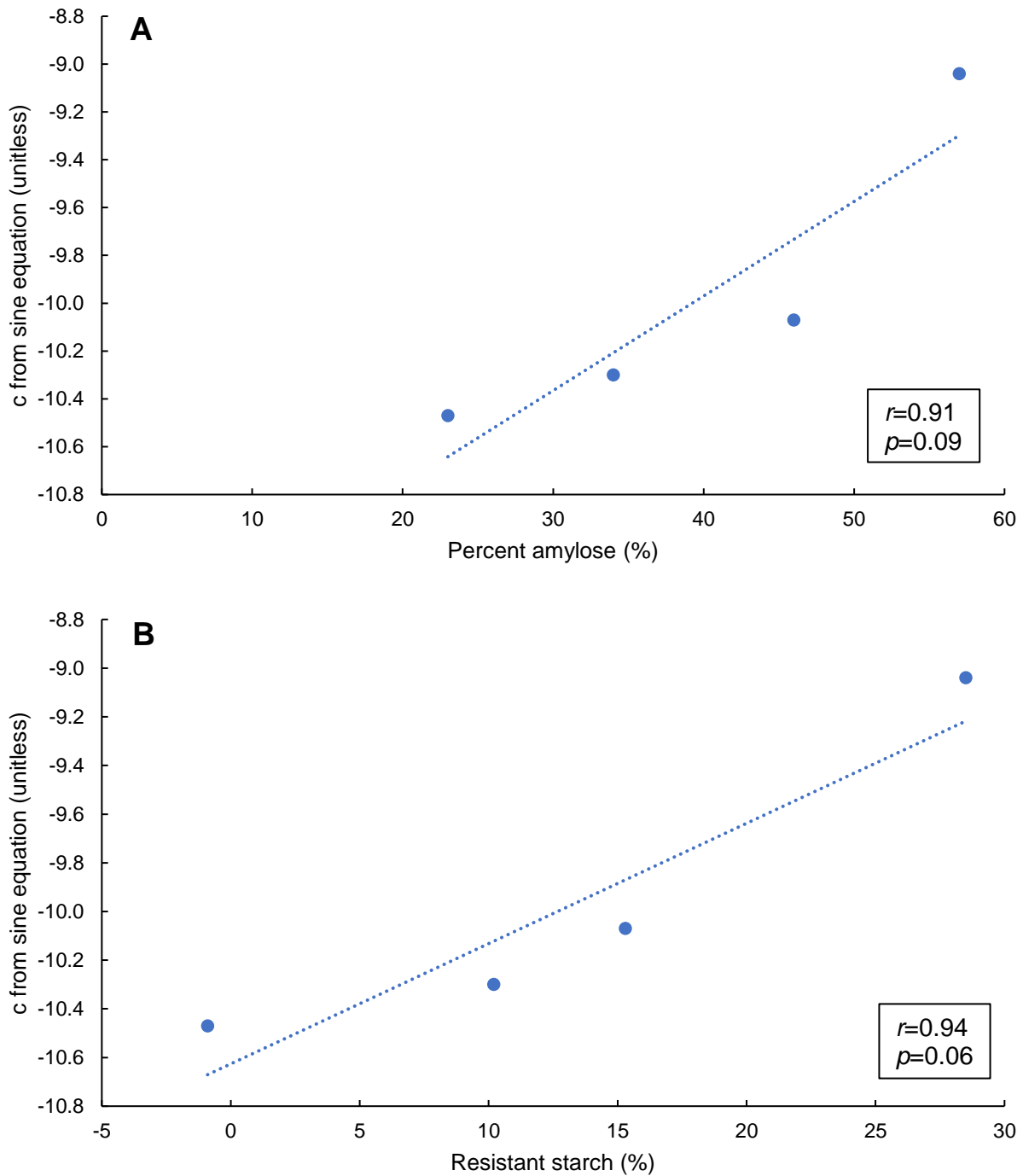


Figure 5.13 Relationships between carbohydrate components and  $c$  parameter values from sine equation curve fitting for null mice fed the Conventional starch diet, 53% Resistant starch diet, 35% Resistant starch diet, and 18% Resistant starch diet, all without the amyloglucosidase (AMG) supplement. Correlation between amylose percentage and  $c$  (A). Correlation between resistant starch amount and  $c$  (B). Correlation coefficients and  $p$ -values from linear regression are shown for both analyses.

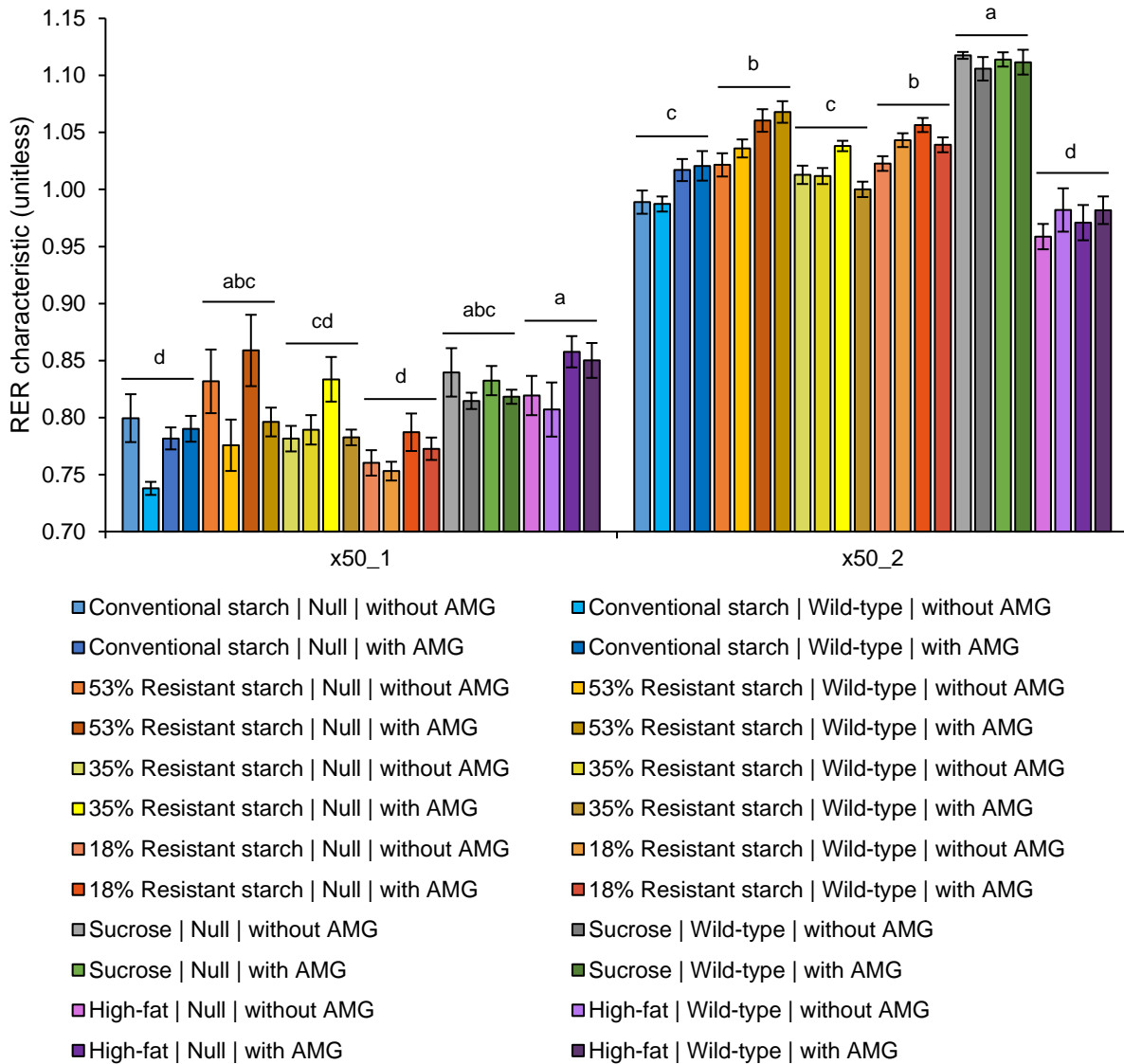


Figure 5.14 Median RER values from the bimodal PRCF distributions of RER modeled for individual mice using the Mixed Weibull Cumulative Distribution function.  $x_{50_1}$  represents the median RER for the first mode, while  $x_{50_2}$  represents the median RER for the second mode. Error bars indicate  $\pm$  standard error of the mean. Groups not sharing the same letters within each parameter are significantly different in main effect for diet ( $p < 0.05$ ). Statistically significant main effects for cycle (with vs. without AMG) and genotype (null vs. wild-type) were observed for the  $x_{50_1}$  parameter ( $p < 0.05$ ), and a statistically significant main effect for cycle (with vs. without AMG) was observed for the and  $x_{50_2}$  parameter ( $p < 0.05$ ). AMG, amyloglucosidase.

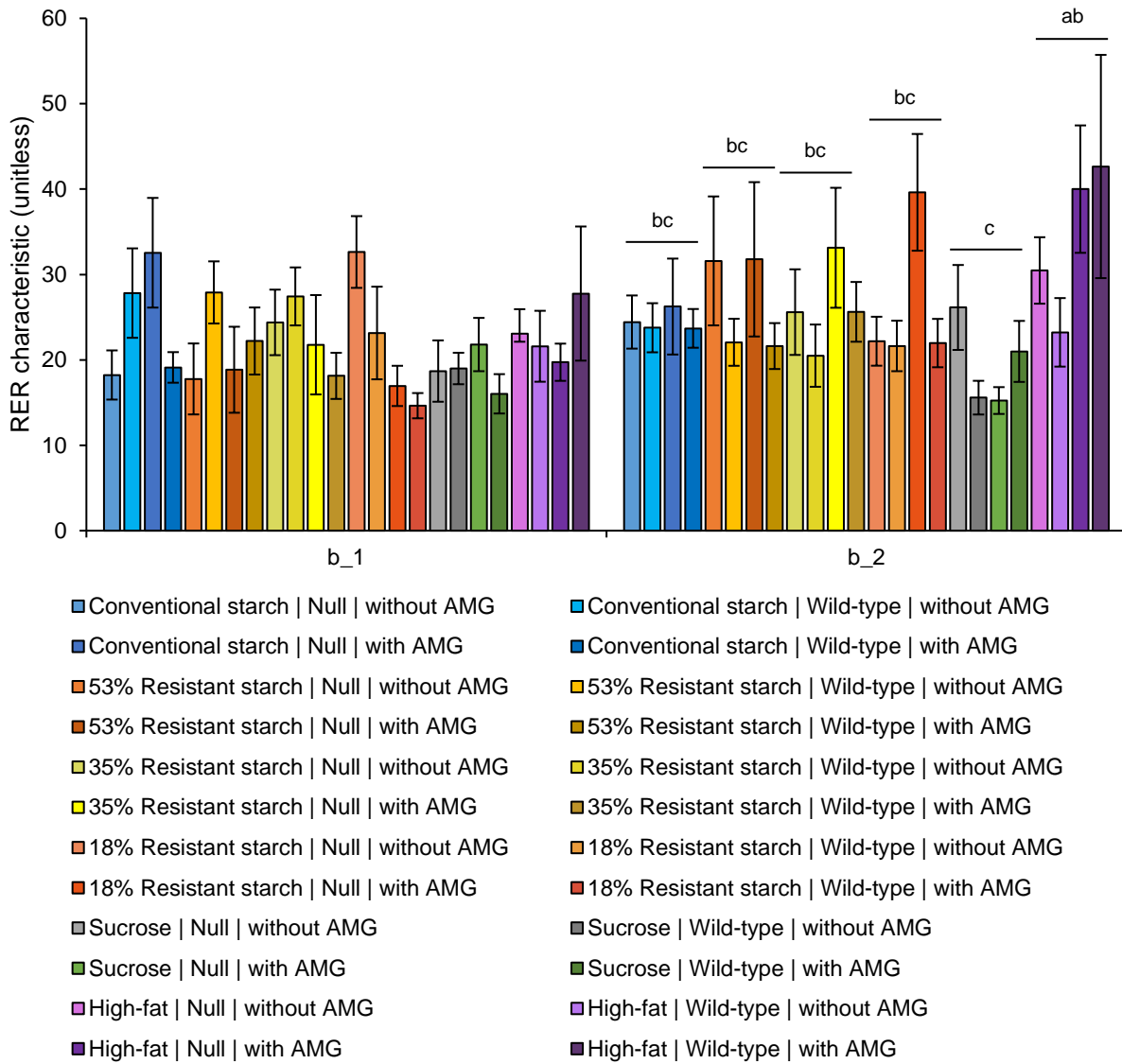


Figure 5.15 Distribution breadth constants (slopes) from the bimodal PRCF distributions of RER modeled for individual mice using the Mixed Weibull Cumulative Distribution function.  $b_1$  represents the median RER for the first mode, while  $b_2$  represents the median RER for the second mode. Error bars indicate  $\pm$  standard error of the mean. Groups not sharing the same letters within each parameter are significantly different in main effect for diet ( $p < 0.05$ ). Statistically significant main effects for cycle (with vs. without AMG) and genotype (null vs. wild-type) were observed for the  $b_2$  parameter ( $p < 0.05$ ). AMG, amyloglucosidase.

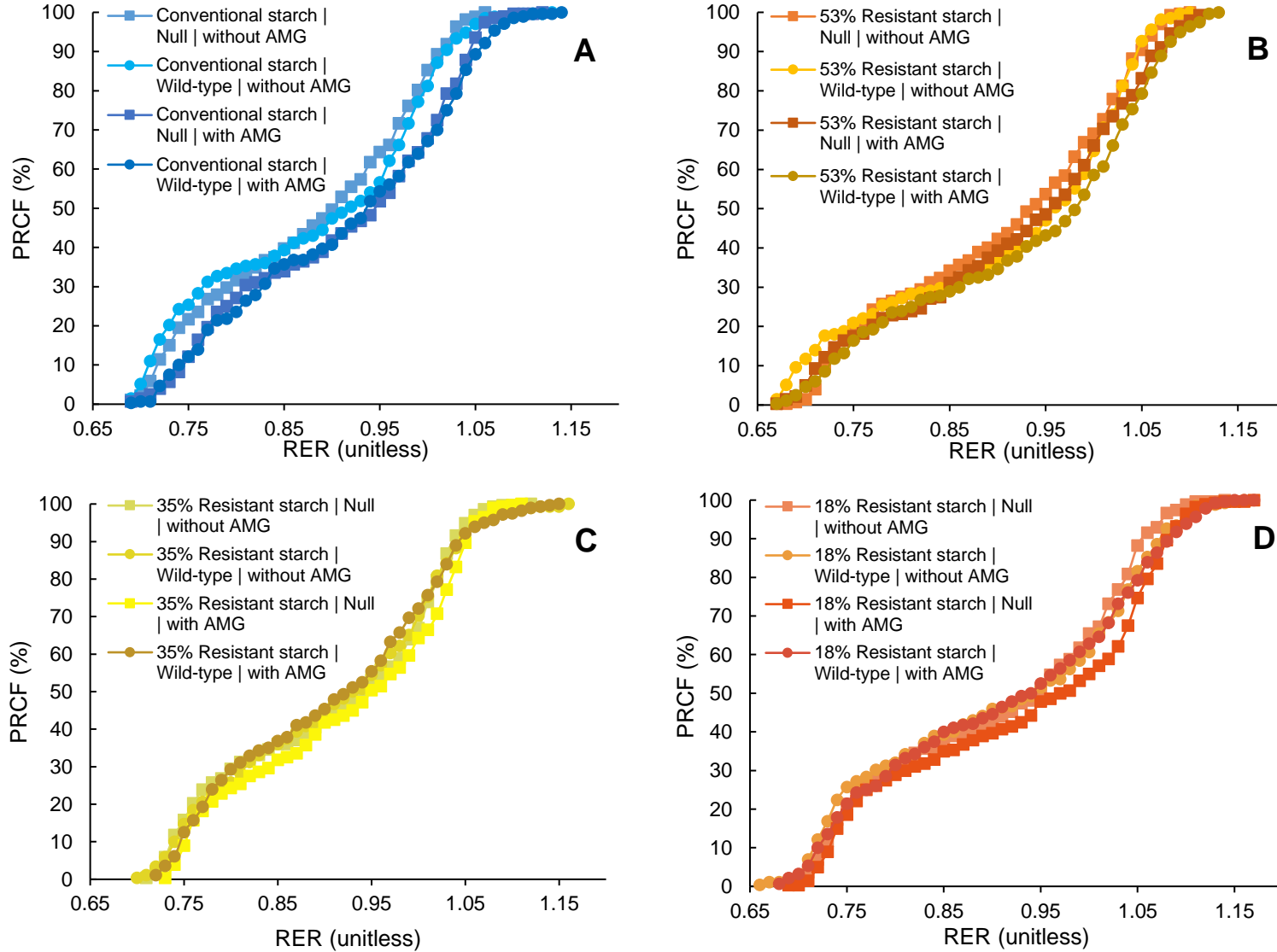


Figure 5.16 Percent relative cumulative frequency (PRCF) curves for pooled RER data from all mice per diet (diet × mouse genotype × cycle). Split per diet: Conventional starch (A), 53% Resistant starch (B), 35% Resistant starch (C), 18% Resistant starch (D).

Figure 5.16, continued.

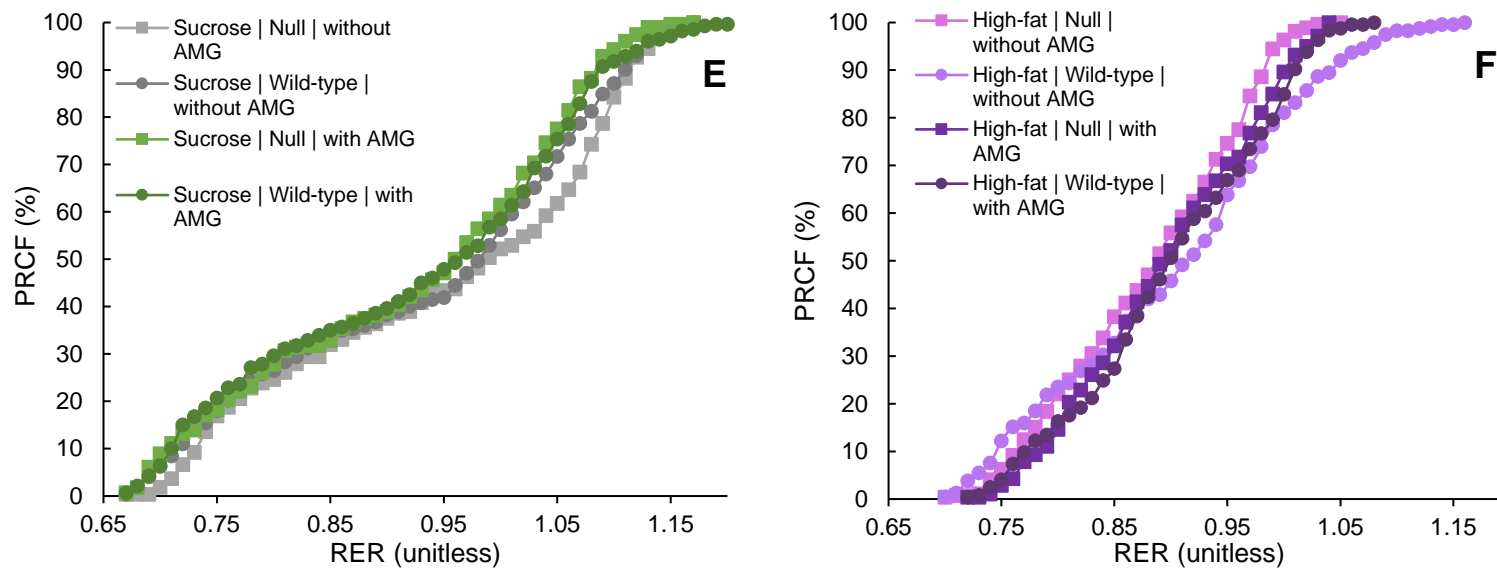


Figure 5.16 (continued). Percent relative cumulative frequency (PRCF) curves for pooled RER data from all mice per diet (diet × mouse genotype × cycle). Split per diet: Sucrose (E), High-fat (F). AMG, amyloglucosidase.

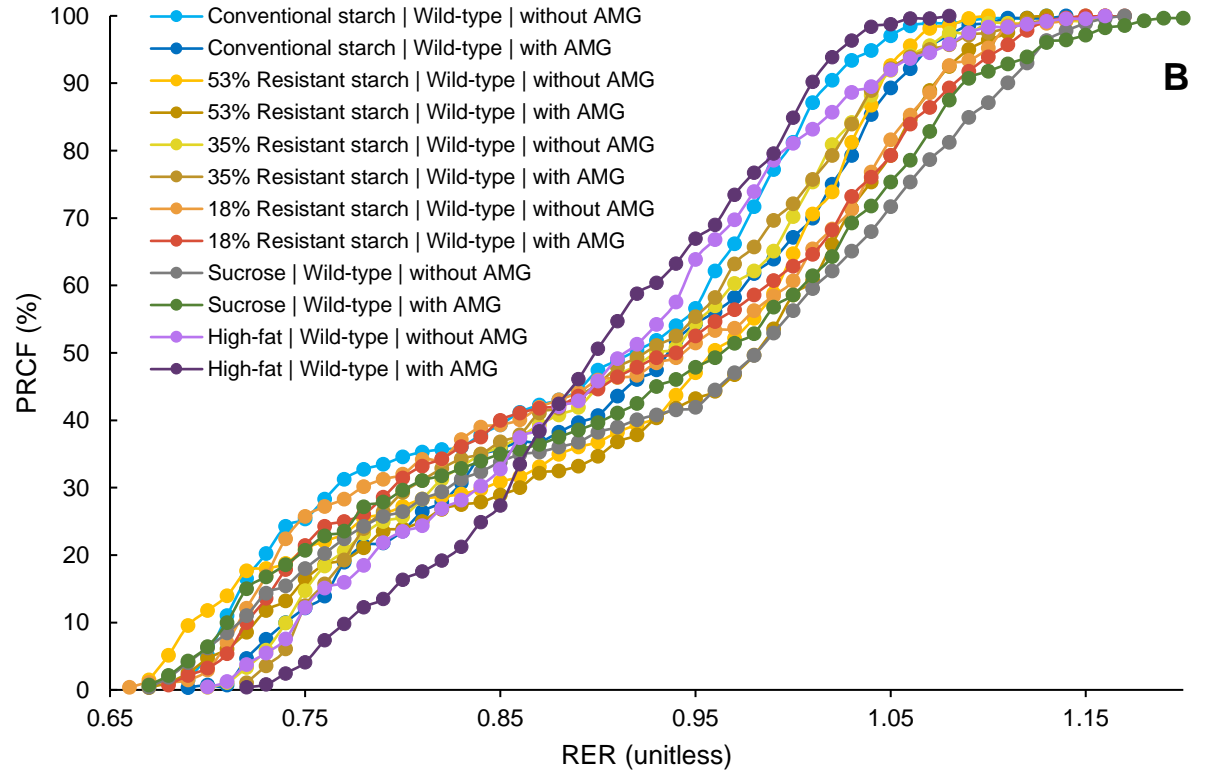
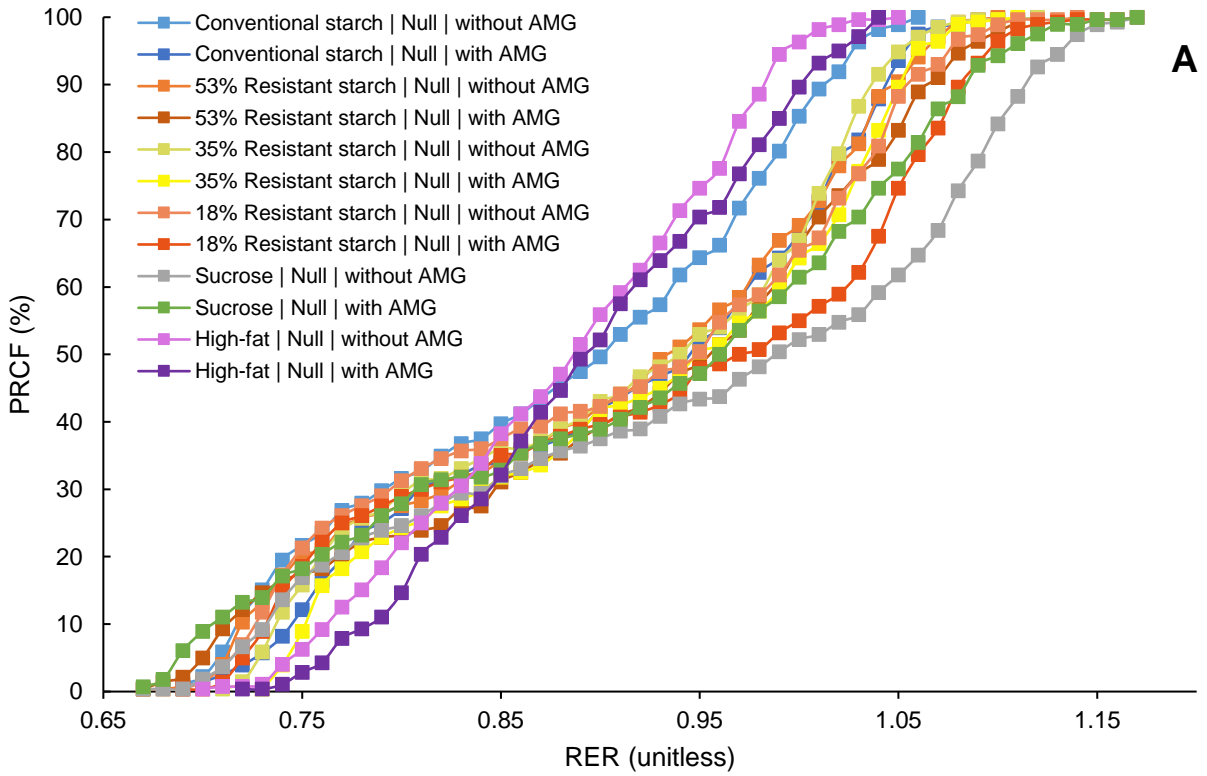


Figure 5.17 Percent relative cumulative frequency (PRCF) curves for pooled RER data from all mice per diet (diet × mouse genotype × cycle). Split by genotype: null (A), wild-type (B). AMG, amyloglucosidase.

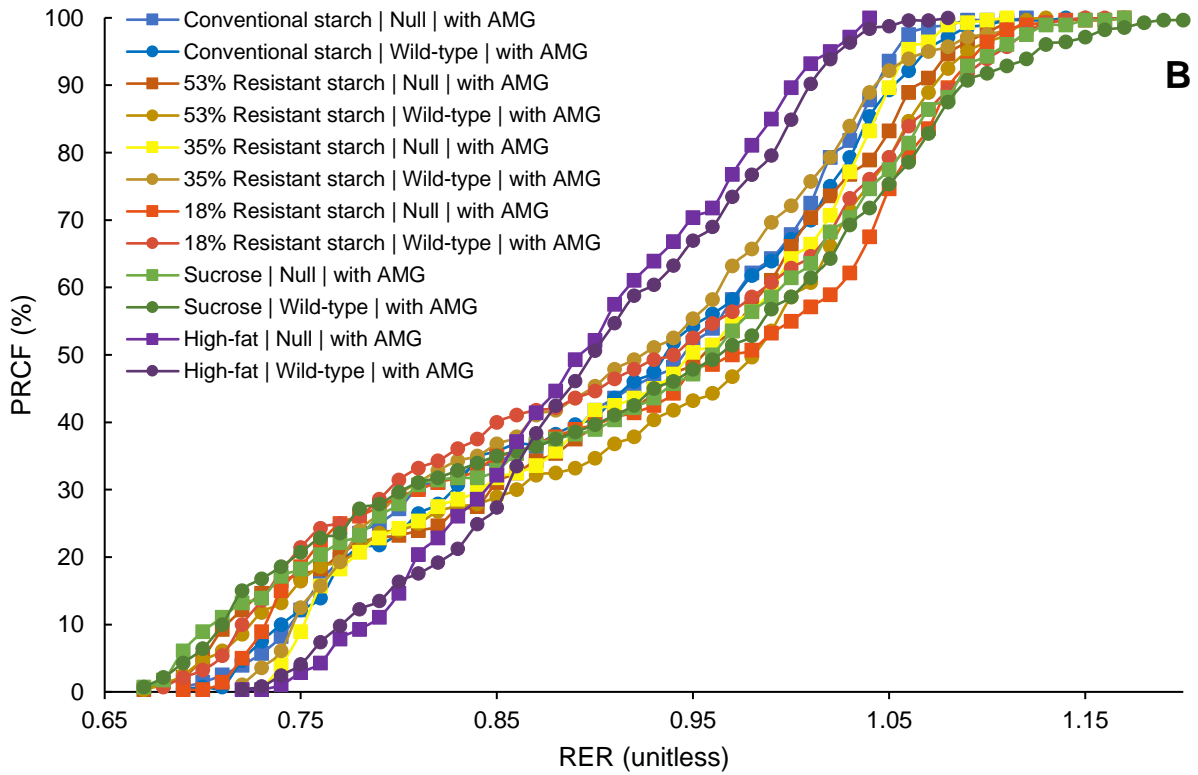
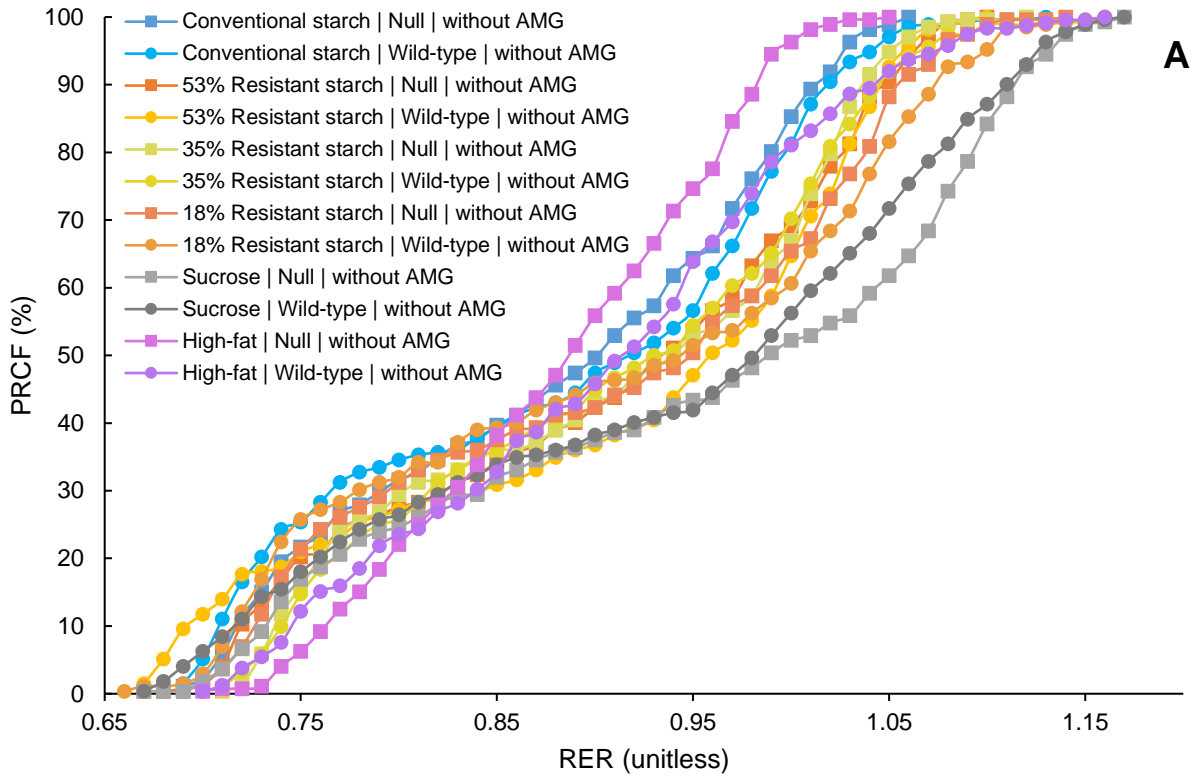


Figure 5.18 Percent relative cumulative frequency (PRCF) curves for pooled RER data from all mice per diet (diet  $\times$  mouse genotype  $\times$  cycle). Split by cycle: without AMG (A), with AMG (B). AMG, amyloglucosidase.

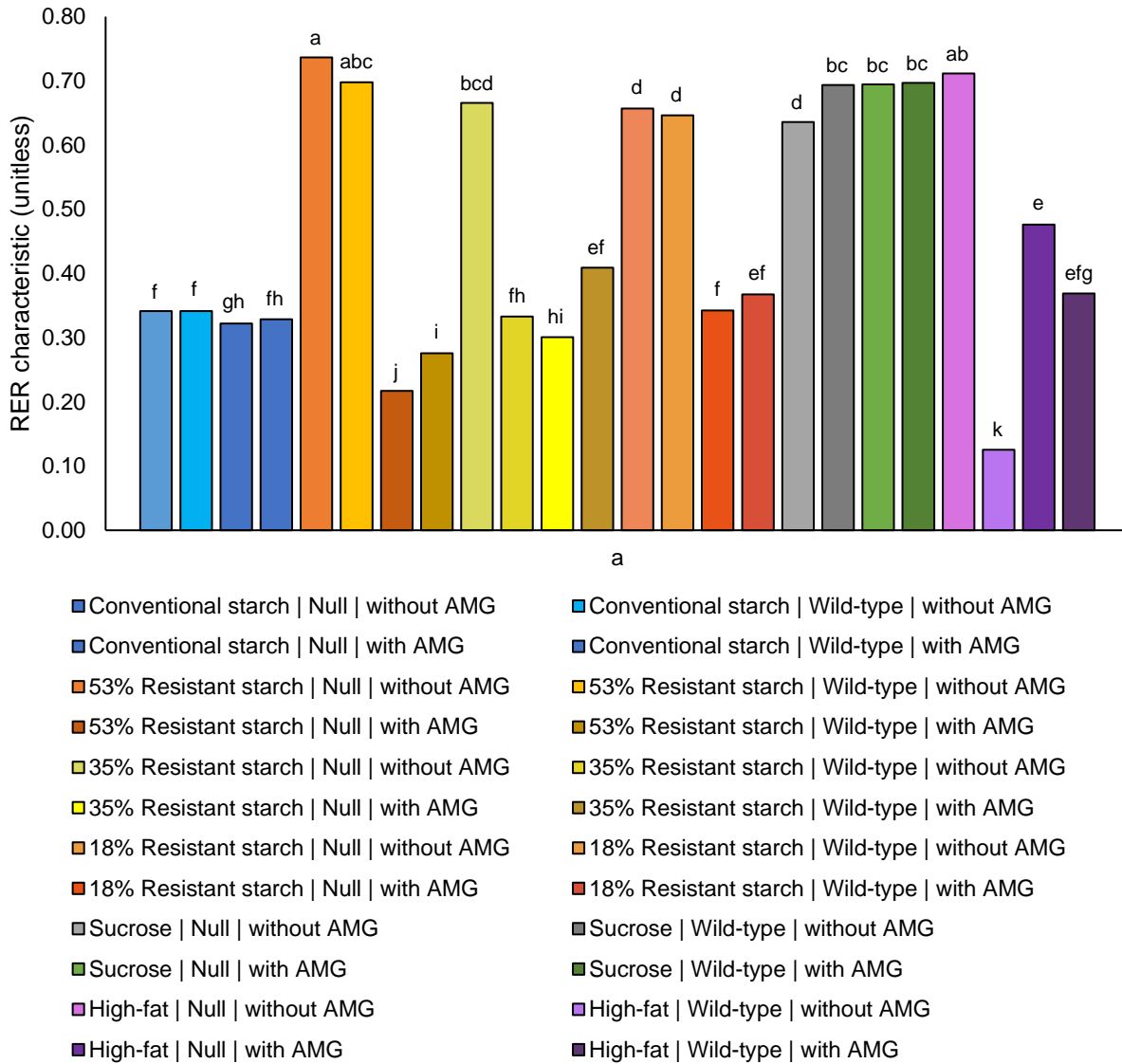


Figure 5.19 Median  $\alpha$  values from the bimodal PRCF distributions of RER modeled for pooled data from all mice using the Mixed Weibull Cumulative Distribution function. Error bars indicate  $\pm$  standard error of the mean. Groups not sharing the same letters within each parameter are significantly different ( $p < 0.05$ ). AMG, amyloglucosidase.

## CHAPTER 6. CONCLUSION

### 6.1 Summary and overall conclusions

Evidence indicating the potential benefits of some slowly digestible carbohydrates and moderated starch digestion on the control of food intake and body weight regulation is growing. However, the specific characteristics of digestible carbohydrates that give rise to such effects *in vivo* are incompletely understood. In this work, we have examined the physicochemical and *in vitro* digestive properties of pearl millet couscous compared to wheat couscous; the satiety effects, gastric emptying rate, and glycemic response of pearl millet-based foods compared to wheat couscous and white rice in humans; and substrate utilization for metabolism as well as metabolic flexibility of resistant starch (high-amylose corn starch) diets compared to conventional starch (raw corn starch), sucrose, and high-fat diets in mice. Summaries of these investigations and considerations for future work to further advance our understanding of slowly digestible carbohydrate-related enhancements in the regulation of food intake and body weight are described below.

The first experimental chapter, Chapter 3, examined how pearl millet couscous particles broke down in a simulated gastric environment compared to wheat couscous. Specific focus was placed on whether physicochemical properties of the couscous affected particle breakdown and starch hydrolysis in order to better understand the slow gastric emptying of pearl millet couscous in a Malian population. The particle size of flour starting material and initial couscous particle size was controlled. Our results showed that millet couscous broke down into small, more numerous particles than wheat couscous, regardless of initial controlled particle size, but millet couscous had a slower starch hydrolysis (digestion) property per unit surface area. From this investigation, we reason that the slow starch digestion property of pearl millet may enable it to activate the ileal brake and in turn delay gastric emptying, independent of its particle breakdown in the stomach. This work was published in *Food and Function* (Hayes, Swackhamer, et al., 2020).

The second experimental chapter, Chapter 4, investigated the subjective satiety, gastric emptying, and glycemic response of pearl millet-based foods compared to wheat couscous and white rice in a U.S. population. This complemented the previous trial in Mali (Cisse et al., 2018), by controlling flour and couscous particle sizes for the self-made treatments, comparing couscous

from two different grain sources (pearl millet and wheat), examining glycemic response, and testing effects in a U.S. population. An additional part of this investigation was the utilization of an advanced gastrointestinal digestion system to study if viscosity of these foods in the stomach was potentially affecting gastric emptying. Some of the results from this work were unexpected, as the pearl millet-based foods did not delay gastric emptying compared to white rice and wheat couscous. However, one type of pearl millet-based food (self-made millet couscous) promoted satiety and all millet-based foods (and wheat couscous) had lower glycemic response than white rice. We also found that viscosity in the simulated stomach was quite low and thus we propose, as in the previous study, that the slow digestion property of pearl millet is the cause of its benefits. The difference in gastric emptying between the U.S. and Malian populations requires further study, but we propose that there may be diet-induced changes affecting ileal brake and/or gut-brain axis signaling to alter how the body responds to slowly digestible carbohydrates. This work was published in *British Journal of Nutrition* (Hayes, Gozzi, et al., 2020).

The third experimental chapter, Chapter 5, focused on how altering carbohydrate digestion – through using mice lacking maltase-glucoamylase (versus wild-type), feeding diets with different levels of carbohydrate digestibility, and providing amyloglucosidase supplement – impacted the ability of the body to oxidize carbohydrate vs. fat for energy and to switch between using carbohydrate and fat (i.e. metabolic flexibility). This research ties more closely into whole-body energy metabolism and thus has implications for body weight regulation that are somewhat peripheral to the control of food intake. Regardless, they may have implications on deposition of adipose tissue (Sparks et al., 2009), insulin sensitivity (Malin et al., 2013), and even neuronal fuel use in the brain (Bernier et al., 2020; Reichenbach et al., 2018). In this investigation, we also devised and employed new approaches to assess metabolic flexibility using mathematical modeling of patterns in respiratory exchange ratio (i.e. substrate metabolism). Our results indicated that increasing carbohydrate digestion rate generally increased carbohydrate oxidation, but that moderated carbohydrate digestion promoted fat oxidation and metabolic flexibility. We propose that slow or moderated carbohydrate digestion may allow for a good balance between carbohydrate and fat oxidation that enhances metabolic flexibility. These findings expand our understanding of slowly digestible carbohydrates and reveal their potential advantages on substrate utilization by the body.

## 6.2 Future directions

Establishing a better understanding of the potential benefits of slowly digestible carbohydrates is no easy endeavor. Studies that are carefully designed to control for different carbohydrate factors can help advance our efforts in this area.

Our findings from Chapter 3 indicate the slow gastric emptying rate of pearl millet couscous observed in Mali (Cisse et al., 2018) is unlikely to be due to the resistance of particle breakdown in the stomach. Instead, our evidence suggests pearl millet has a slow digestion property which may be related to its content of amylose with an intermediate chain length. However, starch fine structural properties, intact cellular structure, or the phenolic content of pearl millet may also be contributing factors, and thus this warrants further exploration. This study did reveal that millet couscous types with different initial particle sizes broke down into particles of similar size during gastric simulation, which informed the design of our subsequent human study. Additional research pursuits to identify physicochemical characteristics of slowly digestible carbohydrates with established *in vivo* benefits (i.e. ability to trigger the ileal brake or gut-brain axis) would be worthwhile, for these characteristics could then be used to design carbohydrates with similar desirable effects.

The results from Chapter 4 perhaps complicate our understanding of the ability of slowly digestible carbohydrates to trigger the ileal brake and perhaps also the gut-brain axis, as pearl millet-based foods did not delay gastric emptying rate in the U.S. population tested, as we had shown that they did in a Malian cohort. Despite the lack of difference in gastric emptying, the self-made millet couscous had lower hunger ratings and higher fullness ratings, and all the pearl millet-based foods (as well as the wheat couscous) had lower glycemic response than white rice. We observed that the overall gastric half-emptying times for the foods in our study was approximately 3 h, which is similar to the half-emptying times observed for white rice, boiled potatoes, and well-cooked pasta in the Mali study (Cisse et al., 2018). Because we reason that the Malian population generally consumes pearl millet-based foods on a regular basis while the U.S. population does not, we hypothesize that there could be diet-induced changes in enteroendocrine L-cell signaling to affect the gut-brain axis and ileal brake that alter the sensitivity of the body to respond to slowly digestible carbohydrates. Adaptation of small intestinal L-cells may be one potential mechanism for these changes. One way to test this hypothesis would be to compare gastric emptying rates, appetitive responses, and glycemic responses following prolonged consumption of a slowly

digestible carbohydrate compared to a rapidly digestible carbohydrate in a Malian population. Additional studies in mice could help reveal the mechanism(s) for these proposed changes (e.g. L-cells, hormones, neuronal signaling). A further insight gained from this investigation was that viscosity did not appear to impact the gastric emptying of pearl millet couscous. Mechanistic work in mice to evaluate mechanoreceptor activation during gastric emptying of highly viscous foods such as pearl millet thick porridge may provide additional clarification on this topic.

In the experiments of Chapter 5, we discovered that higher carbohydrate digestion increased carbohydrate oxidation, which seems logical, but this in turn decreased fat oxidation, which may not be most ideal for metabolism. Furthermore, our evidence suggested that moderated carbohydrate digestion, such as the use of slowly digestible carbohydrate, increased fat oxidation and increased metabolic flexibility. Because previous work on metabolic flexibility has largely focused on its connection with conditions such as type 2 diabetes, exercise, and energy use directed by brain neurons, among others, there appears to be great potential to further study the connection between metabolic flexibility and diets with different degrees of carbohydrate digestion. In our study, we focused more specifically on raw corn starch (slowly digestible starch) and high-amylose corn starch (resistant starch), leaving comparisons between rapidly digestible and slowly digestible carbohydrates for further exploration. It may also be beneficial to measure insulin sensitivity and body weight change after longer periods of diet exposure and to relate them back to metabolic flexibility using the approaches we proposed, as this would more directly connect the outcomes to disease. It is also worthy to note that future experiments in this area should include measurements of food intake and activity level while the animals are housed within the indirect calorimetry chambers. A further area of study is to examine how altering carbohydrate digestion affects the toggling between substrate oxidation and fermentation in mice, which is especially relevant for resistant starches such as the one we used. A sophisticated system has been developed that would be a beneficial tool for such investigations (Fernández-Calleja et al., 2018).

With highly complex, multi-faceted challenges such as obesity in our midst, the need for multidisciplinary approaches to overcome such obstacles becomes increasingly apparent. In this dissertation work, we utilized *in vitro*, *in vivo*, and modeling approaches to make strides to better understand how carbohydrates with slow digestion may promote targeted effects on the body, ranging from gastric emptying to postprandial glycemia to metabolism. However, there are numerous other disciplines that may eventually be integrated with future pursuits in this area in

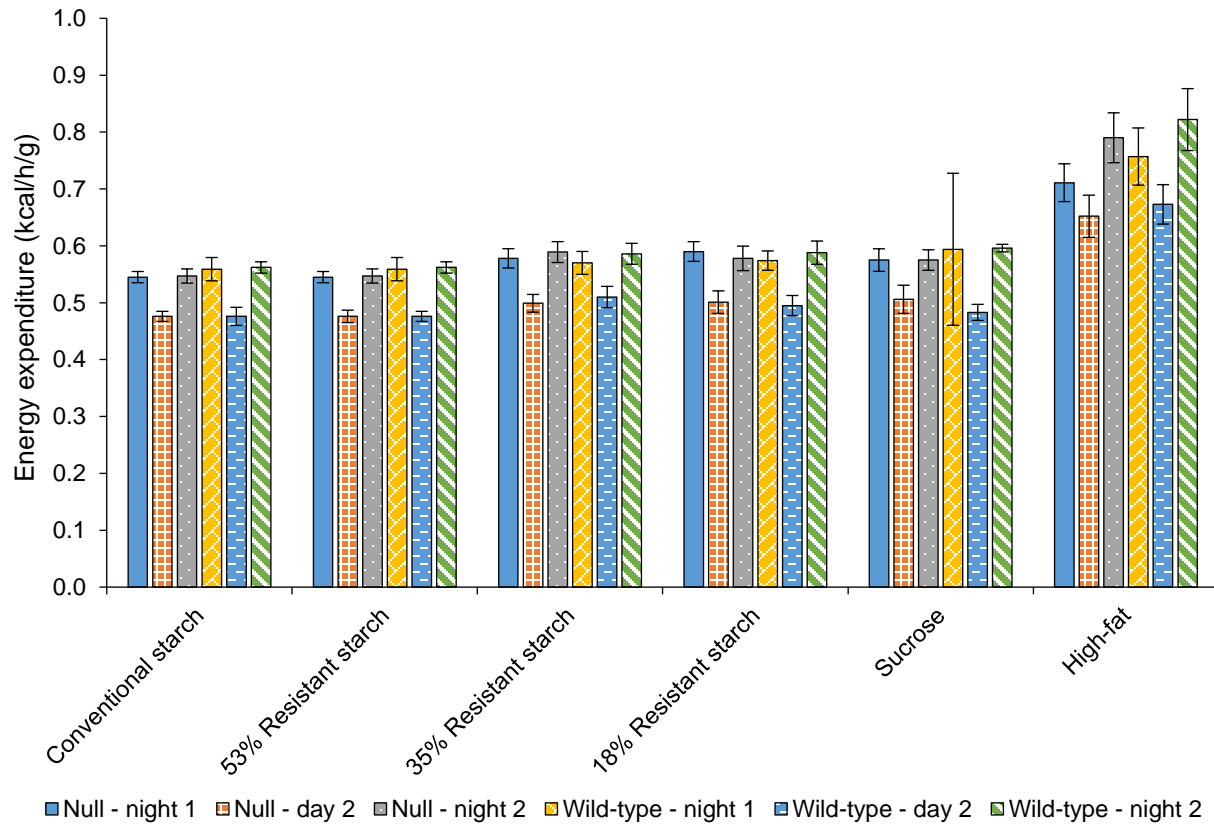
order to generate a more comprehensive understanding of the functions of slowly digestible carbohydrates, such as neuroscience, endocrinology, and gastroenterology. This is especially important for studying the control of food intake, as the circumstances surrounding food consumption involve reward, memory (Suarez et al., 2020; Zheng et al., 2009), and cultural practices/societal norms (Bu & Go, 2008; Syrjälä et al., 2017) along with homeostatic signaling (Beutler et al., 2017; Morton et al., 2006) to control eating. Much work remains to be done in connecting fundamental food characteristics to these areas.

### 6.3 References

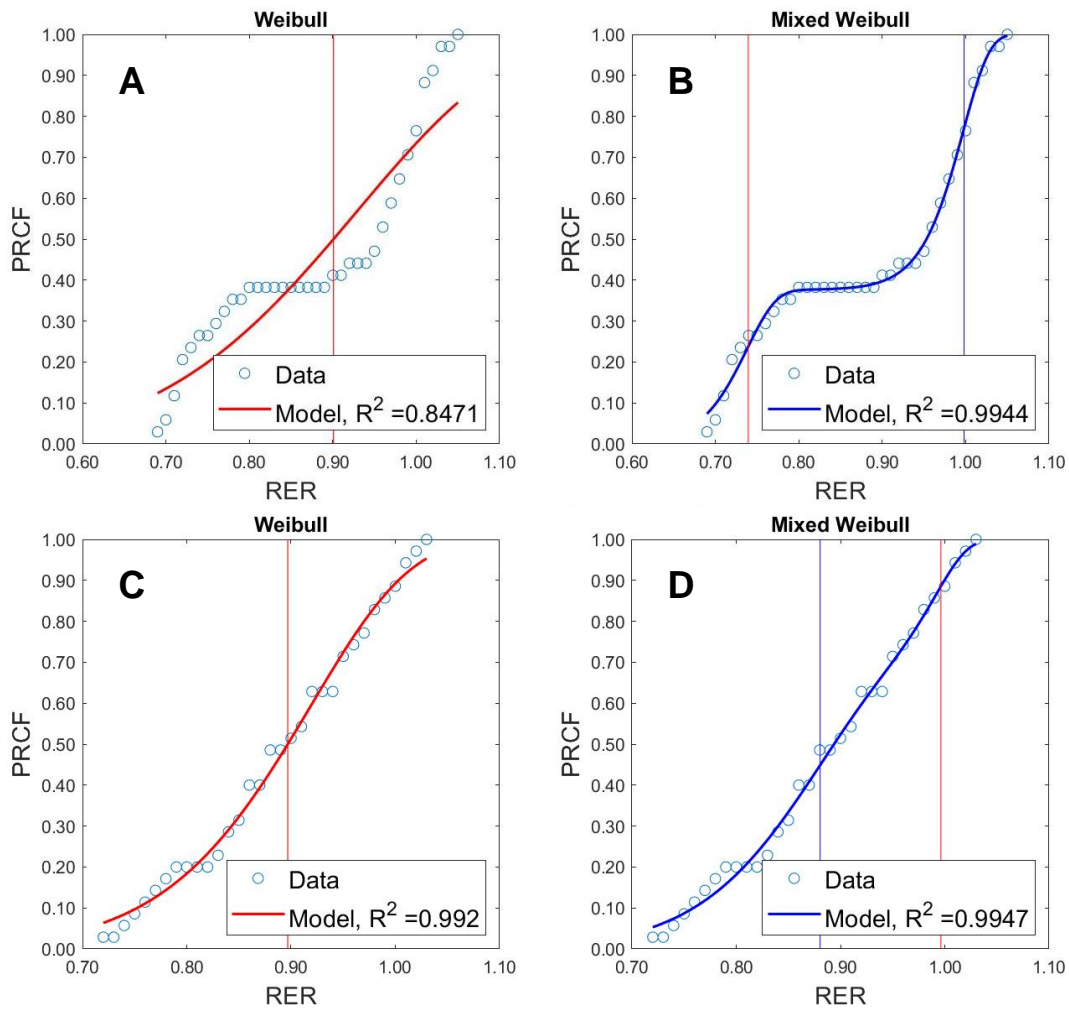
- Bernier, L. P., York, E. M., Kamyabi, A., Choi, H. B., Weiling, N. L., & MacVicar, B. A. (2020). Microglial metabolic flexibility supports immune surveillance of the brain parenchyma. *Nature Communications*, *11*(1). <https://doi.org/10.1038/s41467-020-15267-z>
- Beutler, L. R., Chen, Y., Ahn, J. S., Lin, Y.-C., Essner, R. A., & Knight, Z. A. (2017). Dynamics of Gut-Brain Communication Underlying Hunger. *Neuron*, *96*(2), 461-475.e5. <https://doi.org/10.1016/j.neuron.2017.09.043>
- Bu, O. B., & Go, A. S. (2008). Perceived trustworthiness of online shops. *Journal of Consumer Behaviour*, *50*(October), 35–50. <https://doi.org/10.1002/cb>
- Cisse, F., Erickson, D. P., Hayes, A. M. R., Opekun, A. R., Nichols, B. L., & Hamaker, B. R. (2018). Traditional Malian solid foods made from sorghum and millet have markedly slower gastric emptying than rice, potato, or pasta. *Nutrients*, *10*(2), 124. <https://doi.org/10.3390/nu10020124>
- Fernández-Calleja, J. M. S., Konstanti, P., Swarts, H. J. M., Bouwman, L. M. S., Garcia-Campayo, V., Billecke, N., Oosting, A., Smidt, H., Keijer, J., & van Schothorst, E. M. (2018). Non-invasive continuous real-time in vivo analysis of microbial hydrogen production shows adaptation to fermentable carbohydrates in mice. *Scientific Reports*, *8*(1), 15351. <https://doi.org/10.1038/s41598-018-33619-0>
- Hayes, A. M. R., Gozzi, F., Diatta, A., Gorissen, T., Swackhamer, C., Bellmann, S., & Hamaker, B. R. (2020). Some pearl millet-based foods promote satiety or reduce glycaemic response in a crossover trial. *British Journal of Nutrition*, 1–31. <https://doi.org/10.1017/S0007114520005036>
- Hayes, A. M. R., Swackhamer, C., Mennah-Govela, Y. A., Martinez, M. M., Diatta, A., Bornhorst, G. M., & Hamaker, B. R. (2020). Pearl millet (*Pennisetum glaucum*) couscous breaks down faster than wheat couscous in the Human Gastric Simulator, though has slower starch hydrolysis. *Food & Function*, *11*(1), 111–122. <https://doi.org/10.1039/C9FO01461F>
- Malin, S. K., Haus, J. M., Solomon, T. P. J., Blaszcak, A., Kashyap, S. R., & Kirwan, J. P. (2013). Insulin sensitivity and metabolic flexibility following exercise training among different obese insulin-resistant phenotypes. *American Journal of Physiology-Endocrinology and Metabolism*, *305*(10), E1292–E1298. <https://doi.org/10.1152/ajpendo.00441.2013>
- Morton, G. J., Cummings, D. E., Baskin, D. G., Barsh, G. S., & Schwartz, M. W. (2006). Central nervous system control of food intake and body weight. *Nature*, *443*(7109), 289–295. <https://doi.org/10.1038/nature05026>

- Reichenbach, A., Stark, R., Mequinion, M., Denis, R. R. G., Goularte, J. F., Clarke, R. E., Lockie, S. H., Lemus, M. B., Kowalski, G. M., Bruce, C. R., Huang, C., Schittenhelm, R. B., Mynatt, R. L., Oldfield, B. J., Watt, M. J., Luquet, S., & Andrews, Z. B. (2018). AgRP Neurons Require Carnitine Acetyltransferase to Regulate Metabolic Flexibility and Peripheral Nutrient Partitioning. *Cell Reports*, 22(7), 1745–1759. <https://doi.org/10.1016/j.celrep.2018.01.067>
- Sparks, L. M., Ukropcova, B., Smith, J., Pasarica, M., Hymel, D., Xie, H., Bray, G. A., Miles, J. M., & Smith, S. R. (2009). Relation of adipose tissue to metabolic flexibility. *Diabetes Research and Clinical Practice*, 83(1), 32–43. <https://doi.org/10.1016/j.diabres.2008.09.052>
- Suarez, A. N., Liu, C. M., Cortella, A. M., Noble, E. E., & Kanoski, S. E. (2020). Ghrelin and Orexin Interact to Increase Meal Size Through a Descending Hippocampus to Hindbrain Signaling Pathway. *Biological Psychiatry*, 87(11), 1001–1011. <https://doi.org/10.1016/j.biopsych.2019.10.012>
- Syrjälä, H., Luomala, H. T., & Autio, M. (2017). Fluidity of places in everyday food consumption: Introducing snackscapes. *International Journal of Consumer Studies*, 41(6), 761–768. <https://doi.org/10.1111/ijcs.12389>
- Zheng, H., Lenard, N. R., Shin, A. C., & Berthoud, H. R. (2009). Appetite control and energy balance regulation in the modern world: Reward-driven brain overrides repletion signals. *International Journal of Obesity*, 33(S2), S8–S13. <https://doi.org/10.1038/ijo.2009.65>

## APPENDIX A. SUPPLEMENTARY MATERIALS

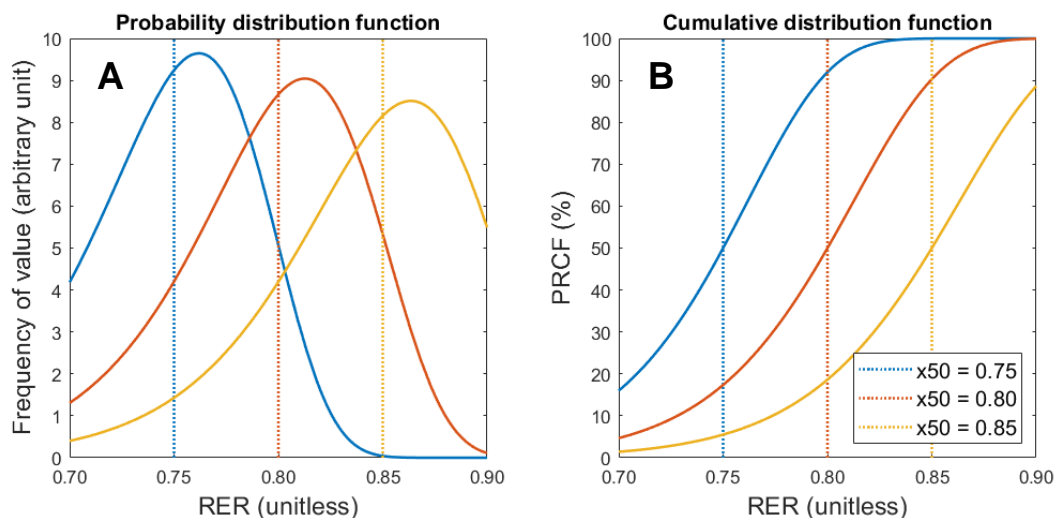


Supplementary Figure A.1 Energy expenditure split by 12-h periods (day/night) for null and wild-type mice fed 6 different diets ( $n=8$  each group). Error bars represent  $\pm$  standard error of the mean (SEM).



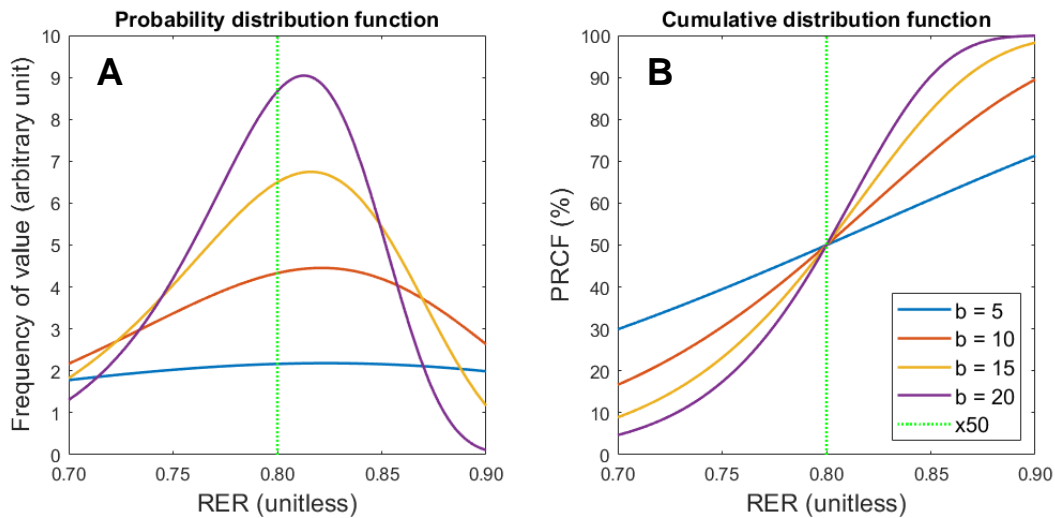
Supplementary Figure A.2 Examples of model curves for percent relative cumulative frequency (PRCF) of respiratory exchange ratio (RER) for individual mice. Example 1 (A and B): Weibull Cumulative Distribution function curve fit (A) and Mixed Weibull Cumulative Distribution function curve fit (B) for data from a wild-type mouse consuming the Conventional starch diet without amyloglucosidase; in this scenario, the Mixed Weibull Cumulative Distribution function (more complex model) had a better fit because the F ratio was less than 0.0001, and the  $R^2$  was greatly improved using this model (0.847 for Weibull vs. 0.994 for Mixed Weibull). Example 2 (C and D): Weibull Cumulative Distribution function curve fit (C) and Mixed Weibull Cumulative Distribution function curve fit (D) for data from a wild-type mouse consuming the High-fat diet with amyloglucosidase; in this scenario, the Weibull Cumulative Distribution function (simpler model) was had a better fit because the F ratio was greater than 0.0001, and the  $R^2$  was very similar between the two models (0.992 for Weibull vs. 0.995 for Mixed Weibull). Vertical red lines in A and C represent  $x_{50}$  (median RER). Vertical red and blue lines in B and D represent  $x_{50,1}$  and  $x_{50,2}$  (median RER values for the two “modes”), respectively. Note that the PRCF values on the y-axis have been divided by 100 so that they range from 0 to 1 instead of 0 to 100. PRCF, percent relative cumulative frequency; RER, respiratory exchange ratio.

Weibull: different  $x_{50}$  but the same  $b$

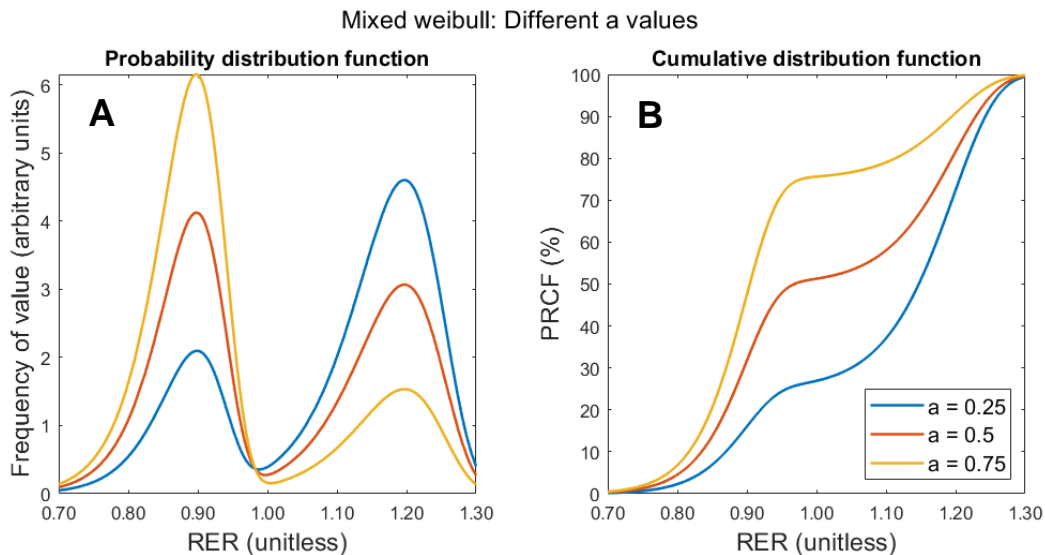


Supplementary Figure A.3 Weibull parameter exploration for percent relative cumulative frequency (PRCF) analysis of respiratory exchange ratio (RER): different  $x_{50}$  but the same  $b$ . Probability distribution function indicating theoretical non-cumulative distributions of data with three different  $x_{50}$  values (A). Cumulative distribution function [Weibull Cumulative Distribution function] for the same  $x_{50}$  values (B). Smooth curves indicate curves of distribution. Dotted lines indicate  $x_{50}$  RER values, which are the median RER values of the respective distributions. As shown in the figure, greater  $x_{50}$  shifts the curve to the right, indicating higher RER. au, arbitrary unit; PRCF, percent relative cumulative frequency; RER, respiratory exchange ratio.

Weibull: same  $x_{50}$  but different  $b$

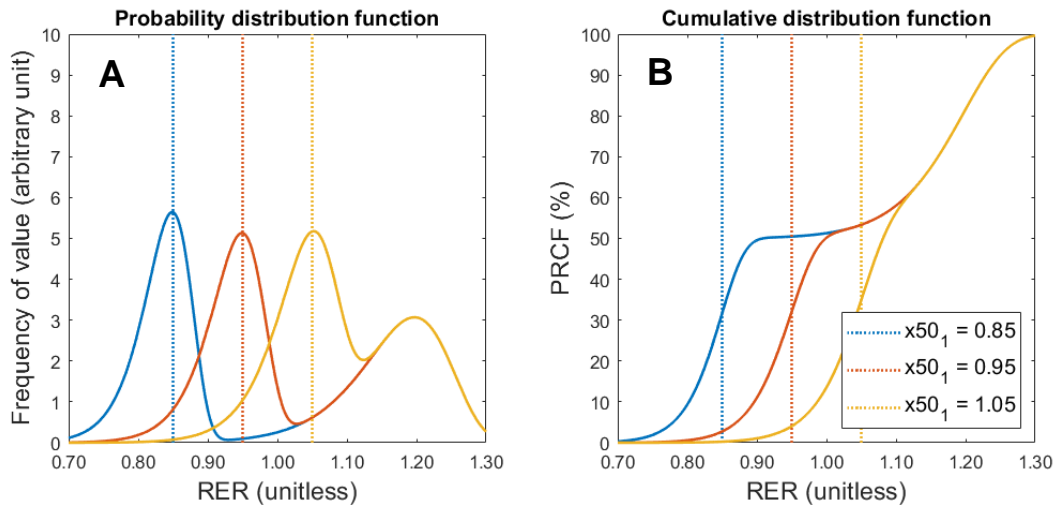


Supplementary Figure A.4 Weibull parameter exploration for percent relative cumulative frequency (PRCF) analysis of respiratory exchange ratio (RER): different  $b$  but the same  $x_{50}$ . Probability distribution function indicating theoretical non-cumulative distributions of data with three different  $b$  values (A). Cumulative distribution function [Weibull Cumulative Distribution function] for the same  $b$  values (B). Smooth curves indicate curves of distribution. Dotted green line indicates  $x_{50}$  RER value, which is the median RER and is the same each distribution because each has the same  $x_{50}$ . As shown in the figure, greater  $b$  causes the curves to be steeper for a narrower region, indicating a greater proportion of RER values fall within the selected narrowing range (narrower spread). au, arbitrary unit; PRCF, percent relative cumulative frequency; RER, respiratory exchange ratio.



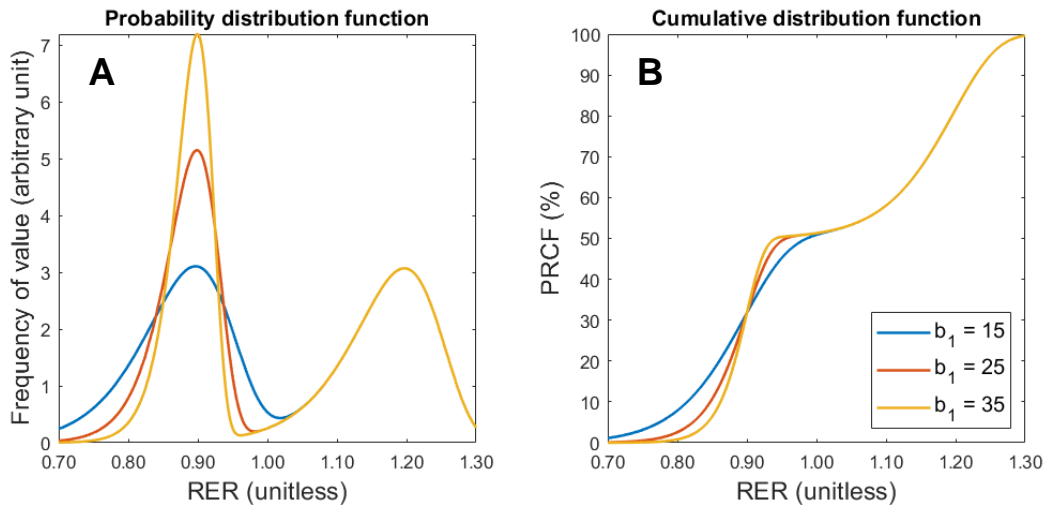
Supplementary Figure A.5 Mixed Weibull parameter exploration for percent relative cumulative frequency (PRCF) analysis of respiratory exchange ratio (RER): different  $\alpha$  but the same  $x_{50,1}$ ,  $x_{50,2}$ ,  $b_1$ , and  $b_2$ . Probability distribution function indicating theoretical non-cumulative distributions of data with three different  $\alpha$  values (A). Cumulative distribution function [Mixed Weibull Cumulative Distribution function] for the same  $\alpha$  values (B). Smooth curves indicate curves of distribution. Note that the Mixed Weibull can be used for a bimodal distribution, while the Weibull (normal, non-mixed version) is more suitable for a unimodal distribution. Related to RER, the first mode represents fat oxidation and the second mode represents carbohydrate oxidation. As shown in the figure, greater  $\alpha$  causes a greater proportion of the distribution to be allocated to the first mode and consequently a lesser proportion of the distribution constitutes the second mode. In practical terms, this means a greater  $\alpha$  shifts RER toward increased fat oxidation. au, arbitrary unit; PRCF, percent relative cumulative frequency; RER, respiratory exchange ratio.

Mixed weibull: Different  $x_{50_1}$  values



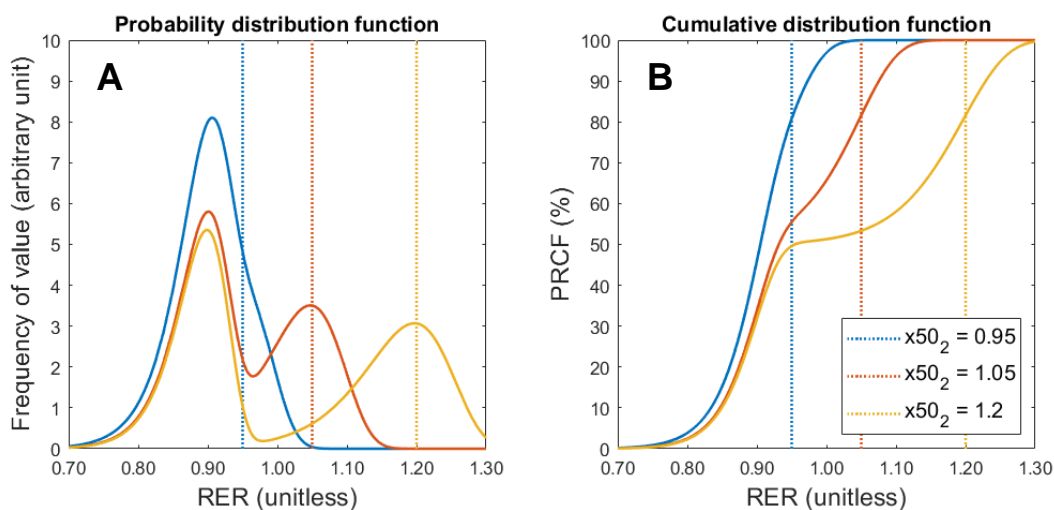
Supplementary Figure A.6 Mixed Weibull parameter exploration for percent relative cumulative frequency (PRCF) analysis of respiratory exchange ratio (RER): different  $x_{50_1}$  but the same  $\alpha$ ,  $x_{50_2}$ ,  $b_1$ , and  $b_2$ . Probability distribution function indicating theoretical non-cumulative distributions of data with three different  $x_{50_1}$  values (A). Cumulative distribution function [Mixed Weibull Cumulative Distribution function] for the same  $x_{50_1}$  values (B). Smooth curves indicate curves of distribution. Dotted lines indicate  $x_{50_1}$  RER values, which are the median RER values of the respective distributions. Note that the Mixed Weibull can be used for a bimodal distribution, while the Weibull (normal, non-mixed version) is more suitable for a unimodal distribution. Related to RER, the first mode represents fat oxidation and the second mode represents carbohydrate oxidation. As shown in the figure, greater  $x_{50_1}$  shifts the curve representing the first mode to the right, which signifies a higher median RER value in the fat oxidation mode. au, arbitrary unit; PRCF, percent relative cumulative frequency; RER, respiratory exchange ratio.

Mixed weibull: Different  $b_1$  values



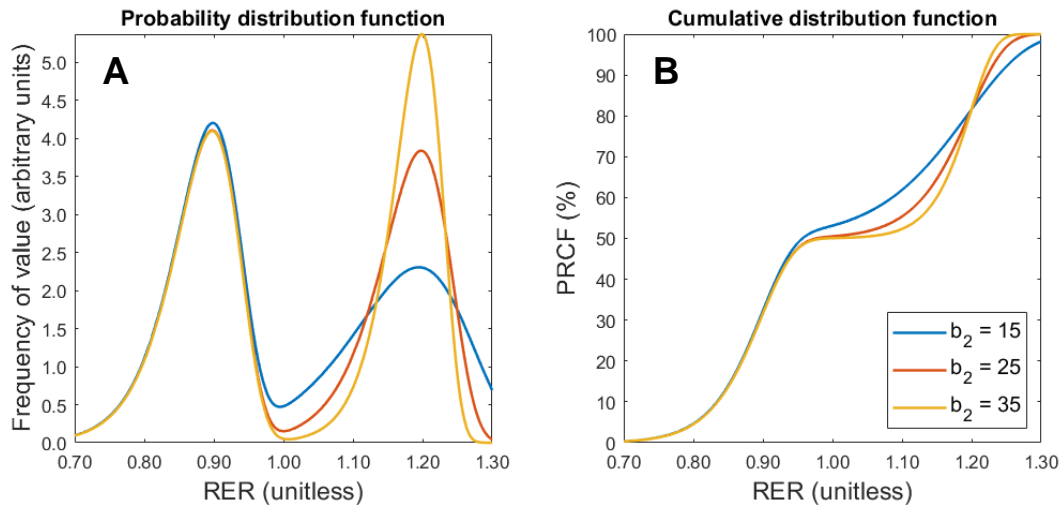
Supplementary Figure A.7 Mixed Weibull parameter exploration for percent relative cumulative frequency (PRCF) analysis of respiratory exchange ratio (RER): different  $b_1$  but the same  $\alpha$ ,  $x_{50,1}$ ,  $x_{50,2}$ , and  $b_2$ . Probability distribution function indicating theoretical non-cumulative distributions of data with three different  $b_1$  values (A). Cumulative distribution function [Mixed Weibull Cumulative Distribution function] for the same  $b_1$  values (B). Smooth curves indicate curves of distribution. Note that the Mixed Weibull can be used for a bimodal distribution, while the Weibull (normal, non-mixed version) is more suitable for a unimodal distribution. Related to RER, the first mode represents fat oxidation and the second mode represents carbohydrate oxidation. As shown in the figure, greater  $b_1$  steepens the curve representing the first mode, which signifies a smaller spread of RER values in the fat oxidation mode. We interpret this to suggest more efficient switching to fat oxidation and thus enhanced metabolic flexibility. au, arbitrary unit; PRCF, percent relative cumulative frequency; RER, respiratory exchange ratio.

Mixed weibull: Different  $x_{50_2}$  values



Supplementary Figure A.8 Mixed Weibull parameter exploration for percent relative cumulative frequency (PRCF) analysis of respiratory exchange ratio (RER): different  $x_{50_2}$  but the same  $\alpha$ ,  $x_{50_1}$ ,  $b_1$ , and  $b_2$ . Probability distribution function indicating theoretical non-cumulative distributions of data with three different  $x_{50_2}$  values (A). Cumulative distribution function [Mixed Weibull Cumulative Distribution function] for the same  $x_{50_2}$  values (B). Smooth curves indicate curves of distribution. Dotted lines indicate  $x_{50_2}$  RER values, which are the median RER values of the respective distributions. Note that the Mixed Weibull can be used for a bimodal distribution, while the Weibull (normal, non-mixed version) is more suitable for a unimodal distribution. Related to RER, the first mode represents fat oxidation and the second mode represents carbohydrate oxidation. As shown in the figure, greater  $x_{50_2}$  shifts the curve representing the second mode to the right, which signifies a higher median RER value in the carbohydrate oxidation mode. au, arbitrary unit; PRCF, percent relative cumulative frequency; RER, respiratory exchange ratio.

Mixed weibull: Different  $b_2$  values



Supplementary Figure A.9 Mixed Weibull parameter exploration for percent relative cumulative frequency (PRCF) analysis of respiratory exchange ratio (RER): different  $b_2$  but the same  $\alpha$ ,  $x_{50_1}$ ,  $x_{50_2}$ , and  $b_1$ . Probability distribution function indicating theoretical non-cumulative distributions of data with three different  $b_2$  values (A). Cumulative distribution function [Mixed Weibull Cumulative Distribution function] for the same  $b_2$  values (B). Smooth curves indicate curves of distribution. Note that the Mixed Weibull can be used for a bimodal distribution, while the Weibull (normal, non-mixed version) is more suitable for a unimodal distribution. Related to RER, the first mode represents fat oxidation and the second mode represents carbohydrate oxidation. As shown in the figure, greater  $b_2$  steepens the curve representing the second mode, which signifies a smaller spread of RER values in the carbohydrate oxidation mode. We interpret this to suggest more efficient switching to carbohydrate oxidation and thus enhanced metabolic flexibility. au, arbitrary unit; PRCF, percent relative cumulative frequency; RER, respiratory exchange ratio.

Supplementary Figure A.10 Institutional Review Board Approval for the human study described in Chapter 4.



HUMAN RESEARCH PROTECTION PROGRAM  
INSTITUTIONAL REVIEW BOARDS

---

<b>To:</b>	BRUCE HAMAKER NLSN 2195A
<b>From:</b>	STEPHEN ELLIOTT, Chair Biomedical IRB
<b>Date:</b>	08/21/2017
<b>Committee Action:</b>	<b>Full Committee Approval</b>
<b>Approval Date:</b>	08/21/2017
<b>IRB Protocol #</b>	1706019348
<b>Study Title</b>	Investigating digestive properties of carbohydrate-based foods
<b>Expiration Date</b>	08/20/2018
<b>Subjects Approved:</b>	25

The above-referenced protocol has been approved by the Purdue IRB. This approval permits the recruitment of subjects up to the number indicated on the application and the conduct of the research as it is approved.

The IRB approved and dated consent, assent, and information form(s) for this protocol are in the Attachments section of this protocol in CoeusLite. Subjects who sign a consent form must be given a signed copy to take home with them. Information forms should not be signed.

**Record Keeping:** The PI is responsible for keeping all regulated documents, including IRB correspondence such as this letter, approved study documents, and signed consent forms for at least three (3) years following protocol closure for audit purposes. Documents regulated by HIPAA, such as Authorizations, must be maintained for six (6) years. If the PI leaves Purdue during this time, a copy of the regulatory file must be left with a designated records custodian, and the identity of this custodian must be communicated to the IRB.

**Change of Institutions:** If the PI leaves Purdue, the study must be closed or the PI must be replaced on the study through the Amendment process. If the PI wants to transfer the study to another institution, please contact the IRB to make arrangements for the transfer.

**Changes to the approved protocol:** A change to any aspect of this protocol must be approved by the IRB before it is implemented, except when necessary to eliminate apparent immediate hazards to the subject. In such situations, the IRB should be notified immediately. To request a change, submit an Amendment to the IRB through CoeusLite.

**Continuing Review/Study Closure:** No human subject research may be conducted without IRB approval. IRB approval for this study expires on the expiration date set out above. The study must be close or re-reviewed (aka continuing review) and approved by the IRB before the expiration date passes. Both Continuing Review and Closure may be requested through CoeusLite.

**Unanticipated Problems/Adverse Events:** Unanticipated problems involving risks to subjects or others, serious adverse events, and serious noncompliance with the approved protocol must be reported to the IRB immediately through CoeusLite. All other adverse events and minor protocol deviations should be reported at the time of Continuing Review.

Supplementary Figure A.11 Institutional Animal Care and Use Committee general protocol information for the mouse study described in Chapter 5.

## Animal Research Protocol

**Protocol Number:** AN-1577

Status: Closed  
Initial Submit Date: 5/5/1997  
Approval Period: 1/22/2013 - 1/21/2016

Category of Experiment: D - Vertebrate, prolonged distress or discomfort

### Section Aa: Title & PI

#### A1. Protocol Title(s):

OVEREXPRESSION OF HUMAN MALTASE-GLUCOAMYLASE AND KNOCKOUT MOUSE MALTASE-GLUCOAMYLASE WITH RESCUE BY HUMAN

#### A2. Principal Investigator

Name:	BUFORD NICHOLS JR	Phone:	713-798-7018
Id:	845577	Fax:	713-798-7057
Department:	PEDIATRICS: NUTRITION	Email:	bnichols@bcm.tmc.edu
Center:		Mail Stn:	CNRC/10064

Does PI have direct contact with animals?: Yes

#### A3. Administrative Contact

Name:	LINDA F KEMPER	Phone:	713-798-7147
Id:	142328	Fax:	713-798-7171
		Email:	lfkemper@bcm.tmc.edu
		Mail Stn:	BCM320

#### A4. Sponsor/Mentor

None

### Section Ab: General Information

#### A5. Additional Research Personnel

Name:	ANTONE OPEKUN	Phone:	713-798-0956
Id:	012621	Fax:	713-798-0951
Department:	MEDICINE: GASTROENTEROLOGY	Email:	aopekun@bcm.tmc.edu
Center:		Mail Stn:	BCM620

Name:	STEPHEN AVERY	Phone:	713-798-7004
Id:	021806	Fax:	713/798-7057
Department:	PEDIATRICS: NUTRITION	Email:	stephen@bcm.tmc.edu
Center:		Mail Stn:	CNRC/10056

#### A6. Funding Source:

QOL Medical, pending

#### A7. Institutions where work will be performed:

CNRC: Children's Nutrition Research Center

## **APPENDIX B. INVESTIGATING THE POTENTIAL OF SLOW-RETROGRADING STARCHES TO REDUCE STALING IN SOFT SAVORY BREAD AND SWEET CAKE MODEL SYSTEMS**

Reprinted with permission. Full citation:

Hayes, A. M. R., Okoniewska, M., Martinez, M. M., Zhao, B., & Hamaker, B. R. (2020). Investigating the potential of slow-retrograding starches to reduce staling over time in soft savory bread and sweet cake model systems. *Food Research International*, 138, 109745. doi: 10.1016/j.foodres.2020.109745.

### **B.1 Abstract**

The potential anti-staling property of starches with slow-retrograding amylopectin was studied in soft wheat bread and cake model systems. Normal rice, waxy rice, and wheat starches were processed by drum drying or extrusion, and native starch was used as a comparator. Extrusion processing causing amylopectin fragmentation can reduce intermolecular retrogradation of rice starch. Starches were incorporated into model breads and cakes as partial replacements for flour on a dry weight basis (3 and 6% for cakes, 5 and 15% for breads). Starches pregelatinized by extrusion had moderate molecular fragmentation, as indicated by RVA and HPSEC-MALLS-RI. Starches previously shown to have lower intermolecular retrograding amylopectin (normal rice, waxy rice) resulted in minor to moderate reductions in hardness and other textural properties as indicated by texture profile analysis (TPA) in breads and cakes upon storage for up to 12 wk. A higher degree of starch fragmentation is suggested to produce lower staling. Incorporation of normal and waxy rice starches resulted in softer breads and cakes than wheat starch, which could be attributed to the shorter external and internal amylopectin chains of rice starch. Higher inclusion (15%) of slow-retrograding waxy rice in the bread model system showed the most potential for anti-staling property.

## B.2 Introduction

Staling results in loss of quality for baked goods in terms of harder texture. Although staling has posed challenges and has been studied extensively over the years, it remains a key issue in many baked products. The most widely used indicator of staling is measurement of the increase in crumb firmness (Gray & BeMiller, 2003). The staling process is complex and incompletely understood. Despite the lack of consensus regarding the mechanism of staling, amylopectin retrogradation is known to be a major contributor (Fadda et al., 2014; Gray & BeMiller, 2003).

Retrogradation, which is a reassociation of starch molecules after gelatinization as driven by formation of double-helices, may occur both intra- and intermolecularly (Jane & Chen, 1992; Martinez et al., 2018; Matalanis et al., 2009; Ring et al., 1987). For staling, amylopectin retrogradation presumably involves intermolecular associations forming large aggregates that change crumb hardness (Ribotta et al., 2004). Matalanis et al. (2009) showed that some starches (e.g. sorghum and maize) have a high tendency to form intermolecular double helices that impact texture, while other starches do not (e.g. rice). Degree of retrogradation, as measured by enthalpy of the endotherm for the melting of amylopectin double helices, was independent of whether intra- or intermolecular associations among amylopectin chains were formed, though a rheological method measured a decrease in the storage modulus ( $G'$ ) in the temperature range of melting of retrograded amylopectin double helices, revealing differences in intermolecular associations. Recently, we showed that starches with external amylopectin A and B1 chain populations with degree of polymerization (DP) of peak maximum exceeding 15.5 glucose units interact via double helical formations and exhibit high propensity to form intermolecular associations (Martinez et al., 2018). Conversely, from this work it was inferred that starches with short external amylopectin chains (less than 14 DP) form fewer intermolecular interactions and thus may exhibit fewer textural changes and at a slower rate, and Matalanis et al. (2009) showed that rice starch, in particular, with shorter amylopectin linear chains neither formed appreciable intermolecular double helices nor changed gel texture over 7 d of cold storage.

Altered intermolecular associations are also related to reduction in overall molecular size of amylopectin resulting from processing, such as using high-shear extrusion (Bindzus et al., 2002; Colonna et al., 1984; Davidson et al., 1984; Roman et al., 2018; Roman, Campanella, et al., 2019). Notably, typical increases in  $G'$  over a 7-d storage period were diminished for extruded rice, wheat, and maize flours with fragmented amylopectin compared to the gelatinized flour counterparts,

indicative of decreased formation of intermolecular associations (Roman et al., 2018). However, the type of starch also must be considered, as amylopectin fragmentation imparted through extrusion of banana starch was found to increase intermolecular associations in a banana starch-water gel system (Roman, Campanella, et al., 2019). Here, we thought a combination of the appropriate starch and high-temperature high-shear extrusion to fragment amylopectin could serve as an approach to reduce staling in baked products.

Our aim was to use slow-retrograding amylopectin to retard staling in bread and cake model systems. We reasoned that incorporation of starch to reduce retrogradation through a decrease in intermolecular associations could be a mechanism by which starches can improve texture and reduce staling during product storage. The objectives were two-fold. Firstly, the effect of partial flour replacement with starches possessing amylopectin with previously identified slow intermolecular retrogradation properties was tested to reduce staling/textural changes in breads and cakes. We hypothesized that starches with amylopectin structures that form fewer intermolecular interactions during retrogradation (i.e. have shorter external and internal chains) would impede or slow staling/textural changes. Secondly, the impact of the same starches with extrusion processing to fragment starch (compared to drum-dried pregelatinized starches where there is no fragmentation) was tested to further reduce staling/textural changes. We hypothesized that extrusion to pregelatinize and molecularly fragment starches would result in fewer intermolecular interactions during retrogradation and thus would produce highly dispersed starch suspensions that would impede or slow staling/textural changes. Due to their shorter external ( $DP < 14$ ) and internal amylopectin chains, rice and waxy rice starches were selected to retard retrogradation and wheat starch with longer chains was used as a more rapidly retrograding comparator. Ultimately, we sought to identify a means to reduce staling in baked products.

## **B.3 Methods**

### **B.3.1 Materials**

Normal rice (PenPure 30, PP30) and waxy rice (PenPure 37, PP37) starch samples were purchased from Ingredion, and wheat starch (Aytex P) was purchased from Archer Daniels Midland Company (ADM).

### **B.3.2 Processing treatments**

A portion of each type of starch was drum-dried by Custom Drying Solutions (Valparaiso, IN) using a commercial double drum dryer. Starch-water slurries (15.6% solids) were mixed in an agitator for 5 min and pumped onto drum dryer rollers at 30 rpm using a peristaltic pump (Leeson Speedmaster, Regal, Beloit, WI). The drum dryer rollers were maintained at 329°C with a 0.203 mm gap.

Another portion of each starch was extruded at Purdue University using a 30 kg/h small-scale single-screw extruder with restrictions on the screw (Technochem International, Inc., Boone, IA, USA). Prior to extrusion, raw starch samples were hydrated with water (37.5% m.c.) using a Hobart mixer (H600, Planetary mixer, floor model, 60 L capacity, HOBART GmbH, Offenburg, Germany) and then equilibrated at 7°C for 14 h. Samples were allowed to equilibrate at room temperature for 2 h immediately prior to extrusion. An Accu-Rate Bulk Solids Metering feeder (Accu-Rate Inc., Whitewater, WI, USA) was used to control the feed rate into the extruder at 80%. Extrusion conditions were a screw speed of 880-900 rpm and barrel temperature of 130-135°C. Following extrusion, samples were tray-dried in a convection oven at 50°C for 36 h. A summary of samples and processing treatments is shown in Table B.1.

### **B.3.3 Sample preparation post-processing**

Drum-dried and extruded samples were reduced to flour by milling. For drum-dried samples, a pin mill (Alpine, 160 Z, Augsburg, Germany) operated at 5.5 rpm was used for milling, and then a portable sieve shaker (Model Rx-24, W.S. Tyler Inc., Mentor, OH, USA) was used to collect the particle size fraction between 53-180 µm for experimentation. For extruded samples, a hammer mill (Eberbach E3703 Heavy Duty Variable Speed Cutting Mill, Eberbach, Belleville, MI, USA) was used at speed 900 rpm to initially mill samples to pass through a 0.50 mm mesh screen. Samples were then milled in the same pin mill as above (Alpine, 160 Z, Augsburg, Germany), and the same portable sieve shaker was used to collect the particle size fraction between 53-180 µm for experimentation. One portion of starch was also kept in its initial native state and used for experimentation.

### **B.3.4 Starch structural characterization**

In order to obtain relative values of starch fragmentation due to processing, molecular weight distributions of native and processed starches were determined using high-performance size-exclusion chromatography with multi-angle laser light scattering and refractive index detection (HPSEC-MALLS-RI). Previous methods (Moussa et al., 2011) were followed with slight modification. Briefly, 1.5 mL dimethylsulfoxide (DMSO, 90%) was added to 6 mg starch and heated at 80°C for 24 h with agitation at 350 rpm (Eppendorf ThermoMixer C, Eppendorf, Hauppauge, NY, USA). Samples were then centrifuged at 4000 × *g* and starch in supernatants was precipitated with 10 mL ethanol (200 proof), resuspended, and precipitated twice more followed by drying under vacuum. From the resulting dry starch pellets, 2 mg were weighed and mixed with boiling water to obtain a 2 mg/mL concentration; these samples were maintained at 95°C for ≥ 6 h to fully disperse the starch prior to injection. Samples were filtered through 5.0 μm nylon syringe filters immediately prior to being injected on a Sephacryl S500-HR column (Amersham Bioscience, Piscataway, NJ, USA) with filtered purified water containing 0.02% sodium azide used as the eluent. An HPLC pump (Shimadzu LC-10AP pump, Shimadzu Scientific Instruments, Inc., Kyoto, Japan) was used, and chromatograms were obtained using MALLS (WREX-10, Dawn DSP-F, Wyatt Technology Corp., Santa Barbara, CA, USA) and refractive index (Optilab 903 Interferometric Refractometer, Wyatt Technology Corp., Santa Barbara, CA, USA) detectors. Data collection and analysis was done using Astra software version 4.90.08. A Berry plot was used for curve fitting, and molecular weights were determined using a  $dn/dc$  value of 0.146.

### **B.3.5 Starch rheological characterization**

A Rapid Visco Analyzer (RVA; RVA-4, Perten Instruments Instrumentvägen 29, SE-126 53 Hägersten, Sweden) was used to determine pasting profiles for each starch sample. Starch-water slurries were prepared with 8% solids. With the exception of extruded starch samples, all samples were analyzed using the Standard 1 protocol supplied with the instrument. This protocol consisted of holding at 50°C for 1 min, heating at a rate of 12°C/min to 95°C, equilibrating at 95°C for 2.5 min, cooling at a rate of 12°C/min to 50°C, and holding at 50°C for 2 min. For the first 10 s, the RVA mixing paddle speed was 960 rpm, and thereafter the speed was 160 rpm for the remainder

of the experiment. For the extruded samples, a 15 min mixing period at 960 rpm and 50°C was added to the beginning of the protocol to facilitate proper dispersion.

### **B.3.6 Baking**

Proprietary bread and cake formulations provided by a global consumer packaged goods company were used as savory and sweet model intermediate moisture systems, respectively. For the bread model system, 5% and 15% starch replacements for flour (dry weight basis) were evaluated. For the cake model system, 3 and 6% starch replacements for flour (dry weight basis) were evaluated. These different inclusion levels were determined through preliminary trials to maximize percentage of starch inclusion without adversely affecting initial hardness after baking. Control breads and cakes, which had no starch replacement for flour, were also prepared. Breads and cakes were baked in one batch per inclusion level (e.g. breads with 5% starch inclusion were baked in one batch, breads with 15% starch inclusion were baked in one batch, cakes with 3% starch inclusion were baked in one batch). A Commercial KitchenAid mixer (8 quart, NSF-certified commercial stand mixer, KitchenAid Commercial, Benton Harbor, MI, USA) was used for all baking trials.

The bread model consisted of bread flour, treatment starch (5 and 15%, for non-control breads), salt, sugar, a proprietary blend, water (30°C), canola oil, and glycerin. These ingredients were made into dough, proofed, and baked according to a proprietary method. For this model system, the breads were the size of mini-buns (approximately 5 cm width × 4 cm height). Breads were then placed in barrier pouches composed of PAKVF4 material with a water vapor transmission rate of < 0.0005 gr/100 in<sup>2</sup>/24 h and O<sub>2</sub> transmission rate of 0.001/cc/m<sup>2</sup>/24 h (SorbentSystems.com), and promptly sealed. All bread samples were kept at ambient temperature (23-25°C) for the duration of storage. Samples for measurement at different timepoints were stored in separate pouches.

In initial method development for the cake model, levels of starch incorporation used in breads (5 and 15%) were found not suitable, as they produced substantially higher initial hardness than Control cakes. Therefore, levels were set at 3 and 6%. The cake formulation consisted of flour, treatment starch (3 and 6%, for non-control cakes), sucrose, sodium acid pyrophosphate, sodium bicarbonate, salt, water, eggs, glycerin, oil, and lecithin. Cakes were prepared according to a proprietary method and then placed in barrier pouches composed of PAKVF4 material (same as

above for breads, SorbentSystems.com), which were promptly sealed. For this model system, the cakes were the size of cupcakes (approximately 6 cm width × 4.5 cm height). Cake samples were kept at ambient temperature (23-25°C) for the duration of storage. Note: for cakes with 3% starch replacement for flour, the Control cakes were not used because they were not baked on the same day as the test cakes.

Bread and cake samples were analyzed at 0, 1, 4, and 12 wk timepoints (Figure B.1).

### **B.3.7 Texture analysis**

Texture analysis was conducted using a TA-XT2i Texture Analyzer (5 kg load cell) equipped with a Peltier control unit (Stable Micro Systems Ltd., Godalming, Surrey, UK) to control temperature conditions while testing. Temperature conditions of 23 and 80°C within the heating unit were used, with the high temperature used to measure texture melting of amylopectin double helices caused by retrogradation. Breads and cakes were cut into rectangular cuboids (3.7 cm × 3.7 cm × 1.7 cm) using a bread knife, exposing the crumb and removing all crusts. Samples of this dimension were used to maximize the size tested for each bread and cake.

For samples measured at 23°C, each bread and cake were prepared immediately prior to testing to minimize loss of moisture before being subjected to texture analysis. For samples measured at 80°C, breads and cakes were prepared as follows: After cutting, each sample was wrapped in aluminum foil and placed in a drying and heating chamber with forced convection that was pre-heated to 95°C (Binder Model FD 23, Binder Inc., Bohemia, NY, USA). Samples were heated until reaching an internal temperature of 69-74°C, which was 15 min for breads and 20 min for cakes, as determined through initial method development trials. Pre-heating allowed samples to be brought to appropriate temperature while minimizing losses of moisture and heat (that would otherwise occur if samples were heated in the Peltier control unit).

Prepared samples were analyzed by conducting a double compression Texture Profile Analysis (TPA) test using a TA-3 probe (2.54 cm diameter). For all analyses, the test speed was 2.00 mm/s, and compressions proceeded to 50% strain with a 5 × g trigger force. Samples tested at 80°C were evaluated 30 s after removal from the oven. Random sample internal temperature measurements were made using a thermocouple immediately following as a quality check to ensure internal temperatures were maintained at ≥ 69°C during testing. The texture analyzer was calibrated with a 2000 g standard weight prior to use on each testing day.

### **B.3.8 Water activity**

Bread and cake samples were ground using a small-scale commercial grinder (Mr. Coffee, Model IDS77-RB, Cleveland, OH, USA). Water activity of freshly ground samples was measured in duplicate using a water activity meter (Aqua Lab 4TE, Pullman, WA, USA) operated at 25°C and calibrated with 0.500, 0.760, and 0.920 standards immediately before each use.

### **B.3.9 Moisture content**

Moisture content was measured according to AACC International Method 44-15.02 (gravimetric moisture loss), using 5 g ground samples and pre-dried aluminum pans.

### **B.3.10 Image characterization**

Photomacrographic images were captured of bread and cake cross-sections (1 cm thick) within a light cube using the camera function on a Samsung Galaxy S7 mobile device (Seoul, South Korea) with no magnification. Standardized distance (7 cm) was maintained between the camera and the sample for image captures.

### **B.3.11 Statistical analysis**

One-way analysis of variance (ANOVA) was used to determine statistically significant differences between means for all parameters measured. Tukey's test was used to evaluate all pairwise differences between factor level means at the 5% significance level for *post hoc* tests when the model was significant ( $p < 0.05$ ). All analyses were conducted using SAS version 9.4 (SAS Institute Inc., Cary, NC, USA).

## **B.4 Results and Discussion**

### **B.4.1 Starch structural characterization**

Starch fine structural features have previously been shown to drive the formation of intra- versus intermolecular associations (Martinez et al., 2018; Matalanis et al., 2009), which may ultimately affect the rate and extent of staling. Here, we were specifically interested in reducing intermolecular associations by utilizing starches with shorter internal and external amylopectin

chains (i.e. normal and waxy rice starches) compared to the somewhat longer chains of wheat starch; Table B.1), as well as by molecularly fragmenting amylopectin through extrusion. We hypothesized that these strategies would lead to slower staling rate when applied in bread and cake model systems as indicated by reduced hardness. To characterize the extent of molecular fragmentation of starches caused through extrusion, HPSEC-MALLS-RI was performed to compare starch molecular weight distributions. All extruded starches had a lower peak molecular weight fraction than drum-dried and native starches (extruded samples ranging from  $0.85 \times 10^8$  to  $1.18 \times 10^8$  g/mol; native and drum-dried samples ranging from  $1.94 \times 10^8$  to  $2.71 \times 10^8$  g/mol;  $p < 0.001$ ; Table B.2). Differences were statistically significant with the exception of Waxy Rice – Extruded and Wheat – Drum dried. Lower molecular weights observed for extruded samples indicated that starch fragmentation occurred (Davidson et al., 1984; Roman et al., 2018; Sagar & Merrill, 1995).

#### **B.4.2 Starch rheological characterization**

To characterize functionality of the starches before utilizing them in the baked model systems, RVA was performed. As mentioned in Section B.3.5 of the Methods, extruded samples were more difficult to disperse and required gradual addition of water to starch plus a 15 min mixing time in the RVA. Therefore, native and drum-dried (DD) samples are shown in graphs with the same time scale (Figure B.2), while extruded samples are shown in separate graphs with a different time scale (Figure B.3). As seen in Figure B.2, native starches showed pasting temperatures corresponding to gelatinization, while drum-dried starches exhibited initial increases in viscosity that are consistent with pregelatinization (Figure B.2; Juhász & Salgó, 2008). Extruded starches showed minimal initial increases in viscosity, which is indicative of starch fragmentation (Figure B.3; Robin, Théoduloz, & Srichuwong, 2015). The peaks in viscosity at approximately 1100 s for Normal Rice – Extruded and at 1250 s for Wheat – Extruded may be due to a small amount of ungelatinized starch remaining in the processed samples (Figure B.3B) (Juhász & Salgó, 2008). Final viscosity values were higher for native starches and lower for drum-dried and extruded starches, with extruded starches having slightly lower values than drum-dried starches (Figures B.2-B.3), likely due to greater starch disruption and fragmentation of the extruded starches (Robin et al., 2011, 2015).

### **B.4.3 Staling measurement through texture analysis of breads and cakes**

As the indicator of staling, Texture Profile Analysis (TPA) was conducted over storage times (0, 1, 4, 12 wk) for bread and cake model systems, with 5 and 15% starch replacement for flour in breads and 3 and 6% starch replacement for flour in cakes. The 0 wk timepoint was approximately 36 h after baking. The TPA parameters calculated included hardness, springiness, cohesiveness, chewiness, and resilience. Difference in hardness between 23 and 80°C (termed hereafter as “ $\Delta$ Hardness”) was assessed as an indicator of intermolecular associations measured as hardness difference due to the melting of retrograded amylopectin helices. This was confirmed because the internal temperature of the breads and cakes ( $\geq 69^\circ\text{C}$ ) surpassed the conclusion temperature of endotherms for melting retrograded amylopectin helices ( $< 70^\circ\text{C}$ ) (Roman et al., 2018).  $\Delta$ Hardness values are discussed, while values for the other TPA parameters are simply reported in Tables B.3-B.18.

#### *B.4.3.1 Starch performance in breads*

For breads with 5% starch replacement for flour, breads with normal and waxy rice starch treatments, as well as Control breads, generally exhibited both lower  $\Delta$ Hardness and hardness than breads with wheat starch at all timepoints, but with statistical significance only reached between all rice treatments and Wheat – Extruded at the 12 wk timepoint ( $p < 0.001$ ; Figures B.4 and B.5). This is indicative of a moderately lower amount of retrograded amylopectin for normal and waxy rice starches, which supports our first hypothesis that starches with shorter internal and external amylopectin chains, which form fewer intermolecular associations, have slower retrogradation during bread storage.

Somewhat larger effects and differences among treatments emerged overall for breads incorporating 15% starch replacement for flour. Results for  $\Delta$ Hardness at 23 and 80°C showed Waxy Rice – Extruded breads consistently trended with lowest  $\Delta$ Hardness over time and, in general, drum-dried starches trended higher (Figure B.6). Waxy rice – Extruded has significantly lower  $\Delta$ Hardness at 0 wk than all other treatments and Control breads except for Waxy rice – Drum Dried ( $p < 0.05$ ). These results provide some evidence to support our second hypothesis that extrusion to molecularly fragment starch results in fewer intermolecular interactions that in turn slows staling in bread. For hardness values alone, Waxy Rice – Extruded and Waxy Rice – Drum

dried showed significantly lower hardness at 0 wk ( $1531.2 \pm 58.3$  g and  $1732.4 \pm 68.9$  g, respectively) compared to other treatments and Control breads (Figure B.7). Waxy and normal rice samples tended to have lower hardness values over time, again supporting the postulate that starches with shorter external and internal chains form fewer intermolecular associations and thus reduce staling.

#### *B.4.3.2 Starch performance in cakes*

Changes in TPA characteristics occurred in different manners for cakes (Figures B.8-B.11) compared to breads (Figures B.4-B.7).  $\Delta$ Hardness (g) of cakes with 3% starch inclusion level were not large in magnitude (Figure B.8). However, extruded starches tended to exhibit lower  $\Delta$ Hardness overall, with significant differences emerging at 12 wk ( $p < 0.05$ ). For hardness, although overall values among treatment groups were also not great in magnitude, cakes with Wheat – Extruded starch exhibited significantly lower hardness at 12 wk than cakes with Normal Rice – Drum dried ( $p < 0.05$ , Figure B.9).

For cakes with 6% starch replacement for flour, there were no reductions in  $\Delta$ Hardness for rice starches compared to wheat (Figure B.10). Control cakes as well as cakes incorporating native and extruded starches tended to have lower  $\Delta$ Hardness than drum-dried starches, regardless of starch botanical source (Figure B.10). For hardness alone, although differences were not large in magnitude, Waxy Rice – Native cakes had the lowest value at 0 wk ( $1968.5 \pm 72.1$  g), which was significantly different from Wheat – Drum Dried, Wheat – Extruded, Waxy Rice – Extruded, and Normal Rice – Drum Dried at the same timepoint (Figure B.11). Batters for drum-dried treatments were denser (visually observed), which may have contributed to the harder texture of drum-dried cakes.

#### *B.4.3.3 Overall starch performance in breads and cakes*

Moderate, but in many cases significant, reductions in hardness were observed for breads and cakes with inclusion of normal and waxy rice starches. Rice starch possesses shorter internal and external linear chain amylopectin that forms fewer intermolecular associations and is slow retrograding (Martinez et al., 2018; Matalanis et al., 2009; Vamadevan & Bertoft, 2018). As indicated by HPSEC-MALLS-RI, extrusion processing caused a moderate amount of starch

fragmentation (Table B.2), and a notable reduction in hardness over storage time in the bread model system was observed with 15% extruded starch replacement for flour. We reason that a greater extent of starch fragmentation, which would be achieved using twin-screw extrusion, could result in starches with even greater anti-staling potential.

One factor that we did not examine is the potential effect of amylose on staling in the breads and cakes. Through gelatinization during baking, a portion of amylose leaches from starch granules (Fadda et al., 2014; Hug-Iten et al., 1999; Keetels et al., 1996). During cooling after baking, amylose reverts back to an ordered state within a short period of time (minutes to hours), contributing to the initial firmness of baked products (Hug-Iten et al., 1999, 2003). Amylopectin reordering instead takes place slowly over time, occurring on the order of days to months (Ribotta et al., 2004; Ribotta & Le Bail, 2007). Presently, the general consensus is that amylose retrogradation contributes to initial rigidity of starch-containing baked products, while amylopectin retrogradation contributes to the gradual loss of textural quality in such products. An additional point to consider is whether amylose in the pregelatinized state, as was the case for our drum-dried and extruded starch treatments, undergoes retrogradation at a different rate and extent as amylose that was originally in the native state; this could be an area of future investigation.

#### **B.4.4 Water activity and moisture content**

Because staling is also associated with changes in water of baked products (Bosmans et al., 2013), we examined water activity and moisture content at each timepoint for all breads and cakes.

##### *B.4.4.1 Changes in water activity for bread and cake model systems*

Water activity of breads and cakes generally decreased over storage time, with the exception that there were no differences in water activity at 4 and 12 wk timepoints among breads with 5% starch inclusion (Table B.19) or at 1 wk among cakes with 3 and 6% starch inclusion (Table B.20). For the bread model system with 5% starch inclusion, Control breads had the highest water activity values at 0 and 1 wk ( $p < 0.05$ ), however Waxy rice – Drum dried and Wheat – Extruded did not differ from the Control at 0 wk, and differences did not persist at 4 and 12 wk (Table B.19). In breads with 15% starch inclusion, treatments with processed starches (drum-dried and extruded) tended to have lower water activity values over storage time, especially at 0 and 1

wk timepoints, where differences were more pronounced ( $p < 0.05$ ). This was likely due to the fact that these starches were pregelatinized and absorbed water (Gopirajah & Muthukumarappan, 2018; Rodríguez-Miranda et al., 2011).

Water activity of cakes did not decrease over time as much as water activity of breads, likely because cakes had sugar, which helps retain moisture, as well as lower initial water activity than breads. Water activity values for waxy rice treatments trended lower in cakes with 3% starch inclusion level, with significance in difference at the 4 and 12 wk timepoints ( $p < 0.05$ ; Table B.20). For the 6% starch inclusion cakes, Waxy rice – Drum Dried, Waxy rice – Extruded, Wheat – Native, and Wheat – Drum Dried trended lower than the other treatments, with significance reached at 12 wk compared to Normal rice – Extruded, Waxy rice – Native, and Control ( $p < 0.05$ ).

#### *B.4.4.1 Changes in moisture content for bread and cake model systems*

Moisture content level differed between bread and cake model systems (Tables B.21 and B.22). Breads with both starch inclusion levels (5 and 15% replacements for flour) experienced reductions in moisture content by 1-2% over time (Table B.21). Waxy rice treatments tended to have lower moisture content (Waxy Rice – Native was an exception), with differences that became more pronounced over time, reaching statistical significance in some cases at 0, 1, and 4 wk ( $p < 0.05$ ; Table B.21). This is notable because, despite the greater extent of moisture loss over time, the waxy rice treatments generally had lower hardness, indicative of slower staling. Wheat – Native treatments at both inclusion levels showed decreased moisture content over time that was similar in magnitude to the waxy rice starch treatments.

Waxy rice treatments for cakes with 3% starch inclusion level trended lower in moisture content, with significance reached at the 12 wk timepoint ( $p < 0.05$ ; Table B.22). At 6% starch inclusion, Control cakes had higher moisture content than all treatments (Table B.6), with statistically significant differences achieved at 12 wk between Control and all treatments, other than Normal rice – Drum Dried and Normal rice – Extruded ( $p < 0.05$ ). Cakes tended to fluctuate above and below their initial moisture content at the follow-up timepoints (1, 4, and 12 wk), which may be indicative of moisture redistribution upon storage.

Overall, although there were some significant differences among samples at certain timepoints, the moisture content and water activity data demonstrate that there was not a large amount of moisture loss from samples over storage (changes of  $< 0.03$  in water activity and  $< 2\%$

in moisture content), which is notable as otherwise the textural changes could be attributed to drying of the samples.

#### **B.4.5 Image characterization**

Examples of bread and cake images are included in Figures B.12-B.15. The pores in bread and cake crumbs became smaller over storage time, and cake crumbs also seemed to fade in color over time.

#### **B.5 Conclusion**

In summary, inclusion of normal and waxy rice starches resulted in moderate reductions in  $\Delta$ Hardness from 23 to 80°C, as a measurement of degree of retrogradation, by TPA in bread and cake model systems in storage for up to 12 wk. In general, normal and waxy rice starches tended to exhibit more favorable anti-staling effects than wheat starch, which supported the hypothesis that shorter external and internal amylopectin chains of rice starch slows amylopectin retrogradation through fewer intermolecular associations. Furthermore, single-screw extrusion of normal and waxy rice starches to fragment amylopectin had an additional effect of lessened extent of staling in breads and cakes, supporting the idea that amylopectin fragments of starches that initially have relatively short amylopectin internal and external chains form fewer intermolecular associations. Given that the extruder used in this study produced only moderate amylopectin fragmentation, a higher degree of starch fragmentation obtained by twin-screw extrusion could further reduce retrogradation, producing better anti-staling property. Altered water molecular dynamics upon storage of the different starch treatments may be another factor affecting staling, as 5% and 15% waxy rice starch inclusion in the bread model system tended to result in breads with lower moisture content over time. Interestingly, despite their greater moisture loss over time, the waxy rice treatments generally had lower staling, as indicated by lower  $\Delta$ Hardness. Overall, higher inclusion of low intermolecular-retrograding waxy rice in the bread model system (15% starch replacement for flour) showed the most reduction in staling and may, with further starch fragmentation, have anti-staling potential to provide more acceptable, softer stored breads and cakes.

## B.6 References

- AACC International Method 44-15.02. Moisture – Air-Oven Methods.
- Bindzus, W., Livings, S. J., Gloria-Hernandez, H., Fayard, G., van Lengerich, B., & Meuser, F. (2002). Glass Transition of Extruded Wheat, Corn and Rice Starch. *Starch - Stärke*, *54*(9), 393–400. [https://doi.org/10.1002/1521-379X\(200209\)54:9<393::AID-STAR393>3.0.CO;2-W](https://doi.org/10.1002/1521-379X(200209)54:9<393::AID-STAR393>3.0.CO;2-W)
- Bosmans, G. M., Lagrain, B., Ooms, N., Fierens, E., & Delcour, J. A. (2013). Biopolymer interactions, water dynamics, and bread crumb firming. *Journal of Agricultural and Food Chemistry*, *61*(19), 4646–4654. <https://doi.org/10.1021/jf4010466>
- Colonna, P., Doublier, J. L., Melcion, J. P., de Monredon, F., & Mercier, C. (1984). Extrusion-cooking and drum drying of wheat starch. Physical and macromolecular modifications. *Cereal Chemistry*, *61*, 538–543.
- Davidson, V. J., Paton, D., Diosady, L. L., & Larocque, G. (1984). Degradation of Wheat Starch in a Single Screw Extruder: Characteristics of Extruded Starch Polymers. *Journal of Food Science*, *49*(2), 453–458. <https://doi.org/10.1111/j.1365-2621.1984.tb12441.x>
- Fadda, C., Sanguinetti, A. M., Del Caro, A., Collar, C., & Piga, A. (2014). Bread staling: Updating the view. *Comprehensive Reviews in Food Science and Food Safety*, *13*(4), 473–492. <https://doi.org/10.1111/1541-4337.12064>
- Gopirajah, R., & Muthukumarappan, K. (2018). Effect of extrusion process conditions on the physical properties of tef-oat healthy snack extrudates. *Journal of Food Processing and Preservation*, *42*(3), e13559. <https://doi.org/10.1111/jfpp.13559>
- Gray, J. A., & BeMiller, J. N. (2003). Bread Staling: Molecular Basis and Control. *Comprehensive Reviews in Food Science and Food Safety*, *2*(1), 1–21. <https://doi.org/10.1111/j.1541-4337.2003.tb00011.x>
- Hug-Iten, S., Escher, F., & Conde-Petit, B. (2003). Staling of Bread: Role of Amylose and Amylopectin and Influence of Starch-Degrading Enzymes. *Cereal Chemistry Journal*, *80*(6), 654–661. <https://doi.org/10.1094/CCHEM.2003.80.6.654>
- Hug-Iten, S., Handschin, S., Conde-Petit, B., & Escher, F. (1999). Changes in Starch Microstructure on Baking and Staling of Wheat Bread. *LWT - Food Science and Technology*, *32*(5), 255–260. <https://doi.org/10.1006/fstl.1999.0544>
- Jane, J.-L., & Chen, J.-F. (1992). Effect of amylose molecular size and amylopectin branch chain length on paste properties of starch. *Cereal Chemistry*, *69*, 60–65.
- Juhász, R., & Salgó, A. (2008). Pasting Behavior of Amylose, Amylopectin and Their Mixtures as Determined by RVA Curves and First Derivatives. *Starch - Stärke*, *60*(2), 70–78. <https://doi.org/10.1002/star.200700634>
- Keetels, C. J. A. M., Visser, K. A., van Vliet, T., Jurgens, A., & Walstra, P. (1996). Structure and Mechanics of Starch Bread. *Journal of Cereal Science*, *24*(1), 15–26. <https://doi.org/10.1006/jcrs.1996.0033>
- Martinez, M. M., Li, C., Okoniewska, M., Mukherjee, I., Vellucci, D., & Hamaker, B. (2018). Slowly digestible starch in fully gelatinized material is structurally driven by molecular size and A and B1 chain lengths. *Carbohydrate Polymers*, *197*, 531–539. <https://doi.org/10.1016/j.carbpol.2018.06.021>
- Matalanis, A. M., Campanella, O. H., & Hamaker, B. R. (2009). Storage retrogradation behavior of sorghum, maize and rice starch pastes related to amylopectin fine structure. *Journal of Cereal Science*, *50*(1), 74–81. <https://doi.org/10.1016/j.jcs.2009.02.007>

- Moussa, M., Qin, X., Chen, L. F., Campanella, O. H., & Hamaker, B. R. (2011). High-quality instant sorghum porridge flours for the West African market using continuous processor cooking. *International Journal of Food Science and Technology*, 46(11), 2344–2350. <https://doi.org/10.1111/j.1365-2621.2011.02755.x>
- Ribotta, P. D., Cuffini, S., Leon, A. E., & Anon, M. C. (2004). The staling of bread: an X-ray diffraction study. *European Food Research and Technology*, 218(3), 219–223. <https://doi.org/10.1007/s00217-003-0835-8>
- Ribotta, P. D., & Le Bail, A. (2007). Thermo-physical assessment of bread during staling. *LWT - Food Science and Technology*, 40(5), 879–884. <https://doi.org/10.1016/j.lwt.2006.03.023>
- Ring, S. G., Colonna, P., I'Anson, K. J., Kalichevsky, M. T., Miles, M. J., Morris, V. J., & Orford, P. D. (1987). The gelation and crystallisation of amylopectin. *Carbohydrate Research*, 162(2), 277–293. [https://doi.org/10.1016/0008-6215\(87\)80223-9](https://doi.org/10.1016/0008-6215(87)80223-9)
- Robin, F., Théoduloz, C., Gianfrancesco, A., Pineau, N., Schuchmann, H. P., & Palzer, S. (2011). Starch transformation in bran-enriched extruded wheat flour. *Carbohydrate Polymers*, 85(1), 65–74. <https://doi.org/10.1016/j.carbpol.2011.01.051>
- Robin, F., Théoduloz, C., & Srichuwong, S. (2015). Properties of extruded whole grain cereals and pseudocereals flours. *International Journal of Food Science & Technology*, 50(10), 2152–2159. <https://doi.org/10.1111/ijfs.12893>
- Rodríguez-Miranda, J., Ruiz-López, I. I., Herman-Lara, E., Martínez-Sánchez, C. E., Delgado-Licon, E., & Vivar-Vera, M. A. (2011). Development of extruded snacks using taro (*Colocasia esculenta*) and nixtamalized maize (*Zea mays*) flour blends. *LWT - Food Science and Technology*, 44(3), 673–680. <https://doi.org/10.1016/j.lwt.2010.06.036>
- Roman, L., Campanella, O., & Martinez, M. M. (2019). Shear-induced molecular fragmentation decreases the bioaccessibility of fully gelatinized starch and its gelling capacity. *Carbohydrate Polymers*, 215(March), 198–206. <https://doi.org/10.1016/j.carbpol.2019.03.076>
- Roman, L., Gomez, M., Hamaker, B. R., & Martinez, M. M. (2018). Shear scission through extrusion diminishes inter-molecular interactions of starch molecules during storage. *Journal of Food Engineering*, 238(June), 134–140. <https://doi.org/10.1016/j.jfoodeng.2018.06.019>
- Sagar, A. D., & Merrill, E. W. (1995). Starch fragmentation during extrusion processing. *Polymer*, 36(9), 1883–1886. [https://doi.org/10.1016/0032-3861\(95\)90935-U](https://doi.org/10.1016/0032-3861(95)90935-U)
- Vamadevan, V., & Bertoft, E. (2018). Impact of different structural types of amylopectin on retrogradation. *Food Hydrocolloids*, 80, 88–96. <https://doi.org/10.1016/j.foodhyd.2018.01.029>

Table B.1 Starch samples and processing treatments.

<b>Starch type</b>	<b>Rationale</b>	<b>Processing</b>	<b>Ingredient, Source</b>
Normal rice	Shorter internal and external amylopectin chains (formation of fewer intermolecular interactions during retrogradation)	Native	PenPure 30 (PP30), Ingredion
		Drum-dried	PP30, prepared by Custom Drying Solutions (Valparaiso, IN)
		Extruded	PP30, prepared at Purdue University
Waxy rice	Shorter internal and external amylopectin chains (formation of fewer intermolecular interactions during retrogradation), little/no amylose (decreased hardness)	Native	PenPure 37 (PP37), Ingredion
		Drum-dried	PP37, prepared by Custom Drying Solutions (Valparaiso, IN)
		Extruded	PP37, prepared at Purdue University
Wheat	Comparator, longer internal and external amylopectin chains	Native	Aytex P (hard wheat), ADM
		Drum-dried	Aytex P, prepared by Custom Drying Solutions (Valparaiso, IN)
		Extruded	Aytex P, prepared at Purdue University

Table B.2 Starch molecular weight ( $M_w$ , g/mol). Different letters indicate statistically significant differences between treatments ( $p < 0.05$ ).

<b>Starch treatment</b>	<b>Peak molecular weight (<math>M_w</math>, g/mol) <math>\times 10^8</math></b>
Normal rice - Native	$2.26 \pm 0.26^{ab}$
Normal rice - Drum dried	$2.71 \pm 0.02^a$
Normal rice - Extruded	$0.93 \pm 0.11^d$
Waxy rice - Native	$1.99 \pm 0.31^{ab}$
Waxy rice - Drum dried	$2.65 \pm 0.11^{ab}$
Waxy rice - Extruded	$1.18 \pm 0.02^{cd}$
Wheat - Native	$1.97 \pm 0.15^{ab}$
Wheat - Drum dried	$1.94 \pm 0.02^{bc}$
Wheat - Extruded	$0.85 \pm 0.02^d$

Table B.3 Springiness TPA values (unitless) – bread model system with 5% starch inclusion. Average values  $\pm$  standard error. Different letters indicate statistically significant differences at the same timepoint among treatments (down columns;  $p < 0.05$ ).

Springiness (unitless)	Week 0	Week 1	Week 4	Week 12
5% Normal rice - Native	0.769 $\pm$ 0.020 <sup>a</sup>	0.675 $\pm$ 0.010 <sup>b</sup>	0.754 $\pm$ 0.029 <sup>a</sup>	0.617 $\pm$ 0.002 <sup>b</sup>
5% Normal rice - Drum dried	0.796 $\pm$ 0.002 <sup>a</sup>	0.678 $\pm$ 0.013 <sup>ab</sup>	0.749 $\pm$ 0.034 <sup>a</sup>	0.620 $\pm$ 0.029 <sup>b</sup>
5% Normal rice - Extruded	0.782 $\pm$ 0.007 <sup>a</sup>	0.700 $\pm$ 0.020 <sup>ab</sup>	0.745 $\pm$ 0.038 <sup>a</sup>	0.607 $\pm$ 0.006 <sup>b</sup>
5% Waxy rice - Native	0.779 $\pm$ 0.009 <sup>a</sup>	0.719 $\pm$ 0.020 <sup>ab</sup>	0.763 $\pm$ 0.058 <sup>a</sup>	0.607 $\pm$ 0.003 <sup>b</sup>
5% Waxy rice - Drum dried	0.792 $\pm$ 0.013 <sup>a</sup>	0.680 $\pm$ 0.022 <sup>ab</sup>	0.785 $\pm$ 0.032 <sup>a</sup>	0.620 $\pm$ 0.008 <sup>b</sup>
5% Waxy rice - Extruded	0.790 $\pm$ 0.006 <sup>a</sup>	0.705 $\pm$ 0.002 <sup>ab</sup>	0.775 $\pm$ 0.036 <sup>a</sup>	0.643 $\pm$ 0.026 <sup>b</sup>
5% Wheat - Native	0.804 $\pm$ 0.016 <sup>a</sup>	0.736 $\pm$ 0.013 <sup>ab</sup>	0.679 $\pm$ 0.018 <sup>a</sup>	0.740 $\pm$ 0.001 <sup>a</sup>
5% Wheat - Drum dried	0.823 $\pm$ 0.003 <sup>a</sup>	0.754 $\pm$ 0.021 <sup>ab</sup>	0.718 $\pm$ 0.043 <sup>a</sup>	0.659 $\pm$ 0.021 <sup>ab</sup>
5% Wheat - Extruded	0.822 $\pm$ 0.010 <sup>a</sup>	0.758 $\pm$ 0.016 <sup>a</sup>	0.769 $\pm$ 0.055 <sup>a</sup>	0.678 $\pm$ 0.028 <sup>ab</sup>
Control	0.803 $\pm$ 0.017 <sup>a</sup>	0.731 $\pm$ 0.008 <sup>ab</sup>	0.718 $\pm$ 0.019 <sup>a</sup>	0.632 $\pm$ 0.016 <sup>b</sup>

Table B.4 Cohesiveness TPA values (unitless) – bread model system with 5% starch inclusion. Average values  $\pm$  standard error. Different letters indicate statistically significant differences at the same timepoint among treatments (down columns;  $p < 0.05$ ).

Cohesiveness (unitless)	Week 0	Week 1	Week 4	Week 12
5% Normal rice - Native	0.577 $\pm$ 0.006 <sup>d</sup>	0.485 $\pm$ 0.007 <sup>c</sup>	0.457 $\pm$ 0.004 <sup>a</sup>	0.428 $\pm$ 0.007 <sup>a</sup>
5% Normal rice - Drum dried	0.589 $\pm$ 0.008 <sup>bcd</sup>	0.493 $\pm$ 0.002 <sup>bc</sup>	0.453 $\pm$ 0.016 <sup>a</sup>	0.426 $\pm$ 0.007 <sup>a</sup>
5% Normal rice - Extruded	0.602 $\pm$ 0.012 <sup>abcd</sup>	0.494 $\pm$ 0.002 <sup>abc</sup>	0.452 $\pm$ 0.003 <sup>a</sup>	0.436 $\pm$ 0.005 <sup>a</sup>
5% Waxy rice - Native	0.590 $\pm$ 0.003 <sup>abcd</sup>	0.507 $\pm$ 0.008 <sup>abc</sup>	0.477 $\pm$ 0.009 <sup>a</sup>	0.443 $\pm$ 0.009 <sup>a</sup>
5% Waxy rice - Drum dried	0.590 $\pm$ 0.005 <sup>abcd</sup>	0.488 $\pm$ 0.004 <sup>bc</sup>	0.473 $\pm$ 0.006 <sup>a</sup>	0.439 $\pm$ 0.003 <sup>a</sup>
5% Waxy rice - Extruded	0.583 $\pm$ 0.002 <sup>cd</sup>	0.506 $\pm$ 0.005 <sup>abc</sup>	0.464 $\pm$ 0.009 <sup>a</sup>	0.433 $\pm$ 0.003 <sup>a</sup>
5% Wheat - Native	0.601 $\pm$ 0.003 <sup>abcd</sup>	0.513 $\pm$ 0.008 <sup>abc</sup>	0.466 $\pm$ 0.004 <sup>a</sup>	0.435 $\pm$ 0.003 <sup>a</sup>
5% Wheat - Drum dried	0.613 $\pm$ 0.006 <sup>abc</sup>	0.510 $\pm$ 0.009 <sup>abc</sup>	0.464 $\pm$ 0.007 <sup>a</sup>	0.444 $\pm$ 0.005 <sup>a</sup>
5% Wheat - Extruded	0.618 $\pm$ 0.005 <sup>ab</sup>	0.522 $\pm$ 0.004 <sup>a</sup>	0.486 $\pm$ 0.001 <sup>a</sup>	0.441 $\pm$ 0.002 <sup>a</sup>
Control	0.622 $\pm$ 0.009 <sup>a</sup>	0.515 $\pm$ 0.001 <sup>ab</sup>	0.494 $\pm$ 0.015 <sup>a</sup>	0.450 $\pm$ 0.006 <sup>a</sup>

Table B.5 Chewiness TPA values (g) – bread model system with 5% starch inclusion. Average values  $\pm$  standard error. Different letters indicate statistically significant differences at the same timepoint among treatments (down columns;  $p < 0.05$ ).

Chewiness (g)	Week 0	Week 1	Week 4	Week 12
5% Normal rice - Native	932.5 $\pm$ 34.6 <sup>abc</sup>	838.6 $\pm$ 27.1 <sup>c</sup>	730.0 $\pm$ 91.6 <sup>a</sup>	603.0 $\pm$ 30.5 <sup>c</sup>
5% Normal rice - Drum dried	876.0 $\pm$ 31.9 <sup>bc</sup>	864.4 $\pm$ 24.7 <sup>c</sup>	795.2 $\pm$ 12.1 <sup>a</sup>	620.1 $\pm$ 22.3 <sup>c</sup>
5% Normal rice - Extruded	923.6 $\pm$ 88.3 <sup>abc</sup>	936.3 $\pm$ 9.5 <sup>bc</sup>	806.9 $\pm$ 40.1 <sup>a</sup>	641.4 $\pm$ 20.3 <sup>bc</sup>
5% Waxy rice - Native	865.5 $\pm$ 47.1 <sup>bc</sup>	897.4 $\pm$ 8.5 <sup>bc</sup>	813.2 $\pm$ 81.9 <sup>a</sup>	589.1 $\pm$ 7.7 <sup>c</sup>
5% Waxy rice - Drum dried	899.3 $\pm$ 22.9 <sup>bc</sup>	840.3 $\pm$ 34.1 <sup>c</sup>	805.8 $\pm$ 104.6 <sup>a</sup>	652.6 $\pm$ 15.0 <sup>bc</sup>
5% Waxy rice - Extruded	866.7 $\pm$ 44.0 <sup>bc</sup>	776.3 $\pm$ 53.6 <sup>c</sup>	780.2 $\pm$ 67.7 <sup>a</sup>	670.5 $\pm$ 41.0 <sup>bc</sup>
5% Wheat - Native	982.6 $\pm$ 114.3 <sup>abc</sup>	1050.7 $\pm$ 57.9 <sup>ab</sup>	755.8 $\pm$ 25.4 <sup>a</sup>	949.8 $\pm$ 15.5 <sup>a</sup>
5% Wheat - Drum dried	1102.6 $\pm$ 53.0 <sup>ab</sup>	1044.7 $\pm$ 41.9 <sup>ab</sup>	826.7 $\pm$ 36.5 <sup>a</sup>	765.5 $\pm$ 25.2 <sup>b</sup>
5% Wheat - Extruded	1214.1 $\pm$ 63.2 <sup>a</sup>	1149.4 $\pm$ 5.4 <sup>a</sup>	1049.8 $\pm$ 152.2 <sup>a</sup>	1036.7 $\pm$ 54.9 <sup>a</sup>
Control	728.9 $\pm$ 16.1 <sup>c</sup>	858.5 $\pm$ 13.6 <sup>c</sup>	697.5 $\pm$ 37.3 <sup>a</sup>	670.9 $\pm$ 7.0 <sup>bc</sup>

Table B.6 Resilience TPA values (unitless) – bread model system with 5% starch inclusion. Average values  $\pm$  standard error. Different letters indicate statistically significant differences at the same timepoint among treatments (down columns;  $p < 0.05$ ).

<b>Resilience (unitless)</b>	<b>Week 0</b>	<b>Week 1</b>	<b>Week 4</b>	<b>Week 12</b>
5% Normal rice - Native	0.220 $\pm$ 0.004 <sup>e</sup>	0.177 $\pm$ 0.004 <sup>cd</sup>	0.155 $\pm$ 0.001 <sup>bc</sup>	0.144 $\pm$ 0.003 <sup>b</sup>
5% Normal rice - Drum dried	0.235 $\pm$ 0.007 <sup>cde</sup>	0.183 $\pm$ 0.003 <sup>bcd</sup>	0.151 $\pm$ 0.002 <sup>c</sup>	0.143 $\pm$ 0.003 <sup>b</sup>
5% Normal rice - Extruded	0.241 $\pm$ 0.005 <sup>cd</sup>	0.181 $\pm$ 0.000 <sup>bcd</sup>	0.153 $\pm$ 0.001 <sup>bc</sup>	0.148 $\pm$ 0.001 <sup>ab</sup>
5% Waxy rice - Native	0.226 $\pm$ 0.001 <sup>cde</sup>	0.184 $\pm$ 0.004 <sup>bcd</sup>	0.158 $\pm$ 0.002 <sup>abc</sup>	0.150 $\pm$ 0.004 <sup>ab</sup>
5% Waxy rice - Drum dried	0.229 $\pm$ 0.004 <sup>cde</sup>	0.172 $\pm$ 0.001 <sup>d</sup>	0.153 $\pm$ 0.003 <sup>bc</sup>	0.144 $\pm$ 0.002 <sup>b</sup>
5% Waxy rice - Extruded	0.224 $\pm$ 0.002 <sup>de</sup>	0.183 $\pm$ 0.003 <sup>bcd</sup>	0.154 $\pm$ 0.002 <sup>bc</sup>	0.139 $\pm$ 0.002 <sup>b</sup>
5% Wheat - Native	0.235 $\pm$ 0.002 <sup>cde</sup>	0.190 $\pm$ 0.003 <sup>abc</sup>	0.158 $\pm$ 0.001 <sup>abc</sup>	0.148 $\pm$ 0.001 <sup>ab</sup>
5% Wheat - Drum dried	0.261 $\pm$ 0.003 <sup>ab</sup>	0.196 $\pm$ 0.005 <sup>ab</sup>	0.163 $\pm$ 0.002 <sup>abc</sup>	0.149 $\pm$ 0.003 <sup>ab</sup>
5% Wheat - Extruded	0.267 $\pm$ 0.003 <sup>a</sup>	0.204 $\pm$ 0.003 <sup>a</sup>	0.170 $\pm$ 0.002 <sup>a</sup>	0.151 $\pm$ 0.001 <sup>ab</sup>
Control	0.245 $\pm$ 0.012 <sup>bc</sup>	0.189 $\pm$ 0.002 <sup>bc</sup>	0.165 $\pm$ 0.001 <sup>ab</sup>	0.157 $\pm$ 0.001 <sup>a</sup>

Table B.7 Springiness TPA values (unitless) – bread model system with 15% starch inclusion. Average values  $\pm$  standard error. Different letters indicate statistically significant differences at the same timepoint among treatments (down columns;  $p < 0.05$ ).

Springiness (unitless)	Week 0	Week 1	Week 4	Week 12
15% Normal rice - Native	0.725 $\pm$ 0.005 <sup>de</sup>	0.711 $\pm$ 0.017 <sup>bc</sup>	0.598 $\pm$ 0.003 <sup>b</sup>	0.598 $\pm$ 0.003 <sup>b</sup>
15% Normal rice - Drum dried	0.750 $\pm$ 0.009 <sup>cde</sup>	0.675 $\pm$ 0.015 <sup>cd</sup>	0.606 $\pm$ 0.004 <sup>b</sup>	0.626 $\pm$ 0.048 <sup>ab</sup>
15% Normal rice - Extruded	0.771 $\pm$ 0.005 <sup>bcd</sup>	0.675 $\pm$ 0.006 <sup>cd</sup>	0.585 $\pm$ 0.013 <sup>b</sup>	0.716 $\pm$ 0.026 <sup>ab</sup>
15% Waxy rice - Native	0.707 $\pm$ 0.017 <sup>e</sup>	0.629 $\pm$ 0.017 <sup>d</sup>	0.722 $\pm$ 0.056 <sup>a</sup>	0.758 $\pm$ 0.064 <sup>a</sup>
15% Waxy rice - Drum dried	0.820 $\pm$ 0.008 <sup>ab</sup>	0.727 $\pm$ 0.007 <sup>abc</sup>	0.630 $\pm$ 0.011 <sup>ab</sup>	0.657 $\pm$ 0.033 <sup>ab</sup>
15% Waxy rice - Extruded	0.796 $\pm$ 0.015 <sup>abc</sup>	0.721 $\pm$ 0.012 <sup>abc</sup>	0.612 $\pm$ 0.013 <sup>b</sup>	0.654 $\pm$ 0.018 <sup>ab</sup>
15% Wheat - Native	0.803 $\pm$ 0.016 <sup>ab</sup>	0.776 $\pm$ 0.005 <sup>a</sup>	0.667 $\pm$ 0.018 <sup>ab</sup>	0.639 $\pm$ 0.008 <sup>ab</sup>
15% Wheat - Drum dried	0.823 $\pm$ 0.008 <sup>ab</sup>	0.723 $\pm$ 0.012 <sup>abc</sup>	0.629 $\pm$ 0.017 <sup>ab</sup>	0.658 $\pm$ 0.029 <sup>ab</sup>
15% Wheat - Extruded	0.841 $\pm$ 0.003 <sup>a</sup>	0.740 $\pm$ 0.002 <sup>ab</sup>	0.632 $\pm$ 0.012 <sup>ab</sup>	0.589 $\pm$ 0.006 <sup>b</sup>
Control	0.772 $\pm$ 0.010 <sup>bcd</sup>	0.694 $\pm$ 0.007 <sup>bc</sup>	0.624 $\pm$ 0.019 <sup>ab</sup>	0.602 $\pm$ 0.000 <sup>b</sup>

Table B.8 Cohesiveness TPA values (unitless) – bread model system with 15% starch inclusion. Average values  $\pm$  standard error. Different letters indicate statistically significant differences at the same timepoint among treatments (down columns;  $p < 0.05$ ).

Cohesiveness (unitless)	Week 0	Week 1	Week 4	Week 12
15% Normal rice - Native	0.572 $\pm$ 0.007 <sup>def</sup>	0.501 $\pm$ 0.003 <sup>ab</sup>	0.437 $\pm$ 0.001 <sup>abc</sup>	0.413 $\pm$ 0.005 <sup>ab</sup>
15% Normal rice - Drum dried	0.559 $\pm$ 0.004 <sup>ef</sup>	0.457 $\pm$ 0.004 <sup>d</sup>	0.412 $\pm$ 0.004 <sup>c</sup>	0.392 $\pm$ 0.010 <sup>b</sup>
15% Normal rice - Extruded	0.585 $\pm$ 0.001 <sup>cde</sup>	0.474 $\pm$ 0.003 <sup>cd</sup>	0.420 $\pm$ 0.002 <sup>bc</sup>	0.417 $\pm$ 0.014 <sup>ab</sup>
15% Waxy rice - Native	0.545 $\pm$ 0.006 <sup>f</sup>	0.477 $\pm$ 0.004 <sup>bcd</sup>	0.457 $\pm$ 0.001 <sup>a</sup>	0.435 $\pm$ 0.016 <sup>a</sup>
15% Waxy rice - Drum dried	0.591 $\pm$ 0.004 <sup>cd</sup>	0.478 $\pm$ 0.001 <sup>bcd</sup>	0.423 $\pm$ 0.008 <sup>abc</sup>	0.400 $\pm$ 0.006 <sup>ab</sup>
15% Waxy rice - Extruded	0.593 $\pm$ 0.004 <sup>cd</sup>	0.485 $\pm$ 0.009 <sup>abc</sup>	0.430 $\pm$ 0.008 <sup>abc</sup>	0.402 $\pm$ 0.006 <sup>ab</sup>
15% Wheat - Native	0.611 $\pm$ 0.009 <sup>bc</sup>	0.506 $\pm$ 0.004 <sup>a</sup>	0.454 $\pm$ 0.010 <sup>ab</sup>	0.396 $\pm$ 0.007 <sup>ab</sup>
15% Wheat - Drum dried	0.635 $\pm$ 0.007 <sup>ab</sup>	0.488 $\pm$ 0.008 <sup>abc</sup>	0.444 $\pm$ 0.013 <sup>abc</sup>	0.421 $\pm$ 0.003 <sup>ab</sup>
15% Wheat - Extruded	0.643 $\pm$ 0.007 <sup>a</sup>	0.495 $\pm$ 0.002 <sup>abc</sup>	0.454 $\pm$ 0.008 <sup>ab</sup>	0.418 $\pm$ 0.002 <sup>ab</sup>
Control	0.572 $\pm$ 0.005 <sup>def</sup>	0.481 $\pm$ 0.005 <sup>bcd</sup>	0.435 $\pm$ 0.004 <sup>abc</sup>	0.417 $\pm$ 0.002 <sup>ab</sup>

Table B.9 Chewiness TPA values (g) – bread model system with 15% starch inclusion. Average values  $\pm$  standard error. Different letters indicate statistically significant differences at the same timepoint among treatments (down columns;  $p < 0.05$ ).

Chewiness (g)	Week 0	Week 1	Week 4	Week 12
15% Normal rice - Native	910.8 $\pm$ 21.3 <sup>cde</sup>	979.7 $\pm$ 54.5 <sup>cd</sup>	716.9 $\pm$ 7.8 <sup>bc</sup>	675.0 $\pm$ 4.3 <sup>b</sup>
15% Normal rice - Drum dried	1267.7 $\pm$ 14.5 <sup>b</sup>	1091.3 $\pm$ 35.7 <sup>bc</sup>	836.3 $\pm$ 17.6 <sup>abc</sup>	954.2 $\pm$ 45.4 <sup>ab</sup>
15% Normal rice - Extruded	1008.7 $\pm$ 27.4 <sup>cd</sup>	1030.2 $\pm$ 9.8 <sup>cd</sup>	715.7 $\pm$ 57.4 <sup>bc</sup>	858.4 $\pm$ 57.5 <sup>ab</sup>
15% Waxy rice - Native	779.1 $\pm$ 42.1 <sup>ef</sup>	840.0 $\pm$ 33.5 <sup>d</sup>	804.6 $\pm$ 60.6 <sup>abc</sup>	939.7 $\pm$ 126.2 <sup>ab</sup>
15% Waxy rice - Drum dried	840.1 $\pm$ 35.0 <sup>def</sup>	942.6 $\pm$ 33.7 <sup>cd</sup>	648.0 $\pm$ 10.3 <sup>c</sup>	716.4 $\pm$ 67.3 <sup>ab</sup>
15% Waxy rice - Extruded	723.4 $\pm$ 28.3 <sup>f</sup>	943.9 $\pm$ 23.2 <sup>cd</sup>	635.3 $\pm$ 17.1 <sup>c</sup>	687.3 $\pm$ 22.3 <sup>b</sup>
15% Wheat - Native	1068.6 $\pm$ 12.8 <sup>c</sup>	1276.9 $\pm$ 42.6 <sup>ab</sup>	933.4 $\pm$ 27.2 <sup>a</sup>	917.0 $\pm$ 70.2 <sup>ab</sup>
15% Wheat - Drum dried	1445.9 $\pm$ 34.5 <sup>a</sup>	1393.2 $\pm$ 86.4 <sup>a</sup>	933.7 $\pm$ 49.5 <sup>a</sup>	862.6 $\pm$ 69.3 <sup>ab</sup>
15% Wheat - Extruded	1331.8 $\pm$ 69.9 <sup>ab</sup>	1332.3 $\pm$ 29.8 <sup>a</sup>	898.1 $\pm$ 60.7 <sup>ab</sup>	1028.0 $\pm$ 72.4 <sup>a</sup>
Control	1070.4 $\pm$ 23.9 <sup>c</sup>	1032.5 $\pm$ 72.3 <sup>cd</sup>	769.7 $\pm$ 43.2 <sup>abc</sup>	766.0 $\pm$ 11.6 <sup>ab</sup>

Table B.10 Resilience TPA values (unitless) – bread model system with 15% starch inclusion. Average values  $\pm$  standard error. Different letters indicate statistically significant differences at the same timepoint among treatments (down columns;  $p < 0.05$ ).

Resilience (unitless)	Week 0	Week 1	Week 4	Week 12
15% Normal rice - Native	0.205 $\pm$ 0.005 <sup>d</sup>	0.176 $\pm$ 0.001 <sup>b</sup>	0.153 $\pm$ 0.000 <sup>bcd</sup>	0.140 $\pm$ 0.001 <sup>bc</sup>
15% Normal rice - Drum dried	0.224 $\pm$ 0.002 <sup>bcd</sup>	0.169 $\pm$ 0.003 <sup>bc</sup>	0.151 $\pm$ 0.001 <sup>cd</sup>	0.141 $\pm$ 0.003 <sup>bc</sup>
15% Normal rice - Extruded	0.230 $\pm$ 0.002 <sup>bc</sup>	0.173 $\pm$ 0.001 <sup>b</sup>	0.148 $\pm$ 0.001 <sup>d</sup>	0.137 $\pm$ 0.001 <sup>c</sup>
15% Waxy rice - Native	0.180 $\pm$ 0.004 <sup>e</sup>	0.159 $\pm$ 0.002 <sup>c</sup>	0.145 $\pm$ 0.001 <sup>d</sup>	0.141 $\pm$ 0.006 <sup>bc</sup>
15% Waxy rice - Drum dried	0.229 $\pm$ 0.003 <sup>bc</sup>	0.170 $\pm$ 0.001 <sup>bc</sup>	0.146 $\pm$ 0.003 <sup>d</sup>	0.135 $\pm$ 0.002 <sup>c</sup>
15% Waxy rice - Extruded	0.225 $\pm$ 0.003 <sup>bcd</sup>	0.173 $\pm$ 0.004 <sup>b</sup>	0.149 $\pm$ 0.002 <sup>d</sup>	0.136 $\pm$ 0.002 <sup>c</sup>
15% Wheat - Native	0.244 $\pm$ 0.007 <sup>b</sup>	0.192 $\pm$ 0.003 <sup>a</sup>	0.169 $\pm$ 0.004 <sup>ab</sup>	0.144 $\pm$ 0.003 <sup>abc</sup>
15% Wheat - Drum dried	0.285 $\pm$ 0.004 <sup>a</sup>	0.194 $\pm$ 0.004 <sup>a</sup>	0.166 $\pm$ 0.002 <sup>abc</sup>	0.153 $\pm$ 0.002 <sup>ab</sup>
15% Wheat - Extruded	0.294 $\pm$ 0.007 <sup>a</sup>	0.198 $\pm$ 0.001 <sup>a</sup>	0.174 $\pm$ 0.001 <sup>a</sup>	0.155 $\pm$ 0.001 <sup>a</sup>
Control	0.214 $\pm$ 0.004 <sup>cd</sup>	0.171 $\pm$ 0.004 <sup>bc</sup>	0.154 $\pm$ 0.001 <sup>bcd</sup>	0.146 $\pm$ 0.001 <sup>abc</sup>

Table B.11 Springiness TPA values (unitless) – cake model system with 3% starch inclusion. Average values  $\pm$  standard error. No statistically significant differences were found between treatments at each timepoint (down columns), thus no letters indicating significance have been included.

<b>Springiness (unitless)</b>	<b>Week 0</b>	<b>Week 1</b>	<b>Week 4</b>	<b>Week 12</b>
3% Normal rice - Native	0.802 $\pm$ 0.003	0.756 $\pm$ 0.005	0.729 $\pm$ 0.003	0.695 $\pm$ 0.019
3% Normal rice - Drum dried	0.786 $\pm$ 0.014	0.779 $\pm$ 0.026	0.749 $\pm$ 0.016	0.717 $\pm$ 0.006
3% Normal rice - Extruded	0.803 $\pm$ 0.016	0.764 $\pm$ 0.030	0.756 $\pm$ 0.038	0.692 $\pm$ 0.013
3% Waxy rice - Native	0.777 $\pm$ 0.004	0.760 $\pm$ 0.021	0.719 $\pm$ 0.000	0.697 $\pm$ 0.017
3% Waxy rice - Drum dried	0.780 $\pm$ 0.010	0.776 $\pm$ 0.012	0.750 $\pm$ 0.010	0.700 $\pm$ 0.020
3% Waxy rice - Extruded	0.783 $\pm$ 0.013	0.730 $\pm$ 0.004	0.716 $\pm$ 0.007	0.676 $\pm$ 0.009
3% Wheat - Native	0.801 $\pm$ 0.011	0.775 $\pm$ 0.010	0.701 $\pm$ 0.005	0.690 $\pm$ 0.012
3% Wheat - Drum dried	0.786 $\pm$ 0.018	0.770 $\pm$ 0.009	0.724 $\pm$ 0.004	0.701 $\pm$ 0.012
3% Wheat - Extruded	0.774 $\pm$ 0.012	0.751 $\pm$ 0.013	0.714 $\pm$ 0.004	0.651 $\pm$ 0.019

Table B.12 Cohesiveness TPA values (unitless) – cake model system with 3% starch inclusion. Average values  $\pm$  standard error. Different letters indicate statistically significant differences among treatments at the same timepoint (down columns;  $p < 0.05$ ).

<b>Cohesiveness (unitless)</b>	<b>Week 0</b>	<b>Week 1</b>	<b>Week 4</b>	<b>Week 12</b>
3% Normal rice - Native	0.332 $\pm$ 0.014 <sup>ab</sup>	0.214 $\pm$ 0.016 <sup>a</sup>	0.217 $\pm$ 0.005 <sup>a</sup>	0.151 $\pm$ 0.007 <sup>b</sup>
3% Normal rice - Drum dried	0.334 $\pm$ 0.014 <sup>ab</sup>	0.264 $\pm$ 0.005 <sup>a</sup>	0.224 $\pm$ 0.007 <sup>a</sup>	0.210 $\pm$ 0.008 <sup>a</sup>
3% Normal rice - Extruded	0.366 $\pm$ 0.007 <sup>a</sup>	0.205 $\pm$ 0.006 <sup>a</sup>	0.203 $\pm$ 0.007 <sup>a</sup>	0.174 $\pm$ 0.009 <sup>ab</sup>
3% Waxy rice - Native	0.321 $\pm$ 0.003 <sup>ab</sup>	0.229 $\pm$ 0.022 <sup>a</sup>	0.199 $\pm$ 0.005 <sup>a</sup>	0.170 $\pm$ 0.001 <sup>b</sup>
3% Waxy rice - Drum dried	0.347 $\pm$ 0.018 <sup>ab</sup>	0.233 $\pm$ 0.012 <sup>a</sup>	0.223 $\pm$ 0.020 <sup>a</sup>	0.181 $\pm$ 0.010 <sup>ab</sup>
3% Waxy rice - Extruded	0.335 $\pm$ 0.008 <sup>ab</sup>	0.208 $\pm$ 0.004 <sup>a</sup>	0.196 $\pm$ 0.017 <sup>a</sup>	0.158 $\pm$ 0.011 <sup>b</sup>
3% Wheat - Native	0.333 $\pm$ 0.009 <sup>ab</sup>	0.226 $\pm$ 0.014 <sup>a</sup>	0.183 $\pm$ 0.009 <sup>a</sup>	0.148 $\pm$ 0.005 <sup>b</sup>
3% Wheat - Drum dried	0.330 $\pm$ 0.011 <sup>ab</sup>	0.235 $\pm$ 0.016 <sup>a</sup>	0.208 $\pm$ 0.014 <sup>a</sup>	0.187 $\pm$ 0.005 <sup>ab</sup>
3% Wheat - Extruded	0.328 $\pm$ 0.019 <sup>ab</sup>	0.203 $\pm$ 0.011 <sup>a</sup>	0.205 $\pm$ 0.011 <sup>a</sup>	0.148 $\pm$ 0.010 <sup>b</sup>

Table B.13 Chewiness TPA values (g) – cake model system with 3% starch inclusion. Average values  $\pm$  standard error. Different letters indicate statistically significant differences among treatments at the same timepoint (down columns;  $p < 0.05$ ).

Chewiness (g)	Week 0	Week 1	Week 4	Week 12
3% Normal rice - Native	879.5 $\pm$ 54.0 <sup>a</sup>	502.1 $\pm$ 98.4 <sup>ab</sup>	663.6 $\pm$ 48.5 <sup>a</sup>	373.8 $\pm$ 11.6 <sup>bc</sup>
3% Normal rice - Drum dried	1075.4 $\pm$ 59.7 <sup>a</sup>	891.2 $\pm$ 41.2 <sup>a</sup>	628.9 $\pm$ 54.4 <sup>a</sup>	715.7 $\pm$ 57.8 <sup>a</sup>
3% Normal rice - Extruded	951.9 $\pm$ 72.6 <sup>a</sup>	455.9 $\pm$ 31.0 <sup>b</sup>	544.3 $\pm$ 66.1 <sup>a</sup>	437.2 $\pm$ 59.1 <sup>bc</sup>
3% Waxy rice - Native	851.4 $\pm$ 64.8 <sup>ab</sup>	724.5 $\pm$ 149.7 <sup>ab</sup>	517.2 $\pm$ 5.8 <sup>a</sup>	471.5 $\pm$ 32.6 <sup>bc</sup>
3% Waxy rice - Drum dried	951.3 $\pm$ 130.0 <sup>a</sup>	629.3 $\pm$ 95.6 <sup>ab</sup>	571.4 $\pm$ 87.5 <sup>a</sup>	501.7 $\pm$ 94.4 <sup>abc</sup>
3% Waxy rice - Extruded	722.9 $\pm$ 55.4 <sup>ab</sup>	427.9 $\pm$ 40.0 <sup>b</sup>	497.9 $\pm$ 110.1 <sup>a</sup>	370.0 $\pm$ 30.9 <sup>bc</sup>
3% Wheat - Native	796.1 $\pm$ 51.3 <sup>ab</sup>	575.7 $\pm$ 81.6 <sup>ab</sup>	440.2 $\pm$ 35.8 <sup>a</sup>	310.0 $\pm$ 24.6 <sup>c</sup>
3% Wheat - Drum dried	927.6 $\pm$ 71.6 <sup>a</sup>	528.6 $\pm$ 91.0 <sup>ab</sup>	541.9 $\pm$ 101.0 <sup>a</sup>	575.2 $\pm$ 22.3 <sup>ab</sup>
3% Wheat - Extruded	871.1 $\pm$ 103.9 <sup>a</sup>	468.8 $\pm$ 40.7 <sup>b</sup>	584.0 $\pm$ 75.9 <sup>a</sup>	321.2 $\pm$ 28.6 <sup>c</sup>

Table B.14 Resilience TPA values (unitless) – cake model system with 3% starch inclusion. Average values  $\pm$  standard error. Different letters indicate statistically significant differences among treatments at the same timepoint (down columns;  $p < 0.05$ ).

<b>Resilience</b>	<b>Week 0</b>	<b>Week 1</b>	<b>Week 4</b>	<b>Week 12</b>
3% Normal rice - Native	0.121 $\pm$ 0.003 <sup>a</sup>	0.093 $\pm$ 0.008 <sup>a</sup>	0.098 $\pm$ 0.001 <sup>a</sup>	0.067 $\pm$ 0.004 <sup>b</sup>
3% Normal rice - Drum dried	0.129 $\pm$ 0.004 <sup>a</sup>	0.114 $\pm$ 0.005 <sup>a</sup>	0.098 $\pm$ 0.002 <sup>a</sup>	0.096 $\pm$ 0.005 <sup>a</sup>
3% Normal rice - Extruded	0.129 $\pm$ 0.002 <sup>a</sup>	0.086 $\pm$ 0.003 <sup>a</sup>	0.090 $\pm$ 0.002 <sup>a</sup>	0.080 $\pm$ 0.004 <sup>ab</sup>
3% Waxy rice - Native	0.122 $\pm$ 0.005 <sup>a</sup>	0.102 $\pm$ 0.010 <sup>a</sup>	0.089 $\pm$ 0.002 <sup>a</sup>	0.078 $\pm$ 0.001 <sup>ab</sup>
3% Waxy rice - Drum dried	0.130 $\pm$ 0.008 <sup>a</sup>	0.097 $\pm$ 0.005 <sup>a</sup>	0.095 $\pm$ 0.004 <sup>a</sup>	0.080 $\pm$ 0.006 <sup>ab</sup>
3% Waxy rice - Extruded	0.124 $\pm$ 0.003 <sup>a</sup>	0.086 $\pm$ 0.003 <sup>a</sup>	0.087 $\pm$ 0.006 <sup>a</sup>	0.069 $\pm$ 0.005 <sup>b</sup>
3% Wheat - Native	0.128 $\pm$ 0.005 <sup>a</sup>	0.095 $\pm$ 0.006 <sup>a</sup>	0.082 $\pm$ 0.003 <sup>a</sup>	0.066 $\pm$ 0.002 <sup>b</sup>
3% Wheat - Drum dried	0.128 $\pm$ 0.004 <sup>a</sup>	0.095 $\pm$ 0.006 <sup>a</sup>	0.093 $\pm$ 0.007 <sup>a</sup>	0.086 $\pm$ 0.002 <sup>ab</sup>
3% Wheat - Extruded	0.124 $\pm$ 0.007 <sup>a</sup>	0.088 $\pm$ 0.004 <sup>a</sup>	0.093 $\pm$ 0.005 <sup>a</sup>	0.068 $\pm$ 0.005 <sup>b</sup>

Table B.15 Springiness TPA values (unitless) – cake model system with 6% starch inclusion. Average values  $\pm$  standard error. Different letters indicate statistically significant differences at the same timepoint among treatments (down columns;  $p < 0.05$ ).

Springiness (unitless)	Week 0	Week 1	Week 4	Week 12
6% Normal rice - Native	0.821 $\pm$ 0.010 <sup>ab</sup>	0.775 $\pm$ 0.003 <sup>ab</sup>	0.735 $\pm$ 0.010 <sup>a</sup>	0.748 $\pm$ 0.019 <sup>a</sup>
6% Normal rice - Drum dried	0.776 $\pm$ 0.007 <sup>abc</sup>	0.761 $\pm$ 0.008 <sup>ab</sup>	0.742 $\pm$ 0.014 <sup>a</sup>	0.729 $\pm$ 0.019 <sup>a</sup>
6% Normal rice - Extruded	0.778 $\pm$ 0.011 <sup>abc</sup>	0.749 $\pm$ 0.010 <sup>ab</sup>	0.725 $\pm$ 0.007 <sup>a</sup>	0.685 $\pm$ 0.004 <sup>a</sup>
6% Waxy rice - Native	0.827 $\pm$ 0.003 <sup>a</sup>	0.754 $\pm$ 0.011 <sup>ab</sup>	0.750 $\pm$ 0.009 <sup>a</sup>	0.731 $\pm$ 0.034 <sup>a</sup>
6% Waxy rice - Drum dried	0.786 $\pm$ 0.017 <sup>abc</sup>	0.782 $\pm$ 0.010 <sup>a</sup>	0.755 $\pm$ 0.009 <sup>a</sup>	0.759 $\pm$ 0.018 <sup>a</sup>
6% Waxy rice - Extruded	0.770 $\pm$ 0.007 <sup>bc</sup>	0.792 $\pm$ 0.028 <sup>a</sup>	0.747 $\pm$ 0.015 <sup>a</sup>	0.734 $\pm$ 0.016 <sup>a</sup>
6% Wheat - Native	0.803 $\pm$ 0.019 <sup>abc</sup>	0.761 $\pm$ 0.021 <sup>ab</sup>	0.721 $\pm$ 0.020 <sup>a</sup>	0.691 $\pm$ 0.008 <sup>a</sup>
6% Wheat - Drum dried	0.770 $\pm$ 0.011 <sup>bc</sup>	0.758 $\pm$ 0.003 <sup>ab</sup>	0.744 $\pm$ 0.009 <sup>a</sup>	0.732 $\pm$ 0.035 <sup>a</sup>
6% Wheat - Extruded	0.756 $\pm$ 0.009 <sup>c</sup>	0.713 $\pm$ 0.006 <sup>b</sup>	0.700 $\pm$ 0.012 <sup>a</sup>	0.682 $\pm$ 0.010 <sup>a</sup>
Control	0.800 $\pm$ 0.007 <sup>abc</sup>	0.780 $\pm$ 0.010 <sup>a</sup>	0.717 $\pm$ 0.008 <sup>a</sup>	0.695 $\pm$ 0.012 <sup>a</sup>

Table B.16 Cohesiveness TPA values (unitless) – cake model system with 6% starch inclusion. Average values  $\pm$  standard error. Different letters indicate statistically significant differences at the same timepoint among treatments (down columns;  $p < 0.05$ ).

Cohesiveness (unitless)	Week 0	Week 1	Week 4	Week 12
6% Normal rice - Native	0.332 $\pm$ 0.008 <sup>abc</sup>	0.258 $\pm$ 0.018 <sup>abc</sup>	0.204 $\pm$ 0.007 <sup>bc</sup>	0.184 $\pm$ 0.003 <sup>abc</sup>
6% Normal rice - Drum dried	0.321 $\pm$ 0.010 <sup>bcd</sup>	0.275 $\pm$ 0.013 <sup>ab</sup>	0.221 $\pm$ 0.005 <sup>abc</sup>	0.215 $\pm$ 0.005 <sup>a</sup>
6% Normal rice - Extruded	0.333 $\pm$ 0.009 <sup>abc</sup>	0.265 $\pm$ 0.003 <sup>abc</sup>	0.208 $\pm$ 0.004 <sup>abc</sup>	0.171 $\pm$ 0.004 <sup>bc</sup>
6% Waxy rice - Native	0.314 $\pm$ 0.007 <sup>cd</sup>	0.225 $\pm$ 0.008 <sup>bc</sup>	0.202 $\pm$ 0.007 <sup>bc</sup>	0.164 $\pm$ 0.009 <sup>c</sup>
6% Waxy rice - Drum dried	0.356 $\pm$ 0.003 <sup>ab</sup>	0.277 $\pm$ 0.005 <sup>a</sup>	0.234 $\pm$ 0.011 <sup>ab</sup>	0.185 $\pm$ 0.012 <sup>abc</sup>
6% Waxy rice - Extruded	0.361 $\pm$ 0.004 <sup>a</sup>	0.276 $\pm$ 0.004 <sup>ab</sup>	0.207 $\pm$ 0.007 <sup>abc</sup>	0.179 $\pm$ 0.012 <sup>abc</sup>
6% Wheat - Native	0.313 $\pm$ 0.007 <sup>cd</sup>	0.238 $\pm$ 0.009 <sup>abc</sup>	0.196 $\pm$ 0.013 <sup>bc</sup>	0.158 $\pm$ 0.012 <sup>c</sup>
6% Wheat - Drum dried	0.346 $\pm$ 0.006 <sup>abc</sup>	0.286 $\pm$ 0.008 <sup>a</sup>	0.246 $\pm$ 0.004 <sup>a</sup>	0.208 $\pm$ 0.007 <sup>ab</sup>
6% Wheat - Extruded	0.324 $\pm$ 0.007 <sup>abcd</sup>	0.219 $\pm$ 0.015 <sup>c</sup>	0.199 $\pm$ 0.008 <sup>bc</sup>	0.178 $\pm$ 0.004 <sup>abc</sup>
Control	0.290 $\pm$ 0.011 <sup>d</sup>	0.261 $\pm$ 0.010 <sup>abc</sup>	0.188 $\pm$ 0.005 <sup>c</sup>	0.162 $\pm$ 0.008 <sup>c</sup>

Table B.17 Chewiness TPA values (g) – cake model system with 6% starch inclusion. Average values  $\pm$  standard error. Different letters indicate statistically significant differences at the same timepoint among treatments (down columns;  $p < 0.05$ ).

Chewiness (g)	Week 0	Week 1	Week 4	Week 12
6% Normal rice - Native	650.0 $\pm$ 45.2 <sup>abc</sup>	825.5 $\pm$ 168.1 <sup>ab</sup>	566.0 $\pm$ 20.3 <sup>ab</sup>	581.9 $\pm$ 26.7 <sup>abc</sup>
6% Normal rice - Drum dried	617.3 $\pm$ 37.9 <sup>abc</sup>	797.7 $\pm$ 57.0 <sup>ab</sup>	606.1 $\pm$ 32.5 <sup>ab</sup>	703.3 $\pm$ 42.9 <sup>ab</sup>
6% Normal rice - Extruded	497.0 $\pm$ 47.7 <sup>c</sup>	722.6 $\pm$ 36.2 <sup>ab</sup>	577.1 $\pm$ 29.6 <sup>ab</sup>	471.0 $\pm$ 33.1 <sup>bc</sup>
6% Waxy rice - Native	511.1 $\pm$ 27.6 <sup>bc</sup>	517.4 $\pm$ 1.8 <sup>b</sup>	599.3 $\pm$ 58.4 <sup>ab</sup>	440.8 $\pm$ 58.1 <sup>c</sup>
6% Waxy rice - Drum dried	634.5 $\pm$ 46.7 <sup>abc</sup>	815.3 $\pm$ 46.6 <sup>ab</sup>	679.8 $\pm$ 62.5 <sup>ab</sup>	545.9 $\pm$ 52.7 <sup>abc</sup>
6% Waxy rice - Extruded	668.9 $\pm$ 6.2 <sup>ab</sup>	793.3 $\pm$ 45.9 <sup>ab</sup>	496.3 $\pm$ 50.2 <sup>b</sup>	491.7 $\pm$ 50.0 <sup>bc</sup>
6% Wheat - Native	526.7 $\pm$ 30.8 <sup>bc</sup>	526.3 $\pm$ 16.0 <sup>b</sup>	492.6 $\pm$ 115.7 <sup>b</sup>	422.4 $\pm$ 36.9 <sup>c</sup>
6% Wheat - Drum dried	729.6 $\pm$ 25.2 <sup>a</sup>	1037.0 $\pm$ 34.7 <sup>a</sup>	820.4 $\pm$ 35.6 <sup>a</sup>	755.8 $\pm$ 74.3 <sup>a</sup>
6% Wheat - Extruded	623.6 $\pm$ 9.0 <sup>abc</sup>	601.7 $\pm$ 106.3 <sup>b</sup>	493.4 $\pm$ 65.4 <sup>b</sup>	519.9 $\pm$ 42.8 <sup>abc</sup>
Control	491.2 $\pm$ 5.7 <sup>c</sup>	798.6 $\pm$ 54.3 <sup>ab</sup>	458.5 $\pm$ 10.8 <sup>b</sup>	458.8 $\pm$ 55.1 <sup>bc</sup>

Table B.18 Resilience TPA values (unitless) – cake model system with 6% starch inclusion. Average values  $\pm$  standard error. Different letters indicate statistically significant differences at the same timepoint among treatments (down columns;  $p < 0.05$ ).

<b>Resilience (unitless)</b>	<b>Week 0</b>	<b>Week 1</b>	<b>Week 4</b>	<b>Week 12</b>
6% Normal rice - Native	0.127 $\pm$ 0.002 <sup>abc</sup>	0.112 $\pm$ 0.010 <sup>abc</sup>	0.095 $\pm$ 0.002 <sup>ab</sup>	0.088 $\pm$ 0.002 <sup>ab</sup>
6% Normal rice - Drum dried	0.128 $\pm$ 0.006 <sup>abc</sup>	0.118 $\pm$ 0.005 <sup>ab</sup>	0.096 $\pm$ 0.002 <sup>ab</sup>	0.097 $\pm$ 0.003 <sup>a</sup>
6% Normal rice - Extruded	0.131 $\pm$ 0.004 <sup>ab</sup>	0.109 $\pm$ 0.001 <sup>abc</sup>	0.092 $\pm$ 0.001 <sup>ab</sup>	0.074 $\pm$ 0.002 <sup>b</sup>
6% Waxy rice - Native	0.116 $\pm$ 0.003 <sup>cd</sup>	0.094 $\pm$ 0.001 <sup>c</sup>	0.094 $\pm$ 0.004 <sup>ab</sup>	0.076 $\pm$ 0.006 <sup>ab</sup>
6% Waxy rice - Drum dried	0.132 $\pm$ 0.001 <sup>ab</sup>	0.113 $\pm$ 0.003 <sup>abc</sup>	0.098 $\pm$ 0.004 <sup>ab</sup>	0.094 $\pm$ 0.008 <sup>ab</sup>
6% Waxy rice - Extruded	0.135 $\pm$ 0.001 <sup>a</sup>	0.114 $\pm$ 0.001 <sup>abc</sup>	0.087 $\pm$ 0.004 <sup>b</sup>	0.080 $\pm$ 0.005 <sup>ab</sup>
6% Wheat - Native	0.117 $\pm$ 0.002 <sup>bcd</sup>	0.097 $\pm$ 0.002 <sup>bc</sup>	0.087 $\pm$ 0.007 <sup>b</sup>	0.073 $\pm$ 0.005 <sup>b</sup>
6% Wheat - Drum dried	0.136 $\pm$ 0.002 <sup>a</sup>	0.125 $\pm$ 0.003 <sup>a</sup>	0.111 $\pm$ 0.002 <sup>a</sup>	0.096 $\pm$ 0.005 <sup>ab</sup>
6% Wheat - Extruded	0.128 $\pm$ 0.001 <sup>abc</sup>	0.099 $\pm$ 0.007 <sup>bc</sup>	0.089 $\pm$ 0.002 <sup>ab</sup>	0.084 $\pm$ 0.002 <sup>ab</sup>
Control	0.110 $\pm$ 0.003 <sup>d</sup>	0.108 $\pm$ 0.004 <sup>abc</sup>	0.082 $\pm$ 0.001 <sup>b</sup>	0.074 $\pm$ 0.004 <sup>b</sup>

Table B.19 Water activity values ( $a_w$ , unitless) – bread model system with 5% and 15% starch inclusions. Average values  $\pm$  standard error of the mean. Different letters indicate statistically significant differences at the same timepoint among treatments (down columns;  $p < 0.05$ ).

Water activity ( $a_w$ , unitless)					Water activity ( $a_w$ , unitless)				
Starch treatment	Week 0	Week 1	Week 4	Week 12	Starch treatment	Week 0	Week 1	Week 4	Week 12
Control	0.848 $\pm$ 0.000 <sup>a</sup>	0.845 $\pm$ 0.001 <sup>a</sup>	0.834 $\pm$ 0.000 <sup>a</sup>	0.825 $\pm$ 0.000 <sup>a</sup>	Control	0.839 $\pm$ 0.000 <sup>b</sup>	0.838 $\pm$ 0.000 <sup>bc</sup>	0.825 $\pm$ 0.001 <sup>a</sup>	0.812 $\pm$ 0.002 <sup>bcd</sup>
5% Normal rice - Native	0.846 $\pm$ 0.000 <sup>bc</sup>	0.843 $\pm$ 0.000 <sup>b</sup>	0.834 $\pm$ 0.000 <sup>a</sup>	0.826 $\pm$ 0.000 <sup>a</sup>	15% Normal rice - Native	0.836 $\pm$ 0.001 <sup>cd</sup>	0.836 $\pm$ 0.001 <sup>cd</sup>	0.824 $\pm$ 0.000 <sup>a</sup>	0.811 $\pm$ 0.001 <sup>bcd</sup>
5% Normal rice - Drum dried	0.843 $\pm$ 0.000 <sup>e</sup>	0.840 $\pm$ 0.000 <sup>de</sup>	0.834 $\pm$ 0.000 <sup>a</sup>	0.824 $\pm$ 0.001 <sup>a</sup>	15% Normal rice - Drum dried	0.833 $\pm$ 0.000 <sup>ef</sup>	0.833 $\pm$ 0.000 <sup>ef</sup>	0.823 $\pm$ 0.000 <sup>a</sup>	0.814 $\pm$ 0.000 <sup>bcd</sup>
5% Normal rice - Extruded	0.845 $\pm$ 0.000 <sup>cde</sup>	0.840 $\pm$ 0.000 <sup>cde</sup>	0.830 $\pm$ 0.001 <sup>a</sup>	0.826 $\pm$ 0.000 <sup>a</sup>	15% Normal rice - Extruded	0.835 $\pm$ 0.000 <sup>de</sup>	0.835 $\pm$ 0.001 <sup>de</sup>	0.826 $\pm$ 0.001 <sup>a</sup>	0.817 $\pm$ 0.000 <sup>b</sup>
5% Waxy rice - Native	0.844 $\pm$ 0.000 <sup>cde</sup>	0.839 $\pm$ 0.000 <sup>e</sup>	0.830 $\pm$ 0.001 <sup>a</sup>	0.824 $\pm$ 0.000 <sup>a</sup>	15% Waxy rice - Native	0.843 $\pm$ 0.000 <sup>a</sup>	0.844 $\pm$ 0.000 <sup>a</sup>	0.832 $\pm$ 0.002 <sup>a</sup>	0.823 $\pm$ 0.000 <sup>a</sup>
5% Waxy rice - Drum dried	0.847 $\pm$ 0.000 <sup>ab</sup>	0.842 $\pm$ 0.001 <sup>bc</sup>	0.830 $\pm$ 0.002 <sup>a</sup>	0.823 $\pm$ 0.001 <sup>a</sup>	15% Waxy rice - Drum dried	0.825 $\pm$ 0.000 <sup>g</sup>	0.825 $\pm$ 0.001 <sup>g</sup>	0.814 $\pm$ 0.001 <sup>b</sup>	0.809 $\pm$ 0.000 <sup>d</sup>
5% Waxy rice - Extruded	0.844 $\pm$ 0.001 <sup>de</sup>	0.839 $\pm$ 0.000 <sup>e</sup>	0.829 $\pm$ 0.002 <sup>a</sup>	0.823 $\pm$ 0.000 <sup>a</sup>	15% Waxy rice - Extruded	0.832 $\pm$ 0.001 <sup>f</sup>	0.832 $\pm$ 0.000 <sup>f</sup>	0.823 $\pm$ 0.004 <sup>ab</sup>	0.813 $\pm$ 0.001 <sup>bcd</sup>
5% Wheat - Native	0.846 $\pm$ 0.001 <sup>bcd</sup>	0.842 $\pm$ 0.000 <sup>bcd</sup>	0.833 $\pm$ 0.002 <sup>a</sup>	0.823 $\pm$ 0.001 <sup>a</sup>	15% Wheat - Native	0.837 $\pm$ 0.000 <sup>bc</sup>	0.839 $\pm$ 0.000 <sup>b</sup>	0.825 $\pm$ 0.002 <sup>a</sup>	0.815 $\pm$ 0.001 <sup>bc</sup>
5% Wheat - Drum dried	0.843 $\pm$ 0.001 <sup>e</sup>	0.841 $\pm$ 0.000 <sup>cde</sup>	0.834 $\pm$ 0.000 <sup>a</sup>	0.826 $\pm$ 0.001 <sup>a</sup>	15% Wheat - Drum dried	0.835 $\pm$ 0.001 <sup>cd</sup>	0.833 $\pm$ 0.000 <sup>ef</sup>	0.826 $\pm$ 0.002 <sup>a</sup>	0.809 $\pm$ 0.001 <sup>cd</sup>
5% Wheat - Extruded	0.846 $\pm$ 0.000 <sup>abc</sup>	0.843 $\pm$ 0.001 <sup>b</sup>	0.834 $\pm$ 0.001 <sup>a</sup>	0.828 $\pm$ 0.000 <sup>a</sup>	15% Wheat - Extruded	0.836 $\pm$ 0.000 <sup>cd</sup>	0.837 $\pm$ 0.000 <sup>bc</sup>	0.827 $\pm$ 0.000 <sup>a</sup>	0.814 $\pm$ 0.002 <sup>bcd</sup>

Table B.20 Water activity values ( $a_w$ , unitless) – cake model system with 3% and 6% starch inclusions. Average values  $\pm$  standard error of the mean. Different letters indicate statistically significant differences at the same timepoint among treatments (down columns;  $p < 0.05$ ).

Starch treatment	Water activity ( $a_w$ , unitless)				Starch treatment	Water activity ( $a_w$ , unitless)			
	Week 0	Week 1	Week 4	Week 12		Week 0	Week 1	Week 4	Week 12
Control	N/A*	N/A*	N/A*	N/A*	Control	0.731 $\pm$ 0.000 <sup>abc</sup>	0.720 $\pm$ 0.001 <sup>a</sup>	0.736 $\pm$ 0.000 <sup>a</sup>	0.733 $\pm$ 0.000 <sup>a</sup>
3% Normal rice - Native	0.732 $\pm$ 0.002 <sup>abc</sup>	0.731 $\pm$ 0.001 <sup>a</sup>	0.729 $\pm$ 0.000 <sup>a</sup>	0.718 $\pm$ 0.000 <sup>e</sup>	6% Normal rice - Native	0.729 $\pm$ 0.000 <sup>c</sup>	0.729 $\pm$ 0.002 <sup>a</sup>	0.734 $\pm$ 0.000 <sup>ab</sup>	0.722 $\pm$ 0.000 <sup>abcd</sup>
3% Normal rice - Drum dried	0.734 $\pm$ 0.001 <sup>ab</sup>	0.722 $\pm$ 0.002 <sup>a</sup>	0.722 $\pm$ 0.000 <sup>cd</sup>	0.724 $\pm$ 0.001 <sup>bc</sup>	6% Normal rice - Drum dried	0.729 $\pm$ 0.002 <sup>bc</sup>	0.724 $\pm$ 0.003 <sup>a</sup>	0.732 $\pm$ 0.001 <sup>b</sup>	0.723 $\pm$ 0.002 <sup>abcd</sup>
3% Normal rice - Extruded	0.740 $\pm$ 0.001 <sup>a</sup>	0.732 $\pm$ 0.001 <sup>a</sup>	0.724 $\pm$ 0.001 <sup>bc</sup>	0.721 $\pm$ 0.001 <sup>cd</sup>	6% Normal rice - Extruded	0.729 $\pm$ 0.001 <sup>c</sup>	0.725 $\pm$ 0.003 <sup>a</sup>	0.734 $\pm$ 0.001 <sup>ab</sup>	0.728 $\pm$ 0.003 <sup>abc</sup>
3% Waxy rice - Native	0.740 $\pm$ 0.002 <sup>a</sup>	0.730 $\pm$ 0.000 <sup>a</sup>	0.725 $\pm$ 0.001 <sup>bc</sup>	0.720 $\pm$ 0.000 <sup>de</sup>	6% Waxy rice - Native	0.730 $\pm$ 0.000 <sup>bc</sup>	0.726 $\pm$ 0.004 <sup>a</sup>	0.735 $\pm$ 0.001 <sup>ab</sup>	0.730 $\pm$ 0.001 <sup>ab</sup>
3% Waxy rice - Drum dried	0.734 $\pm$ 0.001 <sup>ab</sup>	0.729 $\pm$ 0.001 <sup>a</sup>	0.720 $\pm$ 0.001 <sup>d</sup>	0.718 $\pm$ 0.000 <sup>e</sup>	6% Waxy rice - Drum dried	0.737 $\pm$ 0.000 <sup>a</sup>	0.730 $\pm$ 0.002 <sup>a</sup>	0.728 $\pm$ 0.000 <sup>c</sup>	0.718 $\pm$ 0.001 <sup>cd</sup>
3% Waxy rice - Extruded	0.724 $\pm$ 0.003 <sup>c</sup>	0.726 $\pm$ 0.000 <sup>a</sup>	0.727 $\pm$ 0.001 <sup>ab</sup>	0.714 $\pm$ 0.001 <sup>f</sup>	6% Waxy rice - Extruded	0.736 $\pm$ 0.001 <sup>ab</sup>	0.730 $\pm$ 0.000 <sup>a</sup>	0.727 $\pm$ 0.001 <sup>c</sup>	0.715 $\pm$ 0.003 <sup>d</sup>
3% Wheat - Native	0.732 $\pm$ 0.002 <sup>abc</sup>	0.734 $\pm$ 0.011 <sup>a</sup>	0.730 $\pm$ 0.000 <sup>a</sup>	0.725 $\pm$ 0.001 <sup>ab</sup>	6% Wheat - Native	0.736 $\pm$ 0.001 <sup>ab</sup>	0.731 $\pm$ 0.002 <sup>a</sup>	0.722 $\pm$ 0.001 <sup>d</sup>	0.715 $\pm$ 0.004 <sup>d</sup>
3% Wheat - Drum dried	0.734 $\pm$ 0.001 <sup>ab</sup>	0.723 $\pm$ 0.000 <sup>a</sup>	0.720 $\pm$ 0.000 <sup>d</sup>	0.720 $\pm$ 0.000 <sup>de</sup>	6% Wheat - Drum dried	0.731 $\pm$ 0.002 <sup>abc</sup>	0.724 $\pm$ 0.003 <sup>a</sup>	0.735 $\pm$ 0.001 <sup>ab</sup>	0.720 $\pm$ 0.001 <sup>bcd</sup>
3% Wheat - Extruded	0.728 $\pm$ 0.001 <sup>bc</sup>	0.722 $\pm$ 0.001 <sup>a</sup>	0.729 $\pm$ 0.001 <sup>a</sup>	0.727 $\pm$ 0.000 <sup>a</sup>	6% Wheat - Extruded	0.730 $\pm$ 0.002 <sup>bc</sup>	0.726 $\pm$ 0.001 <sup>a</sup>	0.735 $\pm$ 0.001 <sup>ab</sup>	0.725 $\pm$ 0.000 <sup>abcd</sup>

\*Control cakes not used because they were not baked on the same day as the test cakes with 3% starch replacement for flour.

Table B.21 Moisture content values (wet basis, %) – bread model system with 5% and 15% starch inclusions. Average values  $\pm$  standard error of the mean. Different letters indicate statistically significant differences at the same timepoint among treatments (down columns;  $p < 0.05$ ).

Starch treatment	Moisture content (wet basis, %)				Starch treatment	Moisture content (wet basis, %)			
	Week 0	Week 1	Week 4	Week 12		Week 0	Week 1	Week 4	Week 12
Control	27.1 $\pm$ 0.0 <sup>ab</sup>	27.0 $\pm$ 0.1 <sup>a</sup>	26.7 $\pm$ 0.1 <sup>ab</sup>	26.1 $\pm$ 0.0 <sup>ab</sup>	Control	26.1 $\pm$ 0.0 <sup>b</sup>	26.1 $\pm$ 0.1 <sup>ab</sup>	25.9 $\pm$ 0.1 <sup>a</sup>	24.8 $\pm$ 0.1 <sup>cd</sup>
5% Normal rice - Native	26.6 $\pm$ 0.0 <sup>d</sup>	27.0 $\pm$ 0.0 <sup>a</sup>	26.6 $\pm$ 0.3 <sup>abc</sup>	26.5 $\pm$ 0.1 <sup>a</sup>	15% Normal rice - Native	25.4 $\pm$ 0.0 <sup>c</sup>	25.6 $\pm$ 0.3 <sup>bc</sup>	25.3 $\pm$ 0.1 <sup>b</sup>	24.6 $\pm$ 0.1 <sup>de</sup>
5% Normal rice - Drum dried	26.4 $\pm$ 0.0 <sup>ef</sup>	26.8 $\pm$ 0.1 <sup>ab</sup>	26.9 $\pm$ 0.1 <sup>a</sup>	26.5 $\pm$ 0.1 <sup>a</sup>	15% Normal rice - Drum dried	25.9 $\pm$ 0.0 <sup>b</sup>	25.9 $\pm$ 0.0 <sup>abc</sup>	25.9 $\pm$ 0.1 <sup>a</sup>	25.2 $\pm$ 0.1 <sup>abc</sup>
5% Normal rice - Extruded	26.6 $\pm$ 0.0 <sup>de</sup>	26.7 $\pm$ 0.0 <sup>abc</sup>	26.7 $\pm$ 0.1 <sup>ab</sup>	26.4 $\pm$ 0.2 <sup>a</sup>	15% Normal rice - Extruded	26.0 $\pm$ 0.0 <sup>b</sup>	25.7 $\pm$ 0.0 <sup>bc</sup>	26.0 $\pm$ 0.0 <sup>a</sup>	25.4 $\pm$ 0.1 <sup>ab</sup>
5% Waxy rice - Native	26.4 $\pm$ 0.0 <sup>c</sup>	26.2 $\pm$ 0.0 <sup>e</sup>	25.8 $\pm$ 0.1 <sup>d</sup>	25.5 $\pm$ 0.0 <sup>b</sup>	15% Waxy rice - Native	26.1 $\pm$ 0.0 <sup>b</sup>	26.5 $\pm$ 0.2 <sup>a</sup>	25.9 $\pm$ 0.0 <sup>a</sup>	25.5 $\pm$ 0.0 <sup>a</sup>
5% Waxy rice - Drum dried	27.2 $\pm$ 0.0 <sup>a</sup>	26.5 $\pm$ 0.0 <sup>cde</sup>	26.2 $\pm$ 0.0 <sup>bcd</sup>	25.7 $\pm$ 0.1 <sup>b</sup>	15% Waxy rice - Drum dried	24.9 $\pm$ 0.1 <sup>d</sup>	24.8 $\pm$ 0.0 <sup>d</sup>	24.5 $\pm$ 0.1 <sup>c</sup>	24.1 $\pm$ 0.0 <sup>f</sup>
5% Waxy rice - Extruded	26.9 $\pm$ 0.0 <sup>bc</sup>	26.2 $\pm$ 0.0 <sup>e</sup>	26.0 $\pm$ 0.1 <sup>cd</sup>	25.7 $\pm$ 0.0 <sup>b</sup>	15% Waxy rice - Extruded	25.6 $\pm$ 0.0 <sup>c</sup>	25.4 $\pm$ 0.0 <sup>cd</sup>	25.3 $\pm$ 0.1 <sup>b</sup>	24.5 $\pm$ 0.0 <sup>ef</sup>
5% Wheat - Native	26.9 $\pm$ 0.1 <sup>f</sup>	26.2 $\pm$ 0.0 <sup>de</sup>	26.1 $\pm$ 0.0 <sup>bcd</sup>	25.7 $\pm$ 0.1 <sup>b</sup>	15% Wheat - Native	25.4 $\pm$ 0.0 <sup>c</sup>	25.6 $\pm$ 0.0 <sup>bc</sup>	25.2 $\pm$ 0.0 <sup>b</sup>	24.4 $\pm$ 0.0 <sup>ef</sup>
5% Wheat - Drum dried	27.0 $\pm$ 0.0 <sup>abc</sup>	26.5 $\pm$ 0.2 <sup>bcd</sup>	26.5 $\pm$ 0.2 <sup>abc</sup>	26.3 $\pm$ 0.3 <sup>a</sup>	15% Wheat - Drum dried	26.4 $\pm$ 0.1 <sup>a</sup>	26.0 $\pm$ 0.0 <sup>abc</sup>	25.8 $\pm$ 0.1 <sup>a</sup>	25.1 $\pm$ 0.1 <sup>bc</sup>
5% Wheat - Extruded	27.1 $\pm$ 0.1 <sup>ab</sup>	27.0 $\pm$ 0.0 <sup>a</sup>	27.2 $\pm$ 0.2 <sup>a</sup>	26.6 $\pm$ 0.0 <sup>a</sup>	15% Wheat - Extruded	26.5 $\pm$ 0.0 <sup>a</sup>	26.3 $\pm$ 0.0 <sup>a</sup>	26.1 $\pm$ 0.1 <sup>a</sup>	25.3 $\pm$ 0.1 <sup>ab</sup>

Table B.22 Moisture content values (wet basis, %) – cake model system with 3% and 6% starch inclusions. Average values  $\pm$  standard error of the mean. Different letters indicate statistically significant differences at the same timepoint among treatments (down columns;  $p < 0.05$ ).

Starch treatment	Moisture content (wet basis, %)				Starch treatment	Moisture content (wet basis, %)			
	Week 0	Week 1	Week 4	Week 12		Week 0	Week 1	Week 4	Week 12
Control	N/A*	N/A*	N/A*	N/A*	Control	16.3 $\pm$ 0.1 <sup>bc</sup>	16.0 $\pm$ 0.0 <sup>a</sup>	16.7 $\pm$ 0.1 <sup>ab</sup>	16.9 $\pm$ 0.2 <sup>a</sup>
3% Normal rice - Native	16.3 $\pm$ 0.0 <sup>ab</sup>	16.2 $\pm$ 0.0 <sup>bcd</sup>	15.7 $\pm$ 0.0 <sup>bc</sup>	16.0 $\pm$ 0.1 <sup>bcd</sup>	6% Normal rice - Native	15.6 $\pm$ 0.0 <sup>d</sup>	16.0 $\pm$ 0.0 <sup>a</sup>	16.2 $\pm$ 0.1 <sup>cdef</sup>	16.2 $\pm$ 0.1 <sup>bcd</sup>
3% Normal rice - Drum dried	16.3 $\pm$ 0.0 <sup>ab</sup>	16.5 $\pm$ 0.0 <sup>ab</sup>	15.3 $\pm$ 0.0 <sup>b</sup>	16.5 $\pm$ 0.1 <sup>ab</sup>	6% Normal rice - Drum dried	16.4 $\pm$ 0.1 <sup>bc</sup>	16.0 $\pm$ 0.1 <sup>a</sup>	16.8 $\pm$ 0.1 <sup>a</sup>	16.6 $\pm$ 0.2 <sup>ab</sup>
3% Normal rice - Extruded	16.4 $\pm$ 0.0 <sup>a</sup>	16.7 $\pm$ 0.2 <sup>a</sup>	15.3 $\pm$ 0.1 <sup>c</sup>	15.7 $\pm$ 0.1 <sup>a</sup>	6% Normal rice - Extruded	16.3 $\pm$ 0.1 <sup>bc</sup>	15.8 $\pm$ 0.1 <sup>a</sup>	16.6 $\pm$ 0.2 <sup>abc</sup>	16.4 $\pm$ 0.2 <sup>abc</sup>
3% Waxy rice - Native	15.9 $\pm$ 0.0 <sup>c</sup>	16.6 $\pm$ 0.1 <sup>ab</sup>	15.5 $\pm$ 0.0 <sup>c</sup>	15.3 $\pm$ 0.0 <sup>ab</sup>	6% Waxy rice - Native	16.2 $\pm$ 0.1 <sup>c</sup>	15.7 $\pm$ 0.1 <sup>a</sup>	16.2 $\pm$ 0.1 <sup>def</sup>	15.9 $\pm$ 0.0 <sup>cde</sup>
3% Waxy rice - Drum dried	16.6 $\pm$ 0.1 <sup>a</sup>	16.6 $\pm$ 0.1 <sup>ab</sup>	15.6 $\pm$ 0.2 <sup>bc</sup>	15.3 $\pm$ 0.0 <sup>ab</sup>	6% Waxy rice - Drum dried	16.7 $\pm$ 0.1 <sup>ab</sup>	16.5 $\pm$ 0.2 <sup>a</sup>	16.0 $\pm$ 0.0 <sup>ef</sup>	15.6 $\pm$ 0.0 <sup>efg</sup>
3% Waxy rice - Extruded	15.8 $\pm$ 0.1 <sup>c</sup>	16.2 $\pm$ 0.1 <sup>bc</sup>	16.3 $\pm$ 0.1 <sup>a</sup>	15.1 $\pm$ 0.0 <sup>bc</sup>	6% Waxy rice - Extruded	16.9 $\pm$ 0.1 <sup>a</sup>	16.3 $\pm$ 0.3 <sup>a</sup>	15.8 $\pm$ 0.0 <sup>fg</sup>	15.4 $\pm$ 0.0 <sup>fg</sup>
3% Wheat - Native	16.3 $\pm$ 0.0 <sup>ab</sup>	15.7 $\pm$ 0.0 <sup>de</sup>	16.5 $\pm$ 0.2 <sup>a</sup>	15.7 $\pm$ 0.0 <sup>de</sup>	6% Wheat - Native	16.2 $\pm$ 0.0 <sup>c</sup>	15.9 $\pm$ 0.3 <sup>a</sup>	15.4 $\pm$ 0.0 <sup>g</sup>	15.3 $\pm$ 0.0 <sup>g</sup>
3% Wheat - Drum dried	16.5 $\pm$ 0.1 <sup>a</sup>	15.6 $\pm$ 0.0 <sup>e</sup>	16.3 $\pm$ 0.1 <sup>a</sup>	15.9 $\pm$ 0.1 <sup>e</sup>	6% Wheat - Drum dried	16.3 $\pm$ 0.0 <sup>bc</sup>	16.4 $\pm$ 0.1 <sup>a</sup>	16.4 $\pm$ 0.1 <sup>bcde</sup>	15.8 $\pm$ 0.1 <sup>def</sup>
3% Wheat - Extruded	16.0 $\pm$ 0.1 <sup>bc</sup>	15.5 $\pm$ 0.0 <sup>e</sup>	16.2 $\pm$ 0.2 <sup>ab</sup>	16.2 $\pm$ 0.1 <sup>e</sup>	6% Wheat - Extruded	15.9 $\pm$ 0.0 <sup>cd</sup>	15.8 $\pm$ 0.3 <sup>a</sup>	16.5 $\pm$ 0.1 <sup>abcd</sup>	16.2 $\pm$ 0.1 <sup>bcd</sup>

\*Control cakes not used because they were not baked on the same day as the test cakes with 3% starch replacement for flour.

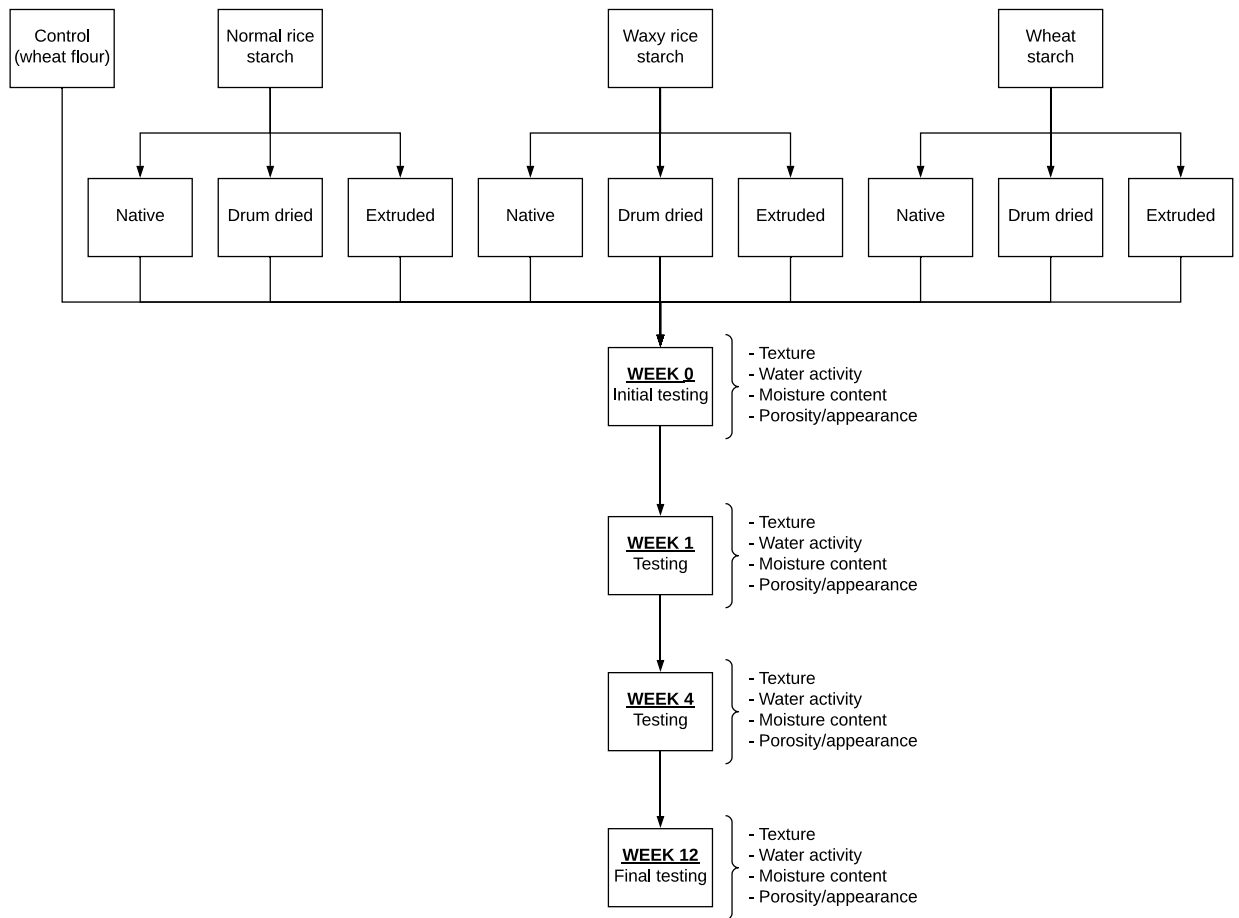


Figure B.1 Experimental design diagram for baking experiments. Diagram summarizes experiments for one inclusion level of one model system.

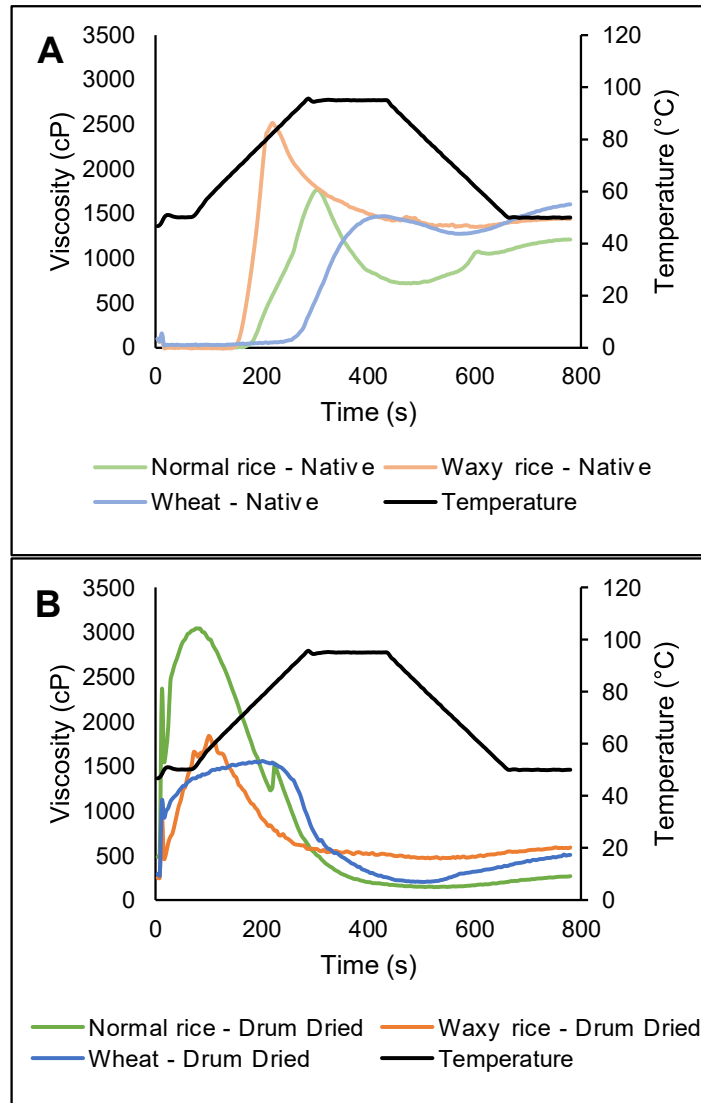


Figure B.2 Average viscosity (cP) over time for native and drum-dried starch samples from the Rapid Visco Analyzer. A: Profiles for native normal rice, waxy rice, and wheat starches. B: Profiles for drum-dried normal rice, waxy rice, and wheat starches.

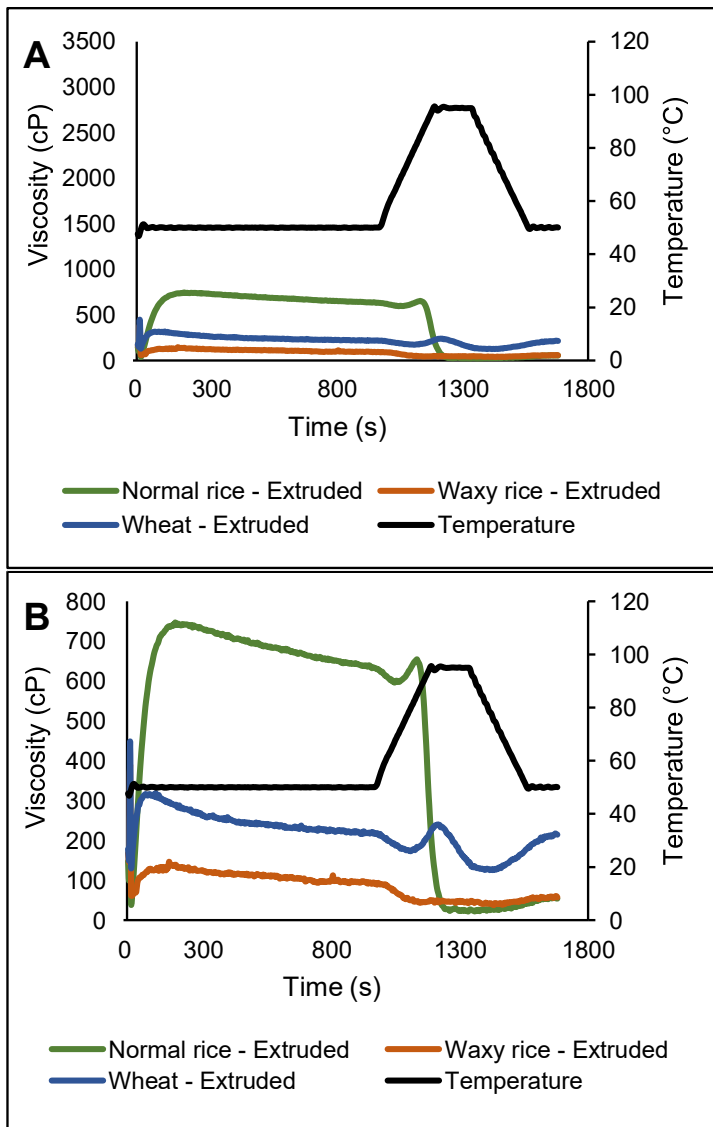


Figure B.3 Average viscosity (cP) over time for extruded starch samples from the Rapid Visco Analyzer. A: Profiles for extruded normal rice, waxy rice, and wheat starches. B: Profiles with smaller y-axis scale for extruded normal rice, waxy rice, and wheat starches.

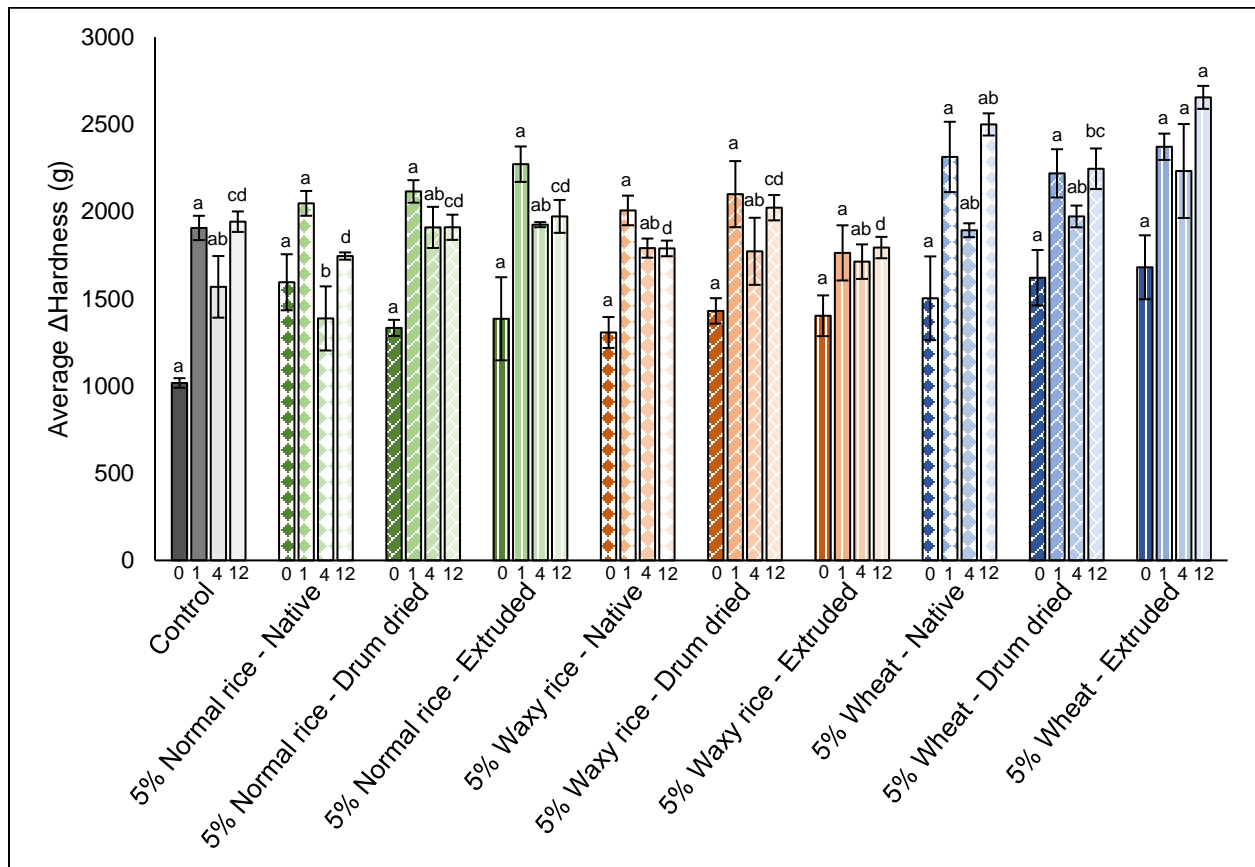


Figure B.4  $\Delta$ Hardness (g) (difference in hardness from 23 to 80°C, as measurement of degree of retrogradation) of breads with 5% starch inclusion level measured at 0, 1, 4, and 12 wk timepoints. Control breads had no starch replacement for flour. Average values  $\pm$  standard error of the mean are shown. Different letters indicate statistically significant differences among the treatments (starch source and processing method) at the same timepoint ( $p < 0.05$ ).

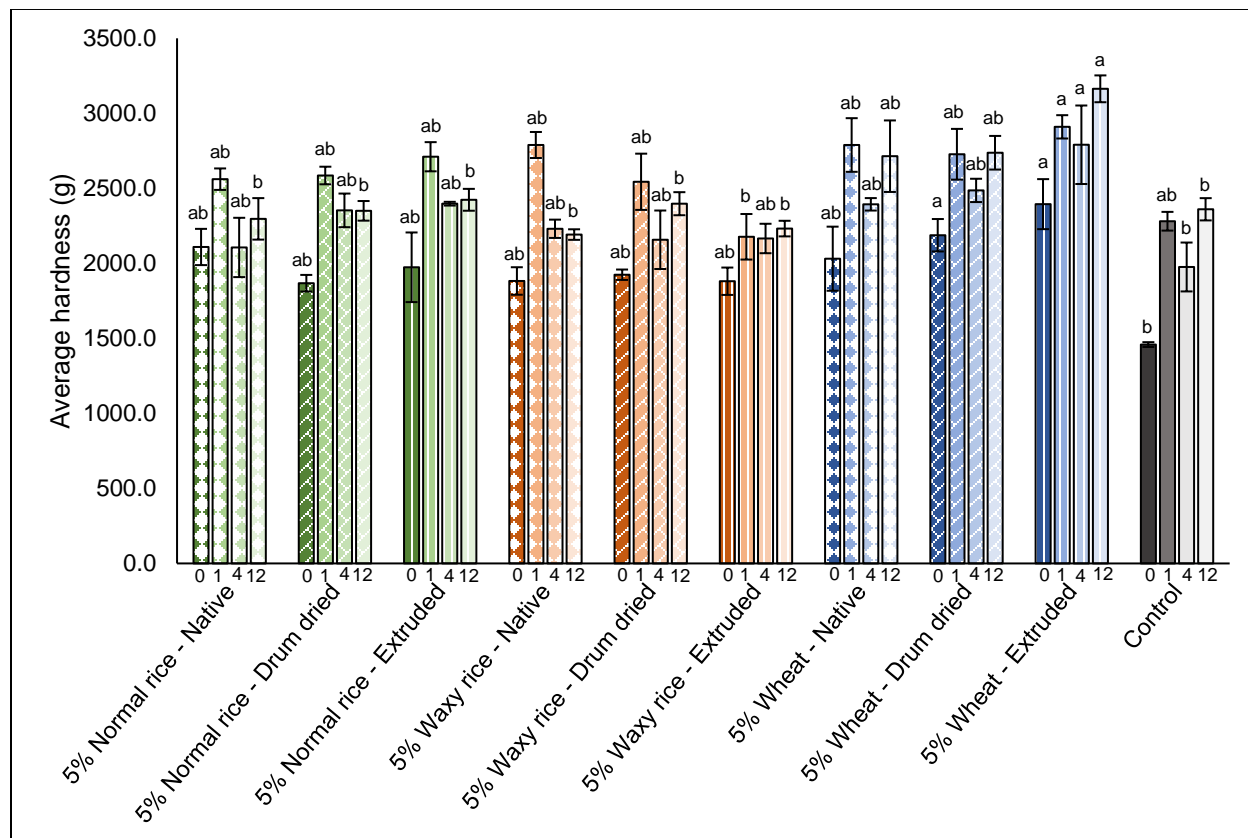


Figure B.5 Hardness (g) of breads with 5% starch inclusion level at 0, 1, 4, and 12 wk timepoints. Average values  $\pm$  standard error of the mean. Different letters indicate statistically significant differences among treatments at the same timepoint ( $p < 0.05$ ).

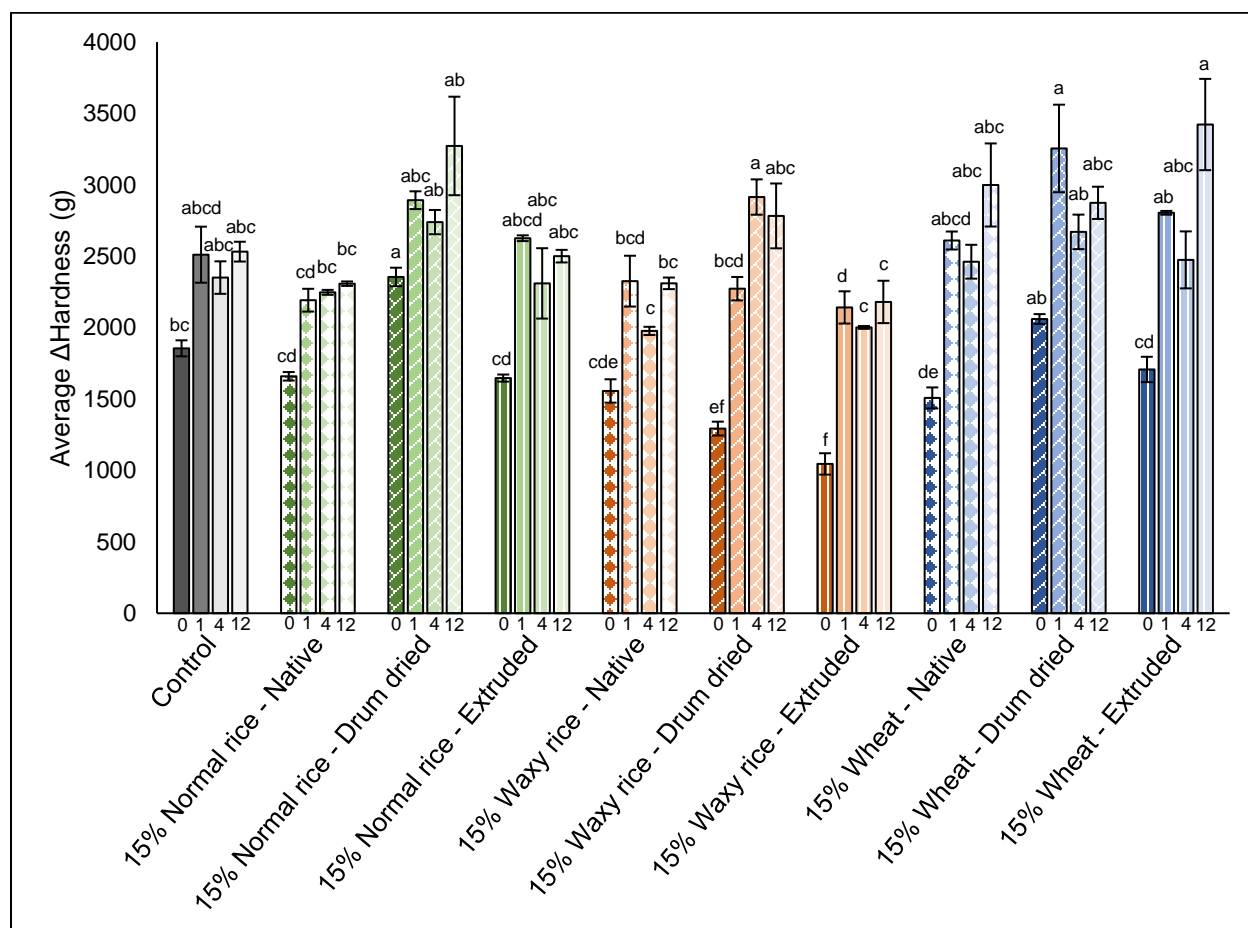


Figure B.6  $\Delta$ Hardness (g) (difference in hardness from 23 to 80°C, as measurement of degree of retrogradation) of breads with 15% starch inclusion level measured at 0, 1, 4, and 12 wk timepoints. Control breads had no starch replacement for flour. Average values  $\pm$  standard error of the mean are shown. Different letters indicate statistically significant differences among the treatments (starch source and processing method) at the same timepoint ( $p < 0.05$ ).

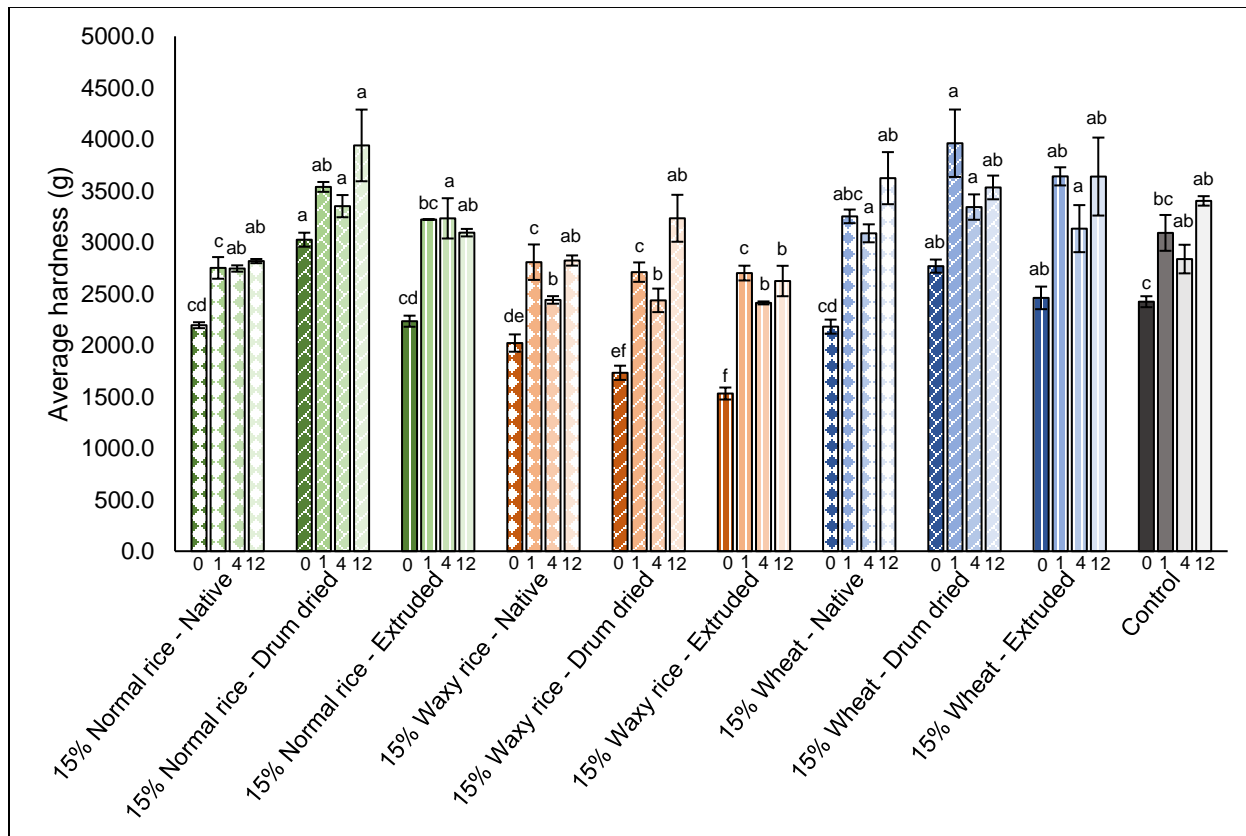


Figure B.7 Hardness (g) of breads with 15% starch inclusion level at 0, 1, 4, and 12 wk timepoints. Average values  $\pm$  standard error of the mean. Different letters indicate statistically significant differences among treatments at the same timepoint ( $p < 0.05$ ).

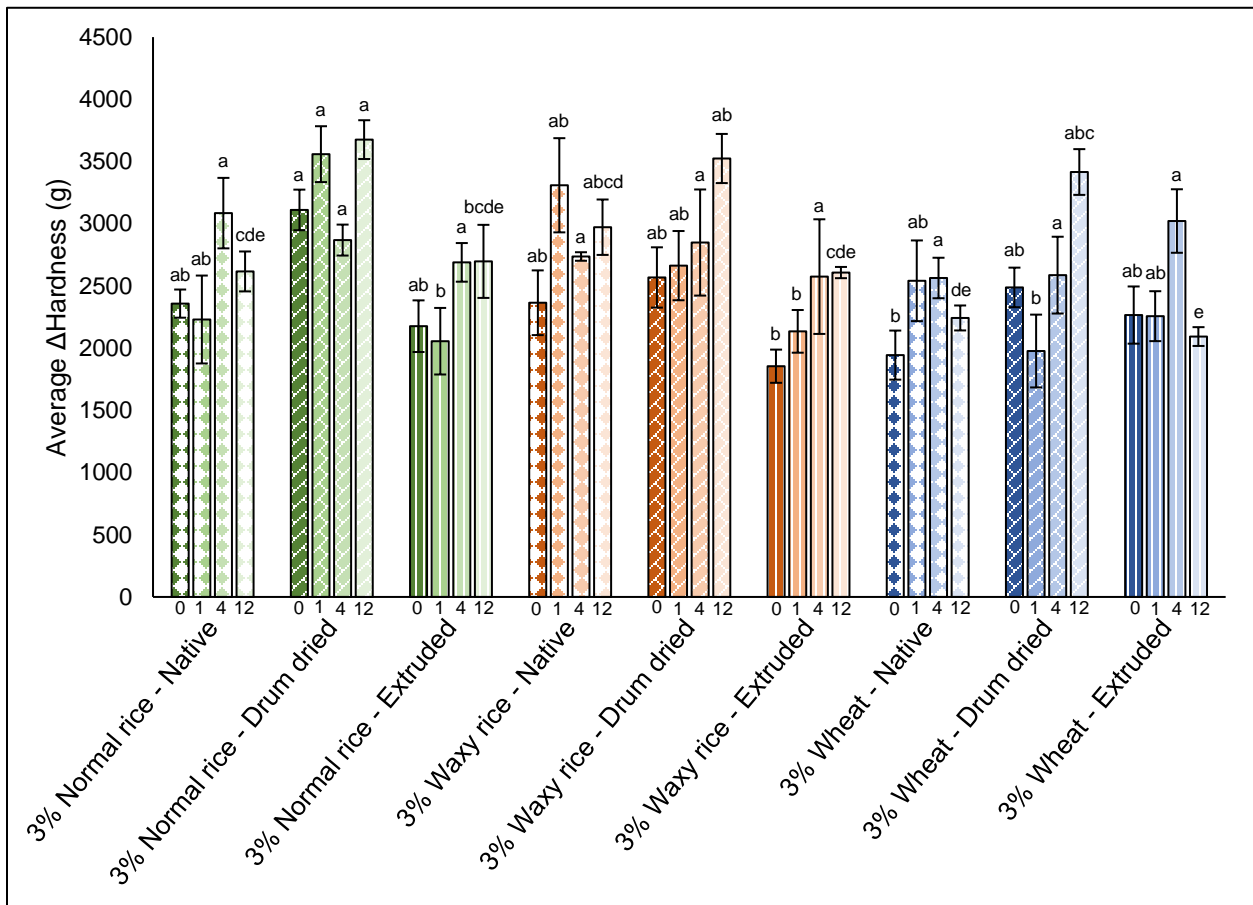


Figure B.8  $\Delta$ Hardness (g) (difference in hardness from 23 to 80°C, as measurement of degree of retrogradation) of cakes with 3% starch inclusion level measured at 0, 1, 4, and 12 wk timepoints. Average values  $\pm$  standard error of the mean are shown. Different letters indicate statistically significant differences among the treatments (starch source and processing method) at the same timepoint ( $p < 0.05$ ).

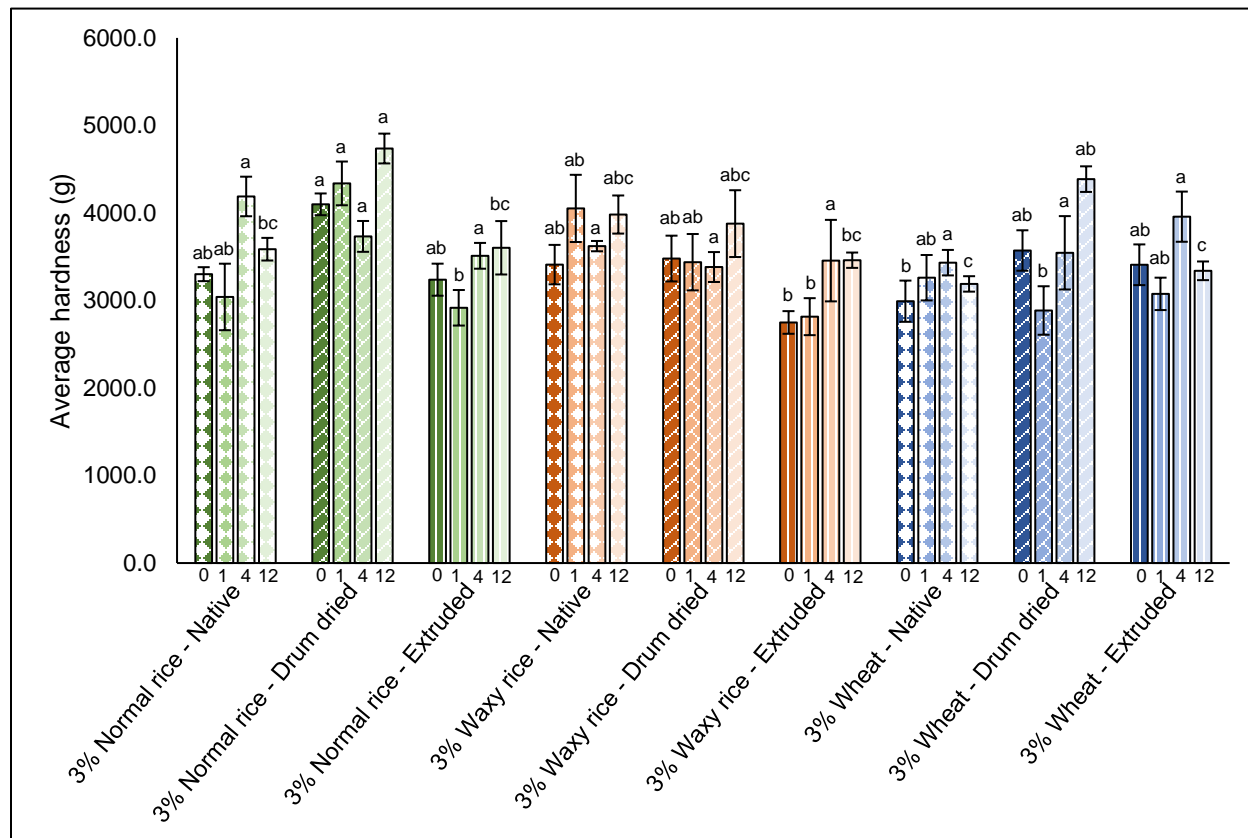


Figure B.9 Hardness (g) of cakes with 3% starch inclusion level at 0, 1, 4, and 12 wk timepoints. Average values  $\pm$  standard error of the mean. Different letters indicate statistically significant differences among treatments at the same timepoint ( $p < 0.05$ ).

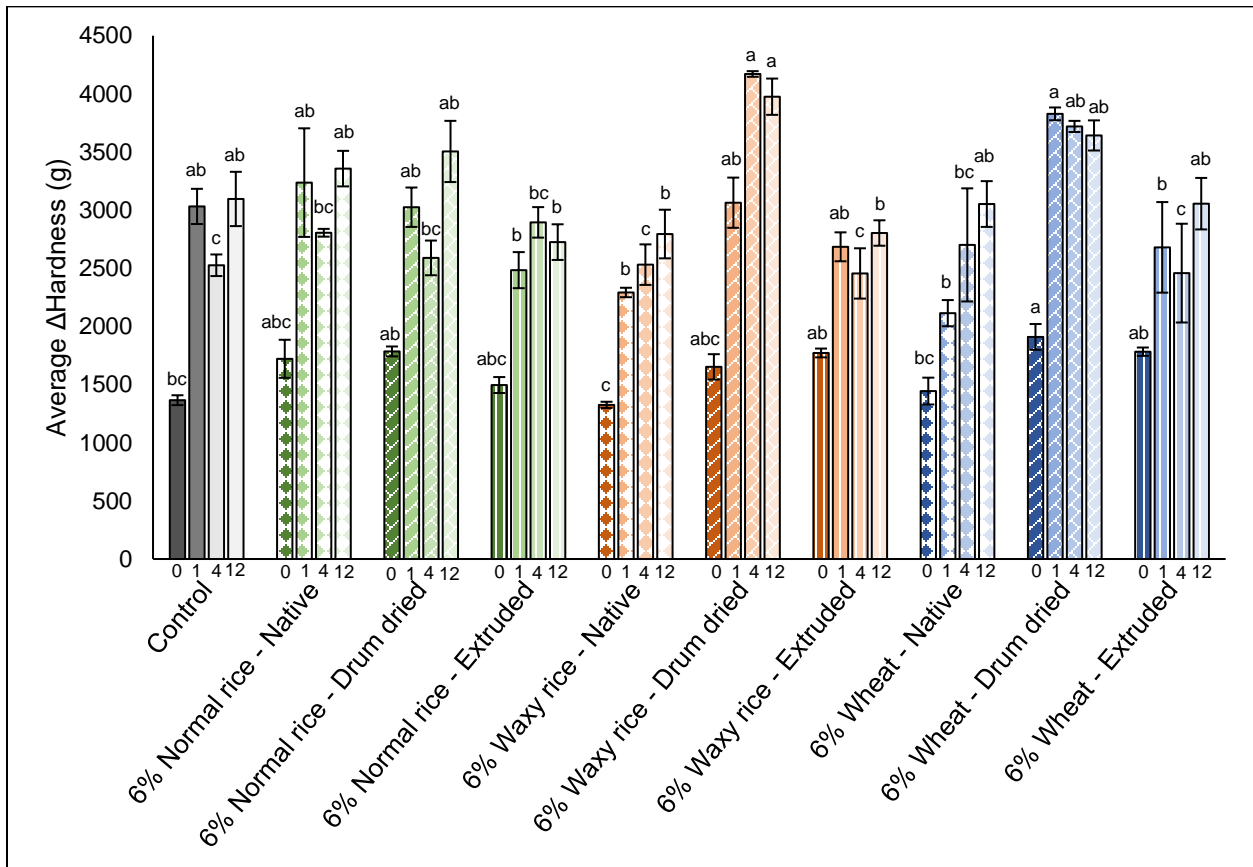


Figure B.10  $\Delta$ Hardness (g) (difference in hardness from 23 to 80°C, as measurement of degree of retrogradation) of cakes with 6% starch inclusion level measured at 0, 1, 4, and 12 wk timepoints. Control cakes had no starch replacement for flour. Average values  $\pm$  standard error of the mean are shown. Different letters indicate statistically significant differences among the treatments (starch source and processing method) at the same timepoint ( $p < 0.05$ ).

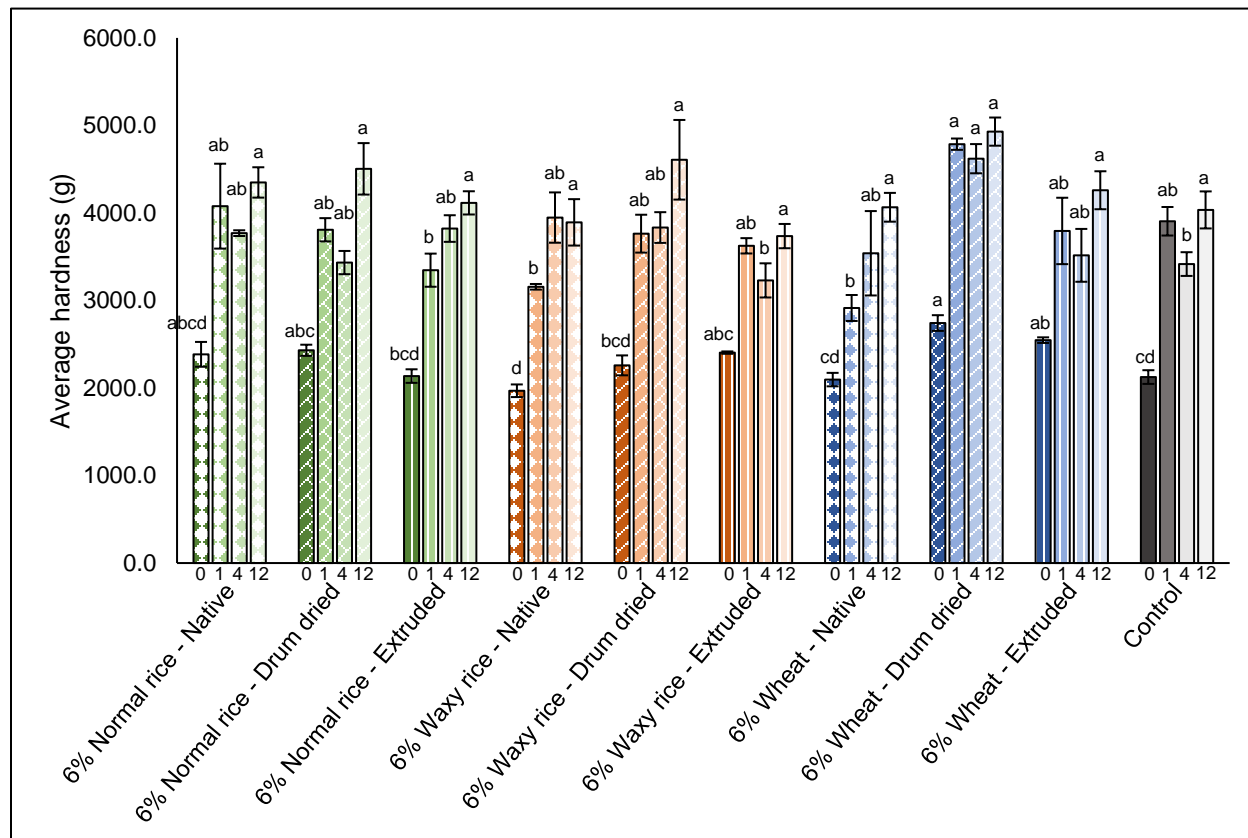


Figure B.11 Hardness (g) of cakes with 6% starch inclusion level at 0, 1, 4, and 12 wk timepoints. Average values  $\pm$  standard error of the mean. Different letters indicate statistically significant differences among treatments at the same timepoint ( $p < 0.05$ ).



Control – baked with 5% breads at wk 0



Control – baked with 5% breads at wk 4



5% Normal Rice – Native at wk 0



5% Normal Rice – Native at wk 4



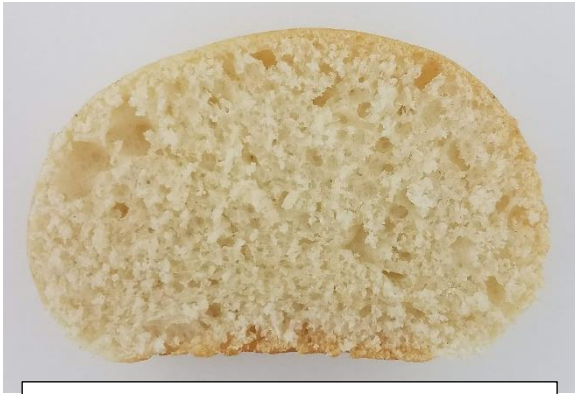
5% Waxy Rice – Native at wk 0



5% Waxy Rice – Native at wk 4

Figure B.12 Select images of breads with 5% starch inclusion.

Figure B.12, continued.



5% Wheat – Native at wk 0



5% Wheat – Native at wk 4



Control – baked with 15% breads at wk 0



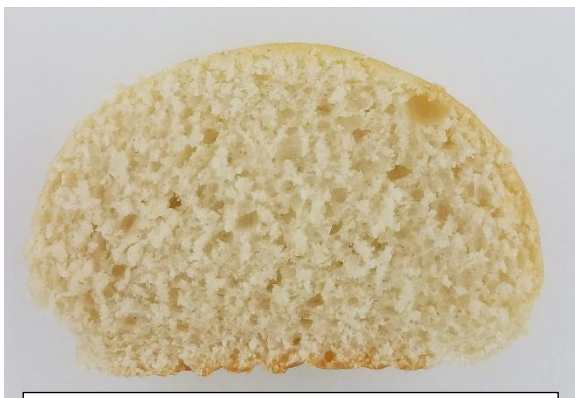
Control – baked with 15% breads at wk 4



15% Normal Rice – Extruded at wk 0



15% Normal Rice – Extruded at wk 4



15% Waxy Rice – Extruded at wk 0



15% Waxy Rice – Extruded at wk 4

Figure B.13 Select images of breads with 15% starch inclusion.

Figure B.13, continued.



15% Wheat – Extruded at wk 0



15% Wheat – Extruded at wk 4



3% Normal Rice – Drum dried at wk 0



3% Normal Rice – Drum dried at wk 12



3% Waxy Rice – Drum dried at wk 0



3% Waxy Rice – Drum dried at wk 12



3% Wheat – Drum dried at wk 0



3% Wheat – Drum dried at wk 12

Figure B.14 Select images of cakes with 3% starch inclusion.



Control – baked with 6% cakes at wk 0



Control – baked with 6% cakes at wk 12



6% Normal Rice – Extruded at wk 0



6% Normal Rice – Extruded at wk 12



6% Waxy Rice – Extruded at wk 0



6% Waxy Rice – Extruded at wk 12

Figure B.15 Select images of cakes with 6% starch inclusion.

Figure B.15, continued.



6% Wheat – Extruded at wk 0



6% Wheat – Extruded at wk 12

# VITA

**ANNA M.R. HAYES**

## EDUCATION

---

**Purdue University**, West Lafayette, IN

Direct Enrollment for Doctoral Degree: Food Science August 2014-February 2021

- Overall GPA: 3.99
- Andrews Fellowship Award Recipient
- Dual concentration – Foods for Health and Ingestive Behavior
- Graduate Research Assistant – Laboratory of Dr. Bruce Hamaker

**St. Catherine University**, St. Paul, MN

Bachelor of Science: Food and Nutrition Science August 2010-May 2014

Bachelor of Arts: Spanish

- Overall GPA: 4.00
- Class of 2014 Valedictorian
- Academic Dean's List – *Summa Cum Laude*
- Antonian Honors Program Scholar
- Recipient of Top Senior Honors Project Award

**Pontificia Universidad Católica Madre y Maestra**

January-April 2012

Santiago, Dominican Republic

Liberal Arts Council on International Educational Exchange (CIEE) Study Abroad Program

Spring 2012 Semester, Full Spanish Immersion Program, 4-month Homestay with Dominican family

## PUBLICATIONS

---

1. **Hayes AMR**, Gozzi F, Diatta A, Gorissen T, Swackhamer C, Bellmann S, Hamaker BR. (2020). Some pearl millet-based foods promote satiety and reduce glycaemic response in a crossover trial. *British Journal of Nutrition*. doi: 10.1017/S0007114520005036.
2. **Hayes AMR**, Okoniewska M, Martinez MM, Zhao B, Hamaker BR. (2020). Investigating the potential of slow-retrograding starches to reduce staling over time in soft savory bread and sweet cake model systems. *Food Research International*. 138:109745. doi: 10.1016/j.foodres.2020.109745.
3. Fang F, **Hayes AMR**, Watanabe H, Campanella OH, Hamaker BR. (2020). Isomaltodextrin strengthens model starch gels and moderately promotes starch retrogradation. *International Journal of Food Science & Technology*. doi: 10.1111/ijfs.14782.
4. **Hayes AMR**, Gundersen C, Coleman-Jensen A, Miller D, Eicher-Miller H. (2020). Session 3 discussion: Food insecurity. *Physiology & Behavior*. 224:113051. doi: 10.1016/j.physbeh.2020.113051.

5. Roman L, Yee J, **Hayes AMR**, Bertoft E, Hamaker BR, Martínez MM. (2020). On the role of the internal chain length distribution of amylopectins during retrogradation: double helix lateral aggregation and slow digestibility. *Carbohydrate Polymers*. 246:116633. doi: 10.1016/j.carbpol.2020.116633.
6. Fang F, Luo X, BeMiller JN, Schaffter S, **Hayes AMR**, Woodbury TJ, Hamaker BR, Campanella OH. (2020). Neutral hydrocolloids promote shear-induced elasticity and gel strength of gelatinized waxy potato starch. *Food Hydrocolloids*. 107:105923. doi: 10.1016/j.foodhyd.2020.105923.
7. Hasek LY, Phillips RJ, **Hayes AMR**, Kinzig K, Zhang G, Powley TL, Hamaker BR. (2020). Carbohydrates designed with different digestion rates modulate gastric emptying response in rats. *International Journal of Food Sciences and Nutrition*. 71:839-844. doi: 10.1080/09637486.2020.1738355.
8. **Hayes AMR**, Swackhamer C, Mennah-Govela Y, Martinez MM, Diatta A, Bornhorst GM, Hamaker BR. (2020). Pearl millet (*Pennisetum glaucum*) couscous breaks down faster than wheat couscous in the Human Gastric Simulator, though has slower starch hydrolysis. *Food & Function*. 11:111-122. doi: 10.1039/c9fo01461f. **Selected as front cover article for January 2020 journal issue.**
9. Veile A, Kramer K, Fiese B, **Hayes A**. (2018). Session 1 discussion: Time allocation across subsistence economies. *Physiology & Behavior*. 193(B):209-210. doi: 10.1016/j.physbeh.2018.05.020.
10. Cisse F, Erickson DP, **Hayes AMR**, Opekun AR, Nichols BL, Hamaker BR. (2018). Traditional Malian solid foods made from sorghum and millet have markedly slower gastric emptying than rice, potato or pasta. *Nutrients*. 10:124. doi: 10.3390/nu10020124.
11. Cisse F, Pletsch EA, Erickson DP, Chegeni M, **Hayes AMR**, Hamaker BR. (2017). Preload of slowly digestible carbohydrate microspheres decreases gastric emptying rate of subsequent meal in humans. *Nutrition Research*. 45:46-51. doi: 10.1016/j.nutres.2017.06.009.
12. **Hayes AMR**, Howe SC, Burgess-Champoux TL. (2015). Enhancing whole grain, fiber, and iron content of pancakes: Impacts on quality attributes and adult receptivity. *Journal of Student Research*. 4(2):36-43. Accessible from <http://www.jofsr.com/index.php/path/article/view/185>.

#### **PAPER UNDER REVIEW**

---

1. Diarra M, Torres-Aguilar P, **Hayes AMR**, Cisse F, Nkama I, Hamaker BR. Malian thick porridges (*tô*) of pearl millet are made thinner in urban than rural areas and decrease satiety. *Food and Nutrition Bulletin*. Under review (submitted April 28, 2020).

#### **BOOK CHAPTER**

---

**Hayes AMR**, Jones JM. Cultural Differences in Processing and Consumption, in *Encyclopedia of Food Grains* (Second Edition), Academic Press, Oxford, 2016, p. 35-42. ISBN 9780123947864. <http://dx.doi.org/10.1016/B978-0-12-394437-5.00073-5>

## PROFESSIONAL PRESENTATIONS

---

1. **Hayes AMR**, Kingery A, Hamaker BR. (2020, July 13-15). Development and utilization of a semester-long product development team project for first- and second-year undergraduate students to promote student engagement. Institute of Food Technologists Annual Expo (IFT20), virtual event. (poster presentation by Hayes AMR)
2. **Hayes AMR**, Hamaker BR. (2019, November 3-5). Improving understanding of pearl millet-based foods for satiety. Cereals & Grains 19. Cereals & Grains Association (formerly AACC International) Annual Meeting, Denver, CO, USA. (invited; oral presentation by Hayes AMR)
3. Roman L, Yee J, **Hayes AMR**, Bertoft E, Hamaker BR, Martínez MM. (2019, November 3-5). Amylose and amylopectin roles in the structurally-driven formation of slowly digestible starch from fully gelatinized starch. Cereals & Grains 19. Cereals & Grains Association (formerly AACC International) Annual Meeting, Denver, CO, USA. (oral presentation by Roman L)
4. Roman L, Yee J, **Hayes AMR**, Bertoft E, Hamaker BR, Martínez MM. (2019, October 31-November 2). Amylose and amylopectin roles in the structurally-driven formation of slowly digestible starch from fully gelatinized starch. Starch Roundtable, Denver, CO, USA. (oral presentation by Roman L)
5. **Hayes AMR**, Gozzi F, Hamaker BR. (2019, July 9-13). Slow gastric emptying rate for pearl millet-based foods in Mali is not observed in a U.S. population, though shows a slow digestion property. Society for the Study of Ingestive Behavior Annual Meeting, Utrecht, Netherlands. (poster presentation by Hayes AMR)
6. Hudson JL, Braun E, Wang Y, **Hayes AMR**, Hill ER, Couture SC, Douglas SM, Reister EJ, Hunter SR, Cheon E, McGowan B, Gunaratna NS, Mattes RD, Higgins KA. (2019, June 8-11). Systematic review and meta-analysis on the effect of portion size and ingestive frequency on energy intake and body weight among adults in randomized controlled trials. Nutrition 2019. American Society for Nutrition Annual Meeting, Baltimore, MD, USA. (poster presentation by collective group)
7. Chegeni M, **Hayes AMR**, Gonzalez TD, Manderfeld MM, Menon R, Holschuh N, Lim J, Hamaker BR. (2018, October 21-23). Slowly digestible carbohydrates reduce gastric emptying in humans suggesting activation of the ileal brake. Cereals & Grains 18. AACC International Annual Meeting, London, UK. (poster presentation by Hayes AMR)
8. Torres-Aguilar P, Yepez X, **Hayes AMR**, Martínez MM, Hamaker BR. (2018, October 21-23). Effect of pearl millet extrusion on the formation of amylose-lipid complexes and their slow digestion property. Cereals & Grains 18. AACC International Meeting, London, UK. (oral presentation by Torres-Aguilar P/Hamaker BR)
9. **Hayes AMR**, Swackhamer C, Martínez MM, Mennah-Govela YA, Bornhorst GM, Hamaker BR. (2018, July 15-18). Breakdown rate of couscous made from pearl millet versus wheat in a simulated gastric environment linked to gastric emptying. Institute of Food Technologists Annual Expo (IFT18), Chicago, IL, USA. (poster presentation by Hayes AMR)

10. **Hayes AMR**, Martínez MM, Swackhamer C, Mennah-Govela YA, Bornhorst GM, Hamaker BR. (2018, April 9-12). Insights to the delayed gastric emptying rate and slow digestibility of pearl millet couscous. Sorghum in the 21<sup>st</sup> Century, Cape Town, South Africa. (poster presentation by Hayes AMR)
11. **Hayes AMR**, Martínez MM, Hamaker BR. (2017, October 8). Investigating the slow digesting property of pearl millet couscous. Cereals 17. American Association of Cereal Chemists International (AACCI) Annual Meeting, San Diego, CA, USA. (oral presentation by Hayes AMR)
12. Martínez MM, Bertoft E, **Hayes AMR**, Hamaker BR. (2017, October 8). “Zipper model” explains intermolecular re-associations of starch molecules. Cereals 17, AACCI Annual Meeting, San Diego, CA, USA. (oral presentation by Martínez MM)
13. Martínez MM, Bertoft E, **Hayes AMR**, Hamaker BR. (2017, October 7). “Zipper model” explains intermolecular re-associations of starch molecules. Starch Roundtable, San Diego, CA, USA. (oral presentation by Martínez MM)
14. **Hayes AMR**, Mattes RD. (2017, October 2-4). The effect of snacking on lipid metabolic biomarkers: a review. The Pace of Life and Feeding: Health Implications. Ingestive Behavior Research Center (IBRC) International Conference, West Lafayette, IN, USA. (poster presentation by Hayes AMR)
15. Cisse F, Erickson DP, Opekun AR, Nichols BL, **Hayes AMR**, Hamaker BR. (2015, October 18-21). Sorghum and millet exhibit slower gastric emptying than pasta, potatoes, and rice. American Association of Cereal Chemists International Centennial Meeting, Minneapolis, MN, USA. (poster display)
16. **Hayes AMR**, Marquart L, Maschoff B. (2014). Fast-casual restaurant surveillance - Whole grain menu offerings and opportunities. Grains for Health Foundation (GHF) GrainUp Consortium 2014 annual meeting, Minneapolis, MN, USA. (oral presentation by Hayes AMR)
17. **Hayes AMR**, Burgess-Champoux TL. (2014). Enhancing the nutritional quality of flour tortillas: An investigation of consumer receptivity to a fortified tortilla product. National Conference on Undergraduate Research (NCUR) 2014, Lexington, KY, USA. (oral presentation by Hayes AMR and NCUR Proceedings 2014 publication: <http://www.ncurproceedings.org/ojs/index.php/NCUR2014/article/view/952/498>)
18. **Hayes AMR**, Burgess-Champoux TL. (2014). Enhancing the nutritional quality of flour tortillas: An investigation of consumer receptivity to a fortified tortilla product. St. Catherine University Antonian Honors Project Seminar. St. Paul, MN, USA. (oral presentation by Hayes AMR and St. Catherine University SOPHIA publication: [http://sophia.stkate.edu/shas\\_honors/32/](http://sophia.stkate.edu/shas_honors/32/))
19. **Hayes AMR**, Burgess-Champoux TL. (2014). Enhancing the nutritional quality of flour tortillas: An investigation of consumer receptivity to a fortified tortilla product. Minnesota Academy of Nutrition and Dietetics (MAND) 2014 annual meeting, St. Cloud, MN, USA. (poster presentation by Hayes AMR)

20. **Hayes AMR**, Burgess-Champoux T. (2014). The efficacy of alternative treatments in maintaining metabolic control of Glycogen Storage Disease (GSD) Type I: A systematic review. Minnesota Academy of Nutrition and Dietetics (MAND) 2014 annual meeting, St. Cloud, MN, USA. (poster presentation by Hayes AMR)
21. **Hayes AMR**, Howe SC, Burgess-Champoux TL. (2013). Enhancing whole grain, fiber, and iron content of pancakes: Impacts on quality attributes and adult receptivity. Minnesota Academy of Nutrition and Dietetics (MAND) 2013 annual meeting, Bloomington, MN, USA. (poster presentation by Hayes AMR)

## AWARDS & ACCOMPLISHMENTS

---

- Phi Tau Sigma Dr. Gideon ‘Guy’ Livingston Scholarship Recipient, 2020
- Phi Kappa Phi Honor Society Inductee, October 2019
  - Through Phi Kappa Phi chapter at St. Catherine University to commemorate installation of new chapter at the University in 2019
- Purdue Graduate Student Government Travel Grant Recipient (top tier), August 2019
- Institute of Food Technologists (IFT) Carbohydrate Division, Outstanding Service Award, 2019, 2020
- Purdue University Certificate of Practice in College Teaching, 2019
- Cereals & Grains 18 (AACC International Annual Meeting), Nutrition Division Best Student Research Award, 2018
- Institute of Food Technologists Annual Food Expo (IFT18), Poster Competition Finalist, 2018
- Institute of Food Technologists (IFT) Feeding Tomorrow Graduate Scholarship Recipient, 2018-2019
- Phi Tau Sigma Honors Society Chapter of the Year, 2018 and 2020
  - Awarded to Hoosier Chapter at Purdue University
  - Chapter President in 2018, with lead role in completing and submitting nomination materials for this honor
  - Chapter Secondary Secretary in 2020, with role in completing and submitting nomination materials for this honor
- Phi Tau Sigma Honors Society for Food Science and Technology Inductee, June 2015
- Institute of Food Technologists (IFT) Feeding Tomorrow Graduate Scholarship Recipient, 2014-2015
- Andrews Fellowship Recipient (2-year award), Purdue University, 2014
- St. Catherine University Mary E. McCahill Memorial Award Recipient, May 2014
  - Most prestigious award of St. Catherine University
  - Presented to a senior student who has consistently demonstrated outstanding leadership, academic excellence, loyalty and service to the university throughout her years
- St. Catherine University Class of 2014 Valedictorian
- St. Catherine University Academic Dean’s List - *Summa Cum Laude* Latin Honors, September 2010-May 2014
- St. Catherine University Antonian Honors Program Scholar, September 2010-May 2014
- St. Catherine University Top Senior Honors Project Award Recipient, May 2014

- St. Catherine University Baccalaureate Student Commencement Speaker Nominee, March 2014
- St. Catherine University Bonnie Jean Kelly and Joan Kelly Award for Excellence in Scholarly Writing – Honorable Mention, May 2014
- Phi Beta Kappa (PBK) Liberal Arts Honor Society Inductee, March 2014
- Kappa Gamma Pi (KGP) Catholic College Graduate Honor Society Inductee, March 2014
- Sigma Delta Pi (SDP) Spanish Honor Society Inductee, April 2013
  - Chapter President, April 2013-May 2014
- Kappa Omicron Nu (KON) Human Sciences Honor Society Inductee, April 2012
  - Chapter Vice President, May 2013-2014
- Minnesota Soybean Research & Promotion Council Scholarship Recipient, April 2013
- Sister James Agnes Fogarty Home Economic Scholarship Recipient, April 2012 & April 2013
- Mayo Innovation Scholar, November 2012-April 2013
  - Mayo Innovation Scholars Program, Rochester, MN
  - Initiative of the Medtronic Foundation, Mayo Clinic, & MN Private College Council
  - Collaborated with a team of three other undergraduate students and one graduate student to conduct research on an assigned inventive topic
  - Presented conclusions in paper and presentation format to professionals at Mayo Clinic
- St. Catherine University Freshman Chemistry Award Recipient, May 2011
- Catholic Order of Foresters Scholarship Recipient, May 2010
- Citizens Bank Minnesota Scholarship Recipient, May 2010

## **WORK EXPERIENCE**

---

**Graduate Research Assistant** August 2014-present  
 Department of Food Science, Purdue University, West Lafayette, IN  
 Whistler Center for Carbohydrate Research, Purdue University, West Lafayette, IN

- Design and conduct food and nutrition science related experiments in the laboratory of Dr. Bruce Hamaker
- Assist other students and scholars with use and organization of lab equipment
- *Note: Medical leave of absence from Fall 2015 through Summer 2016*

**Graduate Teaching Instructor** January-May 2019  
 Department of Food Science, Purdue University, West Lafayette, IN

- Designed and carried out FS 162 Introduction to Food Processing Course
- Incorporated a mixture of lectures, laboratory activities/experiments in the Pilot Plant and Product Development Laboratory, guest speakers, and field trips (Conagra and Frito-Lay) into the course curriculum
- Integrated a semester-long group product development project with components of marketing pitches, group presentations, and individual written reports
- Earned the Certificate of Practice in College Teaching from Purdue University

**Manuscript Editor/Reviser** October 2016-April 2018  
 West Lafayette, IN

- Reviewed and edited manuscripts, ensuring adherence to proper English grammatical rules and appropriate scientific style

**Science, Basic Statistics, & Physics Tutor** August 2012-May 2014

O'Neill Center for Academic Development, St. Catherine University, St. Paul, MN

Department of Mathematics & Physics, St. Catherine University, St. Paul, MN

- Assisted students with coursework in general chemistry, organic chemistry, biochemistry, biology, psychology, basic statistics, and calculus-based physics
- Assessed and accommodated students' strengths/weaknesses, identified unique needs for help, and developed efficient strategies to help multiple students with diverse backgrounds

**Research & Development - Food Science Intern** May 2013-August 2013

Michael Foods, Inc., Gaylord, MN

- Conducted projects relating to eggs as food ingredients – liquid egg products, liquid and dried enzyme-modified egg products, while maintaining accurate and detailed records of all tasks undertaken
- Learned and applied analytical methods for pH, free fatty acid, viscosity, salt, color, solids/moisture, and texture using various sample products
- Presented a completed project to the Research & Development staff at Michael Foods and to students and faculty at St. Catherine University

**Inorganic Laboratory Intern** May 2011-August 2012

Minnesota Valley Testing Laboratories, New Ulm, MN

- Prepared potable water samples and filtered water samples for metals analyses
- Performed analyses for moisture (vacuum oven method), fat (Mojonnier method), and scorched particles
- Maintained a clean work environment, ensured calibration of lab instruments, and assisted others

**TEACHING EXPERIENCE**

---

- Introduction to Food Law and Regulations (FS 340), guest lecturer, Spring 2018, Spring 2019, Spring 2020
- Introduction to Food Processing (FS 162), course instructor (of record), Spring 2019
- Cereal Chemistry and Processing (FS 455), guest lecturer, Fall 2018

**MENTEES**

---

- Fanny Gozzi, Undergraduate student visiting scholar from France (IUT University Institut of Technology of Bethune), April-July 2018
- Katherine Franko, Undergraduate student, May-August 2018

**PROFESSIONAL AFFILIATIONS & COMMUNITY INVOLVEMENT**

---

Institute of Food Technologists (IFT)

September 2013-present

- Student member; member of the Student Association, Indiana Section, and Great Plains Sub-Section (former member of Minnesota Section)
- Feeding Tomorrow Graduate Scholarship Recipient, 2014-2015 & 2018-2019
- College Bowl team member 2014-2016

- Student Session Monitor at IFT16 Annual Conference
  - Division Champion Team member (invited position), 2020-2021
  - Carbohydrate Division Leadership Team Volunteer
    - Secretary (2020-2021), Action Group Co-Lead (2020-2021), Newsletter Lead (2019-2020), Student Outreach Lead (2018-2020), Newsletter contributor (2016-2018)
- Phi Tau Sigma Honor Society June 2015-present
- Hoosier Chapter at Purdue
    - Secondary Treasurer, 2018-2020
    - President, 2017-2018
    - Vice President, 2016-2017
  - Program Committee member (national level), 2020-2021
- Institute of Food Technologists Student Association (IFTSA) July 2018-present
- Area Meeting Co-chair, Midwest Area, 2018-2019
  - Purdue IFTSA Chapter President, 2018-2019
- American Association of Cereal Chemists International (AACCI) April 2015-present  
*Name changed to Cereals & Grains Association, September 2019*
- Cereals & Grains Student Association President, 2019-2020
  - AACCI/Cereals & Grains Student Association Vice President, 2018-2019
  - AACCI/Cereals & Grains Board of Directors – Student Representative, 2018-2019
  - AACCI Student Association Online Communicator, 2017-2018
  - Travel Award Recipient to Cereals 17 and Cereals & Grains 18, Annual Meetings in 2017 and 2018
- Purdue University College of Agriculture Graduate Student Advisory Board August 2019-2020
- Representative for the Department of Food Science
  - Provide input on programs and activities that will enhance the graduate experience
  - Promote excellence and professionalism in graduate education for all students
- Purdue University Food Science Graduate Student Association August 2014-present
- President, June 2018-2019
  - Treasurer, September 2014-May 2015
  - Organize and facilitate enriching opportunities for 80+ fellow graduate students
  - Wrote successful grant to obtain funding through the Purdue Graduate Student Government
  - Assisted at various events – Molecular Gastronomy night, Wine & Cheese night, International Dinner, Holiday Party, Breakfast hours, etc.
  - Purdue University AgWeek and Spring Fest planner and volunteer
- Purdue University Ingestive Behavior Graduate Student Association August 2014-present
- Treasurer, September 2017-2018
  - Event Planner, May 2015-September 2017
- Purdue Graduate Student Government (PGSG) September 2014-October 2015
- Academic & Professional Development (APD) committee member, September 2014-April 2015
  - APD co-chair, April 2015-October 2015
  - Planned and facilitated Public Speaking & Poster Presentation Workshops and the Next Generation Scholars Event for 80 middle school youth

- Head organizer of Etiquette Seminar for 50 graduate students (April 7, 2015)

#### **RECENT VOLUNTEERING & SERVICE**

---

- Mental Health First Aid, certified aider, November 11, 2019
- Purdue Student Food Insecurity Committee member, May 2019-present
- Lafayette Regional Science and Engineering Fair Judge, March 6, 2015; March 3, 2017; March 2, 2018; March 8, 2019; March 26, 2020
- Purdue Extension Booth Volunteer at the Indiana State Fair, 2016 and 2017
- Food Finders – J.P. Lisack Community Food Pantry bi-weekly volunteer, Lafayette, IN, June 2016-2017
- Springification/Boiler Blast community outreach event volunteer, Purdue University, April 9, 2016
- Food Finders Food Bank volunteer, Lafayette, IN, March 31, 2016
- Project Move Out volunteer, Purdue University, May 9, 2015
- Martin Luther King, Jr. Day of Service volunteer, Purdue University, January 19, 2015; January 16, 2017